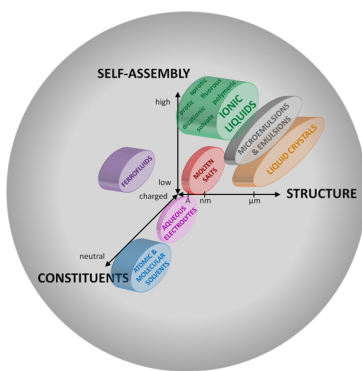


## Structure and Nanostructure in Ionic Liquids

Robert Hayes,<sup>†,§</sup> Gregory G. Warr,<sup>‡</sup> and Rob Atkin<sup>\*,†</sup>

<sup>†</sup>Discipline of Chemistry, The University of Newcastle, NSW 2308, Callaghan, Australia

<sup>‡</sup>School of Chemistry, The University of Sydney, NSW 2006, Sydney, Australia



### CONTENTS

1. Introduction	6358
1.1. Solvent Structure	6358
1.2. Overview and Scope	6358
2. Liquid Salts	6360
2.1. What Is an Ionic Liquid?	6361
2.2. Classification by Structure	6361
2.2.1. Protic ILs	6361
2.2.2. Aprotic ILs	6362
2.2.3. Other IL Subclasses	6362
2.3. IL Solvent Properties	6362
3. The Bulk Structure of Ionic Liquids	6362
3.1. Crystal Lattice Structure	6362
3.2. Supramolecular Solvent Structure	6364
3.2.1. Ion Pairs or Free Ions	6364
3.2.2. H-Bond Networks	6365
3.2.3. Ion Clusters	6366
3.3. Self-Assembled Solvent Structures	6367
3.3.1. Micelle-like Nanostructure	6367
3.3.2. Mesoscopic Nanostructures	6368
3.4. Novel Ion Types That Self-Assemble	6377
3.4.1. Fluorous ILs	6377
3.4.2. Dicationic ILs	6377
3.4.3. Polymeric ILs	6378
3.4.4. Magnetic ILs	6378
3.4.5. Solvate ILs	6379
3.5. Effect of External Variables	6380
3.5.1. Temperature	6380
3.5.2. Electric Field	6381
3.5.3. Pressure	6381
3.6. Solvation Structures in ILs	6381
3.6.1. Uncharged Solutes	6381
3.6.2. Charged Solutes	6381
3.6.3. IL Mixtures	6382
3.7. Some Remarks on IL Dynamics	6383
4. The Structure of the Solid–Ionic Liquid Interface	6383
4.1. Charged Nonmetal Interfaces	6384
4.2. Carbon Interfaces	6386
4.3. Metal Interfaces	6386
4.4. IL Electrical Double Layer Structure	6388
4.5. IL Films	6390
4.6. Do Solid and Liquid IL Phases Coexist?	6391
5. The Relationship between Bulk and Interfacial IL Arrangements	6391
6. How Does IL Structure Compare to Other Solvents?	6391
6.1. In the Bulk Phase	6391
6.2. At Solid Interfaces	6394
7. Discussion	6394
7.1. Factors That Dictate Self-Assembly in ILs	6395
7.1.1. Coulombic Interactions	6395
7.1.2. Solvophobic Interactions	6395
7.1.3. Packing Geometry	6395
7.1.4. Hydrogen Bonding	6395
7.1.5. IL–Surface Interactions	6395
7.2. How To Control IL Self-Assembly	6396
7.2.1. In the Bulk Phase	6396
7.2.2. At the Solid Interface	6396
7.3. Exploiting (Nano)structure to Make Things	6397
7.3.1. Nanoscience and Nanomaterials	6397
7.3.2. Organic Synthesis	6398
7.3.3. Electrodeposition	6399
7.3.4. Medicines and Medical Research	6399
7.4. Exploiting (Nano)structure to Process Things	6399
7.4.1. Cellulose Dissolution	6399
7.4.2. Mineral Extraction	6400
7.4.3. Energy Storage	6400
7.4.4. Microfluidics	6401
7.4.5. CO <sub>2</sub> Capture	6401
7.4.6. Biomolecule Stabilization	6401
7.4.7. Nuclear Fuel Processing	6401
7.5. Exploiting (Nano)structure to Transport Things	6401
7.5.1. Lubrication	6401
7.5.2. Fuels	6402
8. Conclusions	6402
8.1. Outlook	6402
Author Information	6403
Corresponding Author	6403
Present Address	6403
Notes	6403
Biographies	6403
Acknowledgments	6403
Glossary	6404
References	6405

Received: July 31, 2014

Published: June 1, 2015

## 1. INTRODUCTION

*"If you want to understand function, study structure!"<sup>1</sup>*  
Francis H. Crick

Much of chemistry is concerned with the study of reactions and processes in solution, that is, where liquids are used as solvents.<sup>2,3</sup> The solvent is the (excess) liquid phase in which one or more solutes are dissolved to form a homogeneous solution. Until recently, the constituents of solvents, whether they be water, alcohols, hydrocarbons, fluorocarbons, ammonia, tetrahydrofuran, carboxylic acids, amides, or supercritical CO<sub>2</sub>, have overwhelmingly been molecular.

Some of the most interesting problems in chemistry research, and many of the most important ones facing society, can be addressed using solvents. Today, solvents are employed in a diverse range of technologies and applications involved in making (medicines, foods, plastics), processing (minerals extraction, analytical separation, surface coatings, energy storage, CO<sub>2</sub>-capture), and transporting things (fuels, lubricants). Even with the increasing miniaturization of science and devices,<sup>4,5</sup> solvents remain a convenient and widely used medium in which to do chemistry. All of this translates to an enormous economic demand for solvents; the global market for solvents is worth billions of dollars, and is growing steadily.

There are several drawbacks associated with the use of solvents relating to environmental, health, or safety issues, which are subject to strict legislation in many countries. First, considerable energy input is required throughout all stages of the solvent life cycle from manufacture through disposal. Most solvent feedstocks are finite as they are derived from petrochemical or fresh water resources. Nonaqueous solvents are also frequently toxic if ingested and are prone to bioaccumulation in natural environments. As solvents are often volatile, there are problems related to storage, transport, and atmospheric pollution. Together, these pose serious short- and long-term challenges to their use, and can affect the living standards of all people.

Against this astounding backdrop of knowledge, the prevailing question is not "Is a solvent needed?" but rather "What is the right solvent for my process?" Notably, "solvent-free" reaction conditions<sup>6</sup> are in their infancy (microwave irradiation,<sup>6</sup> flow chemistry<sup>7</sup>) or are significantly more expensive to the chemist, and some have their own environmental issues. Thus, in the short to medium term, the majority of reactions will still be conducted in solvents, either traditional or chemically modified liquids. It is simply not feasible to replace all solvents in a short time period. However, a lack of innovation in solvent technology could have serious consequences. Today's chemistry will not function on yesterday's solvents, and tomorrow's chemistry will need new solvent developments.

### 1.1. Solvent Structure

One key area of solvent research ripe for investigation is linked to structure, and how this controls liquid properties. How are liquid molecules organized in the bulk? Over what length and time scales does solvent structure exist? What are the interactions responsible for liquid structure? Can liquid structure be controllably tuned? Is there a relationship between solvent structure and performance?

Of the three forms of matter (solids, liquids, and gases), the physical structure of liquids is the least well-understood; Tabor's famous description of liquids as the "Cinderella of modern physics"<sup>8</sup> still holds true today as a unified theory of liquid structure has not been established. Elucidation of molecular organization in liquids is challenging because they are an

intermediate phase, with features common to both solids and gases.<sup>2</sup> There are also still gaps in our knowledge of the forces that control structure on tiny dimensions.<sup>9–11</sup>

Until recently, liquids were thought to be structurally homogeneous systems; Bernal's classic picture of liquids as homogeneous, coherent, and essentially irregular<sup>12</sup> strongly influenced thinking in the scientific community. Liquid structure was believed to be similar to the parent solid, albeit much more disordered because molecules diffuse rapidly and randomly through the liquid. This would mean that structure exists only over negligible distances and time scales. However, in the past decade or so, advances in theoretical, computational, and experimental techniques have provided unprecedented resolution pictures of the physical structure of liquids,<sup>13–17</sup> which was recently the focus of a Faraday Discussions meeting in 2013.<sup>18</sup> Mounting evidence suggests that liquids possess reasonably well-defined structure in the bulk phase and at interfaces, and that this structure underpins solvent behavior.

### 1.2. Overview and Scope

Ionic liquids (ILs) are fluids that exemplify these features. They are solvents that can participate in a variety of attractive interactions ranging from the weak, nonspecific, and isotropic forces (e.g., van der Waals,<sup>19</sup> solvophobic,<sup>20</sup> dispersion<sup>21</sup> forces) to strong (Coulombic), specific, and anisotropic forces (e.g., hydrogen bonding,<sup>22</sup> halogen bonding,<sup>23</sup> dipole–dipole, magnetic dipole, electron pair donor/acceptor interactions). The diversity and strength of intermolecular forces in ILs fine-tune local arrangements in the bulk and near interfaces. However, some interactions have an entropic contribution, paving the way for complex, higher order self-assembled structures. The amphiphilic nature of many ions provides a basis for ordering akin to ionic surfactant systems; open to question is whether the ion–ion interactions induce strong association or self-assembly. To date, almost every known physical chemistry technique has been used to investigate structure in ILs. This has yielded a wealth of sometimes conflicting data. The purpose of this Review is to trace the development of models used to describe IL bulk structure and show how ion self-assembly underpins much of their complex chemical and physical behavior. Our aims in examining IL structure are (1) to develop a unified map of the solvent architectures reported in ILs and (2) to discover both common and complementary elements for their rational design.

This Review is also motivated by increased demand for structure–property relationships in ILs. Over and over again in the literature, the concept of "IL structure" features prominently, with authors emphasizing that one IL outperforms another (molecular liquid or IL) solvent in a given process. This has enabled ILs to be aggressively pursued across all areas of chemistry, physics, biology, and materials science, which is the subject of numerous reviews,<sup>24–35</sup> books,<sup>36–42</sup> special issues in high-impact journals,<sup>43–51</sup> conference proceedings, and online databases.<sup>52</sup> A survey of these reviews shows that our understanding of IL fundamentals (mp, bp, conductivity, density, vapor pressure, etc.) in relation to chemical structure is reasonably advanced. Likewise, chemists have developed a well-resourced toolbox of reactions for preparing different ion chemical structures.<sup>53,54</sup> Approximate<sup>55–57</sup> and classical<sup>58–60</sup> theories are now available, which can predict general IL phase behavior and viscosity, although ion arrangements are once again ignored in these theories because the liquid is modeled as a continuum of ions of fixed molecular volume and density.

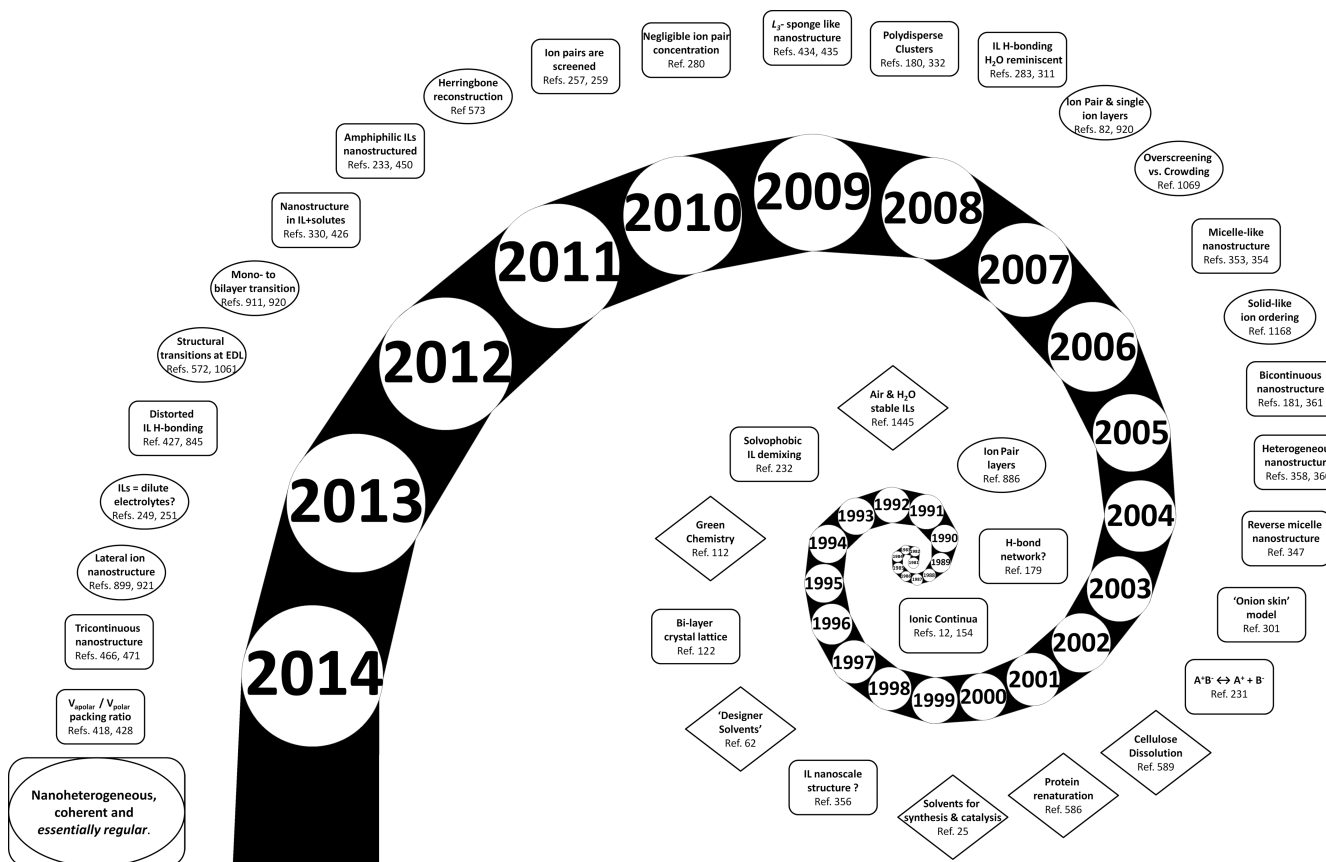


**Figure 1.** A brief history of (nano)structure in ionic liquids, which has been driving interest in ILs even before it was widely appreciated. The area of each year's circle is proportional to the number of "ionic liquid" or "ionic liquids" publications based on an ISI web of science search. The rectangular boxes and ovals highlight advances in scientific understanding of bulk and interfacial IL structure (respectively). Diamonds highlight other important milestones.

Thus, despite intense interest and continuing experimental success, widespread integration of ILs has yet to occur; ILs have certainly left the "Ivory Tower",<sup>61</sup> yet the number of IL-patents and general use in industry<sup>35</sup>/everyday life lags behind their hype as "designer solvents".<sup>62</sup> While there have been some significant achievements, price (per unit volume) remains a hurdle and limits most applications to small-scale niche processes.<sup>63</sup> More importantly, the sheer number of potential ILs<sup>64</sup> (estimated at as high as  $10^{18}$  pure ILs accessible, excluding IL mixtures<sup>65–68</sup>), which provides enormous scope for scientific innovation, means that the use of ILs often results in reduced efficiencies or deviations from expected behavior. It is simply not realistic to switch to an IL solvent and expect an improved outcome. These effects are usually attributed to high liquid viscosity (mass transport effects) or the presence of impurities<sup>67</sup> (e.g., water), in some cases correctly. However, in most instances, the physical arrangement of ions in the bulk or at interfaces plays a key role in determining process efficiency.

The general lack of understanding of IL structure and how it differs from molecular solvents means research is at a crossroads; ILs are not "just another" class of solvents, and even similar ILs can dramatically change reaction outcomes.<sup>69</sup> Likewise, ILs that were once prototypical species are atypical,<sup>70</sup> and dissolved impurities (which alter ion arrangements) are being treated with decreased hostility.<sup>71</sup> There are also many barriers for ILs to take their place in the environmental challenges of the 21st century.<sup>72</sup> For all of these reasons,

increased understanding of IL (nano)structure and the role it plays in IL function is necessary.

We are not alone in recognizing this problem. The bulk structure of ILs is the topic of several technical reviews,<sup>73–81</sup> notably by Castner et al.,<sup>74</sup> Weingärtner,<sup>76</sup> and Greaves and Drummond.<sup>79,80</sup> IL interfacial structure has also been reviewed by our group<sup>82–85</sup> as well as by other researchers.<sup>86–90</sup> However, these papers are narrowly defined as (1) not all IL types are examined, (2) no consideration is given as to how this differs from structure in other (usually molecular) solvents, (3) they focus on only (one) experiment/simulation technique, and (4) the link between bulk and interfacial solvent structure is not examined. Moreover, because of the annual number of publications in ILs, these reviews have rapidly become outdated. Our Review addresses all of these topics and shows that ion self-assembly underpins much of ILs complex chemical and physical behavior. In the same way that understanding of the physical principles of membrane organization<sup>91,92</sup> changed the way we think about biological function and surfactant thermodynamics, knowledge of the way IL ions are arranged will drive future progress and enable the cost/benefit ratio to become favorable.

We start by introducing ionic liquids as both salts and solvents, and then focus on the bulk structure of ILs. The main emphasis is on protic and aprotic ILs, although other novel ion types, the effect of external variables, solvation structures, and IL dynamics are considered. The structure of the solid–IL interface is discussed in section 4 for a variety of substrates. In section 5, the relationship between bulk and interfacial structure is examined,

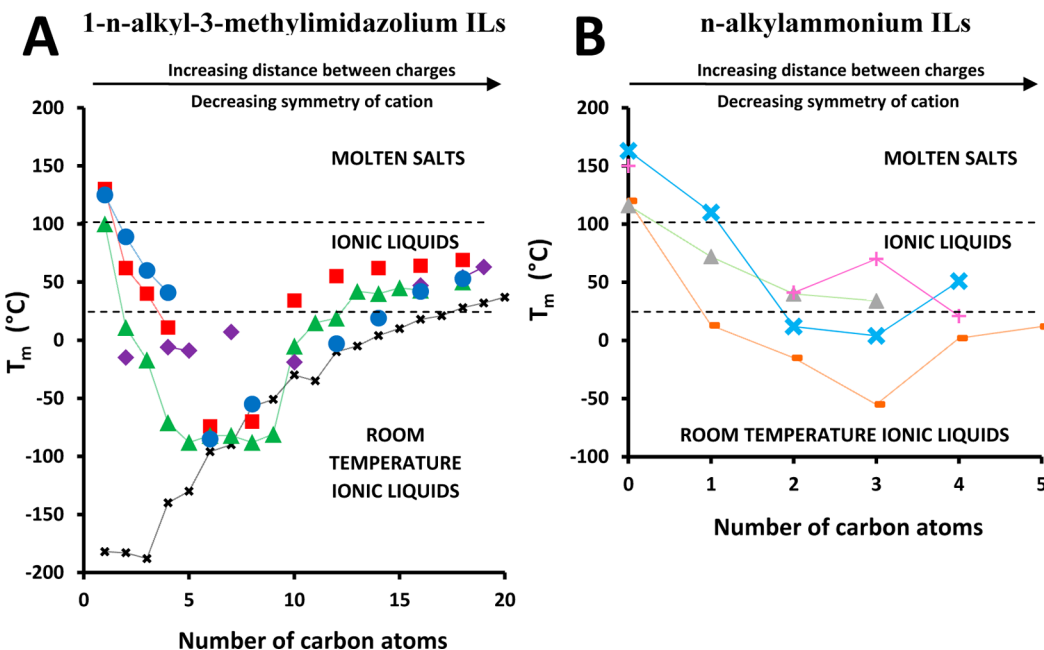


**Figure 2.** Melting point ( $T_m$ ) as a function of cation alkyl chain length ( $n$ ) for salts systems with (A) 1- $n$ -alkyl-3-methylimidazolium and (B)  $n$ -alkylammonium cations.  $n$ -Alkane data ( $n = 1 - 20, x$ ) are also shown for comparison. The trend in  $T_m$  is consistent across all salts: low  $n$  values  $T_m > 100$  °C; intermediate  $n$  values  $50$  °C  $< T_m < 100$  °C then  $T_m <$  °C  $25$ ; and large  $n$  values  $50$  °C  $< T_m < 100$  °C. Dashed lines indicate the boundaries between molten salts ( $T_m > 100$  °C) ILs ( $T_m \leq 100$  °C) and RTILs ( $T_m \leq 25$  °C). In (A), hexafluorophosphate ( $\text{PF}_6^-$ , red ■), tetrafluoroborate ( $\text{BF}_4^-$ , green ▲), bis(perfluoromethyl-sulfonyl)imide ( $\text{NTf}_2^-$ , purple ♦), and chloride ( $\text{Cl}^-$ , blue ●); data sourced from refs 119–122. In (B), nitrate ( $\text{NO}_3^-$ , blue ×), formate ( $\text{HCO}_2^-$ , orange ■), hydrogen sulfate ( $\text{HSO}_4^-$ , yellow-green ▲), and thiocyanate ( $\text{SCN}^-$ , pink +) sourced from unpublished data and ref 28. Note, data points for zero carbon atoms in (B) correspond to the  $\text{NH}_4^+[\text{X}]^-$  salt.

which has implications for ion arrangements at other interfaces (air–liquid<sup>90</sup> or liquid–liquid<sup>93,94</sup>) not directly considered in this Review. Section 6 compares and contrasts the structure formed in ILs to other common solvents. The key findings are discussed in broader context in section 7, and present a critical examination of how to control self-assembly in ILs. In section 8, we conclude this Review and provide outlook to the field of structure and nanostructure in ILs.

In surveying the literature, we have been ambitious in terms of the scope of phenomena treated here and variety of self-assembled structures evident in ILs. Of course, there will be papers that are overlooked and we apologize for these oversights. For the most part, we highlight the key developments and areas of disagreement so as to draw out the strengths and limitations of this model for IL structure. For the most part, we leave aside discussion of related specialist topics including transportation,<sup>95,96</sup> ionicity,<sup>97–99</sup> polarity,<sup>100–102</sup> and polarizability<sup>103,104</sup> as these merit their own review in more detail than we can provide here. Thus, our hope is that this Review helps scientists think intuitively about IL self-assembly, the forces that control it, the length scales on which it occurs, and how this provides an overarching framework for interpretation of IL behavior.

## 2. LIQUID SALTS

One hundred years ago, the German chemist Walden made a startling discovery: a pure salt (ethylammonium nitrate, EAN) that was liquid at ambient temperatures.<sup>105</sup> Until then, it was never suspected that ions could form a liquid at room temperature unless diluted in a molecular solvent; established theories of liquids dealt with uncharged molecules (water, benzene, ethanol) or atomic fluids (mercury, argon, bromine), and Arrhenius had only recently proved the existence of ions in solution.<sup>106</sup> EAN was strikingly similar to water in many respects

as it was clear, colorless, odorless, with solid-like density (1.21 g cm<sup>-3</sup>) and reasonably high viscosity. However, Walden's key finding was its electrical conductivity, a property intrinsic to all liquids that contain mobile ions.<sup>32</sup> The conductivity of EAN was consistent with a composition of (nearly) purely anions and cations. This conclusion was based on Walden's earlier studies of aqueous electrolytes<sup>107</sup> in which a relationship between viscosity, molar conductivity, and density was proposed. For these reasons, Walden is widely credited with conceiving the field of liquid salts, despite reports by earlier workers creating similar materials, with melting points just above room temperature.<sup>108</sup>

The science of liquid salts or “ionic liquids” has progressed leaps and bounds since the days of Walden. In particular, the last three decades have been marked by exponential growth in publications (Figure 1), with discoveries spanning all of chemistry<sup>27,109</sup> such that the field has now substantially outgrown (but not left) its roots in electrochemistry<sup>110,111</sup> and organic synthesis.<sup>25</sup> Nowadays, IL research is truly an interdisciplinary area, with chemists, physicists, biologists, engineers, and simulators using them to tackle important scientific problems. This has been spurred by green chemistry movement,<sup>112</sup> and the relative ease with which IL solvents can be integrated into existing systems.

Key to their emergence and impact is their pronounced solvent (nano)structure, which has been driving interest in ILs even before it was widely appreciated. Consider the solubilities of materials in ILs. As early as the 1950s, ILs were shown to dissolve both polar and apolar compounds. This is incompatible with standard models of liquids of uniform polarity; solvents can be either polar or nonpolar and thus prefer to dissolve similar materials according to the dictum “like dissolves like”.

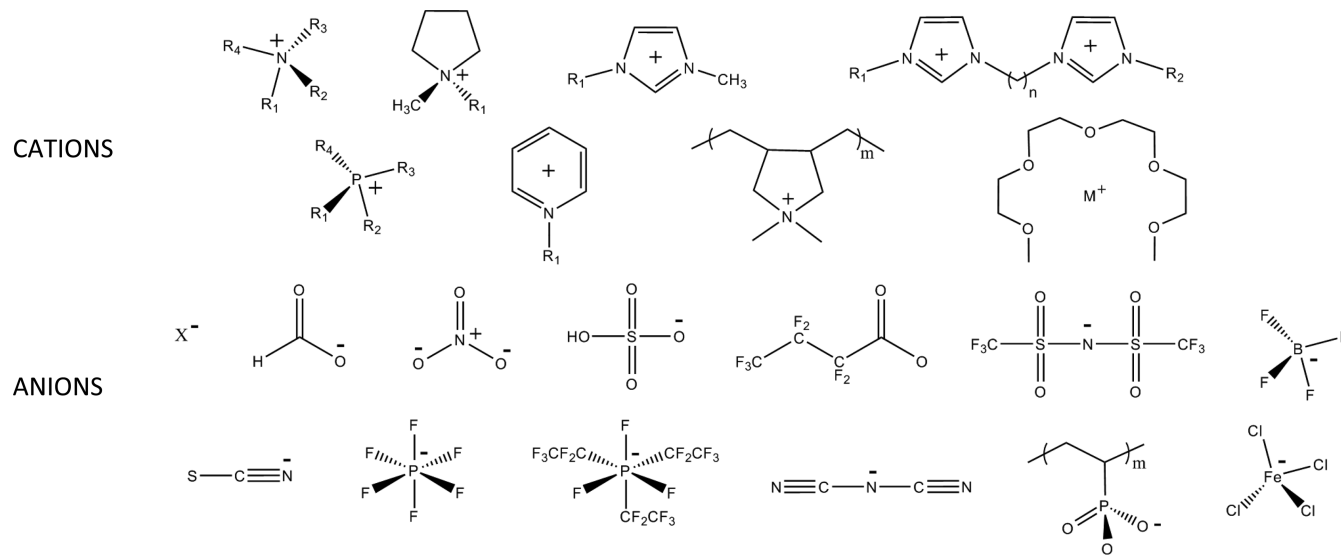


**Figure 3.** Some chemical structures of representative cations and anions used in protic, aprotic, dicationic, polymeric, magnetic, and solvate ionic liquids. From left to right, the cations (top row) include: ammonium, pyrrolidinium, 1-methyl-3-alkylimidazolium, 1,3-bis[3-methylimidazolium-1-yl]alkane; (second row) phosphonium, pyridinium, poly(diallyldimethylammonium), metal ( $M^+$ ) tetraglyme. The anions include (third row) halides, formate, nitrate, hydrogen sulfate, heptafluorobutyrate, bis(perfluoromethylsulfonyl)imide, tetrafluoroborate, (bottom row) thiocyanate, hexafluorophosphate, tris(pentafluoroethyl)trifluorophosphate, dicyanamide, poly(phosphonic acid), and tetrachloroferrate.

## 2.1. What Is an Ionic Liquid?

Ionic liquids (ILs) are a subset of molten salts with melting points ( $T_m$ ) below 373 K. In Walden's original paper on EAN, he described a class materials as "water-free salts... which melt at relatively low temperatures, about up to 100 °C."<sup>113</sup> This definition was later reaffirmed and codified in a NATO workshop in Crete in 2000.<sup>114</sup> Definitions are important and relevant as the field is still relatively young; the term "ionic liquids" was originally coined in reference to silicate slags with  $T_m > 1000$  K,<sup>29</sup> and similar materials have been described in the literature with names including "fused salts", "pure liquid electrolyte", "liquid salt", "ionophore", "organic ionic melts", or "molten salt at room temperature".<sup>29,110,115</sup> Although the term "ionic liquid" has widespread acceptance, the definition has recently attracted criticism as it is based on a somewhat arbitrary physical property (melting point) for a temperature relevant to a molecular solvent (water).<sup>116</sup> Some authors also distinguish between ILs ( $T_m < 373$  K) and room-temperature ionic liquids (RTILs) ( $T_m < 298$  K). In this Review, the acronym "IL" is preferred and indicates an ionic compound with  $T_m < 373$  K, while "molten salt" is used for systems with  $T_m > 373$  K.

ILs exist as liquids at ambient temperatures because of their chemical structure. The anion and cation are chosen precisely to destabilize the solid-phase crystal. Thus, while there are no set rules to making an IL, in general this can be achieved within a relatively large window of ion structures by balancing ion–ion interactions and symmetry as shown in Figure 2. For instance, the cation alkyl chain must be long enough to reduce Coulombic forces and disrupt lattice packing, but not be too long ( $\sim n < 12$ ) as this will increase salt mp despite the enhanced asymmetry; cohesive interactions increase with length of nonpolar groups as per linear alkanes. However, Davis et al. recently showed a way around this and produced low melting salts from very long chain ( $>C_{16}$ ) cations by introducing a *cis* double bond "kink" on the alkyl group.<sup>117</sup> This is similar to homeoviscous adaptation in cell membranes<sup>118</sup> and highlights the complex array of packing and chemical factors that controls IL melting point.

## 2.2. Classification by Structure

ILs, like solvents generally, are usually classified on the basis of chemical structure. However, ILs possess structural features reminiscent of molten salts, ionic surfactants, ionic crystals,<sup>123</sup> and molecular liquids, and the number of potential neat ILs is enormous.<sup>64</sup> This makes classifying ILs challenging, as multiple labels are often appropriate for a given IL, depending whether the anion, cation, or a functional group is considered most important. Protic<sup>28</sup> and aprotic<sup>124</sup> ILs are the two most common IL types, based on the well-established division between proton-donating (protic) and nonproton-donating (aprotic) molecular solvents.<sup>125</sup> However, this definition is not so rigid as it would seem; Davis et al. characterized dicationic ILs with one protic and one aprotic charge center, enabling both functionalities to be expressed.<sup>126</sup> Figure 3 shows a sample of representative popular anion and cation chemical structures.

**2.2.1. Protic ILs.** Protic ILs (PILs) are formed by proton transfer from an equimolar combination of a Brønsted acid and a Brønsted base.<sup>28</sup> This means that PILs are generally simpler and cheaper to prepare than other IL classes as there are no byproducts. In nature, proton transfer is ubiquitous, and thus it was a pleasant surprise that a naturally occurring PIL was recently characterized in the literature.<sup>127</sup> While proton transfer is a chemical equilibrium (leading in some cases to a non-negligible population of neutral species), PILs can be treated as pure mixtures of ions. This is because most PILs show "good" ionic behavior as compared to ideal aqueous KCl solutions from Walden plots of molar conductivity versus fluidity.<sup>128</sup>

H-bond donor and acceptor sites are created on the ions due to proton transfer. This means that PILs can H-bond (cf., sections 3.2.2 and 7.1.4). The mechanism of proton transfer in PILs is still unclear, although it may be similar to Grotthuss-like behavior in molecular protic solvents with labile protons "hopping" between ions along H-bonds.<sup>129,130</sup> Proton transfer in PILs has been implicated in many properties (vapor pressure,<sup>131</sup> thermal stability,<sup>58</sup> catalytic activity,<sup>28</sup> conductivity,<sup>131</sup> protein stabilization<sup>132</sup>) or for PILs explosives.<sup>133</sup> Thus, understanding their H-

**Table 1.** Properties of EAN (a PIL) and  $[C_4mim]PF_6$  (an AIL) As Compared to Water, Molten NaCl (at 850 °C), and Hg(I)<sup>a</sup>

property	solvent type					
	atomic	molecular		molten salt	ionic liquid	
	mercury	water	benzene	molten sodium chloride	ethylammonium nitrate (EAN)	1-butyl-3-methylimidazolium hexafluorophosphate ( $[C_4mim]PF_6$ )
chemical structure	Hg	$H_2O$	$C_6H_6$	NaCl	$[CH_3CH_2NH_3^+] [NO_3^-]$	$[C_4mim^+] [PF_6^-]$
appearance	silver, luster	clear, colorless	clear, colorless	clear, colorless	clear, colorless	clear, colorless
mp (°C)	-38.8	0	5.5	801	12 <sup>b</sup>	10 <sup>f</sup>
bp (°C)	356.7	100	80.1	1413	255 <sup>b</sup>	409 <sup>j</sup>
$\rho$ (g cm <sup>-3</sup> )	13.534	0.9970	0.8765	1.539	1.21 <sup>c</sup>	1.366 <sup>k</sup>
$\eta$ (Pa s)	$1.526 \times 10^{-3}$	$8.95 \times 10^{-4}$	$6.076 \times 10^{-4}$	$12.5 \times 10^{-4}$	$35.9 \times 10^{-4c}$	$36.9 \times 10^{-4l}$
P (Pa)	2.67	3173	12 700	128	0.49 <sup>d</sup>	$<10^{-2m}$
$n_D$	1.000933	1.332	1.5011	1.436 <sup>p</sup>	1.4535 <sup>c</sup>	1.411 <sup>i</sup>
$D \times 10^{-6}$ (cm <sup>2</sup> s <sup>-1</sup> )	85 <sup>q</sup>	22.99 <sup>r</sup>	22.07 <sup>s</sup>	Na <sup>+</sup> 80.1 Cl <sup>-</sup> 63.5	$[CH_3CH_2NH_3^+] 0.158, ^e$ $[NO_3^-] 0.151^e$	$[C_4mim]^+ 1.5, ^j [PF_6]^- 1.8^j$
$\gamma_{LV}$ (mN m <sup>-1</sup> )	486.5	72.8	28.88	111.7 <sup>t</sup>	47.3 <sup>b</sup>	43.8 <sup>n</sup>
$\kappa$ (S cm <sup>-1</sup> )	10 <sup>s</sup>	$5.5 \times 10^{-4}$	$4.4 \times 10^{-17u}$	0.256	$2.69 \times 10^{-2b}$	$1.4 \times 10^{-3i}$
$\epsilon$	1.00074	78.4	2.284	1.6 <sup>t</sup>	$26.3 \pm 0.5^f$	$14.0 \pm 0.7^f$
C (J mol <sup>-1</sup> K <sup>-1</sup> )	27.98	75.3	134.8	66.9	206 <sup>g</sup>	406 <sup>k</sup>
$\lambda$ (W m <sup>-1</sup> K <sup>-1</sup> )	8.3	0.6065 <sup>v</sup>	0.1405 <sup>w</sup>	0.497 <sup>x</sup>	0.245 <sup>h</sup>	0.145 <sup>o</sup>

<sup>a</sup>Melting point (mp), boiling point (bp), density ( $\rho$ ), viscosity ( $\eta$ ), vapor pressure (P), refractive index ( $n_D$  at 589 nm), diffusion coefficient (D), liquid–vapor surface tension ( $\gamma_{LV}$ ), ionic conductivity ( $\kappa$ ), dielectric constant ( $\epsilon$ ), molar heat capacity (C). Data for molten NaCl and mercury are obtained from ref 154 unless otherwise specified. Sources for water and benzene data are from ref 155 (298 K, 1 atm pressure) unless otherwise specified. IL data are from references as follows: <sup>b</sup>From ref 28. <sup>c</sup>From ref 156. <sup>d</sup>From ref 157 (at 106 °C). <sup>e</sup>From ref 158. <sup>f</sup>From ref 159. <sup>g</sup>From ref 160. <sup>h</sup>From ref 161. <sup>i</sup>From ref 162. <sup>j</sup>From ref 163. <sup>k</sup>From ref 164. <sup>l</sup>From ref 165. <sup>m</sup>From ref 166. <sup>n</sup>From ref 167. <sup>o</sup>From ref 168. <sup>p</sup>From ref 169. <sup>q</sup>From ref 170. <sup>r</sup>From ref 171. <sup>s</sup>From ref 172. <sup>t</sup>From ref 173. <sup>u</sup>From ref 174. <sup>v</sup>From ref 175. <sup>w</sup>From ref 176. <sup>x</sup>From ref 177.

bonding structures may provide insight into PIL solvent behavior.

**2.2.2. Aprotic ILs.** Aprotic ILs (AILs) do not share a common structural feature as do PILs. AILs can span a range of anion and cation chemical structures, some of which H-bond and some of which do not. Most early studies of AILs were confined to halometallate ions,<sup>134</sup> but this has now expanded to include an enormous array of chemical structures. AIL preparation is generally more expensive and complicated than PILs, often involving multistep reactions.<sup>53,54</sup> This is because ions are formed by the covalent bond formation between two functional groups. In most instances, this leads to a solvent that is more thermally and electrochemically stable than the corresponding PIL; Walden plots frequently show “good” ionic behavior for AILs.

**2.2.3. Other IL Subclasses.** Several other IL subclasses are reported in the literature, based upon distinct structural features, for example, a chiral center (chiral ILs),<sup>135</sup> a paramagnetic atom/group (magnetic ILs),<sup>136</sup> a divalent ion (divalent ILs), a polymeric or polymerizable ion (polymeric ILs<sup>137</sup>), a fluorocarbon moiety (fluorous ILs<sup>138</sup>), or a coordinated ion (solvate ILs<sup>139</sup>). There are also reports of amino acid ILs<sup>140</sup> and aryl alkyl ILs<sup>141</sup> named from specific functional groups introduced on the ions. Notably, polymeric, fluorous, and magnetic ILs have an analogous solvent type among polymer melts,<sup>142,143</sup> fluorous solvents,<sup>144</sup> or ferrofluids<sup>145,146</sup> (respectively), enabling the cross-fertilization of chemistries and guiding future research into these ILs types.

### 2.3. IL Solvent Properties

It is not possible to identify a general set of IL properties due to the structural diversity of the ions. In principle, the only solvent property common to ILs is ionic conductivity, because they contain mobile ions.<sup>32</sup> Broadly, ILs have solvent properties that are quite different from atomic, diatomic, or aprotic molecular liquids, but similar to polar protic liquids, molten salts, or

bicontinuous microemulsions (cf., Table 1). This is related to the nature of their ions and solvent structure.

There is growing evidence to suggest that the ability to support amphiphile self-assembly is widespread among ILs.<sup>147–153</sup> In a recent review by Greaves and Drummond,<sup>79</sup> it was concluded that ILs are now the largest known class of self-assembly media for amphiphiles; prior to 2006, only 16 solvents (14 molecular liquids and two ILs) were known to do this. Currently, 37 PILs and 11 AILs have been shown to promote amphiphile self-assembly in some fashion, limited only by surfactant solubility. Thus, it is possible that this is another common IL trait, due to the unique solvation environment in the bulk phase.

## 3. THE BULK STRUCTURE OF IONIC LIQUIDS

Historically, ILs were thought to fall within the traditional picture of molecular liquids as homogeneous, coherent, and essentially irregular<sup>12</sup> systems. Most researchers regarded the IL bulk structure as similar to a highly concentrated salt solution or a molten salt. Recently, however, the models used to describe ILs have increasingly suggested they are structured solvents, from supramolecular (ion pairs, ion clusters) to mesoscopic (H-bond networks, micelle-like, and bicontinuous morphologies) length scales (cf., Figure 4). Understanding this structure is key to unraveling their complex physical, chemical, and dynamic behavior.

### 3.1. Crystal Lattice Structure

What can we learn from the crystal lattice structure of ILs? In the same way that the structure of molecular liquids can be inferred from its parent solid crystal, IL crystal structures are expected to provide clues to ion arrangements in the liquid phase. In fact, IL bulk structure was initially inferred from the structure of crystal analogues; the ion arrangements were assumed to be isotropic, with some local resemblance to the solid or (in some instances) liquid crystal state. Thus, melting was thought to induce a behavior similar to that of molecular liquids, where a high

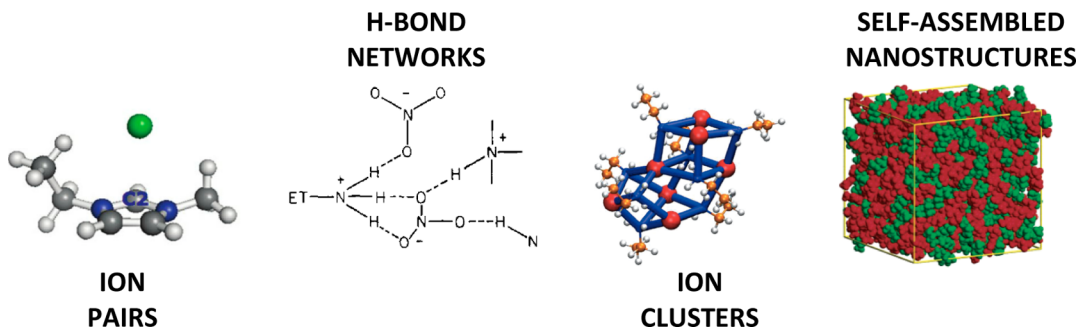


**Figure 4.** Different models for the bulk structure of ionic liquids. See text for details. Reproduced with permission from refs 178 (Copyright 2011 American Chemical Society), 179 (Copyright 1981 American Chemical Society), 180 (Copyright 2009 American Chemical Society), and 181 (Copyright 2006 American Chemical Society).

structured crystal phase decays into a disorganized liquid. Conclusions of early influential reviews by Welton,<sup>25</sup> “[ILs] are unlikely to have great differences in their structures and interionic interactions (compared to molten salts)”, or Dupont, “1,3-dialkylimidazolium [ILs] possess analogous structural patterns in both the solid and liquid phase... although significant randomness in organization is necessary to describe the structure of a liquid”,<sup>73</sup> are typical of this prevailing opinion. This has been extended recently with *quasi-*<sup>182</sup> or *pseudo-*<sup>183,184</sup> lattice models, which view the bulk ion organization as a collapsed solid crystal. More broadly, knowledge of IL crystal structure provides direct insight into the way that the IL melts<sup>185,186</sup> and facilitate “anticrystal engineering”<sup>187–189</sup> to extend the range of salts that can be used as IL solvents.

Evidence of polar/nonpolar segregation, analogous to amphiphilic self-assembly structures in a liquid and widespread in the crystal structure of conventional amphiphiles,<sup>190</sup> is seen in every report of IL crystal structure. 1-Alkyl-3-methylimidazolium halide ILs [ $C_n\text{mim}$ ]X (where  $n = 12–18$ ) have been shown to arrange into well-defined, bilayer crystal lattices. The overall structure of these IL liquid crystal phases is best described as sheets of imidazolium rings and anions, separated by a domain of interdigitated alkyl chains (layer–layer separations of 2.4–3.3 nm), cf., Figure 5. A H-bond network forms within this lattice.<sup>191</sup>

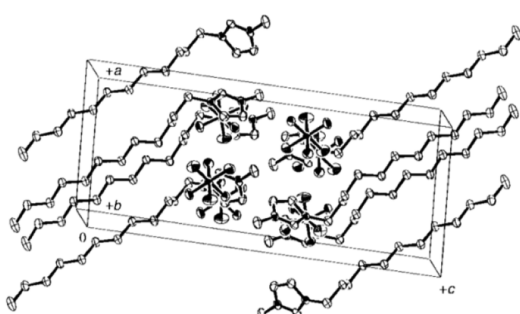


**Figure 5.** Unit cell of  $[C_{12}\text{mim}]PF_6$  (mp 55 °C). Reproduced with permission from ref 122. Copyright 1998 The Royal Society of Chemistry.

Similar results were obtained for alkylpyridinium<sup>192,193</sup> or short chain imidazolium salts.<sup>194–196</sup> The interlayer distance was inversely proportional to the anion’s ability to form a 3-D H-bond network, with smallest cation–cation spacing for  $Cl^-$  anions and largest for  $NTf_2^-$  anions.<sup>120</sup> NMR experiments showed the nature of the H-bond network in the lattice is highly anion dependent for the same imidazolium ILs.<sup>197,198</sup>

Cation alkyl chains can adopt different conformations in the bilayer, leading to crystal polymorphs. For instance, X-ray diffraction has shown that multiple polymorphs can be obtained from  $C_4\text{mim}^+$  cations with  $Cl^-$ ,  $Br^-$ ,  $I^-$ ,  $[BF_4]^-$ , or  $[PF_6]^-$  anions.<sup>199</sup> Monoclinic (*trans-trans*) or orthorhombic (*gauche-trans*) crystals of these  $C_4\text{mim}^+$  ILs are possible, depending on butyl group conformations. Complementary Raman spectroscopy data revealed an equilibrium of both structures was present, and that interconversion between them may hinder crystallization and thus lower the mp below 100 °C.<sup>200,201</sup>

Anions can also have different rotational conformations in the bulk crystal. X-ray diffraction was used to show that the popular, noncoordinating  $NTf_2^-$  anion in  $C_1\text{mim}[NTf_2]$  adopts the *cis* conformer in the crystal phase,<sup>202</sup> supported by bifurcated cation–anion C–H···O<sup>203</sup> H-bonds. Interestingly, later neutron diffraction measurements by Hardacre et al. revealed the *trans* geometry is favored in the bulk liquid,<sup>204</sup> suggesting the *cis* form is more a result of ion close packing in the lattice. (Other ILs show opposite *cis-trans* conformer populations for the solid and liquid phases.<sup>205</sup>)

Only one paper has examined the crystal lattice structure of a genuine PIL below its melting point.<sup>206</sup> Recently, the crystal structure of ethylammonium nitrate (EAN, mp 12 °C) was reported by Henderson et al.<sup>206</sup> and compared to ethylammonium chloride (mp 110 °C)<sup>207</sup> and propylammonium chloride.<sup>208</sup> EAN’s unit cell, shown in Figure 6, is composed of two lamellar-like cation layers with alkyl chains segregated together and ammonium groups pointing “up” or “down”. Half anions are situated between ammonium groups to form an ionic domain. The remaining nitrate ions are interspersed between cation alkyl groups. On the basis of this crystal structure, a lamellar-like liquid morphology may be expected in pure EAN and other primary alkylammonium PILs.

Pure 1-alkyl-3-methylimidazolium ( $>C_{14}$ )<sup>209–211</sup> or alkylammonium ( $C_6–C_{18}$ )<sup>212–214</sup> molten salts with very long cation alkyl chains and some PILs with short alkyl chains<sup>215</sup> form smectic thermotropic liquid crystal phases between their solid and liquid states. The nature of this self-assembled structure is crucial to function.<sup>216</sup> Such lamellar-like smectic phases also exhibit segregation of charged polar and apolar domains, regardless of the nature of the anion (halides,<sup>213,217–219</sup> alkanesulfonates,<sup>220</sup> pyroglutamates,<sup>221</sup> naphthalenesulfonates,<sup>222</sup> benzenesulfonates<sup>223</sup>). Interestingly, there is also evidence of alkyl chain lateral organization in the apolar domains, which likely contributes to their high melting points, above 100 °C.<sup>224</sup> Surprisingly, H-bonding was shown to have a strong effect on the temperature stability of the phases,<sup>225</sup> yet the structure

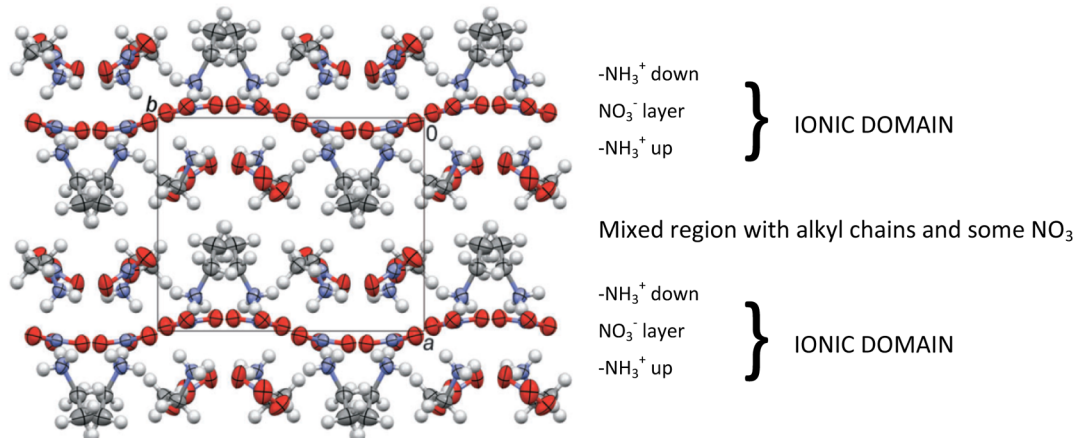


**Figure 6.** Crystal structure of EAN at 260 K. C gray, H white, N blue, and O red. Reproduced with permission from ref 206. Copyright 2012 PCCP Owner Societies.

was essentially invariant. Segregation of nonpolar from polar, H-bonding moieties in both crystal and liquid crystal structures thus suggests the potential for similar patterns of self-assembly in the bulk liquid phase of ILs with smaller nonpolar groups ( $C_2$ – $C_8$ ).

### 3.2. Supramolecular Solvent Structure

**3.2.1. Ion Pairs or Free Ions.** Ion pairs are the simplest repeat unit in ILs. Thus, it is tempting to depict local arrangements in terms of the likely ion pair structure plus a concentration of “free” ions. Many ILs are also known to evaporate as ion pairs,<sup>226–228</sup> which suggest that they may be present in the bulk phase. Historically, the concept was important for the study of aqueous electrolyte solutions as well as the criticality or phase transitions of Coulomb fluids<sup>229</sup> and was first proposed by Bjerrum<sup>230</sup> for a pair of oppositely charged ions dispersed in water that behave as one unit. Because ILs represent an infinitely concentrated or solventless ionic solution, tight (or intimate/contact) ions pairs would be expected in this model, and have been studied in a variety of ways for ILs.

The observation of critical behavior in mixtures of EAN and octanol<sup>231</sup> was used to suggest ion pairs in EAN. Weingärtner et al. derived ion pair association constants from conductivity measurements that were 1–2 orders of magnitude larger than predicted by Bjerrum<sup>230</sup> for ion pairs in aqueous solution. This suggested that liquid EAN exists in a chemical equilibrium between ion pairs and “free” ions:  $EA^+[NO_3^-] \rightleftharpoons EA^+ + NO_3^-$ . The key conclusion, however, was that ion pairs are much more favored in the pure IL bulk than in corresponding solutions of aqueous electrolytes because H-bonds were thought to stabilize the ion pair by shielding the long-range Coulombic forces in solution. Interestingly, static and dynamic light scattering (DLS) experiments in a follow-up paper showed an EAN–octanol phase transition, consistent with Ising-like behavior.<sup>232</sup> Unlike aqueous electrolyte solutions, a simple mean-field model could not be used to describe the transition. Thus, the authors postulated the contribution of short-range solvophobic interactions that induced “solvophobic demixing” of EAN and octanol. This is important, as it hints possible cation alkyl chain aggregation in pure EAN, which was not conclusively revealed until 2011.<sup>233</sup>

Early dielectric spectroscopy measurements revealed EAN could be described as a system of ion pairs plus free ions.<sup>234</sup> The measured relaxation profile was fitted by assuming ~8% of all ions exist as contact ion pairs (and 92% as free ions). The lifetimes of these ion pairs was found to be in the order of  $10^{-10}$  s at 298 K. This is close to values for anion–cation coupling in

molten alkali metal nitrates  $NaNO_3$  and  $KNO_3$ , but much larger than those in dilute aqueous electrolytes.<sup>235</sup> The enhanced ion pairing in EAN was attributed to anion–cation H-bonds. Assuming no neutral species, the authors estimated the ion pair  $\leftrightarrow$  free ions equilibrium constant to be 142.9.

Sophisticated quantum mechanics or density functional theory (DFT) calculations have been used extensively to study ion pair structures in AILs, optimizing both electronic and molecular structure.<sup>178,236–243</sup> Recently, one of these papers compared ion pair structure of AILs with PILs. Some commonality between IL types was noted, as electrostatics is the most important interaction in the ion pair, governing both relative arrangements and interaction energy.<sup>244</sup>

Ab initio molecular orbital calculations by Izgorodina have shown that  $Cl^-$  anions are stabilized above or below the plane of the  $[C_4mim]^+$  cation ring by Coulombic interactions (cf., Figure 7).<sup>178</sup> Certain positions in the plane of the ring, particularly in

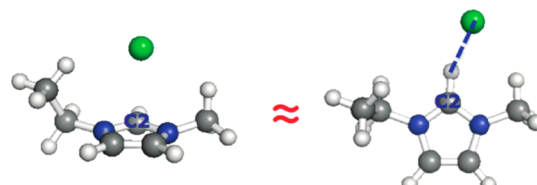


**Figure 7.** Coulombic (left) and H-bonded (right) anion–cation interaction from ab initio molecular orbital calculations. Coulombic interactions favor the anion to be located above or below the imidazolium ring, whereas H-bonded anions interact with the H2 hydrogen. Reproduced with permission from ref 178. Copyright 2011 American Chemical Society.

front of the C2 carbon, are also favored due to anion–cation H-bonds. Interestingly, these H-bonds are relatively long ( $>2.5$  Å) and nonlinear ( $<165^\circ$ ) relative to the ideal H-bond arrangement. The calculations suggest both conformations are present because reduced electrostatic attractions in the ion pair enable other H-bonding-driven structures to form. IR spectroscopy data are consistent with this as a proportion of H-bonds conformers explains the lower than expected vibrational red shift in the anion–cation interaction.<sup>178</sup>

Multinuclear NMR studies with  $C_2mim[X]$  ILs (where X =  $Cl^-$ ,  $Br^-$ , and  $I^-$ ) have suggested contact ion pairs form in the pure AILs, in a quasi-molecular state stabilized by strong H-

bonds.<sup>245</sup> The influence of ion pair effects was also ascribed to chiral transfer effects in the bulk.<sup>246</sup> Likewise, a model for the bulk structure of C<sub>4</sub>mim[1] based on ion pair formation was suggested from absorption spectroscopy.<sup>247</sup> Indirect evidence for ion pairs was also inferred from transport properties of dialkyl-imidazolium ILs, related to the degree of charge localization on the anion.<sup>248</sup> Another important study by Gebbie et al.<sup>249</sup> provides a similar view of the IL bulk from DLVO fits of surface forces apparatus (SFA) data. This paper concluded that C<sub>4</sub>mim[NTf<sub>2</sub>] is a coordinated cation+anion network with a low effective concentration of free ions, akin to descriptions of water as a solution of overwhelmingly neutral H<sub>2</sub>O molecules plus some H<sub>3</sub>O<sup>+</sup> and OH<sup>-</sup> ions. In section 4.1, we address this paper (and the controversy surrounding it<sup>250,251</sup>) in more detail.

However, the weight of scientific evidence is not consistent with a simple ion pair model for IL bulk structure. More recent dielectric spectroscopy data for a range of AILs (imidazolium,<sup>252</sup> pyrrolidinium,<sup>253,254</sup> pyridinium,<sup>253</sup> tetraalkylammonium,<sup>253</sup> and triethylsulfonium<sup>253</sup>) and PILs (EAN,<sup>255</sup> PAN<sup>255</sup>) have revealed no signatures of ion pair formation. This technique is highly sensitive to picosecond-to-nanosecond liquid dynamics, and so should be able to probe orientational relaxations of ion pairs or similar aggregates if they were present. Also, ion pairs were not detected in corresponding NMR measurements that investigate structure on micro to-milliseconds.<sup>256</sup> Thus, if they exist, the lifetimes of any potential ion pairs must be less than a few picoseconds.<sup>76</sup>

These conclusions are in accordance with recent MD simulations<sup>257–259</sup> and theoretical models<sup>260</sup> that explored possible ion pair formation in imidazolium ILs. For C<sub>4</sub>mim-[PF<sub>6</sub>]<sup>257</sup> the cation–anion interaction was best described using the concept of an ion association rather than ion pairs as each ion is not coupled to a single counterion in the ionic atmosphere. Likewise, in Lee et al.’s model, free ions outnumber ion pairs by 2:1, and pairs are stable only for short times (60–140 ps).<sup>260</sup> Further simulations by Lynden-Bell<sup>259</sup> showed that the formation of anion+cation, anion+anion, or cation+cation ion pairs was not important for describing bulk IL structure. These units are only weakly stabilized in pure ILs due to the small physical separation of ions in the bulk. This suggests that the origin of ion pair destabilization is to do with the overscreening of electrostatic charge in the first solvation shell. As multiple co- and counterions can inhabit this region, mutual attraction in a given ion pair is weak, so pairs readily dissociate into individual ions when they form.

Likewise, for most ILs, modeling the bulk as a continuum of anion/cation couples migrating together cannot be reconciled with their characteristically low vapor pressures. Properties such as vapor pressure are controlled by ionicity, as represented in a Walden plot of molar conductivity versus fluidity. An isolated ion pair unit is neutral and thus will not contribute to measured liquid conductivity. Therefore, ILs with a high proportion of ion pairs or larger neutral aggregate structures (section 3.3) should be “poor” ILs because the conductivity will be less than expected from their viscosity. However, most ILs are “good” ILs and have low vapor pressures.<sup>97</sup> The classical explanation of this is that ions must be distributed in a relatively uniform manner in the bulk with each ion surrounded by a shell of opposite charge.<sup>124</sup> Interesting counterexamples to this were recently reported by MacFarlane et al.<sup>261</sup> and Umebayashi et al.<sup>262</sup> In the first report, a novel class of phosphonium-based AILs with chloride or sulfonyl amide anions was shown to behave as neither “good” nor “poor” ILs.<sup>261</sup> Their position on the Walden plot is best described as

liquid ion-pair compounds. Conversely, Umebayashi et al. described a pseudo-PIL from equimolar combination of N-methylimidazole and acetic acid. Raman spectroscopy revealed the concentration of ions is less than 1:100, and yet the system was highly proton conductive,<sup>262</sup> displaying “superionic” behavior. Both of these papers represent compositions and thus structure that is intermediate between molecular liquids and ILs.

In contrast with pure ILs, many reports have suggested that ILs form ion pair structures when they are dissolved in molecular solvents. Many molecular solvents other than water<sup>263–271</sup> appear to support IL ion pair formation. NMR measurements on C<sub>2</sub>mim[X] ILs mixed with propionitrile indicate long-lived anion–cation units.<sup>245</sup> For the same ILs in nonpolar solvents like trichloro- and dichloromethane,  $\pi-\pi$  stacking between C<sub>2</sub>mim<sup>+</sup> cations becomes increasingly important, and anion–cation ion pair association is lost at the expense of cation–cation pairs. Ion pairs of N<sub>4,4,4,4</sub>[I] were invoked to explain total dielectric constant with salt concentration in dichloromethane.<sup>272</sup> Contact and solvent separated anion–cation ion pairs were observed in <sup>1</sup>H-NOESY NMR studies of [C<sub>4</sub>mim<sup>+</sup>]-ILs dissolved in DMSO and CDCl<sub>3</sub>, respectively.<sup>273,274</sup> Similar results have been obtained for wet C<sub>4</sub>mim[BF<sub>4</sub>] and [C<sub>4</sub>mim]BF<sub>4</sub>+DMSO mixtures.<sup>275</sup> The electrochemical stability of several redox probes was thought to depend on ion pairing effects in imidazolium ILs based on cyclic voltammetry (CV) measurements.<sup>276</sup> For example, the unusual two electron wave in the CV spectra of 1,4- and 1,2-dinitrobenzenes was suggested to be related to ion pairing between the [C<sub>4</sub>mim]<sup>+</sup> and dinitrobenzene dianion.<sup>277</sup> MD simulations of C<sub>4</sub>mim[PF<sub>6</sub>] with naphthalene<sup>278</sup> and other aromatics<sup>279</sup> have also showed anion+cation ion pairs and cation +aromatic units across a range of solute concentrations.

Elegant chemical confirmation of these results has been reported by Welton and co-workers,<sup>280</sup> by comparing S<sub>N</sub>2 reaction kinetics in ILs and in IL+molecular solvent mixtures. The S<sub>N</sub>2 reaction incorporated an ionic electrophile, and thus the reaction mechanism relies upon ion pair formation in the bulk. Ion pairs were deduced to be present in IL+molecular solvent mixtures, leading to fast, nonlinear partial-order kinetics. In contrast, slow, pseudo first-order kinetics was observed from the same reaction in the neat ILs. This suggests the ion pair concentration is insignificant as compared to the population of free ions. The absence of a charge-transfer peak in the UV absorption spectrum of ionic probes dissolved in the pure ILs is consistent with this, and points to time-averaged uniform ion association.

Hence, while the concept of ion pairs is useful for electrolyte solutions, it is not easily transferrable to neat ILs; transient as ion pairs may exist in pure ILs with lifetimes less than a few picoseconds, however the overall bulk structure appears to be more complicated than a continuum of anion+cation couples in solution.

**3.2.2. H-Bond Networks.** Evans et al. first suggested a well-defined H-bond structure in an IL. They examined gas solubilities in EAN as a function of temperature.<sup>179</sup> The phase transfer of rare gases and hydrocarbons from cyclohexane to EAN was accompanied by negative enthalpy and entropy values, similar to water. This led them to postulate that proton donor and acceptor sites on the ions may form a 3-D H-bonded network resembling water (cf., Figure 8). This hypothesis explained Evans and co-workers’ previous detection of cationic and nonionic surfactant micelles in EAN<sup>281,282</sup> as solvent H-

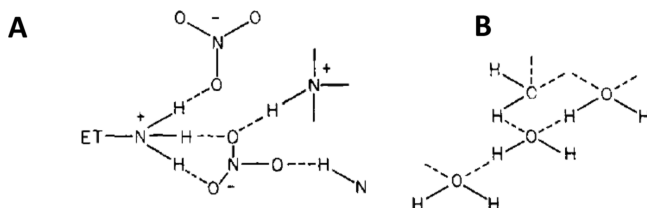


**Figure 8.** Evans et al.’s model of (A) EAN and (B) water’s H-bond network structure. H-bonds are shown as dashed lines. Reproduced with permission from ref 179. Copyright 1981 American Chemical Society.

bonding was thought to be essential for inducing the solvophobic interactions<sup>20</sup> that drive amphiphilic self-assembly.

While this hypothesis was never seriously disputed, H-bonding in PILs such as EAN was only conclusively demonstrated by Ludwig and co-workers in 2009.<sup>283</sup> They measured far-IR spectra of EAN, PAN, and DMAN (dimethylammonium nitrate) in the region ( $30\text{--}600\text{ cm}^{-1}$ ) that excites H-bond bending, stretching, and vibrational modes in molecular liquids. Complementary DFT calculations enabled the spectra to be deconvoluted and specific H-bond interactions assigned. In every PIL, the frequency difference between the asymmetric and symmetric stretches was approximately  $65\text{ cm}^{-1}$ , suggesting comparable H-bonding strengths. The measured peak positions and frequency differences were consistent with the far-IR spectra of pure water. This led the authors to conclude the PIL H-bond networks, while unlikely to be tetrahedral, are structurally reminiscent of water.

Subsequent measurements by the same group<sup>284,285</sup> have quantified the strength of H-bond interactions in PILs using DFT calculations.<sup>286</sup> The energy per ion pair for trimethylammonium nitrate (one H-bond donor) was found to be  $\sim 49\text{ kJ mol}^{-1}$  higher than that for tetramethylammonium nitrate (no H-bond donors), attributed to the formation of a single anion–cation H-bond. Notably, this value is more than double that of H-bonds in water ( $\sim 22\text{ kJ mol}^{-1}$ ) and suggests they possess “moderate” to “strong” H-bonds using established scales.<sup>287</sup>

H-bonding in imidazolium ILs was quite controversial in early structural studies. This is because their contribution to ion arrangements was difficult to decouple from Coulombic interactions. Also, as it does in other systems, the criteria used to define a H-bond affects interpretation,<sup>288</sup> and some ILs may only form a C–H...O<sup>203</sup> type H-bond, which were once famously contentious in chemistry literature.<sup>289</sup> Nowadays, it is widely accepted that AILs can H-bond usually as cation–anion interaction (although anion–anion H-bonds also exist<sup>290</sup>). This has been demonstrated via a variety of experimental (FTIR,<sup>291–295</sup> NMR,<sup>296–298</sup> Raman spectroscopy,<sup>293,299</sup> X-ray,<sup>297,300</sup> or neutron<sup>75,301</sup> scattering) and simulation<sup>299,302–307</sup> techniques. Recent work has highlighted the importance of H-bond time scales on IL properties,<sup>308</sup> a finding that should be relevant to other classes of ILs. Notably too, imidazolium cations bearing a chiral center or small halide anion<sup>304</sup> can build up a 3-D H-bond network like PILs.<sup>297</sup>

Interestingly, a recent spectroscopic study provides evidence of intraionic H-bonds in amino-acid type ILs.<sup>309</sup> This demonstrates that, depending on the IL chemical structures used, H-bonds may form not only between ions, but may stabilize individual ion conformations.

This provides strong evidence of H-bond formation in ILs. Both PILs and AILs can form H-bond networks leading to an associated fluid. To achieve this, the number of donor and acceptor sites must be near equal and located in sterically

accessible positions across both ions. However, the net effect of H-bonds appears to be markedly different in ILs compared to molecular liquids; rather than stabilizing the liquid over the gas by increasing cohesive interactions and inducing a more structured liquid, H-bonds in ILs appear to promote directional interactions at the expense of electrostatic forces<sup>310</sup> favoring the liquid over the solid, possibly by introducing defects in the Coulomb lattice.<sup>311</sup> This promotes higher order arrangements, for example, ion clusters or amphiphilic structures.

**3.2.3. Ion Clusters.** The liquid state has often been modeled as time-dependent molecular clusters of finite size and number. In water, for example, the solvent structure has been described (to varying degrees of success) as “flickering clusters”,<sup>312</sup> linear molecular chains,<sup>313</sup> or larger, unspecified units based on suggestions that it is a mixture of high- and low-density forms.<sup>314</sup> The clustering of molecules in a liquid phase is associated with familiar properties of the system (heat capacity, expansivity, and compressibility) as well as critical phenomena and supercooled or first-order transitions.<sup>315</sup>

Recently, there have been many similar attempts to describe IL bulk structure as a population of (net neutral or net charged) ionic clusters or aggregates. Much of the early work was summarized in an influential review by Dupont, who postulated that ILs form a clustered supramolecular structure to maintain a 3D H-bond network.<sup>73</sup> Some of the more recent cluster research in ILs has been reviewed by Chen et al.<sup>77</sup> However, the notion of ion clusters in the bulk must be interpreted cautiously, because there are no set criteria to define an ion cluster, and distinguishing between an ion pair and ion cluster is arbitrary.<sup>256</sup>

Electrospray ionization mass spectrometry (EI-MS) has been the principal technique employed to corroborate the ion cluster model, in which the bulk structure is depicted as a sea of polydisperse aggregates. EI-MS experiments of AILs have been performed by many groups, with the presence of clusters inferred from high mass/charge ratio fragments.<sup>316–321</sup> Strong conclusions are proposed in these papers, including a set of “magic” numbers for anion/cation interaction<sup>316</sup> or empirical scales for ion association.<sup>317</sup> In most cases, large aggregates were detected of the form  $[C]_a[A]_b$  ( $C$  = cation,  $A$  = anion) for  $a$  and  $b$  values between 2 and 5. More recently, Kennedy and Drummond<sup>322</sup> proposed the PIL bulk is composed of net charged ion clusters. They noticed curiously large ion aggregates from the positive ion spectrum of many pure PILs. In EAN and PAN, the  $C_8A_7^+$  mass/charge ( $m/z$ ) peak was dominant (cf., Figure 9). From these results, the authors proposed the bulk structure of PILs such as EAN and PAN is a polydisperse mixture of aggregated ions, with the  $C_8A_7^+$  cluster most prominent. This suggests a distribution of spherical or oblate spheroid clusters may account for their less than ideal behavior.<sup>323</sup>

Ab initio quantum calculations by Ludwig supported these findings and showed that the  $C_8A_7^+$  aggregate was thermodynamically favored for EAN in the gas phase.<sup>180</sup> The aggregate structure is presented in Figure 9, and was suggested to be the most stable species on because it formed the most compact H-bond network.

An alternate explanation is that the  $C_8A_7^+$  aggregate structure is an artifact of the input parameters in ab initio calculations. For example, DFT calculations on gas-phase clusters of EAN, PAN, or butylammonium nitrate (BAN) show slightly different ion arrangements, with no stabilization of  $C_8A_7^+$  aggregates.<sup>324,325</sup> Likewise, femtosecond infrared spectroscopy (fs-IR) suggests the H-bond network in EAN is not as compact as assumed by

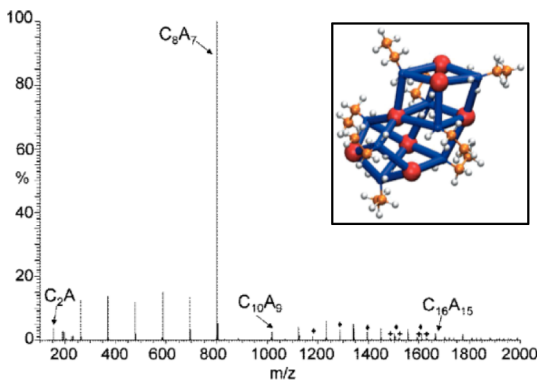


**Figure 9.** ESI-MS positive ion mode of EAN. The  $C_8A_7^+$  aggregate is prominent, with divalent ( $\blacklozenge$ ) and trivalent (+) units. The inset shows ab initio structure of the  $C_8A_7^+$  aggregate ( $C$  = cation,  $A$  = anion). C atoms are orange, H white, and N blue, while anions are represented as red spheres. Reproduced with permission from refs 322 (Copyright 2009 American Chemical Society) and 180 (Copyright 2009 American Chemical Society).

Ludwig, as the ammonium group can reorientate in large angle jumps.<sup>326</sup>

The violent nature of fragmentation in EI-MS experiment may contribute to cluster detection in PILs and AILs. That is, polydisperse aggregates in the mass spectra may not be evidence for underlying structure in the PIL. Notably, fast atom bombardment mass spectrometry (FAB-MS) experiments yield a very different aggregate distribution, with little consistency between clusters, even for the same ILs.<sup>327–329</sup> The ion aggregates were also conspicuously absent when EAN was dissolved in acetone.<sup>322</sup> This finding cannot be reconciled with other data (including by the same group),<sup>330,331</sup> which indicates PIL solution structure is quite robust when mixed with molecular solvents; there is no reason to suggest bulk aggregate formation should be switched off when mixed with a non-H-bonding solvent.

Ion clusters at PIL-air interfaces were suggested by Wakeham et al.<sup>332,333</sup> based on X-ray reflectivity (XRR), sum frequency generation spectroscopy (SFG), and neutral impact collision ion scattering spectroscopy (NICISS) data. Similarly, clusters have been reported at the AIL-air interface.<sup>334</sup> The XRR curves decayed more rapidly than expected for a perfectly smooth surface, indicating a rough or diffuse interface with significant gas interpenetration, which could not be explained by liquid capillary waves. The interfacial structure was postulated to be dotted with small, dynamic clusters of anions and cations in which the short alkyl moieties surround the charged core in a roughly spherical geometry. The SFG and NICISS data support these conclusions, as the hydrophobic alkyl groups were shown to shield the charged groups and protrude outward into the air. Such a structure is consistent with the clusters in Figure 9 and suggests that the enormous air-liquid surface area created upon droplet ionization contributes to aggregate detection. Thus, it appears more likely that EI-MS detects the clustered structure at the IL air-liquid interface, rather than in the bulk.

Rheological measurements by Separovic et al. on many of the same PILs showed them to be shear thinning. This suggests that they form long-lived aggregates much larger than ion pairs that became smaller at high shear rates and with increasing temperature.<sup>335</sup>

Evidence for ion clusters has been provided by IR, Raman, or vibrational spectroscopy experiments.<sup>195,293,336–340</sup> These stud-

ies suggest small, fluctuating hydrogen-bonded aggregates are present in the bulk, often in a conformational equilibrium with two or more rotational forms. Ab initio or DFT calculations of one or two of the cluster units accurately reproduced the measured IR and Raman spectra, thus identifying the absorption bands of different ion-ion interactions. Frequency shifts, due to stronger or weaker than expected associations, could be predicted and compared to similar studies for molecular solvents.<sup>341</sup> This combination of IR/Raman spectroscopy and simulation data enables the mechanism by which H-bonds stretch and bend to be elucidated in several popular ILs. The average ion binding energies in the bulk were also determined as a function of ion structure, and correlated to macroscopic physical properties.

NMR has also been used to suggest possible ion clusters in ILs.<sup>256</sup> This technique was first employed by the Wilkes group, in a series of classic papers on aluminum chloride-based ILs.<sup>342,343</sup> The reported  $^1\text{H}$  and  $^{13}\text{C}$  chemical shifts suggested ion-ion interactions more complex than simple ion pair association. They proposed an IL model built upon oligomeric chains in which each ion interacts with two or more ions of opposite charge. Later publications by Hussey<sup>344</sup> and Watanabe et al.,<sup>345</sup> using more powerful instruments, questioned these conclusions because the expected signature signal splitting from single ions and/or ion aggregates was not observed, meaning that the exchange between ions and their aggregates was faster than the probe time scale. Tokuda et al. have proposed one way around this by calculating the ratio of molar conductivity to ion self-diffusion coefficient,<sup>163,346</sup> as this may be used as quantitative evidence for ionic aggregates in ILs. This suggests that the NMR is likely unsuitable to probe cluster formation in the IL bulk, as the time scales of interest are much shorter than the instrument resolution, so that only time averaged ion solvation can be detected.

### 3.3. Self-Assembled Solvent Structures

**3.3.1. Micelle-like Nanostructure.** Early MD simulations by Margulis<sup>347</sup> proposed a reverse micelle-like structure in AILs [ $C_n\text{mim}$ ] $\text{PF}_6$  ( $n = 6, 8, 10, 12$ ). The spherical anion attracted five or so cations such that the imidazolium heads solvate the negative charge and alkyl chains are expelled outward, producing dynamic, near-spherical aggregates with a polar interior and apolar exterior. This study also indicated the presence of long-lived, nanometer-sized voids in the bulk. The presence of voids or cavities between molecules has often been associated with heterogeneity in disordered phases<sup>348,349</sup> and pure liquids;<sup>350</sup> yet the implications for hole theory were not explored. The void dimensions increased with length of the alkyl chain, which is at odds with experimental studies that show  $\gamma_{LV}$  decreases with increasing chain length,  $n$ .<sup>167,351</sup> As the calculated hole sizes based on known  $\gamma_{LV}$  values for [ $C_n\text{mim}$ ] $\text{PF}_6$ <sup>167</sup> are  $\sim 2\text{--}3$  times larger than observed in the simulation, it is unlikely that hole theory is applicable for describing the equilibrium bulk structure, although it may be useful for dynamic properties.<sup>352</sup>

XRD measurements were used to postulate a micellar-like solvent morphology for [ $C_n\text{mim}$ ] $[\text{PF}_6]$  ILs by Triolo et al.<sup>353</sup> This explained the linear correlation between cation alkyl length and position of the observed bulk correlation length; a 2.1 Å increase was noted for each additional  $\text{CH}_2$ .<sup>354</sup> This is slightly less than twice the increase for nonionic micelles in aqueous solution from the Tanford equation.<sup>355</sup> The alkyl chains were suggested to be weakly interdigitated, due to packing efficiency of apolar groups in the hydrophobic core.

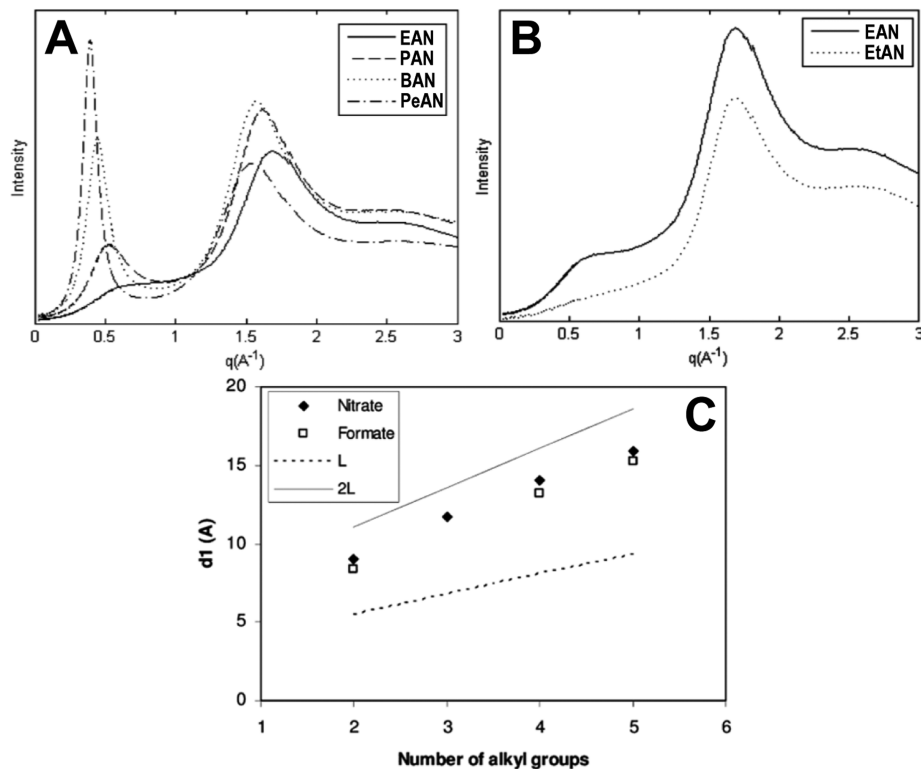


**Figure 10.** Effect of (A) cation alkyl chain length and (B) hydroxyl group addition on SWAXS data. In (A), spectra for ethyl-, propyl-, butyl-, and pentylammonium nitrate. Peak 1 is evident in EAN data in (B), but absent in the corresponding ethanolammonium nitrate (EtAN) spectra. (C) SWAXS peak 1 position, for the ethyl-, propyl-, butyl-, and pentylammonium formates and nitrates. The calculated comparison of 1 and 2 times the cation length  $L$  is included as dotted and solid lines, respectively. Reproduced with permission from ref 354. Copyright 2010 American Chemical Society.

Similar findings were later reported by Greaves et al.<sup>354</sup> for PILs. A micelle-like model for self-assembly in PILs was developed from small- and wide-angle X-ray scattering (SAXS and WAXS) patterns of a wide range alkylammonium, dialkylammonium, trialkylammonium, and cyclic ammonium cations combined with organic or inorganic anions. The SAXS/WAXS peak positions and intensities were systematically characterized as a function of ion structure or solvent/solute dissolution using the micelle-based model. From these data, the cations were thought to form discrete hydrophobic cores surrounded by charged regions. Notably, the bulk correlation was absent in SAXS/WAXS spectra for cations with either hydroxy or methoxy groups, and when the cation was sterically hindered. Likewise, longer cation alkyl chains enhanced long-range order, reminiscent of micelle swelling (cf., Figure 10) based on the Tanford model. This suggests nanostructure is more pronounced with increasing cation amphiphilicity. The choice of anion also influenced the degree of nanostructure, although the structural reason for this order could not be determined.

However, Triolo et al. and Drummond et al. have since moved away from micellar arguments to account for the diffraction peak at low- $q$ , consistent with recent trends in experimental and theoretical studies in the IL community. This is detailed in the next section.

**3.3.2. Mesoscopic Nanostructures.** Schröder et al. made the first suggestion of a mesoscopic solvent IL structure,<sup>356</sup> based on measurements of the diffusion coefficients of three electroactive solutes dissolved in aprotic ILs as a function of water content. Large differences were observed between the diffusion of neutral and charged species when comparing “wet” (up to 25.2 wt % water) IL samples. The authors concluded that binary IL-

water mixtures “may not be regarded as homogeneous solvents, but have to be considered as nanostructured with polar and nonpolar regions.” Later fluorescence spectroscopic data by Hu and Margulis<sup>357</sup> and systematic measurements of physical properties as a function of alkyl chain length by Watanabe et al.<sup>346</sup> were consistent with this. However, another few years elapsed before mesoscopic structure was directly examined.

By 2006, three independent molecular dynamics (MD) simulations suggested AILs self-assemble and form a solvent nanostructure. Wang and Voth<sup>358,359</sup> used a multiscale coarse-grained (CG) computational approach to explore the effect of cation alkyl chain length,  $n$ , on  $\text{C}_n\text{mim}[\text{NO}_3^-]$  (for  $n = 1-4, 6, 8$ ). Urahata and Ribeiro<sup>360</sup> simulated similar ILs with the same cations (for  $n = 1, 2, 4, 8$ ) and tested the effect of various anions ( $\text{F}^-, \text{Cl}^-, \text{Br}^-, \text{PF}_6^-$ ) on structure. Both papers showed cation headgroups and anions are distributed relatively homogeneously in the bulk, but crucially the alkyl tails aggregated together into spatially heterogeneous domains. This effect was more pronounced for longer alkyl chains, suggesting ion amphiphilicity is an important factor in IL structure. For  $n = 1-3$ , tail aggregation was only weakly apparent.

Later MD simulations<sup>181,361</sup> and molar enthalpies of vaporization data<sup>362</sup> by Canongia Lopes et al. supported this picture, but with a few important differences. The charged domains in the liquid were not homogeneously distributed, but formed a continuous three-dimensional network of ionic channels. These regions coexisted with uncharged domains; for short alkyl groups ( $\text{C}_2$ ), small, globular hydrocarbon “islands” form within the (continuous) polar network. Increasing the alkyl chain length ( $\text{C}_6, \text{C}_8$ , and  $\text{C}_{12}$ ) enables hydrocarbon domains to interconnect in a bicontinuous, sponge-like nanostructure. The butyl side

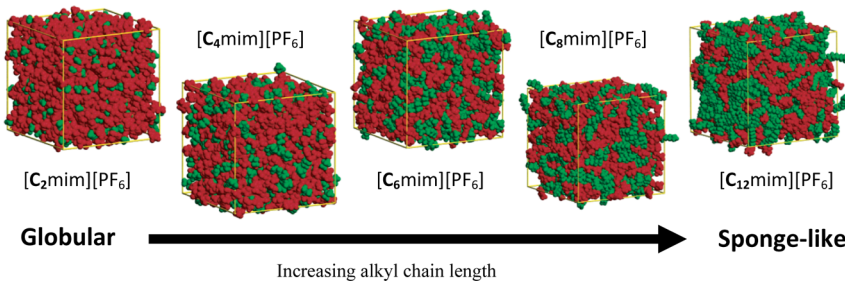


**Figure 11.** Snapshots of the bulk structure of  $[C_n\text{mim}][\text{PF}_6]$  ILs for  $n = 2–12$ . Each box shows 700 IL ion pairs at equilibrium with polar domains (red, anion + cation imidazolium ring) and nonpolar domains (green, cation alkyl chain) observed. Note the box dimensions are not the same length due to differences in ion size and box density. Figures reproduced with permission from ref 181. Copyright 2006 American Chemical Society.

chain ( $C_4$ ) marks the transition between the two solvent morphologies. This progression is shown in Figure 11.

Whether interpreted as indicating a micelle-like structure or other, bicontinuous morphology, XRD data are compelling evidence of self-assembled solvent nanostructure. A well-defined peak emerges for alkyl chains longer than a butyl group, typical of amphiphilic self-assembly.<sup>363</sup> The primary peak position corresponds to distances larger than individual ions or ion pairs, thus demonstrating longer range solvent structure. Altering the anion from the  $\text{Cl}^-$  to the larger, tetrahedral  $\text{BF}_4^-$  had no discernible effect on the diffraction spectra. This highlights the importance of cation nonpolar group aggregation in AIL self-assembly. Recent scattering studies<sup>78,364–367</sup> have proposed the sponge-like nanostructure exists in the bulk phase, which connect when the cation alkyl chain length is greater than or equal to four  $-\text{CH}_2-$  units long. Below this critical length, the liquid structure is understood to be more homogeneous, but containing globular nonpolar domains.

There has since been an abundance of simulations of AILs and their solutions by these<sup>368–373</sup> and other groups,<sup>374–394</sup> most of which confirm the formation of mesoscopic structures. Advances in theory and computational power have enabled fully ab initio quantum models of ILs,<sup>237,325,395–398</sup> allowing the dissection of structure and interaction energies between species, but over a smaller ion ensembles. Often, these simulations can accurately predict liquid properties. The number of published simulations is now sufficient to cross-validate different force fields (AMBER,<sup>390,399</sup> OPLS-AA,<sup>400,401</sup> GROMOS,<sup>402</sup> GAFF,<sup>368</sup> CHARMM,<sup>390</sup> UA-FF<sup>403</sup>) and interaction potentials (polarizable<sup>103,404</sup> vs nonpolarizable<sup>405,406</sup>), so that consistency can be obtained in the models across different ion structures. Specifically, a range of different cations (imidazolium, pyridinium, pyrrolidinium, piperidinium, triazolium, ammonium, phosphonium) and anions (halides,  $\text{PF}_6^-$ ,  $\text{BF}_4^-$ ,  $\text{NO}_3^-$ , chloroaluminate,  $\text{HSO}_4^-$ , OTf, triflate,  $\text{SCN}^-$ ,  $\text{NTf}_2^-$ ) have been examined toward the mesoscopic model (cf., Table 2). The contribution of different ion–ion interactions (electrostatic vs van der Waals,<sup>407,408</sup> dispersion forces,<sup>409</sup> H-bonding,<sup>178,303,306,410</sup>  $\pi-\pi$ <sup>410</sup>) or other molecular effects (e.g., cation symmetry<sup>379,411</sup> or linear/branched/cyclic alkyl groups<sup>412</sup>) has also been explicitly considered. Recent coarse-grained simulations suggest IL nanostructure is quite robust to, or can be enhanced under shear,<sup>413,414</sup> consistent with rheology measurements of neat ILs mixed with molecular solvents.<sup>156,160</sup> For pure simulations, polarizable models should be used to accurately reproduce ion dynamics. Readers interested in further details on IL simulations are referred to several reviews.<sup>373,389,415–417</sup>

Recent simulations by the Canongia Lopes group have shown that different bicontinuous nanostructures can be obtained by

changing cation geometry from imidazolium ( $C_n\text{mim}^+$ ) to trialkylmethylammonium ( $N_{1,n,n,n}^+$ ) or tetraalkylphosphonium ( $P_{n,n,n,n}^+$ ).<sup>418</sup> Close comparison across all of the simulations can be made as the same  $[\text{NTf}_2^-]$  anion was used throughout. These studies emphasize the importance of the volume ratio of charged:uncharged groups ( $V_{\text{alkyl}}:V_{\text{polar}}$ ) and the relative position of the alkyl groups on the cation.  $V_{\text{alkyl}}:V_{\text{polar}}$  loosely defines a packing ratio in the bulk phase. In principle, larger  $V_{\text{alkyl}}:V_{\text{polar}}$  values are obtained for more amphiphilic ions and enforce a stronger segregation of polar and apolar domains. The relative position of the alkyl groups on the cation controls the number and position of anions around the cation, and thus influences the connectivity of the polar domains. For example, the three long, symmetric alkyl groups in  $[\text{N}_{1,4,4,4}]^+$ ,  $[\text{N}_{1,6,6,6}]^+$ , or  $[\text{N}_{1,8,8,8}]^+$  ILs induce a more layered polar and apolar nanostructure,<sup>419</sup> consistent with earlier SAXS study that suggested disordered smectic-A phases in  $[\text{N}_{1,n,n,n}]^+[\text{NTf}_2^-]$  salts.<sup>420</sup> Conversely, in symmetric  $[\text{P}_{n,n,n,n}]^+[\text{NTf}_2^-]$  ILs, increasing  $V_{\text{alkyl}}:V_{\text{polar}}$  makes the cation larger but not more amphiphilic, and poorly defined thread-like network structures result with the anions between the alkyl chain threads, and more likely to be paired with a single cation.

Hardacre et al. have published a number of important articles that use neutron diffraction interpreted through EPSR simulations to investigate the structure in AILs.<sup>75,301,421,422</sup> H/D-isotopic substitution used is similar to that performed for molecular solvents<sup>16,423,424</sup> and PILs.<sup>233,425–428</sup> EPSR fitting of the diffraction spectra can elucidate the local ion–ion distributions in imidazolium ILs as presented in Figure 12. The structural arrangements in these models show significant charge ordering, which in some respects resembles the structure in the crystal state and follows an alternating “onion-skin” shells of cations and anions.<sup>301</sup>  $[\text{C}_1\text{mim}]^+$  cations were examined in these studies with very short alkyl chains, and thus are not amphiphilic. Thus, it is not surprising that IL bulk structure is principally determined by electrostatics as the cations cannot induce segregation. However, the local ion arrangements depicted Figure 12D–F are important as they will be retained with increasing alkyl chain length as the bulk correlation peak emerged (Figure 12A–C); structure in the polar domain is largely unaffected with increasing cation amphiphilicity.

Hardacre et al. recently examined a series of  $[C_n\text{mim}][\text{PF}_6]$  AILs,<sup>422</sup> with alkyl chains long enough to induce cation alkyl chain segregation ( $n = 4, 6, 8$ ). Selective deuteration of the 1-methyl- and 3-alkyl-hydrogens showed a clear bulk correlation peak in all of the ILs, even  $[\text{C}_4\text{mim}][\text{PF}_6]$ . Such a peak is very hard to detect in SAXS or SANS of fully protonated  $[\text{C}_4\text{mim}]^+$  ILs. The overall trend in peak position is the same as that reported in previous scattering experiments. The peak at low- $Q$  moves to

**Table 2.** Reports on Structure of ILs for Different Anion and Cation Combinations As a Function of Alkyl Chain Length  $n^a$ 

ion		technique			
cation	anion	simulation	scattering	other	other notable
Imidazolium					
1-methyl-3-C <sub>n</sub> -imidazolium	NO <sub>3</sub> <sup>-</sup>	MD ( $n = 1\text{--}4,6,8$ ) <sup>358</sup>	ND ( $n = 1$ ) <sup>301</sup>		electron solvation ( $n = 1$ ) <sup>726</sup>
	Cl <sup>-</sup>	MD ( $n = 1$ ) <sup>385,399,803</sup> MC ( $n = 1$ ) <sup>388</sup> ab initio ( $n = 1$ ) <sup>240,397,409</sup>	XRD (14, 18) <sup>804</sup>	Fl <sup>733</sup>	+H <sub>2</sub> O ( $n = 1$ ) <sup>388,608</sup> +alcohol ( $n = 1$ ) <sup>388</sup> +diethyl ether ( $n = 1$ ) <sup>388</sup> proton solvation ( $n = 1$ ) <sup>394</sup> electron solvation ( $n = 1$ ) <sup>724</sup>
	AlCl <sub>4</sub> <sup>-</sup>	MD ( $n = 2$ ) <sup>380,805</sup>			
	CH <sub>3</sub> SO <sub>3</sub> <sup>-</sup>	ab initio ( $n = 1$ ) <sup>409</sup>			
	CH <sub>3</sub> PhSO <sub>3</sub>	ab initio ( $n = 1$ ) <sup>409</sup>			
	N(CN) <sub>2</sub> <sup>-</sup>	ab initio ( $n = 1$ ) <sup>409</sup>			
	PF <sub>6</sub> <sup>-</sup>	MC ( $n = 1$ ) <sup>388</sup> MD ( $n = 1$ ) <sup>399</sup> ab initio ( $n = 1$ ) <sup>409</sup>			+H <sub>2</sub> O <sup>608</sup>
	Br <sup>-</sup>	ab initio ( $n = 1$ ) <sup>409</sup>			+H <sub>2</sub> O ( $n = 8$ ) <sup>602</sup>
	BF <sub>4</sub> <sup>-</sup>	ab initio ( $n = 1$ ) <sup>409</sup>			+ferrocene <sup>638</sup> +benzene ( $n = 8$ ) <sup>633</sup>
	NTf <sub>2</sub> <sup>-</sup>	EPSR ( $n = 1$ ) <sup>204</sup> ab initio ( $n = 1$ ) <sup>240,409</sup>	ND ( $n = 1$ ) <sup>204</sup>		
	HSO <sub>4</sub> <sup>-</sup>			RS ( $n = 2,4$ ) <sup>290</sup>	
1-ethyl-3-methylimidazolium	C <sub>n</sub> -SO <sub>4</sub> <sup>-</sup>	MD ( $n = 2,4,6,8$ ) <sup>806</sup> ab initio ( $n = 1$ ) <sup>409</sup>	XRD ( $n = 2,4,6,8$ ) <sup>806</sup> XRD ( $n = 2,4,6,8$ ) <sup>807</sup>		
	CH <sub>3</sub> PhSO <sub>3</sub> <sup>-</sup>	ab initio <sup>409</sup>			
	AlCl <sub>4</sub> <sup>-</sup>	ab initio <sup>808</sup>	ND <sup>808</sup>		
	SCN <sup>-</sup>	MD <sup>306</sup>			
1-C <sub>n</sub> -3-methylimidazolium	PF <sub>6</sub> <sup>-</sup>	MC ( $n = 4$ ) <sup>393,402</sup> MD ( $n = 4$ ) <sup>257,376,390,399,809,810</sup>  MD ( $n = 1,4$ ) <sup>360,811</sup> MD ( $n = 1,2,3,4$ ) <sup>812,813</sup> EPSR ( $n = 4,6,8$ ) <sup>422</sup>  MD ( $n = 4,7,10$ ) <sup>378</sup>  MD ( $n = 6,8,10$ ) <sup>430</sup>  MD ( $n = 2$ , hydroxyl analogue) <sup>453</sup>	XRD ( $n = 4$ ) <sup>797</sup> XRD ( $n = 4,6,8$ ) <sup>353,811</sup>  ND ( $n = 4,6,8$ ) <sup>422,811</sup> XRC ( $n = 10$ ) <sup>122</sup> EPSR ( $n = 4,6,8$ ) <sup>422</sup>  MD ( $n = 4,7,10$ ) <sup>378</sup>  MD ( $n = 6,8,10$ ) <sup>430</sup>  MD ( $n = 2$ , hydroxyl analogue) <sup>453</sup>	RS ( $n = 4$ ) <sup>199,814</sup> NMR ( $n = 4,6,8,10$ ) <sup>456</sup>  QENS ( $n = 4$ ) <sup>781,782,797</sup> NSE ( $n = 8$ ) <sup>815</sup> Fl <sup>357</sup>	+benzene ( $n = 1$ ) <sup>632</sup> +simple gases ( $n = 4$ ) <sup>646</sup> +CO <sub>2</sub> ( $n = 4$ ) <sup>648,649</sup> +sc-CO <sub>2</sub> ( $n = 4$ ) <sup>655</sup> +naphthalene ( $n = 4$ ) <sup>278</sup> +Li <sup>+</sup> and Na <sup>+</sup> salts ( $n = 4$ ) <sup>689</sup> pressure ( $n = 4$ ) <sup>577\text{--}579</sup> under shear ( $n = 10$ ) <sup>413</sup> +H <sub>2</sub> O <sup>818</sup> +CO <sub>2</sub> ( $n = 4$ ) <sup>648</sup> +Li <sup>+</sup> and Na <sup>+</sup> salts ( $n = 4$ ) <sup>689</sup> pressure ( $n = 4$ ) <sup>580</sup> temp ( $n = 8$ ) <sup>556</sup> H <sub>3</sub> O <sup>+</sup> solvation <sup>729</sup>
1-C <sub>n</sub> -3-methylimidazolium	BF <sub>4</sub> <sup>-</sup>	ab initio ( $n = 2$ ) <sup>409</sup>  MD ( $n = 2$ ) <sup>399</sup>	LAXS ( $n = 2$ ) <sup>816</sup>  XRD ( $n = 4,6,8$ ) <sup>363</sup>	RS ( $n = 4$ ) <sup>199</sup> NMR ( $n = 4$ ) <sup>456,818</sup>	+H <sub>2</sub> O <sup>818</sup> +CO <sub>2</sub> ( $n = 4$ ) <sup>648</sup> +Li <sup>+</sup> and Na <sup>+</sup> salts ( $n = 4$ ) <sup>689</sup> pressure ( $n = 4$ ) <sup>580</sup> temp ( $n = 8$ ) <sup>556</sup> H <sub>3</sub> O <sup>+</sup> solvation <sup>729</sup>
1-C <sub>n</sub> -3-methylimidazolium	NO <sub>3</sub> <sup>-</sup>	MD ( $n = 1,2,3,4$ ) <sup>812,813</sup> MD ( $n = 2$ ) <sup>819,820</sup> MD ( $n = 4$ ) <sup>402</sup> MD ( $n = 6,8,10,12,14,16,18,20,22$ ) <sup>821</sup> MD (hydroxyl analogue, $n = 2\text{--}12$ ) <sup>452</sup> MD ( $n = 2$ , hydroxyl analogue) <sup>453</sup> ab initio ( $n = 1\text{--}4$ , hydroxyl analogue) <sup>240</sup>			+glucose ( $n = 2$ ) <sup>668,669</sup> +cellulose ( $n = 2$ ) <sup>672</sup> +CO <sub>2</sub> ( $n = 4$ ) <sup>650</sup>
1-C <sub>n</sub> -3-methylimidazolium	F <sup>-</sup>	MD ( $n = 1,4$ ) <sup>360</sup> MN ( $n = 2$ ) <sup>377</sup>			
	OAc <sup>-</sup>	MD ( $n = 2$ ) <sup>822</sup> EPSR ( $n = 2$ ) <sup>822</sup> MD ( $n = 4$ ) <sup>382</sup>	ND ( $n = 2$ ) <sup>822</sup>		

Table 2. continued

ion		technique			
cation	anion	simulation	scattering	other	other notable
1-C <sub>n</sub> -3-methylimidazolium	TFA <sup>-</sup>	MD ( <i>n</i> = 4) <sup>382</sup>			+H <sub>2</sub> O ( <i>n</i> = 2) <sup>823</sup>
	Cl <sup>-</sup>	MD ( <i>n</i> = 1,2,4,8) <sup>360</sup>	XRD ( <i>n</i> = 8) <sup>365</sup>	RS ( <i>n</i> = 4) <sup>199,604</sup>	+CO <sub>2</sub> ( <i>n</i> = 4) <sup>650</sup>
		MD ( <i>n</i> = 1,2,3,4) <sup>812,813</sup>	XRD ( <i>n</i> = 3,4,6,8,10) <sup>363</sup>	NMR ( <i>n</i> = 4,6,8,10) <sup>456</sup>	+H <sub>2</sub> O ( <i>n</i> = 4, nitrile analogue) <sup>604</sup>
		ab initio ( <i>n</i> = 2) <sup>409</sup>	SAXS ( <i>n</i> = 12,14,16,18) <sup>120</sup>	DLS ( <i>n</i> = 4) <sup>826</sup>	
		MD ( <i>n</i> = 2) <sup>303</sup>	XRC ( <i>n</i> = 4, nitrile ana- logue) <sup>604</sup>		
		MD ( <i>n</i> = 2, hydroxyl analogue) <sup>453</sup>			
1-C <sub>n</sub> -3-methylimidazolium	Br <sup>-</sup>	MD ( <i>n</i> = 4) <sup>303,824</sup>			
		MD ( <i>n</i> = 8) <sup>365</sup>			
		ab initio ( <i>n</i> = 4) <sup>236,825</sup>			
		MD ( <i>n</i> = 1,2) <sup>360</sup>	XRD ( <i>n</i> = 2) <sup>829</sup>	RS ( <i>n</i> = 4) <sup>199</sup>	+IL ( <i>n</i> = 5) <sup>752</sup>
		ab initio ( <i>n</i> = 2) <sup>409</sup>	XRD ( <i>n</i> = 2,4,6) <sup>828</sup>	IR and UV ( <i>n</i> = 4) <sup>827</sup>	+H <sub>2</sub> O ( <i>n</i> = 6,8) <sup>603</sup>
		ab initio ( <i>n</i> = 4) <sup>824,827</sup>	SAXS ( <i>n</i> = 12,14,16,20) <sup>120</sup>	XAS ( <i>n</i> = 2,4,6,8,10) <sup>830</sup>	
1-C <sub>n</sub> -3-methylimidazolium		MD ( <i>n</i> = 2,4,6) <sup>828</sup>		XANES ( <i>n</i> = 2,4) <sup>831</sup>	
		MD ( <i>n</i> = 4) <sup>258</sup>			
		MD ( <i>n</i> = 4) <sup>382</sup>			
		ab initio ( <i>n</i> = 4) <sup>827</sup>			
	I <sup>-</sup>	ab initio ( <i>n</i> = 4) <sup>824,827</sup>	SAXS ( <i>n</i> = 4) <sup>832</sup>	RS ( <i>n</i> = 4) <sup>199,832</sup>	+H <sub>2</sub> O ( <i>n</i> = 4, nitrile analogue) <sup>604</sup>
		MD ( <i>n</i> = 4) <sup>382</sup>	XRC ( <i>n</i> = 4, nitrile ana- logue) <sup>604</sup>	( <i>n</i> = 4,6,8,10,12) <sup>456</sup>	
1-C <sub>n</sub> -3-methylimidazolium	ClO <sub>4</sub> <sup>-</sup>	ab initio ( <i>n</i> = 1–4, hydroxyl analogue) <sup>240</sup>			
1-C <sub>n</sub> -3-methylimidazolium	NTf <sub>2</sub> <sup>-</sup>	ab initio ( <i>n</i> = 2) <sup>833</sup>	SWAXS ( <i>n</i> = 2–12, 14,16) <sup>411</sup>	RS ( <i>n</i> = 2) <sup>833</sup>	+inorganic salts ( <i>n</i> = 4) <sup>689,690,693</sup>
		MD ( <i>n</i> = 2–10) <sup>448</sup>	SWAXS ( <i>n</i> = 1–10) <sup>366</sup>	FTIR ( <i>n</i> = 2 and 3 analogue) <sup>291</sup>	+ethane and butane ( <i>n</i> = 2,4,6,8,10) <sup>657</sup>
		MD ( <i>n</i> = 2) <sup>834,835</sup>	LAXS ( <i>n</i> = 2) <sup>834</sup>	NMR ( <i>n</i> = 2) <sup>834</sup>	+small molecules ( <i>n</i> = 2,4,8) <sup>661</sup>
		MD ( <i>n</i> = 4) <sup>382</sup>	XRD ( <i>n</i> = 2) <sup>835</sup>	NMR ( <i>n</i> = 2–10,11) <sup>456</sup>	+IL ( <i>n</i> = 5) <sup>752</sup>
		MD ( <i>n</i> = 4,6,8) <sup>470</sup>	XRD ( <i>n</i> = 3,6 and ether analogues) <sup>367</sup>	OKE ( <i>n</i> = 1–10) <sup>366</sup>	pressure ( <i>n</i> = 4) <sup>581</sup>
		MD ( <i>n</i> = 3,6,9 and ether analogues) <sup>451</sup>	XRD ( <i>n</i> = 3,6,9 and ether analogues) <sup>451</sup>	NSE ( <i>n</i> = 6) <sup>836</sup>	+H <sub>2</sub> O ( <i>n</i> = 6) <sup>601</sup>
1-C <sub>n</sub> -3-methylimidazolium		MD ( <i>n</i> = 4,7,10) <sup>374</sup>	SAXS ( <i>n</i> = 12,14,16,18) <sup>120</sup>	NSE ( <i>n</i> = 8) <sup>815</sup>	+acetonitrile ( <i>n</i> = 5) <sup>624</sup>
		MD ( <i>n</i> = 3,4,5 and symm. analogues) <sup>379</sup>			+carbon disulfide ( <i>n</i> = 1–4), ( <i>n</i> = 5) <sup>628,629</sup>
		MD ( <i>n</i> = 2, hydroxyl analogue) <sup>453</sup>			+methanol ( <i>n</i> = 2) <sup>617,618</sup>
		ab initio ( <i>n</i> = 1–4, hydroxyl analogue) <sup>240</sup>			+nanoparticle <sup>837</sup>
					+CO <sub>2</sub> ( <i>n</i> = 3, amine analogue) <sup>652</sup>
					+CO <sub>2</sub> ( <i>n</i> = 6) <sup>654</sup>
1-C <sub>n</sub> -3-methylimidazolium	NPF <sub>2</sub> <sup>-</sup>	MD ( <i>n</i> = 4) <sup>382</sup>			
1-C <sub>n</sub> -3-methylimidazolium	OFT <sup>-</sup>	MD ( <i>n</i> = 2, hydroxyl analogue) <sup>453</sup>		FTIR ( <i>n</i> = 4) <sup>838</sup>	
1-C <sub>n</sub> -3-methylimidazolium	HSO <sub>4</sub> <sup>-</sup>	ab initio ( <i>n</i> = 6) <sup>839</sup>		FTIR ( <i>n</i> = 4) <sup>838</sup>	
1-C <sub>n</sub> -4,5-dibromo-3-methylimidazolium	Br <sup>-</sup>	ab initio ( <i>n</i> = 3) <sup>839</sup>		RS ( <i>n</i> = 2,4) <sup>290</sup>	
1-C <sub>n</sub> -4,5-dibromo-3-methylimidazolium	NTf <sub>2</sub> <sup>-</sup>	ab initio ( <i>n</i> = 4 and didromo analogue) <sup>840</sup>		RD ( <i>n</i> = 6) <sup>839</sup>	
1-C <sub>n</sub> -3-decylimidazolium	Br <sup>-</sup>				+H <sub>2</sub> O ( <i>n</i> = 1,4,7,10) <sup>609</sup>
1-C <sub>n</sub> -3-dodecylimidazolium	Br <sup>-</sup>		SAXS, XRC <sup>210</sup>	NMR <sup>210</sup>	
1-C <sub>n</sub> -3-C <sub>n</sub> -imidazolium	NTf <sub>2</sub> <sup>-</sup>	LAXS ( <i>n</i> = 4) <sup>841</sup>	SWAXS ( <i>n</i> = 1–12) <sup>411</sup>		
		MD ( <i>n</i> = 3,4,5) <sup>379</sup>	LAXS ( <i>n</i> = 4) <sup>841</sup>		
		MD ( <i>n</i> = 2–10) <sup>449</sup>			
1-allyl-3-methylimidazolium		ab initio (Cl <sup>-</sup> , N(CN) <sub>2</sub> <sup>-</sup> , HCO <sub>3</sub> <sup>-</sup> , OAc) <sup>242</sup>		DLS ( <i>n</i> = 4) <sup>826</sup>	
1-methylimidazolium			SWAXS (HBA, OF) <sup>466</sup>		
Ammonium					
methylammonium		ab initio (NO <sub>3</sub> <sup>-</sup> ) <sup>842</sup>	XRC (NO <sub>3</sub> <sup>-</sup> ) <sup>842,843</sup>	Raman (NO <sub>3</sub> <sup>-</sup> ) <sup>842</sup>	+H <sub>2</sub> O (NO <sub>3</sub> <sup>-</sup> ) <sup>844</sup>

Table 2. continued

ion		technique			
cation	anion	simulation	scattering	other	other notable
<b>Ammonium</b>					
ethylammonium	NO <sub>3</sub> <sup>-</sup>	EPSR <sup>233,427,428</sup> MD <sup>435,845</sup> ab initio <sup>180,324,846</sup>	ND <sup>233,427,428</sup> SANS <sup>434</sup> SWAXS <sup>354</sup> XRD <sup>435,845</sup> XRC <sup>206</sup>	DS (HCO <sub>2</sub> <sup>-</sup> ) <sup>802</sup> Walden <sup>58</sup> RS <sup>324,326,846</sup> DS <sup>234,255</sup> EXAFS <sup>715</sup> OKE <sup>255</sup> FAB-MS <sup>327</sup> fs-IR <sup>326</sup> IR <sup>283</sup> TS <sup>847</sup> EI-MS <sup>322</sup> NMR <sup>848</sup> Walden <sup>58</sup> DS <sup>802</sup>	temp (various anions) <sup>354</sup> +H <sub>2</sub> O <sup>331,426</sup> +inorganic salts <sup>688,715,716</sup> +alkanes <sup>330</sup> +alcohols <sup>330</sup> +C <sub>i</sub> E <sub>j</sub> surfactants <sup>662,663</sup> +C <sub>60</sub> <sup>643</sup> +CO <sub>2</sub> <sup>653</sup> +DMSO <sup>641</sup> +cytochrome c <sup>713</sup> electron solvation <sup>726</sup> + glycerol <sup>621</sup>
	HCO <sub>2</sub> <sup>-</sup>	EPSR <sup>427,428</sup> MD (Cl <sup>-</sup> ) <sup>849</sup> EPSR (HSO <sub>4</sub> <sup>-</sup> , SCN) <sup>427,428</sup>	ND <sup>427,428</sup> XRC (Cl <sup>-</sup> ) <sup>849</sup> ND (HSO <sub>4</sub> <sup>-</sup> , SCN) <sup>427,428</sup> SWAXS (G) <sup>354</sup> SWAXS (OA) <sup>466</sup>	DS (HCO <sub>2</sub> <sup>-</sup> ) <sup>802</sup>	temp (NO <sub>3</sub> <sup>-</sup> ) <sup>233</sup>
ethanolammonium	NO <sub>3</sub> <sup>-</sup>	EPSR <sup>233</sup>	ND <sup>233</sup> SWAXS <sup>354</sup> XRD <sup>438</sup> SWAXS <sup>467</sup> SWAXS (HFB, OF, OA) <sup>466</sup>	DS (HCO <sub>2</sub> <sup>-</sup> ) <sup>802</sup>	temp (NO <sub>3</sub> <sup>-</sup> ) <sup>233</sup>
propylammonium		EPSR (NO <sub>3</sub> <sup>-</sup> ) <sup>425,427,428</sup> ab initio (NO <sub>3</sub> <sup>-</sup> ) <sup>324</sup> MD (Cl <sup>-</sup> ) <sup>208</sup>	XRD (NO <sub>3</sub> <sup>-</sup> ) <sup>845</sup> XRD (Cl <sup>-</sup> ) <sup>208</sup> ND (NO <sub>3</sub> <sup>-</sup> ) <sup>425,427,428</sup>	Walden (HCO <sub>2</sub> <sup>-</sup> , OAc) <sup>58</sup> RS (NO <sub>3</sub> <sup>-</sup> ) <sup>324,582</sup> IR (NO <sub>3</sub> <sup>-</sup> ) <sup>283</sup> EI-MS (NO <sub>3</sub> <sup>-</sup> ) <sup>322</sup>	pressure (NO <sub>3</sub> <sup>-</sup> ) <sup>582</sup>
butylammonium		MD (NO <sub>3</sub> <sup>-</sup> and alkanol or methoxyammonium derivatives) <sup>850</sup>	XRD (NO <sub>3</sub> <sup>-</sup> ) <sup>845</sup> SWAXS (HCO <sub>2</sub> <sup>-</sup> ) <sup>354</sup> SWAXS (OA) <sup>466</sup> SWAXS (HCO <sub>2</sub> <sup>-</sup> ) <sup>354</sup> SWAXS (HFB) <sup>466</sup> SWAXS (HCO <sub>2</sub> <sup>-</sup> ) <sup>354</sup> SWAXS (HFB) <sup>466</sup> SWAXS (HCO <sub>2</sub> <sup>-</sup> ) <sup>354</sup> SWAXS (HCO <sub>2</sub> <sup>-</sup> ) <sup>354</sup>	EI-MS (NO <sub>3</sub> <sup>-</sup> ) <sup>322</sup> EI-MS (NO <sub>3</sub> <sup>-</sup> ) <sup>322</sup> RS (NO <sub>3</sub> <sup>-</sup> ) <sup>324</sup> DS (HCO <sub>2</sub> <sup>-</sup> ) <sup>802</sup> EI-MS (NO <sub>3</sub> <sup>-</sup> ) <sup>322</sup> EI-MS (NO <sub>3</sub> <sup>-</sup> ) <sup>322</sup>	+alcohols (HBA, OF) <sup>466</sup>
pentylammonium					
dimethylammonium					
diethylammonium					
triethylammonium					
diethanolammonium				EI-MS (NO <sub>3</sub> <sup>-</sup> ) <sup>322</sup>	
triethanolammonium				EI-MS (NO <sub>3</sub> <sup>-</sup> ) <sup>322</sup>	
trimethylpropylammonium	NTf <sub>2</sub> <sup>-</sup>				electron solvation <sup>726</sup>
2-methoxyethylammonium			SWAXS (NO <sub>3</sub> <sup>-</sup> ) <sup>354</sup> XRD (NO <sub>3</sub> <sup>-</sup> ) <sup>439</sup> SWAXS (HCO <sub>2</sub> <sup>-</sup> ) <sup>354</sup>	EI-MS (NO <sub>3</sub> <sup>-</sup> ) <sup>322</sup>	
2-(2-hydroxyethoxy)ethylammonium	NTf <sub>2</sub> <sup>-</sup>			EI-MS (NO <sub>3</sub> <sup>-</sup> ) <sup>322</sup>	
2-hydroxyethyltrimethylammonium		MD (CH <sub>3</sub> SO <sub>3</sub> <sup>-</sup> and L) <sup>851</sup>		FTIR (CH <sub>3</sub> SO <sub>3</sub> <sup>-</sup> and L) <sup>851</sup>	
N-C <sub>n</sub> -N-ethyl-N,N-dimethyl-ammonium		MD ( <i>n</i> = 4,7,10 and ether analogues) <sup>852</sup>			
tri-C <sub>n</sub> -methyl-ammonium	NTf <sub>2</sub> <sup>-</sup>	MD ( <i>n</i> = 4) <sup>445</sup> MD ( <i>n</i> = 4,6,8) <sup>418</sup>	MD ( <i>n</i> = 4) <sup>445</sup> SAXS ( <i>n</i> = 4,6,8) <sup>420</sup>		temp ( <i>n</i> = 4) <sup>445</sup>
tri-C <sub>n</sub> -octyl-ammonium	NTf <sub>2</sub> <sup>-</sup>		XRD ( <i>n</i> = 2 and ether analogue) <sup>367</sup>		
tetra-C <sub>n</sub> -ammonium	PF <sub>6</sub> <sup>-</sup> I <sup>-</sup> N(CN) <sub>2</sub> <sup>-</sup>	MD ( <i>n</i> = 5) <sup>432</sup> MD ( <i>n</i> = 5) <sup>432</sup> MD ( <i>n</i> = 5) <sup>432</sup>	SAXS ( <i>n</i> = 5) <sup>432</sup> SAXS ( <i>n</i> = 5) <sup>432</sup> SAXS ( <i>n</i> = 5) <sup>432</sup>		
N-ethyl-N,N-dimethyl-N-(2-methoxyethyl)ammonium	NTf <sub>2</sub> <sup>-</sup>	MD <sup>853</sup>			
N-ethyl-N,N-dimethyl-N-butylammonium	NTf <sub>2</sub> <sup>-</sup>	MD <sup>854</sup>			
Pyrrolidinium					
2-pyrrolidinonium			SWAXS (NO <sub>3</sub> <sup>-</sup> , HCO <sub>2</sub> <sup>-</sup> ) <sup>354</sup>		+alcohols (HBA) <sup>466</sup>

Table 2. continued

cation	ion	technique			
		simulation	scattering	other	other notable
<b>Pyrrolidinium</b>					
<i>N</i> -C <sub>n</sub> -N-methylpyrrolidinium	NTf <sub>2</sub> <sup>-</sup>	MD ( <i>n</i> = 3, 4) <sup>336</sup> ab initio ( <i>n</i> = 3, 4) <sup>336</sup> MD ( <i>n</i> = 4) <sup>381,855</sup> MD ( <i>n</i> = 3,4,6,8,10) <sup>856</sup>	SWAXS (HFB) <sup>466</sup> XRC ( <i>n</i> = 1, nitrile functionalized) <sup>857</sup> SAXS ( <i>n</i> = 3,4,6,8,10) <sup>856</sup>	Raman ( <i>n</i> = 3, 4) <sup>336</sup>	+inorganic salt ( <i>n</i> = 1) <sup>692</sup>
	TF <sup>-</sup>	MD ( <i>n</i> = 4) <sup>381</sup>			
	FAP <sup>-</sup>	MD ( <i>n</i> = 4) <sup>381</sup>			
<i>N</i> -C <sub>n</sub> -N-C <sub>n</sub> -pyrrolidinium	NTf <sub>2</sub> <sup>-</sup>	ab initio ( <i>n</i> = 1, nitrile moiety) <sup>857</sup>	XRC ( <i>n</i> = 1, nitrile moiety) <sup>857</sup>		
<b>Phosphonium</b>					
tetra-C <sub>n</sub> -methylphosphonium	NTf <sub>2</sub> <sup>-</sup>	MD ( <i>n</i> = 6) <sup>418</sup>			
tri-C <sub>n</sub> -octyl-phosphonium	NTf <sub>2</sub> <sup>-</sup>		XRD ( <i>n</i> = 2 and ether analogue) <sup>367</sup>		
	OB <sup>-</sup>	MD ( <i>n</i> = 4) <sup>858</sup>			
tri-C <sub>n</sub> -tetradecylphosphonium	NTf <sub>2</sub> <sup>-</sup>	MD ( <i>n</i> = 6) <sup>446</sup> MD ( <i>n</i> = 6) <sup>446,557</sup>	XRD ( <i>n</i> = 6) <sup>446</sup> XRD ( <i>n</i> = 6) <sup>446</sup>		temp ( <i>n</i> = 6) <sup>446,557</sup>
	Cl <sup>-</sup>		XRD ( <i>n</i> = 6) <sup>859</sup>		
	OB <sup>-</sup>	MD ( <i>n</i> = 4, 6) <sup>858</sup>			
<b>Pyridinium</b>					
1-alkylpyridinium	NTf <sub>2</sub> <sup>-</sup>	ab initio (nitrile moiety) <sup>857</sup>	XRC (nitrile moiety) <sup>857</sup>		
	Cl <sup>-</sup>				electron solvation <sup>725</sup>
1-C <sub>n</sub> -pyridinium	BF <sub>4</sub> <sup>-</sup>	ab initio ( <i>n</i> = 4) <sup>860</sup> MD ( <i>n</i> = 4) <sup>860</sup>			
1-C <sub>n</sub> -methylpyridinium	NTf <sub>2</sub> <sup>-</sup>	MD ( <i>n</i> = 6, 8, and 7 isomer) <sup>861</sup>		NMR ( <i>n</i> = 6, 8, and 7 isomer) <sup>861</sup>	+inorganic salt <sup>693</sup>
<b>Pyrrolidinium</b>					
<i>N</i> -C <sub>n</sub> -N-methylpyrrolidinium	NTf <sub>2</sub> <sup>-</sup>	( <i>n</i> = 3,4,6,8,10) <sup>862</sup>	XRD ( <i>n</i> = 3,4,6,8,10) <sup>862</sup> XRD ( <i>n</i> = 3) <sup>863</sup>	Walden ( <i>n</i> = 3) <sup>864</sup>	
1-C <sub>n</sub> -1-methylpyrrolidinium	NTf <sub>2</sub> <sup>-</sup>	MD ( <i>n</i> = 4,5,6,7,8,10) <sup>412</sup> MD ( <i>n</i> = 7 isomer, 8 isomer) <sup>412</sup>	XRD ( <i>n</i> = 4,5,6,7,8,10) <sup>412</sup> XRD ( <i>n</i> = 7 isomer, 8 isomer) <sup>412</sup>		
<i>N</i> -methyl- <i>N</i> -C <sub>n</sub> -pyrrolidinium	NTf <sub>2</sub> <sup>-</sup>	MD ( <i>n</i> = 3) <sup>855</sup> ab initio and MD ( <i>n</i> = 3,4) <sup>336,865</sup> ab initio ( <i>n</i> = 4) <sup>866</sup>		Raman ( <i>n</i> = 3,4) <sup>336,865</sup>	
<b>Piperidinium</b>					
<i>N</i> -C <sub>n</sub> -N-methylpiperidinium	NTf <sub>2</sub> <sup>-</sup>	ab initio ( <i>n</i> = 1,3 nitrile moiety) <sup>857</sup>	SWAXS ( <i>n</i> = 3,4,5,6,7) <sup>867</sup> XRC ( <i>n</i> = 1,3 nitrile moiety) <sup>857</sup>		
<i>N</i> -C <sub>n</sub> -N-methylpiperidinium	NTf <sub>2</sub> <sup>-</sup>	ab initio (nitrile moiety) <sup>857</sup>	XRC (nitrile moiety) <sup>857</sup>		
1-methyl-4-cyanopyridinium	NTf <sub>2</sub> <sup>-</sup>	EPSR <sup>868</sup>	ND <sup>868</sup>		
		MD <sup>868</sup>			
<b>Triazonium</b>					
1-hydroxyethyl-4-amino-1,2,4-triazo- lium	NO <sub>3</sub> <sup>-</sup>	MD <sup>368</sup> ab initio <sup>869</sup>			
1,2,3-triazolium		MD (NO <sub>3</sub> <sup>-</sup> or ClO <sub>4</sub> <sup>-</sup> ) <sup>861</sup>			
1,2,4-triazolium		MD (NO <sub>3</sub> <sup>-</sup> or ClO <sub>4</sub> <sup>-</sup> ) <sup>861</sup>			
4-amino-1,2,4-triazolium		MD (NO <sub>3</sub> <sup>-</sup> or ClO <sub>4</sub> <sup>-</sup> ) <sup>861</sup>			
1-methyl-4-amino-1,2,4-triazolium	ClO <sub>4</sub> <sup>-</sup>	MD <sup>861</sup>			
3-azido-1,2,4-triazolium	NO <sub>3</sub> <sup>-</sup>	ab initio <sup>870</sup>			
<b>Fluorous ILs</b>					
ethylammonium			SWAXS (OF <sup>-</sup> , HFB) <sup>466</sup>		+alcohols (HFB, OF) <sup>466</sup>
ethanolammonium			SWAXS (HFB) <sup>466</sup>		
diethylammonium			SWAXS (HFB) <sup>466</sup>		
triethylammonium			SWAXS (HFB) <sup>466</sup>		
tetraethylammonium			SWAXS (IM <sub>14</sub> ) <sup>468</sup>	NMR (IM <sub>14</sub> ) <sup>468</sup>	
butylammonium		MD (OF) <sup>471</sup>	SWAXS (OF, HFB) <sup>466</sup>		+alcohols (HFB, OF) <sup>466</sup>
tertbutylammonium		MD (FBS) <sup>469</sup>			
1-methylimidazolium			SWAXS (HFB) <sup>466</sup>		
1-C <sub>n</sub> -3-methylimidazolium		MD ( <i>n</i> = 6, FBS) <sup>469</sup>	SWAXS ( <i>n</i> = 2, IM <sub>14</sub> ) <sup>468</sup>	NMR ( <i>n</i> = 2, IM <sub>14</sub> ) <sup>468</sup>	

Table 2. continued

ion		technique			
cation	anion	simulation	scattering	other	other notable
<b>Fluorous ILs</b>					
1-(3,3,4,4,4-pentafluoro-butyl)-3-methylimidazolium		MD ( $\text{Br}^-$ , $\text{I}^-$ , $\text{OAc}^-$ , TFA, $\text{NTf}_2^-$ , $\text{NPf}_2^-$ ) <sup>382</sup>			
1-(3,3,4,4,5,5-heptafluoro-pentyl)-3-methylimidazolium		MD ( $\text{NTf}_2$ ) <sup>470</sup>			
1-(3,3,4,4,5,5,6,6-nonafluoro-hexyl)-3-methylimidazolium		MD ( $\text{NTf}_2$ ) <sup>470</sup>			
1-(3,3,4,4,5,5,6,6,7,7,8,8,8-trideca-fluoro-octyl)-3-methylimidazolium		MD ( $\text{NTf}_2$ ) <sup>470</sup>			
pyrrolidinium			SWAXS (HFB) <sup>466</sup>		
<i>N,N</i> -dimethylpyrrolidinium			SWAXS ( $\text{IM}_{14}$ ) <sup>468</sup>	NMR ( $\text{IM}_{14}$ ) <sup>468</sup>	
<i>N</i> -butyl- <i>N</i> -methylpyrrolidinium			SWAXS ( $\text{IM}_{14}$ , $\text{IM}_{24}$ ) <sup>468</sup>	NMR ( $\text{IM}_{14}$ , $\text{IM}_{24}$ ) <sup>468</sup>	
2-pyrrolidinonium			SWAXS (HFB) <sup>466</sup>		
<b>Dicationic ILs</b>					
di(1-C <sub>n</sub> -3-methylimidazolium)	$\text{NTf}_2^-$	MD ( <i>n</i> = 3,6, 12) <sup>477</sup> MD ( <i>n</i> = 3,6,9,12) <sup>480</sup>	SWAXS ( <i>n</i> = 3,6, 12) <sup>477</sup>		
<b>Magnetic ILs</b>					
1-C <sub>n</sub> -3-methylimidazolium	$[\text{FeCl}_4]^-$		XRC ( <i>n</i> = 2) <sup>532</sup> XRD ( <i>n</i> = 2,4) <sup>528</sup> XRC ( <i>n</i> = 4) <sup>530</sup>	RS ( <i>n</i> = 2,4) <sup>528</sup> IR and RS ( <i>n</i> = 10) <sup>530</sup>	
tri-C <sub>n</sub> -tetradecylphosphonium	$[\text{MnBr}_4]^-$				
<i>N</i> -C <sub>n</sub> -N-methylpyrrolidinium	$[\text{FeCl}_4]^-$				
tetra-C <sub>n</sub> -ammonium	$[\text{FeCl}_4]^-$				
tri-C <sub>n</sub> -methylammonium	$[\text{FeCl}_4]^-$				
<b>Solvate ILs</b>					
group 1 metal ions	TOTO <sup>-</sup>	ab initio ( $\text{Li}^+$ , $\text{Na}^+$ , $\text{K}^+$ ) <sup>555</sup>		Walden <sup>544</sup> Stokes <sup>871</sup>	
Ag <sup>+</sup> complexes	$[\text{NTf}_2]^-$		XRC <sup>554</sup>		

<sup>a</sup>The techniques listed are as follows: molecular dynamics simulations (MD), ab initio methods (ab initio), X-ray diffraction (XRD), neutron diffraction (ND), Raman spectroscopy (RS), nuclear magnetic resonance (NMR), fluorescence (Fl), dielectric spectroscopy (DS), extended X-ray absorption fine structure (EXAFS), X-ray crystallography (XRC), femtosecond-infrared spectroscopy (fs-IR), terahertz spectroscopy (TS), X-ray absorption spectroscopy (XAS), X-ray absorption near edge structure (XANES), neutron spin echo (NSE), quasi elastic neutron scattering (QENS), and Walden (Walden plot). Anion abbreviations are as follows: F<sup>-</sup>, fluoride; Cl<sup>-</sup>, chloride; Br<sup>-</sup>, bromide; I<sup>-</sup>, iodide; NO<sub>3</sub><sup>-</sup>, nitrate; HCO<sub>3</sub><sup>-</sup>, formate; OAc<sup>-</sup>, acetate; SCN<sup>-</sup>, thiocyanate; ClO<sub>4</sub><sup>-</sup>, perchlorate; G<sup>-</sup>, glycolate; L<sup>-</sup>, lactate; TF<sup>-</sup>, triflate; OA<sup>-</sup>, octanoate; CH<sub>3</sub>PhSO<sub>3</sub><sup>-</sup>, tosylate; N(CN)<sup>-</sup>, dicyanamide; TFA<sup>-</sup>, trifluoroacetate; HSO<sub>4</sub><sup>-</sup>, hydrogen sulfate; CH<sub>3</sub>SO<sub>3</sub><sup>-</sup>, methylsulfate; OB, orthoborate; BF<sub>4</sub><sup>-</sup>, tetrafluoroborate; AlCl<sub>4</sub><sup>-</sup>, tetrachloroaluminate; OFT<sup>-</sup>, trifluoromethanesulfonate; NTf<sub>2</sub><sup>-</sup>, bis(trifluoromethylsulfonyl)imide; NPf<sub>2</sub><sup>-</sup>, bis(pentafluoroethylsulfonyl)imide; FAP<sup>-</sup>, tris(perfluoroalkyl)trifluorophosphate; TOTO<sup>-</sup>, oligoether-carboxylate; HFB, heptafluorobutyrate; OF, pentadecafluoroctanoate; FBS<sup>-</sup>, perfluorobutanesulfonate; IM<sub>14</sub>, (nonafluorobutanesulfonyl)(trifluoromethanesulfonyl)imide.

longer distances, sharpens, and becomes more intense with increasing cation chain length. This indicates that the correlation is related to the size of the nonpolar hydrocarbon moiety of the cation, increasing by  $\sim 2 \text{ \AA}$  per methylene unit. The EPSR model results were not consistent with a micelle-like structure because the height and sharpness of the scattering on the peak are less than other features on the diffraction spectra, notably the intraionic peak between  $0.8\text{--}2.0 \text{ \AA}^{-1}$ . This suggests the interionic correlation weakly contributes to the net scattering profile. Second, the peak position is detected at longer length scales than predicted by MD simulations.

On the basis of these observations, Hardacre et al. concluded the peak at low *Q* is not a signature of solvent nanostructure, but instead is a result of changes in cation anisotropy with increasing amphiphilicity. Moreover, the data does not, in isolation, demonstrate the presence of nanostructure beyond an immediate correlation. The picture developed is intermediate to that for [C<sub>1</sub>mim][PF<sub>6</sub>]<sup>75</sup> and long-chain liquid crystalline

ILs;<sup>429</sup> the anions solvate the charge-bearing imidazolium head via Coulombic attraction to form an ionic domain. The alkyl chains fill the void between adjacent ionic domains, and are loosely associated in a bilayer- or sponge-like arrangement consistent with findings for PILs bulk.<sup>233,428</sup> Thus, Hardacre et al.'s disagreement with the concept of IL nanostructure is a matter of language; while signature polar and apolar domains are evident in their data, it is not viewed as being rigid and well-defined separation like in a bicontinuous microemulsion or smectic liquid crystal.

Margulis and co-workers arrived at conclusions similar to those of Hardacre et al.<sup>422</sup> from MD simulations of the bulk structure of [C<sub>6</sub>mim][Cl], [C<sub>8</sub>mim][PF<sub>6</sub>], and [C<sub>10</sub>mim][PF<sub>6</sub>] as compared to the crystal structure of [C<sub>10</sub>mim][PF<sub>6</sub>].<sup>430</sup> The low-*q* feature in all of the liquid phases was proposed to be of the same repeating unit found in the crystal phase, arising due to cation anisotropy. Other MD simulations by this group have

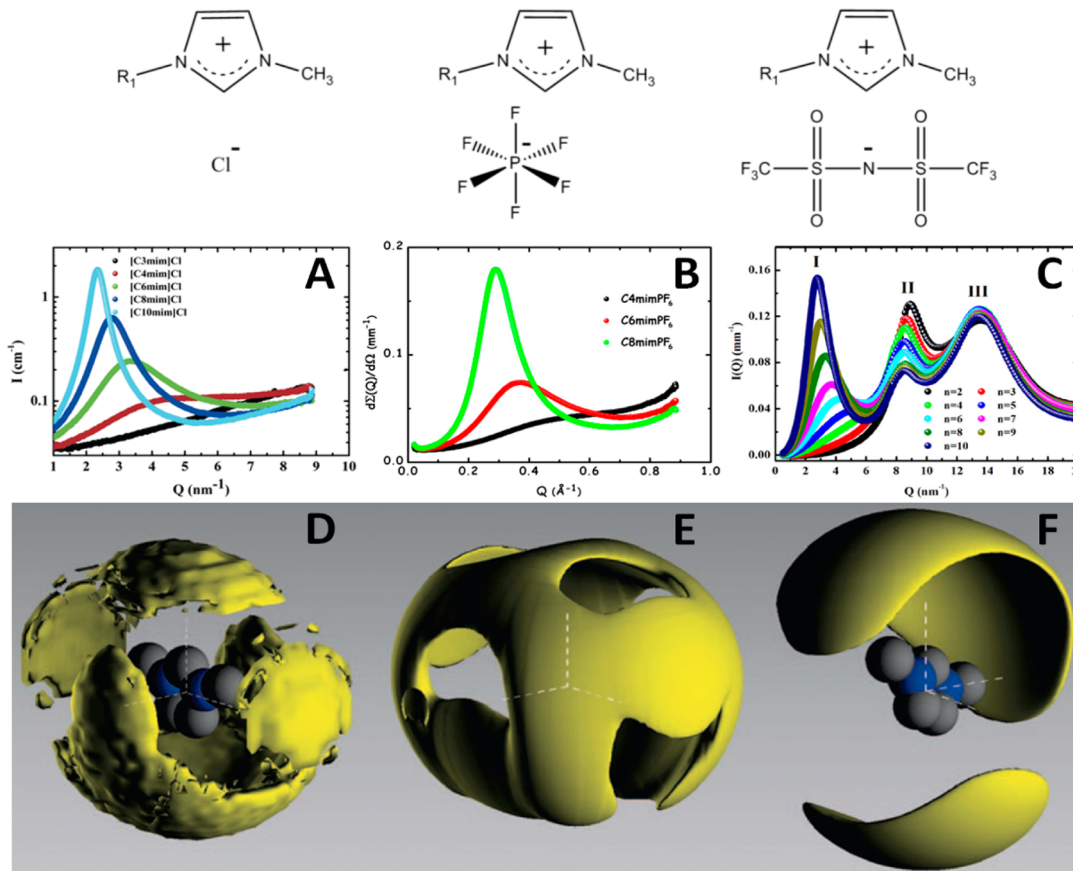


**Figure 12.** Nanostructure in  $C_n$ mim-based ionic liquids. Top (from left to right): Chemical structures of  $[C_n$ mim] $\text{Cl}$ ,  $[C_n$ mim] $\text{PF}_6$ , and  $[C_n$ mim] $\text{NTf}_2$ , respectively. Middle: X-ray diffraction and small-angle X-ray scattering patterns for (A)  $[C_n$ mim] $\text{Cl}$ ,  $n = 3, 4, 6, 8, 10$ , (B)  $[C_n$ mim] $\text{PF}_6$ ,  $n = 4, 6, 8$ , and (C)  $[C_n$ mim] $\text{NTf}_2$   $2 \leq n \leq 10$  AILs at 298 K. Bottom: Corresponding Empirical Potential Structure Refinement (EPSR) modeling of the cation probability distribution around a  $[C_1$ mim] $^+$  cation: (D)  $[C_1$ mim] $\text{Cl}$ , (E)  $[C_1$ mim] $\text{PF}_6$ , and (F)  $[C_1$ mim] $\text{NTf}_2$ . Reproduced with permission from refs 363 (Copyright 2007 American Chemical Society), 353 (Copyright 2008 Elsevier), 75 (Copyright 2007 American Chemical Society), and 366 (Copyright 2009 IOP Publishing).

confirmed this picture for pyrrolidinium<sup>431</sup> and ammonium<sup>432</sup> AILs.

While ion anisotropy may play a role in peak formation, the traditional interpretation of IL scattering data is still widely accepted. In X-ray scattering experiments, the polar domains are known to be the principle scattering units in the liquid phase. Thus, increasing the length of the cation's alkyl chain effectively lowers the concentration of scattering centers in real space with increasing alkyl chain length. This should reduce the peak intensity with alkyl chain length, indicating a less well-ordered system. However, every experimental and computational study has observed the reverse; the peak becomes more pronounced with ion amphiphilicity. For neutron scattering events, the situation is more complicated; yet Hardacre et al.'s data for AILs<sup>422</sup> (and other data for PILs<sup>233,425,428</sup>) are consistent with the expected bulk spacing of a sponge-like L<sub>3</sub>-bicontinuous phase; it is well-established that the scattering peak L<sub>3</sub>-phase is a gauge for bulk self-assembly due to surfactant amphiphilicity.<sup>433</sup>

What is the smallest example of ion self-assembly for an IL? Clear evidence of a bicontinuous nanostructure in EAN (ethyl alkyl chain) was demonstrated in two complementary small angle neutron scattering (SANS)<sup>434</sup> and large angle X-ray scattering (LAXS)<sup>435</sup> papers, which showed structure peaks at low  $Q$  consistent with twice the size of the ion pair dimension. Subsequent neutron diffraction and EPSR simulations have elucidated the nature of this nanostructure in these and a range of

primary alkylammonium PILs (ethyl-, ethanol-, propyl-, and butyl-ammonium cations with nitrate, formate, hydrogen sulfate, or thiocyanate anions).<sup>233,425,427,428,436</sup> All of the amphiphilic PILs self-assemble into bicontinuous, sponge-like nanostructures, with ordered domains of polar and apolar groups. Non-amphiphilic ILs with an ethanolammonium cation formed a clustered morphology,<sup>233</sup> which is broadly consistent with a clathrate-nanostructure inferred by Iglesias et al.<sup>437</sup> Similar conclusions have also been reached via MD simulations of PILs combined with XRD.<sup>438,439</sup>

Evidence of mesoscopic nanostructure in PILs is seen across long and short length scales in the bulk (cf., Figure 13), as well as in the raw scattering data. The PIL nanostructure is found to be largely insensitive to anion type, and becomes more pronounced with increasing cation alkyl chain length.<sup>428</sup> This is perfectly consistent with X-ray data<sup>354</sup> but shows that the scattering data can be explained via non-micelle like organization. On a related note, the ethyl moiety appears to be the smallest alkyl chain that induces self-assembled structure. Ab initio MD simulations<sup>440</sup> of the molten salt methylammonium nitrate (mp 110 °C) revealed no evidence of methyl–methyl aggregation characteristic of self-assembly.

In a further analogy to surfactant mesophases, the area ratios of the respective domains  $a_{\text{alkyl}}/a_{\text{polar}}$  were shown to be a useful predictor of self-assembled morphology in PILs.<sup>428</sup> The  $a_{\text{alkyl}}/a_{\text{polar}}$  was used in place of the well-established packing parameter

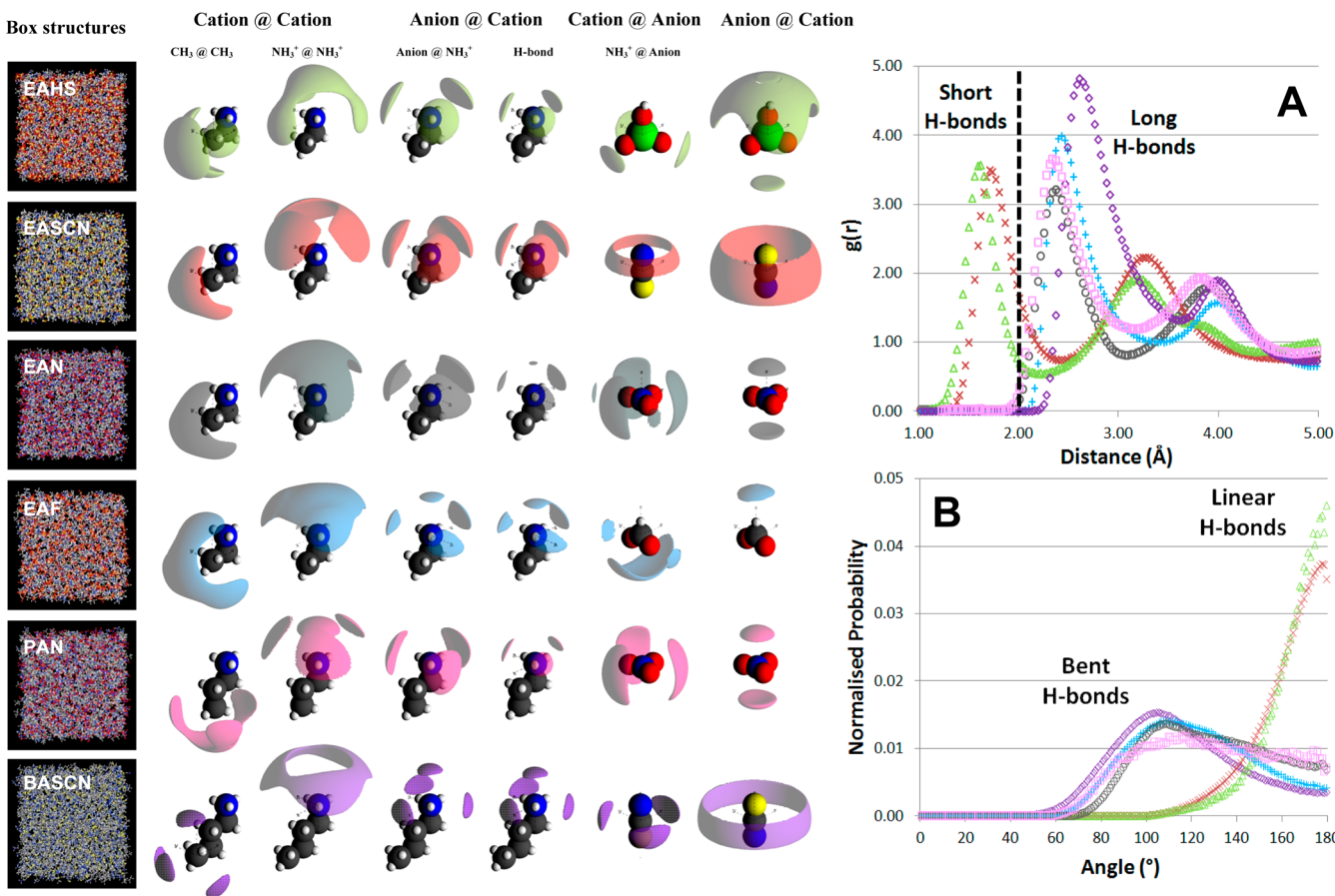


**Figure 13.** Nanostructure in primary alkylammonium protic ILs EAHS (green ▲), EASCN (red ×), EAF (blue +), EAN (●), PAN (pink ■), and BASCN (purple ◆). Column 1 (box structures), column 2 (cation@cation (uncharged@uncharged)), column 3 (cation@cation (charged@charged)), column 4 (anion@cation (charged@charged)), column 5 (anion@cation (H-bonding)), column 6 (cation@anion (charged@charged)), column 7 (anion@anion (charged@charged)). Column 8 (A)  $g(r)$  data and (B) angular distributions for H-bonding interactions in the PILs. The sdf plots in columns 2–7 show 20% probability surfaces. Reproduced with permission from refs 427 (Copyright 2013 Wiley-VCH Verlag GmbH & Co. KGaA) and 428 (Copyright 2014 American Chemical Society).

for surfactant self-assembly<sup>91,92</sup> because PILs are purely ionic media and not dissolved in a second solvent. As expected for sponge-like bicontinuous structures with near-zero mean curvature,<sup>441</sup>  $a_{\text{alkyl}}/a_{\text{polar}}$  values for all PILs varied little and were near 1. This suggests the polar and apolar groups can interpenetrate into two continuous subvolumes, and lies very far from the situation expected for spherical micelles or clusters of nonpolar alkyl chains, where  $a_{\text{alkyl}}/a_{\text{polar}} < 1/3$  or locally cylindrical nonpolar domains for which  $1/3 < a_{\text{alkyl}}/a_{\text{polar}} < 1/2$  (or indeed from the inverse structures of isolated polar domains with  $a_{\text{polar}}/a_{\text{alkyl}} < 1/3$ , or locally cylindrical ionic channels with  $1/3 < a_{\text{polar}}/a_{\text{alkyl}} < 1/2$ ). A packing area ratio near 1 is, however, perfectly consistent with a locally planar bilayer nanostructure analogous to a surfactant sponge or L<sub>3</sub> mesophase.<sup>442–444</sup>

Recently, Castner et al.<sup>445,446</sup> and Shimizu and co-workers<sup>447–449</sup> deconvoluted the total contribution of each ion–ion correlation to the X-ray scattering spectra of several different AILs. The measured structure factor was shown to be a complex combination of many different cation–cation (head–head, head–tail, tail–tail), anion–anion, and cation–anion correlations, any of which may contribute a positive or negative scattering amplitude at different length scales. In general, the lowest  $q$  feature could be attributed to real space distances between ions of the same charge, while the second peak is mostly due to ions of opposite charge. Subsequent features in the

diffraction spectra ( $>3 \text{ \AA}^{-1}$ ) were shown to be intramolecular in nature. These results are consistent with experimental observations of Hardacre et al., but arrive at the mesoscopic model for IL bulk structure because the uncharged cation alkyl tails are aggregated together.

Russina and Triolo recently provided new experimental evidence for the mesoscopic model by comparing the SAXS profiles of [C<sub>6</sub>mim][NTf<sub>2</sub>] and its ether-based counterpart [C<sub>1</sub>OC<sub>2</sub>OC<sub>1</sub>mim][NTf<sub>2</sub>]<sup>450,451</sup> and later extended in a more systematic study of [C<sub>n</sub>mim][NTf<sub>2</sub>] ILs ( $n = 3, 6, 9$ ) and their ether analogues.<sup>451</sup> As these ILs are isoelectronic, the X-ray scattering for core electrons should be identical. However, a clear bulk structure peak at low  $q$  is evident in the alkyl-based ILs but not when ether groups were present. This suggests the bulk structural arrangements in the ILs are different. Because the polyether chain is relatively polar, the driving force for segregation of uncharged groups is weak, and induce kinks along the chain to form a net clustered morphology, similar to that observed in PILs<sup>233</sup> and AILs.<sup>452,453</sup> Thus, only in the amphiphilic ILs is there a bicontinuous solvent structure.

Recent nuclear Overhauser effect (NOE) 2D NMR<sup>454</sup> experiments support these conclusions for phosphonium and ammonium isoelectronic homologues. Thus, the emergence of a correlation peak at low  $Q$  denoting the appearance of mesoscopic bulk structure is related to the presence of a sufficiently

amphiphilic ion, and leads to a bicontinuous arrangement of polar and apolar domains. Revelations of stronger domain segregation with symmetric imidazolium cations<sup>379,455</sup> are consistent with this, as it induces a more amphiphilic cation.

<sup>129</sup>Xe NMR spectroscopy has provided new evidence in support of the mesoscopic model, complemented by MD simulations.<sup>456</sup> A range of popular imidazolium ILs with [Cl<sup>-</sup>], [PF<sub>6</sub><sup>-</sup>], and [NTf<sub>2</sub><sup>-</sup>] anions were studied, and the chemical shift of the <sup>129</sup>Xe signal was used to study bulk structure. Xe is an effective probe of local ion arrangements. It can differentiate between different solvent atom types within the polar and apolar domains, and show how these domains evolve with changes in IL structure. Similar experiments by others groups<sup>457</sup> have shown the broad applicability of this technique to investigate IL structure, although the latter study did not accompany their NMR experiments with MD simulations. This led them to conclude the IL bulk was “cage-like” rather than mesoscopic structure.

X-ray photoelectron spectroscopy (XPS) experiments by the License group have probed the electronic environment (binding energies) of elements in pyrrolidinium-<sup>458</sup> and amino acid-<sup>459</sup> based ILs, as well as of organic reactions in ILs.<sup>460</sup> Notably, the length of the cation alkyl chain was shown to have little effect on the electronic environment of the charged moieties. This means that the electrostatic interactions in the polar domain are largely unaffected by changes in the apolar domain.

### 3.4. Novel Ion Types That Self-Assemble

**3.4.1. Fluorous ILs.** Replacing a hydrocarbon group with the corresponding fluorinated species has a long and interesting history in colloid science<sup>461–463</sup> and chemistry generally,<sup>464,465</sup> because it can induce changes in structure. ILs are no different. Several groups have shown that fluorous analogues of both PILs<sup>466,467</sup> and AILs<sup>382,468–470</sup> are more structured than their nonfluorous counterparts. X-ray scattering,<sup>466–468</sup> NMR,<sup>468</sup> and MD simulations<sup>382,469–471</sup> indicate that tricontinuous nanostructures are formed with fluorous ILs consisting of (1) polar domain of charged groups, (2) apolar domain of hydrocarbon, and (3) fluorous domain of fluorocarbon moieties (cf., Figure 14). Further evidence for this structure was noted in the thermal behavior of these ILs.<sup>469</sup> Overall, these results parallel reports of complex tricontinuous domains in liquid crystals.<sup>472</sup>

Although far fewer papers have dealt with fluorous ILs, a number of key molecular effects have been observed in relation to structure. First, to produce a well-defined fluorocarbon domain, the fluoroalkyl chain must be approximately two carbons longer than for the formation of hydrocarbon domains.<sup>466,467</sup> This is likely because the fluorocarbon and hydrocarbon groups are partially miscible with each other in the bulk, analogous to segregation in mixed micelles.<sup>473</sup> Alternatively, the fluorocarbon group may be less solvophobic than the corresponding hydrocarbon, reducing drive for ions to self-assemble. Second, unlike most amphiphilic ILs, stronger segregation of the solvent domains can be induced by a hydroxyl group at the terminal position on the cation.<sup>466,467</sup> The origin of this in fluorous ILs is still unclear but likely related to the strong electronegativity of fluorine atoms. This in turn promotes stronger solvophobic segregation of the different chemical groups.

**3.4.2. Dicationic ILs.** Dicationic ILs are an interesting subset of ILs akin to bolaform<sup>474</sup> or gemini<sup>475</sup> surfactants.<sup>476</sup> Divalent cations produce much different structures,<sup>477–481</sup> dynamics,<sup>478,482</sup> and thus solvent properties<sup>483,484</sup> than corresponding

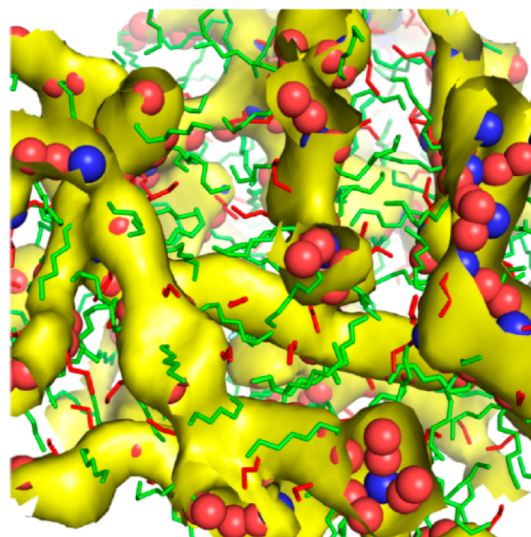


**Figure 14.** Snapshot of the tricontinuous nanostructure in a fluorous IL, butylammonium pentadecafluorooctanoate. Fluorous domains are composed of aggregated green fluorocarbon groups; apolar domains are the red hydrocarbon tails, both of which subsist between the undulating polar domain depicted in yellow. Red and blue spheres show oxygen and nitrogen atoms in the polar domain. Reproduced with permission from ref 471. Copyright 2014 American Chemical Society.

monovalent ILs. In principle, all of the popular cation structures used in monovalent ILs have a dicationic analogue. Studies have so far focused on AILs; we are not aware of any reports of protic dicationic ILs in the literature, likely because it requires transfer of two protons, which may be impossible to achieve (or explosive!) at room temperature. Recently, Davis et al. have characterized dicationic ILs with both protic and aprotic charge centers.<sup>126</sup> Interesting examples of magnetic<sup>485</sup> and polymerizable<sup>486</sup> dicationic ILs have been described in the literature.

As yet, there has only been one experimental study of the ion arrangements in pure dicationic ILs, although some work has been conducted on the interactions and crystal structures of high melting (molten) dicationic salts<sup>487,488</sup> as well as their mixtures with water.<sup>489,490</sup> Recently, SWAXS data for [C<sub>n</sub>(mim)<sub>2</sub>](NTf<sub>2</sub>)<sub>2</sub> (*n* = 3, 6, 12) were published and complemented by fitting with MD simulations.<sup>477</sup> The results are consistent with the larger body of simulation work on dicationic ILs,<sup>478–481</sup> which had been used to predict the expected *S*(*q*) that would be measured in scattering experiments. Bulk structure was shown to depend principally on the “spacer” alkyl chain length separating the cation charge centers, consistent with findings for monovalent PILs and AILs.<sup>363,428,491</sup> This is shown in Figure 15.

Interestingly, the bulk correlation peak at low *Q* is not as pronounced for monocationic ILs, and only emerges once the alkyl chain length is  $\geq 12$ . Anions were shown to have weak contributions toward bulk structure; they strongly interact with the positively charged headgroups, leaving a void of ion density around the alkyl groups (cf., Figure 15). In general, when the alkyl “spacer” group is short, a divalent cation has no significant effect on bulk mesostructure as compared to the monovalent cation IL. Differences arise when the alkyl “spacer” is long, due to the lower entropy, which may adopt a linear (majority) or folded (minority) conformation. This shows that the mesoscopic model of polar/apolar domains holds for dicationic ILs, although a more curved topology is formed.<sup>477,481</sup>

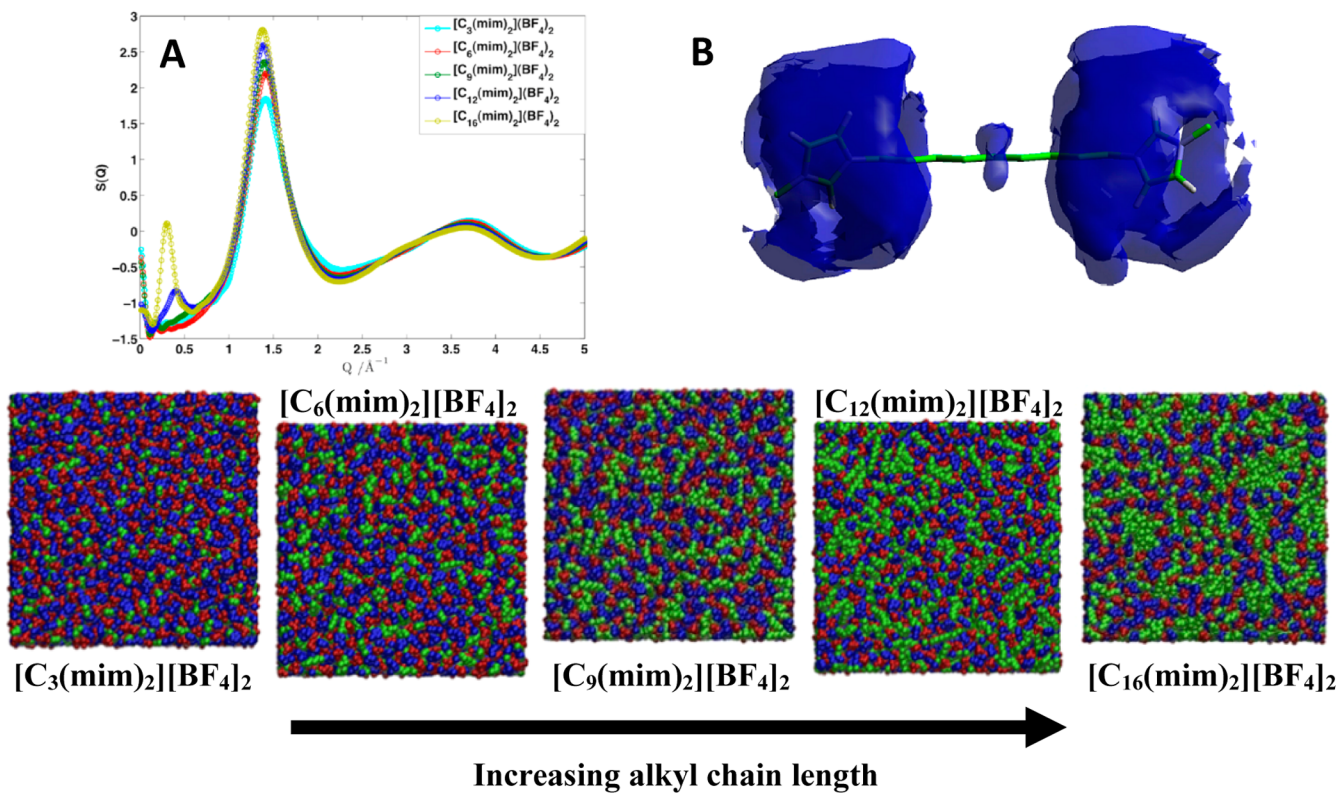


**Figure 15.** Nanostructure in dicationic ILs. (A) Predicted structure factor,  $S(q)$  between  $0\text{--}5.0 \text{ \AA}^{-1}$  from MD simulations for the dicationic  $[\text{C}_n(\text{mim})_2][\text{BF}_4]_2$  ( $n = 3, 6, 9, 12, 16$ ). (B) Spatial distribution functions of  $\text{PF}_6^-$  anion ordering around  $[\text{C}_9(\text{mim})_2]^{2+}$  cation at 450 K. The surface is drawn at 6 times the average ion density, and the lobes are localized around the charged imidazolium headgroups. Bottom row: Snapshots of bulk nanostructure of  $\sim 1000 [\text{C}_n(\text{mim})_2][\text{BF}_4]_2$  ( $n = 3, 6, 9, 12, 16$ ) ion pairs from MD simulation. Blue spheres indicate cationic groups, green spheres are the alkyl “spacer” chains, and red spheres are the anions. Reproduced with permission from refs 479 (Copyright 2012 American Chemical Society) and 481 (Copyright 2013 American Chemical Society).

We are not aware of any studies that examine structure or nanostructure in dianionic ILs. This represents an important extension to this work and would make an interesting comparison to both dicationic and monovalent ILs. Similarly, extensions to trimeric or tetrameric cations or anions should affect both IL structure and dynamics as is seen with oligomeric amphiphiles,<sup>492</sup> and yield novel liquid and solvent properties.

**3.4.3. Polymeric ILs.** ILs have proven to be promising media for polymer self-assembly<sup>147,148,150,493–498</sup> and polymer dispersions, with many interesting applications being explored.<sup>499–501</sup> Recently, there has been some interest in modifying the structure of one of the IL ions so that the liquid is itself polymerizable. These so-called polymeric ionic liquids or poly(ILs) are a versatile class of polyelectrolytes, combining many of the advantages of ILs and the native polymer. A broad range of cationic and anionic poly(ILs) can be made as homopolymers and copolymers of various architectures using polymerizable ion analogues of common aprotic, dicationic,<sup>486</sup> or magnetic<sup>502</sup> ILs. Moreover, all of the well-known free-radical and controlled or “living” polymerization (ATRP, RAFT, ROMP) techniques have been used to prepare poly(ILs). Comprehensive surveys of these materials are available.<sup>137,503,504</sup>

For the purposes of this Review, poly(ILs) represent a novel self-assembling class of IL solvents that form meso- and nanoscale macromolecular architectures with domain sizes up to an order of magnitude larger than common PILs or AILs. Highly ordered and tunable poly(IL) nanoparticles can also be prepared.<sup>505</sup> Like conventional polymer nanostructures, the organization of poly(ILs) is often temperature dependent and is

strongly influenced by the sample preparation. For example, Webber et al. observed lamellar and hexagonally close-packed cylindrical structures in block copolymers in poly(styrene-*b*-4-vinylbenzylalkylimidazolium)  $[\text{NTf}_2]$ , with domain sizes between 39 and 42 nm.<sup>506</sup> The macroscopic ionic conductivity was strongly influenced by the degree of internal order; more strongly connected domains resulted in increased conductivity and vice versa. Interestingly, the lamellar domain sizes of poly(ILs) can be simply adjusted by ion exchange,<sup>507</sup> which is near impossible to achieve in conventional ILs.

While atomic resolution of structures has not been determined for a poly(IL), it is likely that the same factors that govern ion self-assembly in conventional ILs operate in these systems. However, considerations related to packing and chain reptation<sup>508</sup> are likely to be more important, just as they are in conventional polymer self-assembly. Currently, there have been no investigations of the dynamics of poly(ILs). In general, we foresee a bright future for research in poly(ILs) structure, as there are many simple structural effects (block sizes, branching, polymer blends, etc.) awaiting (experimental/theoretical) investigation and a wealth of interesting phase behavior has been reported in similar polyelectrolyte blends.<sup>509–511</sup> This will open more applications of poly(ILs), in the design and scaffolding of new mesostructured materials.

**3.4.4. Magnetic ILs.** Atoms with strong magnetic moments can be incorporated into IL ions. When this occurs, a magnetic interaction is induced in the bulk and a so-called magnetic IL is formed,<sup>136</sup> akin to a ferrofluid.<sup>145,146,512–514</sup> First discovered by Hayashi and Hamaguchi for  $[\text{C}_4\text{mim}][\text{FeCl}_4]$ ,<sup>515</sup> magnetic ILs

are an established, if underused, class of ILs, and to date only the anions have been functionalized with a paramagnetic atom/group.<sup>136,516–519</sup> In particular,  $[\text{FeCl}_4]$ -based magnetic ILs appear to be well disposed to replace  $\text{FeCl}_3$  in Grignard or Friedel–Crafts reactions, as either the solvent, catalytic additive, or both.

Magnetic ILs can be manipulated and recovered by external magnetic fields,<sup>520–522</sup> which can be exploited to template different polymer nanostructures.<sup>523</sup> Surprisingly, memory effects in the bulk liquid have been observed,<sup>524</sup> and the ion ordering changes as a function of pressure.<sup>525</sup> At interfaces, they retain the capacity to self-assemble and interact much like conventional surfactants at interfaces,<sup>526</sup> and so should possess well-defined structure in the bulk, although programmed by a different suite of ion–ion interactions.

Only a handful of studies have examined structure in magnetic ILs, with many of these aimed at characterizing ion speciation in the bulk. Raman scattering and ab initio calculations have been used to study equimolar mixtures of  $[\text{C}_4\text{mim}][\text{Cl}]$  and  $\text{Fe}^{\text{II}}\text{Cl}_2$  or  $\text{Fe}^{\text{III}}\text{Cl}_3$ , to prepare a magnetic IL  $[\text{C}_4\text{mim}][\text{Fe}^x\text{Cl}_x]$  with mixed oxidation states. The results showed both  $[\text{FeCl}_4]^-$  or  $[\text{FeCl}_4]^{2-}$  anions were present with  $[\text{FeCl}_4]^{2-}$  dominant, and adopt a tetrahedral geometry.  $[\text{Fe}_2\text{Cl}_7]^-$  anions were also found when  $\text{Fe}^{\text{II}}\text{Cl}_2$  was added in excess.<sup>527</sup>

de Pedro et al.<sup>528</sup> examined  $[\text{C}_2\text{mim}][\text{FeCl}_4]$  using Raman spectroscopy, which indicated that  $[\text{FeCl}_4]^-$  is the main iron-containing species present, likely in a tetrahedral geometry. XRD measurements were also performed but adequate crystal samples could not be obtained; while Bragg peaks were evident in the diffraction patterns of frozen  $[\text{C}_4\text{mim}][\text{FeCl}_4]$ , they were absent in liquid  $[\text{C}_2\text{mim}][\text{FeCl}_4]$ . This is likely a consequence of instrument resolution rather than the absence of structure. The authors postulated that the liquid phase was composed of a periodic arrangement of ion-pairs, leading to long-range antiferromagnetic ordering.

Freeze-fracture transmission electron microscopy (FF-TEM) experiments indicate a globular nanostructure in  $\text{FeCl}_3/[\text{C}_4\text{mim}]\text{Cl}$  mixtures.<sup>529</sup> The size of these domains was found to be greater than 10 nm, which is much larger than expected for similar nonmagnetic ILs. This is likely related to sample preparation/pretreatment for FF-TEM rather than bulk nanostructure.

Pure crystals of magnetic ILs have been obtained by several groups,<sup>530–533</sup> enabling their structures to be characterized via X-ray crystallography (XRC). Evidence of amphiphilic self-assembly is noted in the crystal structures as they form layered crystal lattices with interlayer distances of  $\sim 6 \text{ \AA}$ , similar to the crystal arrangement of nonmagnetic AILs. A typical example of this for  $[\text{Pyrr}_{14}][\text{FeCl}_4]$  is shown in Figure 16.

Magnetic ILs are more susceptible to manipulation via external magnetic fields than external electric fields. In fact, Garcia-Saiz et al.<sup>525</sup> showed that the layered magnetic IL bulk structure is responsible for three-dimensional magnetic ordering, as it enabled higher-order exchange of magnetic interactions between the planes. This means that the magnetic force is screened to a much lesser extent than electrostatic interactions in the bulk. Assembling of ions under the action of magnetic fields offers a powerful tool to control solvent structure, and may even enable particular ion arrangements to be “pinned”.

There is enormous potential to explore the nature and consequences of ion self-assembly in magnetic ILs. While this has yet to be proven experimentally in the bulk liquid, the ordering appears to be more pronounced than in conventional ILs and to

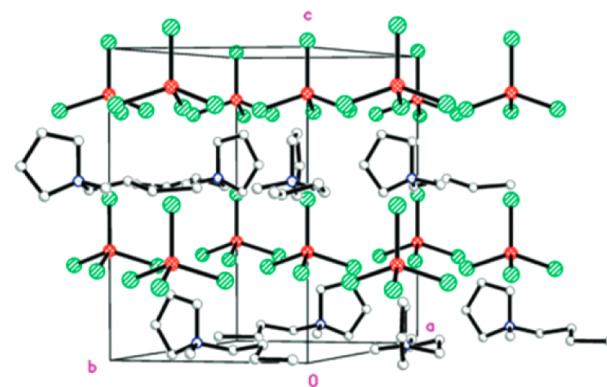


**Figure 16.** Molecular packing of the magnetic IL methylbutylpyrrolidinium tetrachloro-ferrate(III)  $[\text{Pyrr}_{14}][\text{FeCl}_4]$  from XRC. Atom colors are Fe (red), Cl (green) and C (white). Hydrogens are not shown. Reproduced with permission from ref 531. Copyright 2010 PCCP Owner Societies.

have a strong influence on the macroscopic properties of the fluid.

**3.4.5. Solvate ILs.** A well-established design feature of ILs is to seek large ions with the electrostatic charge delocalized and/or sterically hindered. One consequence of this is that most ILs ions are noncoordinating species, and do not spontaneously form larger,  $[\text{C}_x+\text{A}_y]$ -type complexes held together by coordinate covalent bonds (tetrahedral, trigonal bipyramidal, octrahedral, etc.). This means that, while IL ions may resemble ligands, the rich body of structures common to inorganic chemistry<sup>534–536</sup> is absent in the IL bulk as electron transfer between anion and cation is not facilitated. However, coordination complexes can themselves be used as ILs ions,<sup>537</sup> including mercuric ions<sup>538</sup> or the famous ferrocenium cation.<sup>539</sup>

Recently, there has been a growing body of work on such “solvate” or “chelate” IL salts, first proposed by Angell et al.<sup>30</sup> These salts challenge traditional ways of thinking about ILs for a variety of reasons. First, divalent ions can be readily used. Also, molten salt hydrates such as  $[\text{Ca}(\text{H}_2\text{O})_4](\text{NO}_3)_2$  could be considered an IL, due to the stability of many metal aquo ions  $[\text{M}(\text{H}_2\text{O})_n]^{x+}$ .<sup>30,535,540</sup> A recent review by Watanabe et al.<sup>541</sup> discusses the nature and classification of these systems in some detail.

Apart from molten salt hydrates,<sup>540</sup> the first genuine solvate IL appears to have been prepared in 1991 by Rees and Moreno, who synthesized a liquid composed of monomeric barium bisalkoxide.<sup>542</sup> The liquid structure was thought to resemble classic macrocyclic crown ether complexes,<sup>543</sup> with the barium cation centrally coordinated by several anion oxygens. More recently, this has been extended by several groups with oligoether-carboxylate (TOTO),<sup>544–546</sup> trialkylammoniododecarbinate,<sup>547</sup> acetylacetones,<sup>548,549</sup> or glyme<sup>550–553</sup> species, usually coordinated to small, hard inorganic cations. The key structural features for these salts are related to the complexed ion (usually the cation), which must possess strong Lewis-acid chelating groups and be sufficiently flexible to induce multiple directional interactions with the charge center.

To date, only a handful of papers have examined the structure of these systems. Depuydt et al.<sup>554</sup> used XRC on  $\text{Ag}^+$ -containing ILs with melting points above room temperature. The crystals showed the metal ions were coordinated by multiple ligands depending on the  $\text{Ag}^+:\text{ligand}$  concentration, leading to ion pair or chain-like polymeric structures in the solid state. In 2013, Eilmes

and Kubisaik used quantum-chemical calculations and classical molecular dynamics simulations to study the structure of  $[TOTO^-]$ -based salts with alkali metal cations ( $Li^+$ ,  $Na^+$ ,  $K^+$ ).<sup>555</sup> This showed a cross-linked structure in the bulk, with zones of metal ions each coordinated to 4–6 carboxylates on multiple anions (cf., Figure 17). The anion–cation interaction strength was sensitive to cation radius, and decreased in the order  $Li^+ > Na^+ > K^+$ .

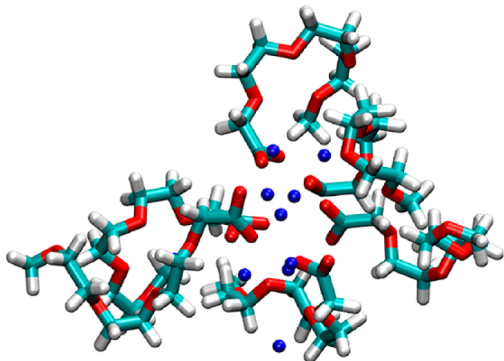


**Figure 17.** Cross-linked structure of  $Na[TOTO]$  solvate IL based on MD simulations. Reproduced with permission from ref 555. Copyright 2013 American Chemical Society.

There are still many unanswered structural and dynamics questions regarding solvate ILs. In general, the field is ripe for X-ray and neutron scattering experiments, as well as computer simulation. The prevailing cross-linked model suggests that ion radius will be key to structure, as it is in macrocycles or other host–guest compounds.<sup>534–536</sup> In a different sense, ion packing is important because the cations are aggregated within a domain confined by multiple chelating species; changes in their shape and thus ion coordination number will influence the nature and extent of cross-linking. Preliminary evidence for this has been observed in comparisons of Walden plots for  $[TOTO^-]$ -based ILs with choline (Ch), tetraalkylammonium (TAA, with ethyl, propyl, butyl groups), or  $Na^+$  cations; Ch $[TOTO]$  and TAA $[TOTO]$  behave as “good ILs”, whereas Na $[TOTO]$  is a “poor IL”.<sup>544</sup> This is likely because the cations in all of the former ILs form a weaker cross-linked structure than in Na $[TOTO]$ . Finally, variation in the functional groups both at the end position and along the backbone of the chelating groups should

influence bulk structure, and we need only look to the rich diversity in inorganic or bioinorganic chemistry for examples of possible new ILs awaiting discovery and characterization.

### 3.5. Effect of External Variables

**3.5.1. Temperature.** The effect of temperature on PILs and AILs nanostructure has been examined via numerous experimental and theoretical techniques. For 1-methyl-3-octyl-imidazolium tetrafluoroborate ( $[C_8mim][BF_4]$ ), the level of structure decreased between 90 K (glassy phase) and 290 K (liquid phase), as is expected for molecular liquids<sup>556</sup> (cf., Figure 18A). This was noted from the change in appearance of the X-ray diffraction correlation peak, which became broader, and at shorter length scales with increasing temperature.<sup>363</sup> Similar findings have been reported for pyrrolidinium-based ILs in systematic measurements by Santos et al.<sup>445</sup> These results compare well with the MD simulations of many groups,<sup>358,385</sup> who calculated a subtle temperature dependence of partial structure factors.

MD and X-ray scattering data surprisingly showed that  $[P_{14,6,6,6}][NTf_2]$  becomes more structured as it is heated between 150 and 400 K, the bulk correlation peak becoming sharper and more pronounced (cf., Figure 18B).<sup>557</sup> This is somewhat counterintuitive as other ILs, molten salts<sup>558</sup> and liquids generally<sup>556</sup> become more disordered with increasing temperature. Subsequent analysis by Hettige et al.<sup>559</sup> demonstrated the origin of this effect by deconvoluting the opposing contributions of the polar and apolar groups to the correlation peak. In short, polar domains were found to become more organized at higher temperatures, whereas the apolar groups became less structured. It was speculated that other ILs may behave in a similar manner.

Hamaguchi et al.<sup>560</sup> developed a novel Raman spectroscopic technique to monitor IL heterogeneity by following the cooling of a photoexcited S1-*trans*-stilbene probe molecule. For molecular solvents,<sup>561</sup> a linear relationship between *cis*–*trans* cooling rates (microscopic effect) and thermal diffusivity (macroscopic effect) is observed. A similar plot could not be produced for AILs, suggesting the ILs are thermally inhomogeneous on the probe’s length scale (cf., Figure 18C). As the apolar groups used by Hamaguchi et al. (ethyl, butyl) are too small relative to the charged groups to form a well-defined mesoscopic nanostructure, the Raman response likely highlights charge ordering, rather than a preferential solvation in a bicontinuous network. Later coherent anti-Stokes Raman scattering (CARS)

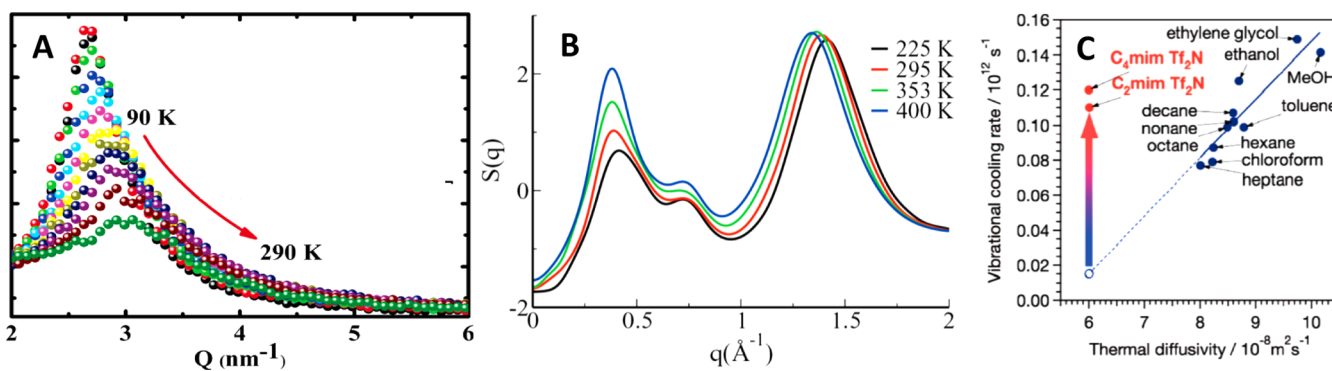


**Figure 18.** Evidence for solvent heterogeneity from temperature effects. Comparison of X-ray diffraction spectra for (A)  $[C_8mim][BF_4]$  and (B)  $[P_{14,6,6,6}][NTf_2]$  at different temperatures. (C) Plot of vibrational cooling rate of excited S1 *trans*-stilbene versus thermal diffusivity; molecular liquids show a linear relationship, while  $[C_4mim][NTf_2]$  and  $[C_2mim][NTf_2]$  do not. Reproduced with permission from refs 363 (Copyright 2007 American Chemical Society), 557 (Copyright 2014 AIP Publishing LLC), and 560 (Copyright 2007 American Chemical Society).

data by this group suggested ILs [ $C_n\text{mim}$ ][ $\text{PF}_6^-$ ] ( $n = 4, 6, 8$ ) have mesoscopic structure, but the possible size range 10–100 nm is too large for meaningful conclusions about ion arrangements.<sup>562</sup>

There are fewer studies of the structure of PILs as a function of temperature, and over a narrower temperature range. Greaves et al.'s X-ray scattering data<sup>354</sup> showed a slight decrease in peak 2 as the sample was heated between 25 and 50 °C, corresponding to a ~1 Å increase in the correlation length. This was attributed to a swelling of the alkyl chains in the micelle structure. Conversely, neutron diffraction patterns for two of these PILs (EAN and EtAN) was invariant over the same temperature range,<sup>233</sup> suggesting that the liquid nanostructure was almost unaltered over this range.

**3.5.2. Electric Field.** Structural changes in an IL subjected to an external electric field were predicted to occur on the basis of MD simulations by Wang,<sup>563</sup> who showed that the native bicontinuous bulk structure of [ $C_{12}\text{mim}$ ][ $\text{NO}_3^-$ ] is first disrupted and then reorganized into nematic-like order with increasing field strength. This was attributed to ion alignment in the direction of the external field. Similar conclusions were reached in a follow-up simulation for a wider variety of AILs<sup>564–566</sup> and IL+water mixtures.<sup>567–569</sup> These findings have important implications for ILs in electrochemistry, or for films confined between charged walls.<sup>570</sup> So far, this effect on the bulk IL structure has not been verified by experimental measurements. It remains questionable whether ILs will behave in such a way under the moderate electric fields used in real world applications; while the ion dynamics may change in accordance with classical electrolyte theories,<sup>571</sup> Debye lengths in ILs are very small, ~0.1 nm, and related experiments at the IL–electrode interface<sup>572–574</sup> show structural changes at most ~5 nm from the surface (see section 4.4).

**3.5.3. Pressure.** Some recent evidence suggests that IL solvent structure is subtly altered by application of an external pressure, as is the case for molecular liquids.<sup>575,576</sup> MD simulations show the cation chain conformation changes from *anti* to *gauche* in [ $C_4\text{mim}$ ][ $\text{PF}_6^-$ ],<sup>577</sup> consistent with Raman spectra of both this IL<sup>578,579</sup> and [ $C_4\text{mim}$ ][ $\text{BF}_4^-$ ].<sup>580</sup> The [ $\text{NTf}_2^-$ ] anion shows analogous behavior when placed under high pressure.<sup>581</sup>

Consideration of these pressure effects naturally leads to the question of how the self-assembled nanostructure changes. Faria et al.<sup>582</sup> reported changes in Raman spectral bands of PAN associated with modes due to both the polar and the apolar groups as the  $\text{PA}^+$  cation changes from *anti* → *gauche*, hinting at mesostructural changes in the liquid. They even postulated that the PIL may become microscopically heterogeneous at sufficient pressure, which would open structural studies based on optical or micro-Raman imaging techniques.

Other indirect evidence of pressure altering IL structure has been noted at the solid interface. IR spectroscopy of gold powder dispersions in [ $C_2\text{mim}$ ][ $\text{NTf}_2^-$ ] observed changes in spectral bands for H-bonding protons on the imidazolium ring.<sup>583</sup> This may be consistent with the IL's near surface structure altering upon application of an external pressure.

### 3.6. Solvation Structures in ILs

In many applications and processes, ILs are not used as pure liquids, but as solvents for one or more dissolved solutes, making IL solvation an important area of research.<sup>24,75</sup> ILs can display excellent solvency for a wide range of substances,<sup>584–588</sup> including those that are difficult to dissolve in common solvents.<sup>589–591</sup> In fact, this can be a drawback in fundamental research as it makes ILs susceptible to contamination,<sup>592</sup> which

can lead to profound changes in behavior.<sup>593</sup> Notably, the reactivity of materials dissolved in ILs is not the same as in a molecular liquid,<sup>24,594–596</sup> due to the intermolecular forces that produce a solvent nanostructure. Thus, the effect of dissolution of a solute on IL nanostructure is a key to future integration of these solvents into industry.

**3.6.1. Uncharged Solutes.** So far, this area has mostly focused on nanostructure in ILs with uncharged solutes. Many different groups have examined the structural effect of water,<sup>269,531,426,597–615</sup> alkanes,<sup>330</sup> alcohols (methanol,<sup>610,616–618</sup> ethanol,<sup>330,466,610,617,619,620</sup> propanol,<sup>330,617</sup> butanol,<sup>330,466,617,619</sup> higher order<sup>619</sup>), Brønsted acid/bases,<sup>331</sup> glycerol,<sup>621</sup> propylene glycol,<sup>622</sup> diethylene glycol,<sup>623</sup> acetonitrile,<sup>624–627</sup> carbon disulfide,<sup>628–630</sup> aromatic molecules,<sup>278,631–634</sup> polyaromatic hydrocarbons,<sup>635</sup> benzyl methacrylate,<sup>636</sup> porphyrins,<sup>637</sup> ferrocene,<sup>638,639</sup> DMSO,<sup>607,640,641</sup> phytantriol,<sup>642</sup>  $\text{C}_{60}$ ,<sup>643,644</sup> carbon nanotubes,<sup>645</sup> simple gases ( $\text{Ar}$ ,<sup>646</sup>  $\text{O}_2$ ,<sup>646,647</sup>  $\text{N}_2$ ,<sup>646,647</sup>  $\text{CO}_2$ ,<sup>646–654</sup> sc- $\text{CO}_2$ ,<sup>655,656</sup> methane<sup>646,647</sup> ethane,<sup>647,657</sup> ethylene,<sup>647,658</sup> butane,<sup>657</sup> phosphine,<sup>659</sup> carbene<sup>660</sup>), various hydrophobic and hydrophilic small molecules,<sup>661</sup> nonionic surfactants,<sup>662,663</sup> polymers (PEG,<sup>496,498,664–666</sup> Pluronics<sup>153,667</sup>), glucose,<sup>668–671</sup> or cellulose<sup>672–677</sup> in both PILs and AILs, examples of which are presented in Figure 19. In most cases, studies have been performed at one, usually low, solute concentration.

Across all of these papers, IL solvents generally resist changes in their nanostructure by accommodating these solutes in either the polar or the apolar domains, depending on solute size, polarity, and amphiphilicity. Thus, a different, but related, nanostructure<sup>426</sup> or population of nanoscale objects<sup>466</sup> forms in the bulk. If the solute cannot be so easily accommodated, a clathrate-type arrangement<sup>631</sup> can form. With increasing concentration of a second component, a transition from contact ion pairs to (solvent-)separated ion pairs and then molecularly dispersed ions has been suggested to occur,<sup>269</sup> akin to the well-understood behavior of ions in molecular liquids.<sup>678–681</sup> As expected, IL ions with sufficiently long alkyl chains will form micelles at high water concentrations, because they resemble ionic surfactants.<sup>613–615,682–685</sup> Perhaps a more interesting question is how are IL micelles solvated<sup>686</sup> as compared to conventional surfactant aggregates<sup>687</sup> and what is the smallest IL amphiphile that forms micelles in aqueous solution?

**3.6.2. Charged Solutes.** There are relatively few studies of the nanostructure of ILs + charged solutes. Inorganic salts show peculiar solubility in ILs. For example, in EAN,  $\text{LiNO}_3$ ,  $\text{KNO}_3$ ,  $\text{Ca}(\text{NO}_3)_2$ , and  $\text{Al}(\text{NO}_3)_3$  are all highly soluble, and yet  $\text{NaNO}_3$  is insoluble.<sup>688</sup> To date, the majority of these solutions have focused on  $\text{Li}^+$  solvation in AILs,<sup>689–696</sup> motivated by interest in  $\text{Li}^+$  batteries.<sup>697</sup> Other papers have characterized the speciation of alkali metal<sup>698</sup> and alkaline earth ions,<sup>699,700</sup> f-block compounds,<sup>701,702</sup> biomolecules (amino acids,<sup>703</sup> peptides,<sup>704–706</sup> or proteins<sup>707–713</sup>), or  $\text{Ru}^{2+}$  dyes<sup>714</sup> aimed at nuclear fuel processing, biopreservation, or organic photovoltaics, respectively. The results show that small, charged solutes completely dissociate in the bulk with the solute ions embedded in the polar domains of the IL nanostructure. For example, inorganic salts dissolved in EAN<sup>688,715–717</sup> have a negligible effect on the solvent nanostructure, because (1) EAN's nanostructure is robust, (2) solute ions were small as compared to the dimensions of the polar domain, or (3) solute ions were dissolved at too low concentrations. There is some evidence to suggest alkaline earth cations can induce more pronounced solvent structure than alkali metals when dissolved in ILs, due to

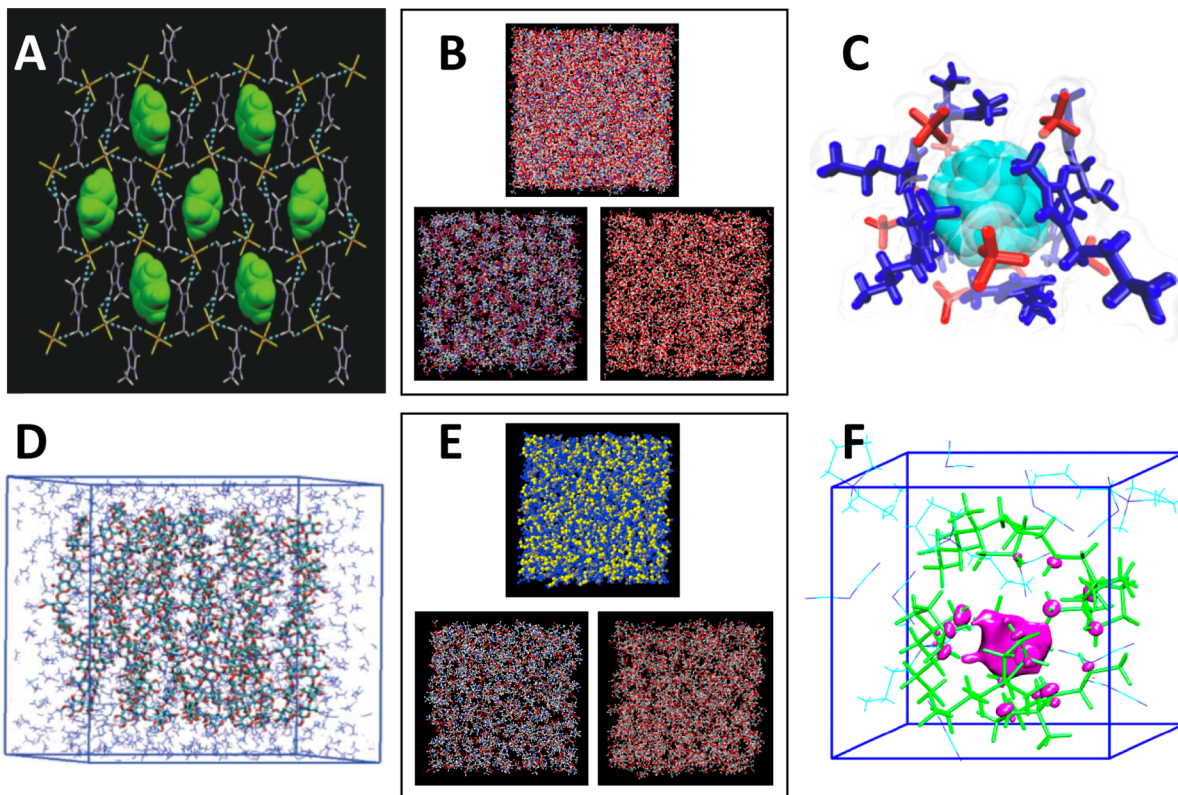


**Figure 19.** Solvation structures in ILs. (A) Liquid clathrate formation in  $[C_1\text{mim}][\text{PF}_6]\cdot0.5C_6\text{H}_6$  (benzene highlighted in green). (B) Three representations of the mesh-like nanostructure in EAN+ $\text{H}_2\text{O}$  1:6 mol:mol mixtures, top = all atoms, bottom left = EAN only, bottom right = water only. (C) Solvation of  $C_{60}$  in  $[C_4\text{mim}][\text{BF}_4]$  ( $[\text{BF}_4]^-$  = red,  $[C_4\text{mim}]^+$  dark blue,  $C_{60}$  = light blue). (D) Solvation of 15 cellulose chains in 990  $[C_4\text{mim}][\text{Ac}]$  ion pairs. (E) Three representations of the nanostructure in EAF+glycerol 50 vol % mixtures, top = polar (blue) and apolar (yellow) groups, bottom left = EAF ion pairs only, bottom right = glycerol only. (F) Pink cavity of an excess electron's spin density within  $[\text{Py}_{1,4}][\text{DCA}]$ . Figures reproduced with permission from refs 631 (Copyright 2003 Royal Society of Chemistry), 426 (Copyright 2012 Wiley-VCH Verlag GmbH & Co. KGaA), 643 (Copyright 2013 Elsevier), 677 (Copyright 2013 Royal Society of Chemistry), 621 (Copyright 2014 PCCP Ownership Societies), and 728 (Copyright 2015 American Chemical Society).

their divalent versus monovalent charge.<sup>718</sup> In other studies, dissolved  $\text{Mg}^{2+}$ <sup>699,700</sup> cations or transition metal ions ( $\text{Cu}^{2+}$ ,  $\text{Ag}^+$ , or  $\text{Zn}^{2+}$ )<sup>719–723</sup> formed coordination complexes with IL anions, and thus changed the local ion self-assembly in the bulk. This is reminiscent of metal ion chelating behavior in aqueous electrolyte solution or that described previously for solvate ILs. The situation for larger charged solutes such as proteins is more complicated, and to date no study has addressed both changes in solvent and biomolecule structure when dissolved in ILs.

Interesting recent extensions of this work include solvation of “dry” electrons,<sup>724–728</sup> protons,<sup>394</sup> or  $\text{H}_3\text{O}^+$  ions<sup>729</sup> in ILs using ab initio MD simulations. Similar to dissolution of small inorganic ions, these species show high affinity for the polar domains of the IL, and induce negligible reorganization of the solvent. Surprisingly, electrons could be localized on either anion or the cation, depending on the HOMO/LUMO gap between molecular orbitals. To understand things like the mechanism of IL (1) charge transfer, (2) proton transport, (3) interaction with radiation, or (4) questions of IL “pH”, “ $\text{pK}_a$ ”, and “acidity”,<sup>58,131,730,731</sup> more research in this area is required, with attention to all classes of ILs, not just aprotics.

Finally, nanoscale structure in pure ILs has often been suggested on the basis of the dissolved molecular,<sup>357,732–738</sup> charged,<sup>732,734,739</sup> or even radical<sup>740–742</sup> probes. While the findings are generally consistent with the mesoscopic model, there is ample evidence to suggest that selective solvation of the probe occurs depending on whether it prefers the polar or apolar

domain. Caution should thus be applied in the interpretation of molecular probe studies that report average solvent properties of inherently nanoheterogeneous media like ILs.

**3.6.3. IL Mixtures.** A special case of IL solvation is when the charged solute is another IL. IL mixtures represent an important extension to the field because solvent mixtures<sup>743</sup> and deep eutectic solvents<sup>744,745</sup> (in chemistry) or double salts<sup>68,746</sup> (in crystallography) sometimes outperform pure components for a given process and can form interesting bulk phase structures.<sup>747–751</sup> For a more wide-ranging discussion in IL mixtures, their properties, and applications, interested readers are directed to several excellent reviews.<sup>65–68</sup>

In general, the self-assembly of IL mixtures is underdeveloped as compared to that previously described for pure ILs, ILs+uncharged solutes, or ILs+molten salts. This is surprising as some of the earliest reported evidence in support of the IL self-assembly model was from optical Kerr effect (OKE) spectroscopy experiments on binary IL mixtures.<sup>752,753</sup> Since then, research has largely focused on (non)ideality of mixing,<sup>754–756</sup> physical and transport properties,<sup>757–760</sup> or general aggregation behavior,<sup>761–763</sup> all of which are consistent with pronounced internal solvent structure. MD simulations,<sup>764–769</sup> SWAXS,<sup>330</sup> IR,<sup>770,771</sup> NMR,<sup>772,773</sup> and XPS<sup>774</sup> have all been used to investigate organization of IL mixtures; however, it is difficult to make wider conclusions about the effect of structure on ideal/nonideal behavior due to the limited data set that encompasses both three-ion and four-ion systems and is largely focused on

AILs. The results indicate that the solvent mixture is different from the structure of the parent ILs, and that polar/apolar segregation of groups is possible. Notably, many cases of “ideal” mixing occur with systems that do not support self-assembly in the bulk. That is, all of the ions are of roughly the same size and nonamphiphilic. However, simulations indicate that binary mixtures of  $[C_6\text{mim}][\text{NTf}_2]$  and  $[C_2\text{mim}][\text{NTf}_2]$  are ideal,<sup>767</sup> yet there is mesoscale structure, albeit not as well-defined as in pure  $[C_6\text{mim}][\text{NTf}_2]$ . This suggests the dissolution of ILs with weakly amphiphilic ions (e.g.,  $[C_2\text{mim}][\text{NTf}_2]$ ) could be used to control the degree of self-assembly of amphiphilic systems (e.g.,  $[C_2\text{mim}][\text{NTf}_2]$ ) and vice versa. This means that it is possible to create strongly structured and weakly structured mixtures by blending ILs, similar to transitions in ternary microemulsions.<sup>775,776</sup>

### 3.7. Some Remarks on IL Dynamics

There have been a number of papers that propose mesoscopic structure in ILs based on techniques that probe ion dynamics or relaxation.<sup>478,777–783</sup> This is similar to implying bicontinuous structure from transient spatial fluctuations in the dynamic regime of microemulsions and colloidal gels.<sup>784–786</sup> In general, ILs show an unusually broad spectrum of non-Arrhenius ion dynamics. As there are no corresponding examples of molecular or complex liquids with similar viscosity, this is usually cited as further evidence toward the mesoscopic structure model of IL structure. However, care must be taken with this interpretation for ILs, as dynamic heterogeneity is not exclusive to structurally heterogeneous systems.<sup>787</sup> Supercooled water is structurally homogeneous but displays the characteristic nongaussian translation and rotational diffusion.<sup>788–790</sup> Indeed the laws of diffusion in model systems are more complicated than originally supposed,<sup>791</sup> and this may have implications for interpreting the dynamics of self-assembled systems. Recent conclusions by Lui et al., “the answer to the question of how polar are ionic liquids very likely depends on when you ask”,<sup>65</sup> are thus incomplete; how polar are ILs is related to both when and where the bulk phase is probed.

Signals in OKE spectroscopy experiments have been used as evidence for an inhomogeneous IL nanostructure on very short time scales. Giraud et al. adduced this from the unusually large number of functions required to fit the OKE spectra of ILs.<sup>792</sup> However, as argued by Chiappe,<sup>793</sup> this is not sufficient evidence for a mesoscopic bulk structure in isolation, and is most likely reflective of strong ion–ion interactions and a high degree of ion association. Later papers by Xiao et al. showed that, unlike molecular solvents, the low frequency intermolecular regions of the OKE spectra ( $200 \text{ cm}^{-1}$ ) of binary mixtures of  $[C_5\text{mim}][\text{NTf}_2]$  and  $[C_5\text{mim}]\text{Br}$  are additive sums of the pure ILs, consistent with ideal solution behavior. The result was explained in the context of the aforementioned MD studies by assuming partitioning of the IL mixture into local domains or “blocks” of the neat ILs in which the polar and nonpolar groups are segregated from one another.<sup>753,794</sup> Further indirect evidence was obtained from experiments with the pure components; while the bulk liquid densities are temperature dependent, OKE spectra were temperature independent.<sup>795</sup> This suggests inhomogeneity in the local densities of the bulk liquids, which could be explained by a mesoscopic solvent structure.

Similarly, indications of a solvent heterogeneity have been made from ion dynamics. Several quasi-elastic neutron scattering (QENS) data have shown long-range diffusional processes that could be attributed to solvent nanostructure.<sup>781,782,796–799</sup>

Likewise, NMR experiments in PILs reveal large, H-bonded aggregates with lifetimes shorter than characteristic time scales of ion diffusion.<sup>800</sup> More recently, femtosecond IR spectroscopy has compared excitation and relaxation modes of  $\text{N}^-\text{H}$  and  $\text{N}^-\text{H}$  covalent bonds in the ionic domain to C–H modes of the apolar domain in primary alkylammonium formate PILs.<sup>783</sup> Unlike alcohols, increasing the cation alkyl chain length had next to no effect on the polar groups dynamics. This is because cation amphiphilicity drives self-assembly (into bicontinuous structures); both the time scales of reorganization and activation barriers for equilibration of alkyl chains in the apolar domain were smaller and independent of the motion of polar moieties in the ionic domain.

In a comprehensive study by Turton and co-workers, EAN and PAN were studied using OKE and dielectric relaxation spectroscopy (DRS) techniques that are sensitive to nitrate anions and alkylammonium cation dynamics, respectively.<sup>255</sup> The solvent relaxation data did not follow the Stokes–Einstein–Debye model, but could only be explained by a network of cooperative H-bonds between  $\text{NH}_3^+$  protons and nitrate oxygens. Both of these results imply an inhomogeneous bulk structure for EAN and PAN, with the alkyl chains aggregated together, consistent with scattering and simulation models detailed previously. The small deviation from Arrhenius behavior suggested that the degree of aggregation of uncharged groups is low as compared to other long chain ( $C_8\text{--}C_{12}$ ) AILs.

Ion dynamics of a solvate IL,  $\text{Na}[\text{TOTO}]$ , has been investigated using Stokes shift<sup>801</sup> and DRS.<sup>546</sup> As compared to imidazolium AILs, ion dynamics were slow and showed near-Arrhenius behavior. The static dielectric constant for  $\text{Na}[\text{TOTO}]$  was intermediate between common PILs<sup>234,802</sup> and AILs.<sup>253</sup>

In Table 2 we map all of these reports of bulk structure for different ILs as a function of ion structure and alkyl chain length  $n$ .

## 4. THE STRUCTURE OF THE SOLID–IONIC LIQUID INTERFACE

The chemistry of solid–liquid interfaces is often very different from that of bulk liquids. This is because close to the interface, the structure and dynamics of solvent molecules are altered,<sup>872,873</sup> and continuum theories (that predict an unstructured bulk liquid) break down.<sup>9</sup> The spatial distribution of solvent molecules or ions at solid–liquid interfaces is thus a central problem in science, as it controls processes as diverse as amphiphile adsorption, colloid stability, lubrication, heterogeneous catalysis, charge transfer, and protein folding.<sup>874–878</sup> The mutual structural effects of the surface and the surrounding liquid on each other determine the properties of the system. Elegant examples of this can be seen at biointerfaces, where the nanoscale organization and dynamics of contacting water and ions<sup>879,880</sup> are precisely controlled to support function.<sup>881</sup>

Since Sir Humphrey Davy’s isolation of alkali metal and alkaline earth elements via melt electrolysis,<sup>882</sup> molten salt interfaces have been used to make many important chemical discoveries. Despite this, IL–solid interfaces remain largely unexploited in chemical processes because their interfacial structure and dynamics has yet to be fully understood.

In 2010, we reviewed structural studies at this interface for both PILs and AILs, with comparison to molecular liquids.<sup>82</sup> Several other reviews of structure at solid–IL interfaces have since emerged,<sup>85–88</sup> including some focused on the electrochemically active interface,<sup>83,84,89</sup> and provide a good overview of

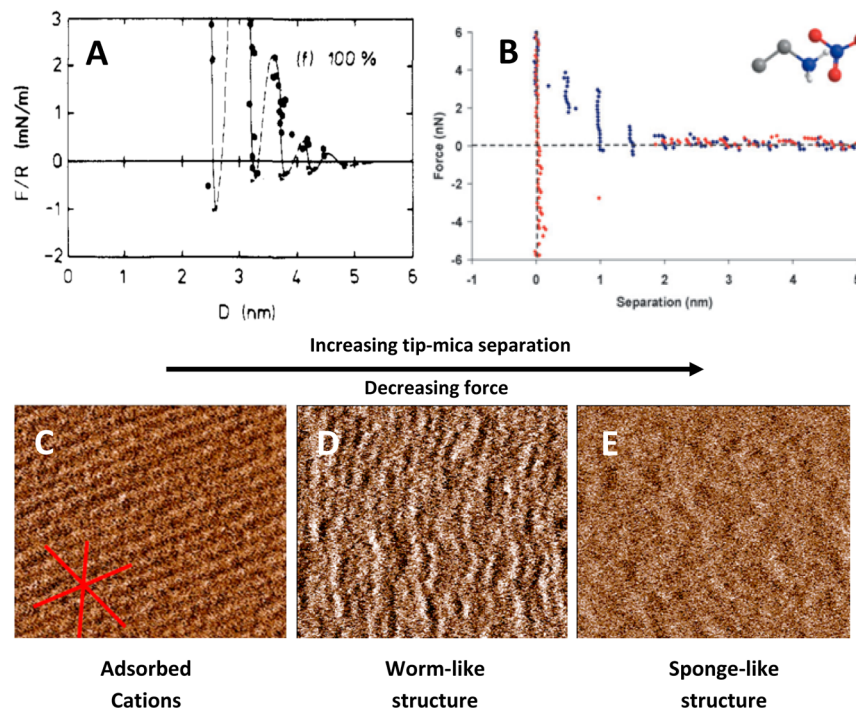


**Figure 20.** Structure of the EAN–mica interface. (A) Oscillatory force profile from SFA measurements. (B) Stepwise AFM force–distance profile. (C–E)  $10 \times 10$  nm soft contact AFM deflection image of the EAN–mica interface for the  $\text{Si}_3\text{N}_4$  tip in soft contact with the (C) innermost ion layer on mica at high force ( $>6$  nN), (D) worm-like innermost ion layer on mica at low force (4–6 nN), and (E) sponge-like structure of the first near surface (ion pair) layer ( $<3$  nN). The three directions of the mica lattice are marked in red on (C). Reproduced with permission from refs 886 (Copyright 1988 American Chemical Society), 920 (Copyright 2007 American Chemical Society), and 902 (Copyright 2013 PCCP Owner Societies).

the problems and challenges of resolving ion arrangements. A brief overview of the structure can be summarized as follows: near the surface, ILs exhibit oscillatory density profiles consistent with ion pair (anion + cation) or bilayer ( $2 \times$  ion pair) dimensions.<sup>85,883–888</sup> This structuring is of fundamentally different origin to solvation layers in molecular liquids<sup>9,889,890</sup> or ABAB packing in molten salts<sup>891–894</sup> because IL ions have the capacity to self-assemble. This provides additional impetus to ion structuring over and above simple geometric constraints (in molecular liquids) or charge ordering (in molten salts). The near-surface organization of ions is best described as layered or lamellar-like and in many respects parallels that found in adsorbed surfactant layers<sup>895,896</sup> but on smaller length scales. In the subsequent section, we highlight recent developments and future directions of the field and draw out the relationship between bulk and interfacial IL structure.<sup>82</sup>

#### 4.1. Charged Nonmetal Interfaces

Mica and silica are important substrates to examine IL interfacial structure. This is because they are smooth and have a net negative surface potential.<sup>897–899</sup> In mica, this charge has been measured to be  $3.2 \times 10^7$  charges per  $\text{cm}^2$  (freshly cleaved),<sup>900</sup> whereas it is less clear for silica because the charge is a consequence of the relative populations of protonated and deprotonated surface hydroxyl groups, which may vary between ILs of differing acidity. Analysis of these data can provide insight into structure near other, less well-defined surfaces.

Recent atomic force microscopy (AFM) experiments have elucidated the lateral organization of molecular liquids and adsorbed ions on solid substrates with subnanometer resolution.<sup>875–878,901</sup> In 2013, this was extended to ILs, in a series of high-precision soft contact, amplitude modulation (AM-) AFM experiments for both PILs<sup>899,902,903</sup> and AILs<sup>902,904</sup> next to a

mica surface (Figures 20 and 21). Notably, the liquid phase itself could be imaged in layers as a function of distance of the imaging tip from the surface.

Surprisingly, the IL structure was laterally inhomogeneous, and reminiscent of soft contact AFM images of self-assembled surfactant aggregates.<sup>905–907</sup> Three different regimes were identified at the EAN–mica interface: (1) a sponge-like nanostructure as in the bulk (far from the interface), (2) a

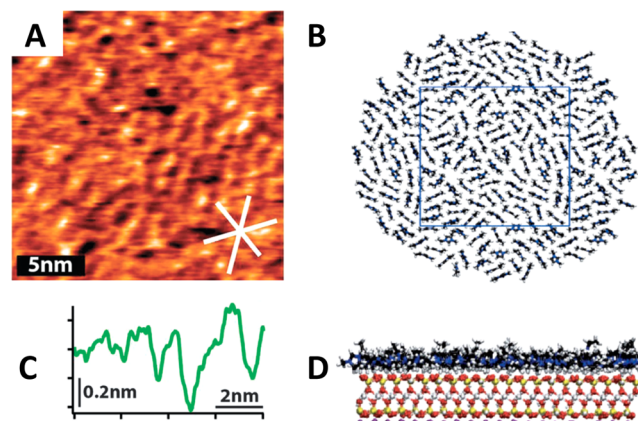


**Figure 21.** Structure of the interfacial layer of  $[\text{C}_4\text{mim}][\text{NTf}_2]$  at the mica interface from AFM experiments (A,C) and MD simulations (B,D). (A) and (B) show the lateral structure of the cations adsorbed in the interfacial layer. (C) and (D) show the  $z$  profile along a side axis. Note colors in the simulation are C = black, H = white, N = blue, O = red, Si = yellow,  $\text{K}^+$  = purple. Reproduced with permission from refs 928 (Copyright 2012 Wiley-VCH Verlag GmbH & Co. KGaA) and 902 (Copyright 2013 PCCP Owner Societies).

more lamellar-like arrangement (close to the interface), and (3) rows of worm-like structures in contact with the surface. When subject to high force, weakly bound ions are expelled from the layer and the worm-like morphology is lost. The confined cation layer blurs features of the underlying hexagonal lattice, and is the origin of markedly lower friction coefficient of EAN confined at high force.<sup>908</sup> Subsequent AM-AFM measurements have shown that both the adsorbed and the near surface structure determines nanoscale friction of this and other IL-coated interfaces.<sup>903</sup> Given the structural simplicity of the EAN and mica surface, these results are far-reaching and suggest that many ILs will exhibit similar patterns of self-assembly at solid–liquid interfaces.

Following Horn et al.'s pioneering research in 1988,<sup>886</sup> the SFA community has recommenced investigations of IL structure at the mica interface.<sup>86,87,249,250,909–919</sup> The main advantage of SFA over AFM is that the surface geometry and absolute separation is known in a SFA experiment. This has enabled the ion orientations in confined films to be resolved from force profiles, exemplified by a crossover structural transition from monolayer to bilayer-type arrangements in pyrrolidinium ILs when the alkyl chain length increases from  $n = 8$  to 10.<sup>911</sup> This is similar to earlier interpretation of AFM data for EAN and PAN.<sup>82,920,921</sup> At the IL–mica interface, Perkin et al.<sup>917,919</sup> also detected quantized friction–load regimes using the SFA, consistent with earlier AFM nanotribology experiments.<sup>908</sup> This was traced to the oscillatory layering of ions; because a unique number of ion layers are confined between the mica walls, each separation has a different friction coefficient and the shear plane can form at the alkyl domain (monolayer arrangement) or ionic domain (bilayer arrangement).<sup>917</sup> Interestingly, several SFA papers find no evidence of oscillatory layering.<sup>249,912,915</sup> This is at odds with much of the recent experimental and theoretical research at the mica– and other solid–IL interfaces. Explanations for this vary, and are usually attributed to surface roughness, remarkably large Debye screening lengths (1–4 nm), or strong repulsions superimposed on the oscillatory forces.

Israelachvili et al.'s<sup>249</sup> most recent publication has been quite controversial in the SFA<sup>250,251</sup> and AFM<sup>922</sup> community. This is because a weak potential-independent attractive force ranging from 3 and 30 nm was measured between the two surfaces (mica at constant charge, gold at constant potential). No corresponding long-range repulsion was observed. Such long-range forces have not been detected by previous SFA or AFM studies of pure ILs, even with instruments of similar force resolution. Furthermore, DLVO fits of the decay length for the attractive force predicted a negligible free ion concentration (0.003%) in the bulk. This led the authors to propose a radical, nonintuitive view that ILs are dilute electrolyte solutions of ion pairs plus a small fraction are dissociated free ions. While the long-range forces in ILs may be real, the main conclusions of the paper are inconsistent with the wider body of experimental and theoretical IL research. An alternate explanation suggests that the DLVO framework is inappropriate because ILs (1) are strongly dissociated<sup>65,280</sup> and show complex dissociation equilibria,<sup>365</sup> (2) ions change allegiance between several close counterions<sup>260,385</sup> and not a single ion pair in the bulk, and (3) only a long-range attractive force is detected; a long-range repulsive force was absent. We note that similar force behavior (long-range attraction, short-range repulsion) has been observed in confinement of a sponge ( $L_3$ ) phase,<sup>923</sup> related to the interfacial tension between bulk sponge ( $L_3$ ) and confinement-induced lamellar ( $L_\alpha$ ) phases. It is likely that a similar effect is operating here but on smaller

dimensions, because the size of the IL's  $L_3$  structure is an order of magnitude lower.

Two recent studies have examined the ion structure at a different type of charged interface: the crystalline salt–IL interface. AILs with cyano-functionalized anions ( $[\text{SCN}]^-$ ,  $[\text{TCM}]^-$ , and  $[\text{DCA}]^-$ ) were studied at near  $\text{NaCl}(100)$  and  $\text{BaF}_2(111)$ .<sup>924</sup> From fitting the SFG spectra, a Helmholtz-like model for ion structure was suggested, similar to results at other interfaces using SFG.<sup>925,926</sup> However, as noted previously,<sup>85</sup> SFG detects structure only where the inversion symmetry is broken, presumed to be a single layer flanking the interface, but is insensitive to any structure subsequent to this out in the bulk. At the  $\text{KCl}(100)$  surface, frequency modulation (FM-) AFM experiments have shown  $[\text{Py}_{14}\text{FAP}$  ion layers normal to the interface. Atomic resolution of the underlying  $\text{KCl}$  lattice could be obtained as well as evidence of tip-induced dissolution of  $\text{K}^+$  and  $\text{Cl}^-$  layers into the IL.<sup>927</sup>

Simulations of charged, nonmetal–IL interfaces are still scarce. The main theoretical hurdle is modeling sufficiently large slabs of the liquid and solid phases to provide insight into structure in both regions. Only one of the current simulations<sup>928,929</sup> accounts for the exchange of potassium ions in the mica lattice. This is important because a freshly cleaved mica surface consists of negatively charged surface groups in a nearly hexagonal (tetragonal) lattice, about one-half of which are neutralized by  $\text{K}^+$  ions.<sup>897</sup> These ions may be dissolved into solution, or remain surface-bound. From an experimental perspective, it is reasonable to assume that  $\text{K}^+$  ions are expelled from the surface as the high concentration and surface active properties of IL ions will prevail. The resulting bulk concentration of dissolved  $\text{K}^+$  is, however, negligible.<sup>910,930</sup>

Classical MD simulations of a thin 4 nm slab of  $[\text{C}_4\text{mim}]\text{[NTf}_2]$  have shown oscillations in ion and charge density normal to the mica interface.<sup>931</sup> These results qualitatively agree with the MD simulations of IL–quartz surfaces<sup>932,933</sup> and with experimental investigations (AFM, SFA, XRR,<sup>930</sup> and SFG<sup>934,935</sup>). More pronounced ion layering was obtained at the mica<sup>928,930</sup> surface using atomistic MD simulations and a more realistic interaction potential. These are shown in Figure 21B and D.

For  $[\text{C}_n\text{mim}]\text{[NTf}_2]$  ILs, Payal and Balasubramanian showed that cations with ethyl- or butyl- substituents ( $n = 2$  or 4) arrange their alkyl tail parallel to the mica surface, but hexyl- and octyl- chains were oriented normal to the interface in a bilayer-like arrangement. Subsequent simulations by the same authors showed similar behavior for  $[\text{NTf}_2]$ -based ILs with either symmetric ( $n = m$ ) or asymmetric ( $n \neq m$ ) imidazolium  $[\text{C}_n\text{C}_m\text{im}]^+$  cations.<sup>936</sup> Zhou et al.'s study was also notable as the model was evaluated against ion layering seen in high-resolution interfacial X-ray scattering data.<sup>930</sup> This provides unambiguous experimental evidence that oscillatory arrangements at the mica interface are not an artifact of confinement; the layering observed in the MD simulations is present at an isolated surface.

Other related surfaces with exchangeable ions are clays such as montmorillonite and kaolinite. MD simulation of IL ion arrangements at these interfaces has recently been achieved.<sup>937,938</sup> IL structure was shown to be similar to that at the mica interface, but the lower (negative) charge density, as well as rougher and more porous solid surface, leads to weaker ion ordering.

In principle, it should be possible to model the IL–mica interface using ab initio, DFT, or other first principle simulation methodologies. Recently, this has been reported for  $[\text{C}_4\text{mim}]\text{[BF}_4]$  at the  $\gamma\text{-Al}_2\text{O}_3$  surface.<sup>939</sup> A monolayer-like structure was

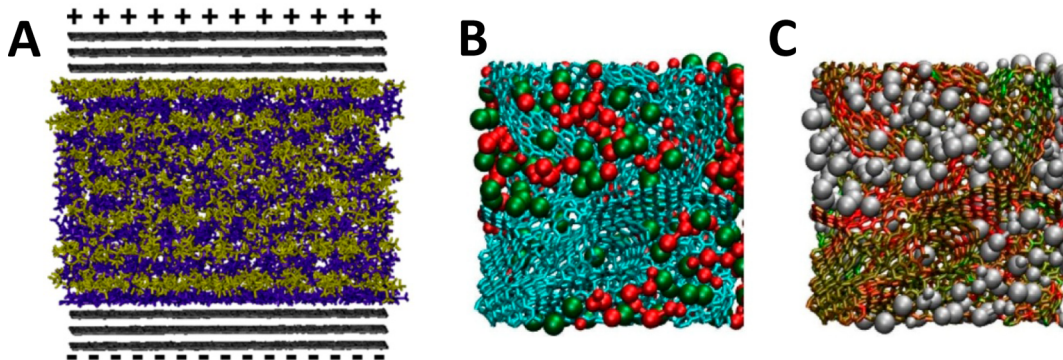


**Figure 22.** Structure of the IL–carbon interface from MD simulations. (A)  $[C_4\text{mim}][\text{NTf}_2]$  organization (cation purple, anion yellow) inside a 5.2 nm graphite nanopore with positive top wall and negative bottom wall. (B) Ion arrangements of  $[C_4\text{mim}][\text{PF}_6]$  (cation red, anion green) and (C) the corresponding charge distribution of the porous carbon electrode held at +0.5 V electrical potential (red for  $q > 0$ , green for  $q < 0$ , yellow for  $q \approx 0$ , ions silver spheres). (C) Reproduced with permission from refs 998 (Copyright 2012 American Chemical Society) and 963 (Copyright 2012 Nature Publishing Group).

seen in the simulation, driven by strong electrostatic interactions between the surface and the ions.

The silica–IL interface has been studied with both surface forces<sup>908,920,940,941</sup> and spectroscopic<sup>942,943</sup> techniques. The data are perfectly consistent with the models developed for the mica interface, by accounting for the lower and uneven charge density as well as increased surface roughness. Thus, like mica, silica can be used as a model substrate for ion arrangements at charged metal electrode surfaces. However, silica–IL interactions are interesting because under certain conditions, they can induce solvent gelation that could be exploited in solar cells.<sup>944–946</sup> Also, silica can be rendered nanoporous, leading to interesting ion self-assembly under confinement.<sup>947–951</sup> Finally, hydrophobic/hydrophilic organic monolayers can be grown from a silica surface, presenting a new way of modifying ion arrangements.<sup>952</sup>

Comprehensive all-atom force field modeling of the silica–IL interface has recently been performed by Canongia Lopes et al.<sup>953</sup> and Li et al.<sup>862</sup> The reciprocal arrangement of cations over negative surface sites and anions over positive surface sites shows that the interface templates the composition of the ion layer immediately adjacent to the surface. This result, while intuitive, is important for describing charged electrode interfaces<sup>89</sup> or ILs close to patchy or omniphobic<sup>954</sup> surfaces.

#### 4.2. Carbon Interfaces

Interest in the solid carbon–IL interface has been fueled by the desire to understand IL solvation of nanotubes,<sup>645</sup> graphene,<sup>955</sup> and  $C_{60}$ <sup>956</sup> as well as applications like supercapacitors<sup>957</sup> where graphite can be used as a cheap electrode material. Graphite is also important because it can be made with subnanometer pores, leading to dramatic increases in capacitance.<sup>958</sup>

Graphite is an atomically smooth, uncharged plane of carbon atoms and thus interacts with ILs differently from mica or silica.<sup>959</sup> As a semimetal, graphite displays interesting surface chemistry quite different from other materials because it is electrically conductive and yet (external or induced) electric fields can penetrate a few angstroms into the bulk.<sup>960</sup> This means that strong interactions with the uncharged or charged IL groups are possible, the first hints of which were noted in interesting gelation behavior of AILs mixed with single-walled carbon nanotubes.<sup>196</sup> In general, experimental measurements have not kept pace with interest in the structure of IL–graphite interface. To fill this void, numerous simulations have been performed (near graphite,<sup>961–980</sup> graphene,<sup>930,981–992</sup> amorphous carbon,<sup>993</sup> nanotube,<sup>961,981,983,989,994–996</sup> nano-

pore<sup>862,963,970,983,997–1002</sup> interfaces), although the results differ widely in the literature mainly because of variation in ILs, input parameters, simulation type, and force field polarizability.

Recently, a consensus structure appears to be emerging that suggests layered ion arrangements close to the surface resulting in an increased solvent density as compared to the bulk<sup>1002,1003</sup> and changes in melting point upon confinement.<sup>1004,1005</sup> Similar results have been reported near a crystalline rubrene interface<sup>1006,1007</sup> or other substrates with a graphite-like hexagonal lattice structure of surface atoms.<sup>1008</sup> On graphite, IL layering varies with applied surface bias and shifts from cation-enriched (negative biases) to anion-enriched (positive biases), similar to that described by Canongia Lopes et al.<sup>953</sup> at a silica substrate, and to experiments at other electrode interfaces (cf., Figures 22–25).<sup>572–574</sup> Some of the simulations can predict observed macroscopic capacitance quite accurately,<sup>963,970,971,975</sup> and the suggested structure has been newly confirmed by electrochemical AFM<sup>968,1009–1011</sup> and XRR<sup>930,987</sup> studies of this interface. Interestingly, the dynamics of ions is related to their relative position near the interface; ions in layers closer to the graphene surface display longer relaxation times and increasingly slaved diffusion.<sup>992</sup> This suggests the degree of ion self-assembly and interactions with the substrate have a key influence on solvent motion, similar to, but more pronounced than that in other solvents.<sup>1012</sup>

Future work at carbon interfaces should also be extended to the study of IL arrangements at surfaces including diamond, coal, bitumen,<sup>1013</sup> charcoal, carbon nanodots, glassy carbon, or polymer substrates generally, where limited data are available.

#### 4.3. Metal Interfaces

It is increasingly clear that the strong IL–surface interaction can drive changes in the structures of both the metal surface and the IL phase. Scanning tunneling microscopy (STM) has been an important tool to probe this at several metal interfaces ( $\text{Au}(111)$ ,<sup>573,574,883,1014–1024</sup>  $\text{Au}(100)$ ,<sup>1018,1022,1025,1026</sup>  $\text{Ag}(111)$ ,<sup>1023,1024,1027</sup> or  $\text{Cu}(111)$ <sup>1028</sup>) with a variety of AILs. Similar reconstructions were reported from surface X-ray scattering at  $\text{Au}(111)$ .<sup>1029</sup> No corresponding investigations with PILs have yet been conducted.

Unlike in molecular liquids,<sup>1030</sup> atomic resolution of surface structure by STM in an IL has not been achieved. This is most likely due to the strong ion adsorption onto the tip in an STM experiment, blurring surface features.<sup>883</sup> However, dramatic changes in the adsorbed ion layer and underlying metal surface

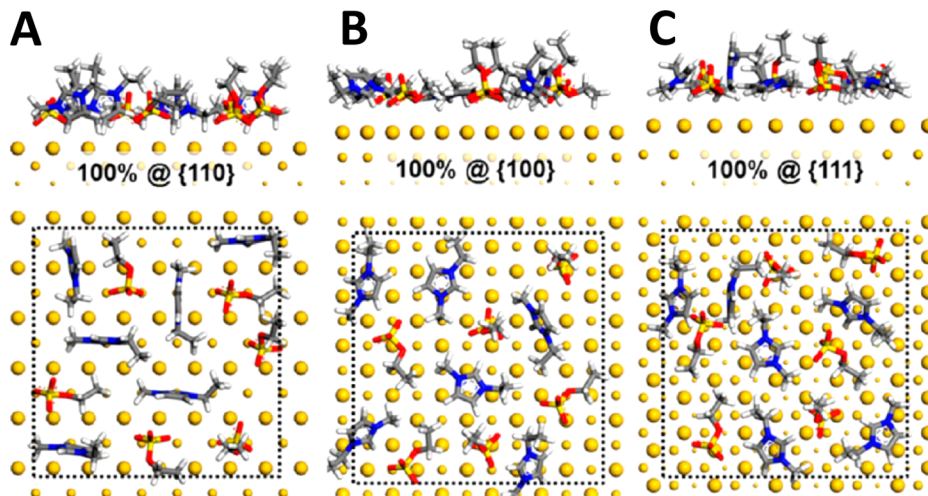


**Figure 23.** Structural arrangement of  $[\text{C}_2\text{mim}][\text{ES}]$  on (A)  $\text{Au}\{110\}$ , (B)  $\text{Au}\{100\}$ , and (C)  $\text{Au}\{111\}$  crystallographic surfaces at 100% surface coverage from MD simulations. Atom colors are as follows: Au (gold), C (gray), N (blue), S (yellow). Reproduced with permission from ref 1055. Copyright 2013 American Chemical Society.

have been characterized, for example, with coil-like<sup>1015</sup> and micelle-like<sup>409</sup> adsorbed ion structures as well as worm-like<sup>883</sup> or  $22 \times \sqrt{3}$  herringbone<sup>573</sup> reconstructions of  $\text{Au}(111)$ . Predicting surface reconstructions in an IL is difficult because the surface arrangement appears to be a complex function of IL chemical structure, crystal lattice plane, surface potential, temperature, and tunneling parameters. Further experiments are required to elucidate the origin of this behavior. At the very least, STM studies suggest that ion–surface interactions will change and possibly degrade the surface structure of electrodes immersed in ILs over time. This poses an important hurdle for future use of ILs in electrochemistry.

In general, papers that probe solvent structure at metal interfaces are geared toward the polarized electrode surfaces to understand the IL electrical double layer structure (cf., section 4.4). However, IL structure at unbiased metal interfaces have been studied with both experiment and theory, and shows strong ion adsorption close to metal surfaces, followed by one or more ion pair layers. As was recently demonstrated for molecular liquids,<sup>1031</sup> this layered arrangement should be transferrable to the IL structure around metal nanoparticles,<sup>837,1032–1034</sup> by accounting for the curvature of the interface relative to the ions.

AFM<sup>883,1035</sup> experiments were performed at  $\text{Au}(111)$  surface and the results are consistent with IL structure at other nonmetallic (mica, silica) surfaces. More recent AFM experiments have attempted to model the system using a massless model of cantilever dynamics.<sup>1036</sup> Related MD simulations have shown that the alkyl chains have well-defined lateral structure even at pressures comparable to that experienced by the ions between the surface and an AFM tip.<sup>1037</sup> Aliaga and Baldelli used SFG to probe the structure at the  $\text{TiO}_2$  surface, with the imidazolium ring of the cation oriented near parallel to the surface.<sup>1038</sup> For metals such as lithium, the IL can react with the surface atoms, leading to diminished near surface liquid structure of several different charged and uncharged species.<sup>1039</sup> Other indirect evidence of ion ordering confined in a silver matrix has been presented.<sup>1040</sup>

Atomic resolution of IL structure has been obtained at the mercury–IL (liquid–liquid) interface,<sup>1041</sup> allowing atomic insight into capacitance profiles.<sup>1042–1044</sup> Synchrotron-based XRR data for Langmuir films of  $[\text{Py}_{1,4}][\text{FAP}]$  were performed at

low and high Hg-surface coverage. Ions were shown to self-assemble across lateral and longitudinal directions. Fits to the reflectivity profile suggest that a checkerboard pattern is formed laterally, while a bilayer structure emerges normal to the interface. This is consistent with the bilayer structure for the same IL at the (smoother, and more well-defined) crystallographic  $\text{Au}(111)$  interface,<sup>572</sup> but is inconsistent with interpretation of XRR data at a sapphire<sup>887,888</sup> substrate.

Interesting spectroscopic experiments have been performed at the metal–IL interface. Harris et al.<sup>1045</sup> used femtosecond two-photon photoemission spectroscopy (TPPE) to study electron solvation in ultrathin films at the  $[\text{Py}_{1,4}][\text{NTf}_2]$ – $\text{Au}(111)$  interface. Electron solvation was found to be ultrafast, which is likely related to the near-surface solvent structure, although the molecular mechanism for this could not be discerned.

For the most part, simulations have played a more prominent role than experiment in describing the ion arrangements at metal interfaces. However, even for model (unbiased) metal surfaces, this is computationally expensive because one must capture many nontrivial ion–ion plus ion–metal interactions over a sufficiently large simulation box. For example, incorporating image charges at a electrode is notoriously difficult<sup>1046</sup> because the electrostatic charge on the ions is (typically) highly delocalized, in flux across many atoms, and, like on the electrode surface, polarizable.

The (rutile)  $\text{TiO}_2$  (110) interface<sup>1047,1048</sup> has been modeled using classical MD simulations, with the orientations of ions adjacent to the interface consistent with SFG measurements.<sup>1049</sup> A number of DFT simulations have also been performed on ILs near the unbiased metal surfaces of  $\text{Li}(100)$ ,<sup>1050,1051</sup>  $\text{Li}(110)$ ,<sup>1051</sup>  $\text{Li}(111)$ ,<sup>1051</sup>  $\text{Al}$ ,<sup>1052</sup>  $\text{Fe}$ ,<sup>1053,1054</sup>  $\text{Ag}(111)$ ,<sup>1027</sup>  $\text{Au}(100)$ ,<sup>1055</sup>  $\text{Au}(110)$ ,<sup>1055</sup>  $\text{Au}(111)$ ,<sup>1055,1056</sup> and  $\text{Cu}(111)$ .<sup>1052</sup> For these simulations to be truly ab initio, a relatively small number of ions (3–8 ion pairs) and surface atoms are studied. Likewise, current DFT models do not reproduce experimentally verified ion layering normal to the interface, yet they are consistent with the ion lateral structure<sup>1027</sup> or the atomic structure<sup>1055</sup> of the underlying metal surface (cf., Figure 23).

The strong interaction between ions and metals may provide a route to separating enantiomers of chiral ILs.<sup>135</sup> This was elegantly demonstrated by Jalili et al.<sup>1057</sup> who showed

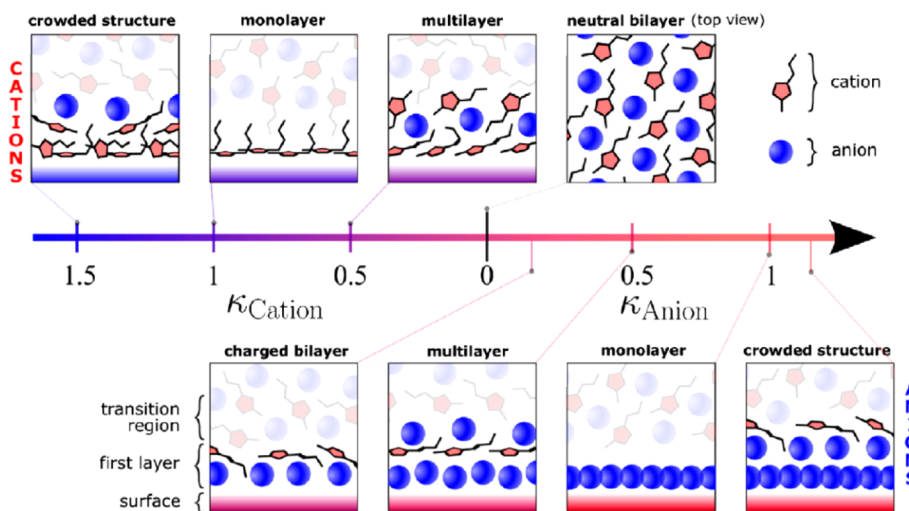


**Figure 24.** Schematic overview of ion arrangements as a function of normalized positive and negative surface charge density from MD simulations. Cations are shown as red pentagons with black tails, while anions are blue spheres. Reproduced with permission from ref 1061. Copyright 2014 Elsevier.

enantiospecific chemisorption of (*R*)- and (*S*)-methyl 2-ammonium chloride propanoate on achiral Al(111) and on chiral Al(854)<sup>5</sup> surfaces via ab initio calculations. It would be interesting to test the broader applicability of this result, that is, whether it could be used to separate mixtures of chiral ions or chiral ILs dissolved in molecular solvents by exploiting the pronounced structuring of ILs at interfaces.

#### 4.4. IL Electrical Double Layer Structure

There have been several important developments in understanding IL structure at the electrified solid–IL interfaces. Fedorov and Kornyshev<sup>1058</sup> provide an excellent overview of the current state of affairs on IL electrical double layer (EDL) research, the structure of which is generally more complicated than expected.<sup>1059–1061</sup> The complexity of the IL EDL arises because many of the basic assumptions key to mean-field models for aqueous EDLs cannot be applied, to which the ability of IL ions to self-assemble adds a further wrinkle. For example, IL ions are typically large with significant charge delocalization, and so cannot be modeled as point charges. Unlike aqueous electrolytes, the pure ionic composition of ILs means that the concentration of ions near the electrode interface simply cannot differ greatly from the bulk, so Debye lengths are considerably smaller, <1 nm. However, some concepts of aqueous electrolyte models cannot be so easily discarded, for example, the finite anion and cation volume, which defines the upper limit for ion packing at the electrode surface. Until a robust model for the IL EDL emerges, their considerable potential in electrochemistry (e.g., electro-deposition,<sup>36,1062</sup> capacitors,<sup>37</sup> dye-sensitized solar cells,<sup>1063,1064</sup> electrowetting<sup>1065–1067</sup>) will likely remain unfulfilled.

Theoretical descriptions of the EDL have progressed rapidly, and continue to provide considerable insight into ion organization. Notably, simulations are now sufficiently advanced such that they often uncover important structural features of the EDL prior to experimental measurement,<sup>1061,1068</sup> much like previous studies of the bulk phase structure.<sup>358,359</sup> Since Kornyshev's landmark study,<sup>1069</sup> DFT,<sup>1070–1074</sup> MC,<sup>1074–1078</sup> MD,<sup>975,1079–1084</sup> and coarse grained<sup>1085–1088</sup> simulations as well as Landau–Ginzburg,<sup>1089,1090</sup> Poisson–Nernst–Planck,<sup>1091,1092</sup> Debye–Falkenhagen,<sup>1093</sup> and Gouy–Chapman–Stern-inspired<sup>1094</sup> models have been developed for a variety of model and real metal interfaces. They all predict many experimentally testable parameters, which can be used to further refine the

structural models and in doing so deepen our understanding of the EDL. Of these, the works of Fedorov et al. provide the most comprehensive roadmap of ion arrangements and structural transitions as a function of surface potential and IL type; the main structural trends are captured by considering (1) normalized excess charge in the first IL ion layer and (2) a parameter related to charge compensation of the surface (cf., Figure 24).<sup>1061,1068</sup> Recently too, the adsorption of water molecules<sup>1095</sup> and also the ferrocene–ferrocenium redox couple<sup>639</sup> were modeled using classical MD simulations. This provides fundamental insight into impurity solvation and electron transfer of reference redox probes at the IL EDL, which is still absent from experimental literature.

Until recently, there has been a considerable debate in the experimental literature about the IL EDL structure. While consensus suggests that ion arrangements vary as a function of potential, the exact structure formed was poorly understood. Early reports using SFG<sup>925,1096,1097</sup> revealed a monolayer structure, whereas other experiments suggested a structure similar to aqueous electrolytes, with an adsorbed ion layer followed by an electrostatically bound diffuse layer.<sup>1098–1100</sup> In early investigations, the EDL structure was widely (if indirectly) probed using electrochemical impedance spectroscopy (EIS). This is because capacitance is a consequence of the relative ion concentrations at the electrode surface, and hence the lateral structure. However, capacitance measurements only provide macroscopically averaged structural information on the relative concentrations of cations and anions at the electrode surface, and there is considerable variation in published data,<sup>969,975,1043,1098,1101–1106</sup> possibly due to the different electrodes, crystallographic planes, pronounced hysteresis effects,<sup>987,1107–1110</sup> or trace impurities.<sup>1095,1111,1112</sup> Thus, to understand the EDL structure, direct measurements on well-defined systems are required.

Experiments at other (solid–IL or air–IL) interfaces have shown that ion organization can extend into the liquid over several nanometers and are thus much more than one ion layer thick; the IL EDL structure must be quite unlike that in aqueous<sup>1113–1116</sup> electrolytes. For this reason, experimental studies of the EDL are shifting toward techniques that can probe ion structure both next to, and further away from, the interface.

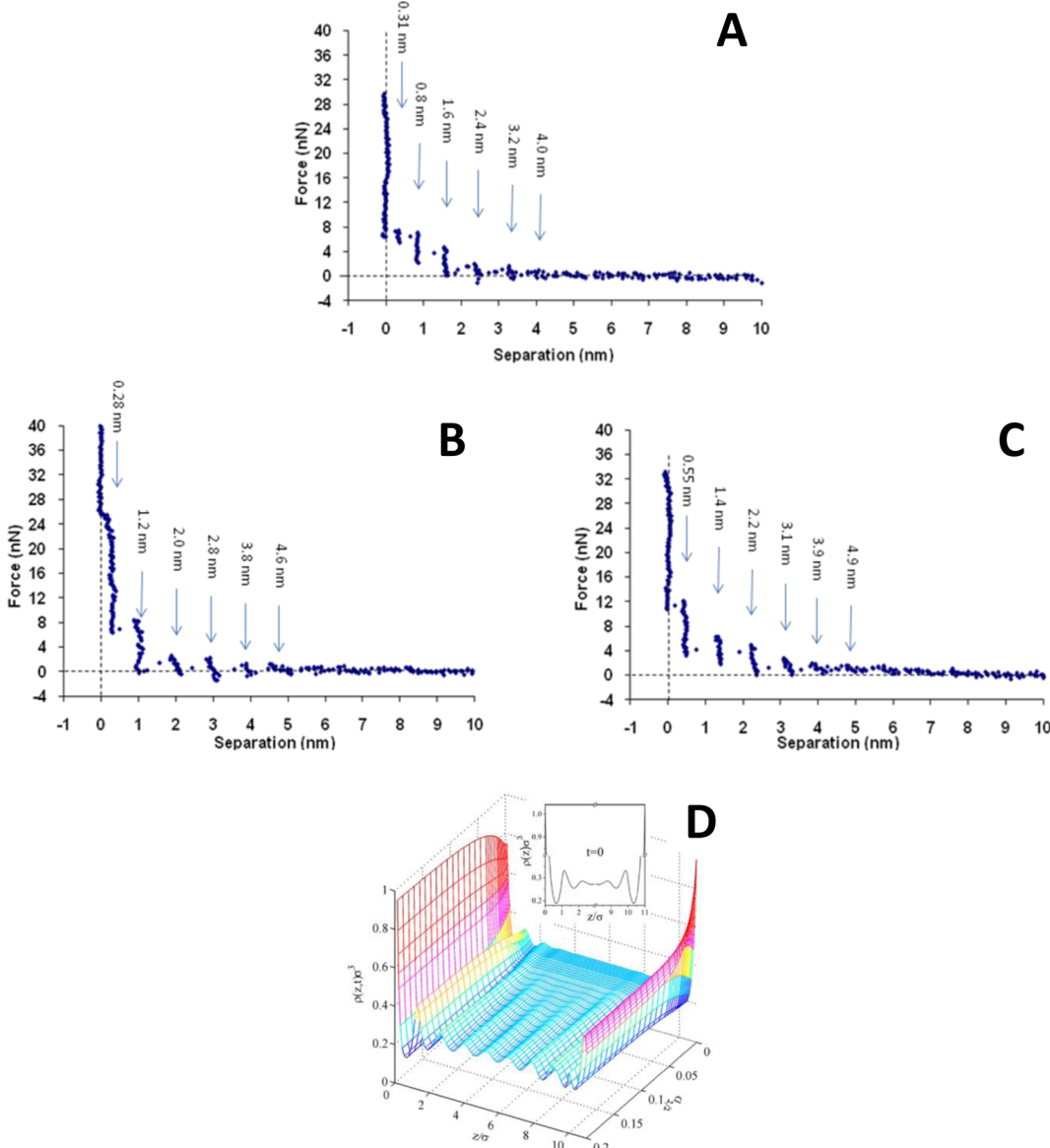


**Figure 25.** Structure of the IL electrical double layer at a polarized metal interface. Typical force versus distance profile for an AFM tip approaching from a Au(111) surface in  $[C_2mim]FAP$  at (A) open circuit potential (ocp,  $-0.18$  V), (B)  $-1.0$  V (vs Pt), and (C)  $+1.0$  V (vs Pt). In (D) the kinetic evolution of near surface cation density as a function of distance from the interface during constant-voltage charging. Reproduced with permission from refs 572 (Copyright 2011 American Chemical Society) and 1133 (Copyright 2014 American Chemical Society).

Nanometer resolution of the IL double layer structure normal to the interface was first obtained via AFM for AILs at an electrified Au(111) interface.<sup>436,572</sup> The setup was similar to corresponding *in situ* electrochemical AFM force measurements for aqueous electrolytes,<sup>1117–1120</sup> yet the findings were quite different; single and ion pair (anion+cation) layers were detected at the electrode interface, which increased in number and became more strongly arranged at higher voltages (cf., Figure 25). This indicated that ion arrangements vary significantly out into the bulk and that the EDL is indeed more than one layer thick. Overall, the data suggests a capacitor-like double layer structure is present in ILs, with a potential decay profile that oscillates between each plane of charge. This has since been extended to a wider range of ILs,<sup>574,922,1121–1126</sup> IL+LiCl mixtures,<sup>574,1112</sup> and pure ILs close to a charged graphite<sup>966,1009–1011,1126</sup> electrode using AFM. In addition, elegant XRR experiments on Au<sup>1127</sup> and graphene<sup>1110</sup> probed the structural reorganization of the layers in

real time as a function of potential. The results showed that ILs were subject to slow potential-dependent kinetics and structural hysteresis, both of which related to the unusually well-defined layering and slow ion dynamics. Together these AFM and XRR results draw a nice parallel to modeling by Lynden-Bell et al.,<sup>1064</sup> and Kornyshev and co-workers,<sup>1075,1089</sup> who could trace the evolution in ion structure in the first and subsequent ion layers with applied bias. Future force work should investigate how lateral structure is affected by applied potential and dissolved electrolytes. Some recent simulations in pure ILs have already begun in this area.<sup>972</sup>

Neutron reflectivity has been employed to study the lateral structure of an IL EDL at a charged gold substrate.<sup>1128</sup> Surprisingly, fits to the reflectivity profiles showed little difference in the interfacial structure at potentials more positive than, more negative than, and close to the point of zero charge. In every case, the ion arrangement structure was best described as a

thin, compact Helmholtz-like cation-enriched layer at the electrode interface, even for positive biases. This was attributed to strong chemisorption of the  $[\text{Py}_{1,4}]^+$  to the gold substrate, although it may also be consistent with ion crowding.<sup>1069</sup> The authors also attempted to reconcile this model with differential capacitance profiles, but at a gold interface different from that in the reflectivity cell. Unfortunately, the  $q$ -range of the instrument meant that any subsequent ion layering could not be discerned. This is important because such layering has been detected for similar ILs using reflectivity experiments<sup>887,888,930,987</sup> including as a function of potential<sup>987</sup> and also with surface forces<sup>883,910</sup> techniques. Thus, to validate this picture of the IL EDL structure, data for more than one solvent contrast should be obtained, using H/D isotopic substitution. This has previously been used on the same instrument to elucidate nonionic surfactant adsorption structure in EAN.<sup>1129</sup>

Surface enhanced infrared<sup>1109,1130</sup> or Raman<sup>1131</sup> spectroscopy (SERAS) and time of flight secondary ion mass spectrometry (ToF-SIMS)<sup>1132</sup> have been used to probe potential-dependent changes in ion density and orientations at electrode interfaces. On an Au surface, SERAS revealed a hysteresis in the exchange and reorientation of ions with applied voltage, beginning with ions far from the interface and then progressively closer to the surface. This is consistent with surface forces<sup>572,573,922,1025</sup> and XRR<sup>1110</sup> as the layers further from the interface are less strongly structured, and so should have more freedom to diffuse. ToF-SIMS experiments were conducted for 1-butyl-2,3-dimethylimidazolium chloride on an electrically conducting polymer actuator interface. Similar potential-dependent changes in near surface structure were noted in the spectra. Surprisingly, the regions of ion accumulation and depletion were found to extend several micrometers away from the electrodes. This is difficult to reconcile with other studies of IL structure reviewed herein as it corresponds to fluctuations on length scales thousands of times larger than individual ions.

It is important to point out that almost all of the papers have examined AIL arrangements; corresponding experimental or theoretical studies of protic, magnetic, or polymeric ILs are absent in the literature. While their electrochemical properties are generally less appealing than AILs<sup>1134</sup> (e.g., higher vapor pressures, smaller electrochemical windows), in applications such as hydrogen fuel cells,<sup>1135,1136</sup> PILs may be more advantageous due to their capacity for proton transfer in the bulk. Similarly, better understanding of polymeric IL self-assembly near electrode surfaces will enable them to be used as novel polymer electrolytes<sup>1137</sup> with tunable conductivity.

#### 4.5. IL Films

The structure and behavior of IL films is important for a range of applications where a small, free-standing amount of IL is spread onto the solid substrate to confer a functional advantage, for example, analytical applications,<sup>1138</sup> lubrication,<sup>1139</sup> catalysis,<sup>24,1140</sup> and corrosion inhibition,<sup>1141</sup> to name a few. In general, layered structures are also observed at the solid–IL film interface. This is because the quantity of IL present, and thus the fluid height normal to the surface, does not moderate the tendency of IL ions to self-assemble. However, He atom scattering experiments suggest at least three ion pairs are required to wet a film surface, which suggests a lower bound for free surface layering.<sup>1142</sup> We note that moisture absorption into such films<sup>1143</sup> should change the ion arrangements, as has been demonstrated for other IL–solid interfaces,<sup>886,1144</sup> although this has not yet been studied in detail.

The static and dynamic structures of thin films of AILs adjacent to various substrates including mica,<sup>1145–1147</sup> silica,<sup>1148</sup> silver,<sup>1149,1150</sup> Au(111),<sup>1151,1152</sup> Ni(111),<sup>1153</sup> Pd(111),<sup>1154,1155</sup> and Al<sub>2</sub>O<sub>3</sub>/NiAl(110)<sup>1155</sup> have been reported. The structure present was characterized using many surface-specific techniques and some vacuum based-techniques, for example, reflection–absorption infrared (RAIRS) or angle resolved XPS spectroscopy, spectra of the latter made possible due to low IL vapor pressures.<sup>1156</sup>

Time scales for, and the possible mechanism of, 2D and 3D film growth of IL films on charged surfaces have been determined on mica.<sup>1145–1147</sup> This is based on known ion arrangements near the solid substrates. On mica, the results are broadly consistent between different studies, and indicate the IL is patchy over micrometer lateral dimensions. Moreover, the film edge advances via surface diffusion, principally attractions between cations and the surface, in accordance with similar studies of wetting phenomena at fluoropolymer<sup>1157</sup> or mesoporous TiO<sub>2</sub><sup>1158</sup> surfaces.

Films of ILs on silica have been less well-studied. Gong et al. reported a transition from a “flat” (anion+cation) layered structure to droplet-like morphology with increasing film thickness.<sup>1148</sup> This behavior may explain revelations of attoliter IL films and IL beads moving along silicon, tin dioxide, and zinc oxide nanowires.<sup>1159</sup>

The lateral and normal structure of ultrathin films of [C<sub>1</sub>mim][NTf<sub>2</sub>] and [C<sub>8</sub>mim][NTf<sub>2</sub>] vapor deposited on Au(111)<sup>1151,1152</sup> and Ni(111)<sup>1153</sup> has been determined. Ion adsorption, orientation, and growth were studied via angle-resolved XPS. In both liquids, anions and cations arrange in a checkerboard manner in the interfacial layer on Au(111). With increasing IL solvent deposited, layer-by-layer buildup is observed to thicknesses of 9 nm,<sup>1160</sup> similar to conclusions from He scattering on Au(111).<sup>1142</sup> For Ni(111), layer-by-layer growth is noted initially, and at submonolayer coverage, ions begin to adopt a bilayered structure. At higher coverage on Ni(111), a transition to a checkerboard-type arrangement occurs.<sup>1161</sup>

Ion adsorption to films can induce changes in the structure of solid surfaces. Ultrathin films of an oxo-functionalized AIL [5-oxo-C<sub>6</sub>mim][NTf<sub>2</sub>] on metal oxide surfaces (CeO<sub>2</sub> and CeO<sub>2-x</sub>) have been studied using *in situ* photoelectron spectroscopy (PES) under high vacuum.<sup>1155</sup> This was motivated by an earlier study of the reactivity of [C<sub>6</sub>C<sub>1</sub>im][NTf<sub>2</sub>] on the same surfaces.<sup>1162</sup> While [5-oxo-C<sub>6</sub>C<sub>1</sub>im][NTf<sub>2</sub>] and [C<sub>6</sub>C<sub>1</sub>im][NTf<sub>2</sub>] interact with CeO<sub>2</sub> in a similar manner, [5-oxo-C<sub>6</sub>C<sub>1</sub>im][NTf<sub>2</sub>] binds to the CeO<sub>2-x</sub> interface via enolate formation, enabling rapid IL decomposition. A similar, but less pronounced, reordering of PtCl<sub>4</sub><sup>-</sup> anions into Pt<sub>2</sub>Cl<sub>8</sub><sup>2-</sup> dianions was observed when [C<sub>4</sub>mim][PtCl<sub>4</sub>] was adsorbed on SiO<sub>2</sub> nanoparticles using X-ray absorption fine structure (XAFS).<sup>1163</sup>

Other vacuum-based techniques have explored IL film structure at metal interfaces. Evidence of ion clusters at a carbon nanotube grid was reported from transmission electron microscopy (TEM).<sup>1164</sup> TEM has also been used to directly visualize the structure and dynamics of polymer assemblies (micelles, vesicles) dissolved in IL films.<sup>1165,1166</sup> Schernich et al. employed time-resolved infrared reflection absorption spectroscopy (TR-IRAS)<sup>1155</sup> on Pd(111), ordered Al<sub>2</sub>O<sub>3</sub>/NiAl(110), and Pd nanoparticles surfaces. An AIL [C<sub>2</sub>mim][OTf] was used and vacuum deposited onto the surface prior to measurement. TR-IRAS revealed differences in ion orientations at the surfaces, attributed to different IL–surface interaction.

#### 4.6. Do Solid and Liquid IL Phases Coexist?

One recent study reported IL liquid and solid phases coexisting at the interface between pure bulk IL and a solid substrate. This is surprising as previously such behavior was only observed for IL layers adsorbed under ultrahigh-vacuum<sup>1027</sup> or when diluted in either methanol or acetone (which provides a driving force for the IL to crystallize<sup>1167</sup>) and the structure probed once the molecular solvent had evaporated.<sup>1158,1168–1170</sup> In 2010, Yokota et al.<sup>1171</sup> showed inhomogeneous solid-like structures are present at the pure IL–mica and IL–HOPG interfaces. To our knowledge, this is the only demonstration of solid-phase formation at a pure IL–solid interface, including for macroscopic measurements.

Canongia Lopes et al.<sup>1172</sup> recently addressed the controversy of solid- and liquid-like phases coexisting at the solid–IL interface. They showed that a solid-like IL structure at the solid interface<sup>1169,1170</sup> can be directly attributed to dissolving the IL salt in an alcohol. Films of pure [C<sub>8</sub>mim][BF<sub>4</sub>] and mixtures of [C<sub>8</sub>mim][BF<sub>4</sub>]+ethanol were deposited on silica and alumina surfaces, and the topographical features were analyzed via AFM. No evidence of solid-like structures was observed in the pure [C<sub>8</sub>mim][BF<sub>4</sub>] over time. In contrast, irregular fractal-type structures grew on the surface in the alcohol mixtures that one might expect from IL crystallization as the ethanol evaporated. Complementary MD simulations presented for the [C<sub>8</sub>mim][BF<sub>4</sub>]-alumina interface are in excellent agreement with the model developed in this Review, consisting of interfacial layer, transition zone, and bulk liquid.<sup>1172</sup>

Other more recent studies cast doubt on the coexistence of solid-like IL structure at solid–IL interfaces. Simulations of pure ILs confined in silica nanopores,<sup>1173</sup> in which there should be a stronger entropic driving force to crystallize, showed ILs remain liquid-like right up to the interface because melting point decreases upon confinement.<sup>1174</sup> Likewise, solid-state NMR measurements of [C<sub>4</sub>mim][PF<sub>6</sub>] adjacent to a silica support<sup>1175</sup> revealed liquid-like behavior close to the surface. As expected, ion mobility was slightly restricted because diffusion was hindered by the interface in the z direction. Thus, it is likely that the unusually rough mica and graphite surfaces, solvent impurities, lack of a sealed AFM fluid cell, or some combination of these contributed to the findings of Yokota et al.<sup>1171</sup>

### 5. THE RELATIONSHIP BETWEEN BULK AND INTERFACIAL IL ARRANGEMENTS

The same ion–ion interactions that drive IL self-assembly in the bulk phase are present at interfaces. This means that bulk and interfacial IL structures are closely related and is why bulk IL-like properties are often detected at interfaces.<sup>90</sup> However, interactions with the second phase (solid, liquid, or air) have an organizing effect. This means that structure related to, but more ordered than, the bulk morphology is present. The majority of experimental studies have so far examined near-surface structure normal to the interface; the lateral arrangement of ions at an interface is less well understood. Normal to the interface the network of polar and nonpolar domains in the bulk is oriented and aligned by the presence of the macroscopic interface, as has been observed in concentrated aqueous surfactant systems.<sup>921,1176</sup> The extent of orientation depends on factors such as surface roughness, surface charge, temperature, and deformability, while molecular factors such as cation amphiphilicity have the most significant influence, as they do in the bulk. For example, EAN forms multiple, well-defined 0.5 nm layers at

the solid– or air–IL interface.<sup>920,1177</sup> EtAN forms at most two, and so decays into its bulk structure much faster than EAN because the hydroxyl group interferes with solvophobic contact between cation alkyl chains.<sup>333,885</sup>

The nanostructures detected in the bulk phase and at interfaces do have several key differences. Ion pairs are routinely observed at interfaces,<sup>87,887,888,910</sup> and yet their concentration in the bulk for most ILs is essentially negligible, with lifetimes of a few picoseconds.<sup>76,252–255</sup> This can be explained as follows: in the bulk each ion has a larger degree of freedom and interacts with multiple counterions,<sup>385</sup> often within a polar domain. Thus, electroneutrality is maintained in the self-assembled structure by each ion associating with several counterions. In contrast, the layered interfacial ion arrangements promote ion pairing. Under confinement, electroneutrality is maintained by “squeezing out” an anion+cation unit, rather than a single ion. The exception to this is when the second surface is highly charged, allowing single cation<sup>572,902</sup> or anion<sup>572</sup> layers to be detected.

### 6. HOW DOES IL STRUCTURE COMPARE TO OTHER SOLVENTS?

#### 6.1. In the Bulk Phase

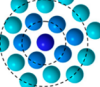
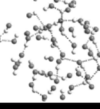
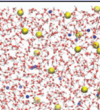
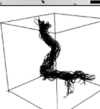
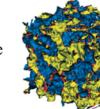
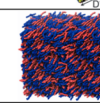
In the bulk phase, the majority of liquids show a favored separation of nearest neighbor molecules. This holds for a range of simple atomic, diatomic, and molecular liquids.<sup>1178–1181</sup> For example, simple atomic liquids (Hg,<sup>1182</sup> Ne,<sup>1183</sup> Ar,<sup>1184</sup> Xe,<sup>1185</sup> etc.) are well-described by the van der Waals model of hard spheres;<sup>1181,1186–1188</sup> the average separation of spheres reflects the strength of repulsive forces, with order created over a few diameters ( $\sigma$ ) oscillating between regions of enhanced and depleted density. Thus, the size and geometry of molecules is important as they define an excluded volume that neighboring proximal molecules cannot encroach upon. Classically, attractive forces provide the uniform background potential (a “mean field”) that stabilizes the liquid phase, and only play a minor role in structure formation. Recently, some authors have suggested attractive forces to be important in solvent dynamics,<sup>1189,1190</sup> although this is not universally accepted.

Diatomic (H<sub>2</sub>,<sup>1191</sup> D<sub>2</sub>,<sup>1192</sup> N<sub>2</sub>,<sup>1193</sup> O<sub>2</sub>,<sup>1193</sup> halogens,<sup>1194</sup> HF,<sup>1195</sup> etc.) or triatomic (CO<sub>2</sub>,<sup>1196</sup> etc.) liquids are consistent with the van der Waals model, but the structure is more complex as molecules are nonspherical and there can be inhomogeneous electron density.

For even larger molecular liquids, a preferred near-neighbor separation and orientation in the bulk emerges. Solvents as diverse as acetone,<sup>423</sup> tetrahydrofuran,<sup>1197</sup> or benzene<sup>16</sup> exhibit a favored molecular arrangement in the first coordination shell (3.5 to  $\sim$ 7 Å). Beyond this ( $>\sim$ 7 Å), structure in all of these liquids falls away rapidly, and a uniform spherical molecular probability is obtained. This shows that liquid structure is present only over small distances in the bulk.

Some molecular liquids possess more well-defined structure. For example, H-bonds<sup>1198</sup> can act cooperatively over several solvation shells leading to a network structure. The classic example of this is water. The consensus scientific view<sup>13,14,424,1199–1202</sup> is that strong H-bonds enable water to build up a 3-D tetrahedral network structure (similar to, but more disordered than, I<sub>h</sub> ice), yet some nontetrahedral structure<sup>1203</sup> may be present. Other protic liquids like methanol,<sup>1204</sup> methylamine,<sup>1204</sup> ammonia,<sup>1205</sup> and glycerol,<sup>1206</sup> as well as their mixtures with water,<sup>747,748,1207–1209</sup> are highly associated in 3D H-bond networks. H-bonding induces

Table 3. Bulk Structure of Ionic Liquids As Compared to Other Solvent Classes<sup>a</sup>

Liquid Type & Examples		Interactions	Bulk Structure		Ref.	$D_{self}$	
			General Comment				
Atomic	Argon (Ar)	R, vdW	vdW model of hard spheres; solvent structure defined by <i>average separation</i> of atoms from repulsive forces. Attractive forces weak. The figure shows hard sphere (2D) packing of the first (deep blue) and second (light blue) solvation shell around a central reference sphere.		None; structure decays in 1-2 $\sigma$ [1217] [1182]	15.3 <sup>[b]</sup> 16.3 <sup>[c]</sup>	
	Mercury (Hg)	R, vdW					
Diatomeric	Hydrogen (H <sub>2</sub> )	R, vdW	vdW model of hard spheres; average separation + some <i>orientation</i> correlations. Attractive forces weak. The figure <sup>[d]</sup> shows a snapshot of liquid HF from <i>ab initio</i> simulations.		None; structure decays in 1-2 $\sigma$ [1191] [1195]	90.1 <sup>[d]</sup> 70 <sup>[e]</sup>	
	Hydrogen Fluoride (HF)	R, vdW, HB					
Molecular	Water (H <sub>2</sub> O)	R, HB, D	Tetrahedral H-bond network		Consistent with vdW model but strong attractive forces emerge. Average molecular separation & orientation. The figure <sup>[f]</sup> shows the most probable local H <sub>2</sub> O@H <sub>2</sub> O structure (tetrahedral).	[424] Structure decays in 1-2 $\sigma$ . Some alcohols show $d$ [16] [749] [1211]	22.99 <sup>[f]</sup> 22.1 <sup>[g]</sup> 1.38 <sup>[h]</sup> 10.4 <sup>[i]</sup>
	Benzene (C <sub>6</sub> H <sub>6</sub> )	R, $\pi$ - $\pi$	Dimers; $\parallel$ displaced $<5 \text{ \AA} < T$ -shape				
	Octanol (CH <sub>3</sub> [CH <sub>2</sub> ] <sub>7</sub> OH)	R, HB, S	Long, thin H-bonded aggregates				
	Formic acid (HCOOH)	R, HB	Cyclic H-bonded dimers				
Aqueous Electrolyte	0.1 M NaCl solution	R, HB, D, C <sub>A/R</sub>	Solvent structure perturbed compared to pure water, similar to the effect of pressure. Varies with dissolved ions ( Hofmeister). The figure <sup>[j]</sup> shows a snapshot of Na <sup>+</sup> (blue) & Cl <sup>-</sup> (yellow) ions solvated in a sea of H <sub>2</sub> O molecules (red & white).		None; structure decays in 1-2 $\sigma$ [1218]	H <sub>2</sub> O: 21.96 <sup>[j]</sup> Na <sup>+</sup> : 12.84 <sup>[k]</sup> Cl <sup>-</sup> : 19.49 <sup>[l]</sup>	
Supercritical	Carbon Dioxide (sc-CO <sub>2</sub> )	R, vdW, D	Varies with temperature pressure & density: isolated molecules, small oligomers (if more gas-like) or clusters, branched chains (if more liquid-like). The figure <sup>[m]</sup> shows a snapshot of sc-CO <sub>2</sub> structure (low density) from MD simulations.		None; structure decays in 1-2 $\sigma$ [1219] [1220]	202 <sup>[m]</sup> 897 <sup>[n]</sup>	
Ferrofluid	~10 nm PIB-coated Fe particles dispersed in H <sub>2</sub> O	SS, M					
Polymer Melt	Polybutadiene	vdW, P	Randomly entangled polymer chains. Often will adopt coil-like conformations (R <sub>g</sub> ). Structure varies with chain length, molecular weight, polydispersity, chemical identity etc. The figure <sup>[o]</sup> shows the trajectories over time of a single chain (400 units) in a polymer melt.		No; likely exceptions [514]	-	
Molten Salt	Sodium Chloride (NaCl)	C <sub>A/R</sub>	Isotropic charge ordering; average separation (sometimes orientation) of ions. The figure shows the schematic of local charge ordering around cations (yellow) and anions (blue).		No; some exceptions [1221]	80.1 <sup>[p]</sup> 63.5 <sup>[q]</sup>	
Ionic Liquid	Protic [C <sub>n</sub> A][NO <sub>3</sub> ]	C <sub>A/R</sub> , HB, S, P	Charge ordering 1 ≤ n ≤ 2 bicontinuous		1.0 nm [428]	0.158 <sup>[r]</sup> 0.151 <sup>[s]</sup>	
	Aprotic [C <sub>n</sub> mim][NTf <sub>2</sub> ]	C <sub>A/R</sub> , HB, S, P	Globular domains 2 ≤ n ≤ bicontinuous		1.2 nm [448]	0.34 <sup>[t]</sup> 0.26 <sup>[u]</sup>	
	Fluorous [C <sub>n</sub> A][OF]	C <sub>A/R</sub> , HB, S, P	Bicontinuous 3 ≤ n ≤ 4 tricontinuous		1.9 nm [467]	NR NR	
	Dicationic [C <sub>n</sub> (mim) <sub>2</sub> ][BF <sub>4</sub> ] <sub>2</sub>	C <sub>A/R</sub> , HB, S, P	Globular domains 1 ≤ n ≤ bicontinuous		2 nm [477]	0.037 <sup>[v]</sup> 0.049 <sup>[w]</sup>	
	Magnetic [C <sub>n</sub> mim][FeCl <sub>4</sub> ] <sup>-</sup>	C <sub>A/R</sub> , S, M, P	NR, similar to aprotics with $\approx n$		1.2 nm [531]	NR NR	
	Polymeric [s-vb-C <sub>n</sub> mim][NTf <sub>2</sub> ]	C <sub>A/R</sub> , S, P	L <sub>α</sub> & H <sub>i</sub> reported. Others possible.		~40 nm [506]	NR NR	
	Solvate [Li(G <sub>4</sub> )][NTf <sub>2</sub> ]	C <sub>A/R</sub> , S, P	Cross-linked charge ordering around M <sup>+</sup> .		~1 nm [555]	NR NR	
Micro-emulsion	AOT/n-decane/brine	H, P	$d$ spacing between domains. Bicontinuous between H <sub>2</sub> O-in-oil & oil-in-H <sub>2</sub> O droplet regimes. Many other self-assembled structures possible. The figure <sup>[o]</sup> shows a MD snapshot of microemulsion structure (water phase blue, oil phase yellow, surfactant red).		10s of nm- μm [1222] [1223]	-	
Liquid Crystal	8CB	H, P	$d$ spacing between domains. Orientational & positional order; various nematic, smectic, columnar etc. structures possible. Self-assembly temp. &/or solvent dependent. The figure <sup>[o]</sup> shows a MD snapshot of 8CB structure with parallel (blue) & antiparallel (red) molecules.		100s of nm- μm [1224]	-	

<sup>a</sup>Repeat correlation length between domains in the bulk ( $d$ ), and self-diffusion coefficient,  $D_{self}$  (characteristic time scale of solvent structure,  $10^{-6} \text{ cm}^2 \text{ s}^{-1}$ ). Abbreviations used for interaction types are as follows: R = repulsive (Born) overlap of electron clouds, vdW = van der Waals interaction,  $\pi-\pi$  = pi-pi interaction, D = dipole interaction, HB = hydrogen-bond interaction, C<sub>A/R</sub> = Coulombic attractions and repulsions, S = solvophobic interaction, H = hydrophobic interaction, SS = steric stabilization, P = packing considerations,  $\sigma$  = molecular diameter, R<sub>g</sub> = radius of gyration, PIB = polyisobutane, s-vb = styrene-vinylbenzyl, C<sub>n</sub>A = primary alkylammonium cation, C<sub>n</sub>mim = 1-alkyl-3-methylimidazolium cation for alkyl chains lengths  $n$ . NR refers to "not reported". Note a rich diversity of structures exists in most liquid types; here, the typical example of solvent structure/key interactions/d is reported for comparison to ILs. <sup>b</sup>From ref 1225. <sup>c</sup>From ref 1226. <sup>d</sup>From ref 1227. <sup>e</sup>From ref 1228. <sup>f</sup>From ref 171. <sup>g</sup>From ref 1225. <sup>h</sup>From ref 1229. <sup>i</sup>From ref 1229. <sup>j</sup>From ref 1230. <sup>k</sup>From ref 1231. <sup>l</sup>From ref 1232. <sup>m</sup>From ref 1233. <sup>n</sup>From ref 1234. <sup>o</sup>From ref 1235. <sup>p</sup>Na<sup>+</sup>, from ref 1236. <sup>q</sup>Cl<sup>-</sup>, from ref 1236. <sup>r</sup>EA<sup>+</sup>, from ref 158. <sup>s</sup>NO<sub>3</sub><sup>-</sup>, from ref 158. <sup>t</sup>C<sub>n</sub>mim<sup>+</sup>, from ref 1237. <sup>u</sup>NTf<sub>2</sub><sup>-</sup>, from ref 1237. <sup>v</sup>[C<sub>n</sub>(mim)<sub>2</sub>]<sub>2</sub>, from ref 479. <sup>w</sup>BF<sub>4</sub><sup>-</sup>, from ref 479. <sup>x</sup>Reproduced with permission from ref 1228. Copyright 2003 AIP Publishing LLC. <sup>y</sup>Reproduced with permission from ref 1238. Copyright 2013 Royal Society of Chemistry. <sup>z</sup>Reproduced with permission from ref 1239. Copyright 2010 AIP Publishing LLC. <sup>aa</sup>Reproduced with permission from ref 1240. Copyright 2004 AIP Publishing LLC. <sup>ab</sup>Reproduced with permission from ref 514. Copyright 2003 Nature Publishing Group. <sup>ac</sup>Reproduced with permission from ref 142. Copyright 1990 AIP Publishing LLC. <sup>ad</sup>Reproduced with permission from ref 1223. Copyright 2013 Royal Society of Chemistry. <sup>ae</sup>Reproduced with permission from ref 1224. Copyright 2013 AIP Publishing LLC.

Table 4. Near Surface Interfacial Structure of Ionic Liquids As Compared to Other Solvent Classes<sup>a</sup>

Interfacial Solvent Structure						
Solvent Type and Examples	Normal Structure (Solvent Order $\perp$ to Interface)			Lateral Structure (Solvent Order $\parallel$ to Interface)		
	General Comment	F (mN/m)	Refs	General Comment	F (mN/m)	Refs
Atomic Liquids	gallium (Ga)	atoms pack in layers; structure decays in 1–5 $\sigma$ layers	no	oscillatory atomic density profile a few $\sigma$ normal to the interface; crystal-like normal and lateral structures possible	NR	1243
Diatomeric Liquids	Lennard-Jones fluid	molecules pack in layers; structure decays in 1–2 $\sigma$ layers	no; likely exceptions	oscillatory molecular density profile a few $\sigma$ normal to the interface; molecules pack in layers; layering more pronounced if molecules spherical, rigid, and nonflexible; preferred orientation in first layer; structure varies with temp., pressure, surface features (roughness, charge etc.) and confinement	NR	1267
Molecular Liquids	octamethylcyclotetrasiloxane water ( $\text{H}_2\text{O}$ ) benzene ( $\text{C}_6\text{H}_6$ ) octane ( $\text{CH}_3[\text{CH}_2]_6\text{CH}_3$ )	molecules pack in layers; structure decays in 1–10 $\sigma$ layers	no; likely exceptions	oscillatory molecular density profile a few $\sigma$ normal to the interface; molecules pack in layers; layering more pronounced if molecules spherical, rigid, and nonflexible; preferred orientation in first layer; structure varies with temp., pressure, surface features (roughness, charge etc.) and confinement	8	1254
Aqueous Electrolytes	0.1 M NaCl solution	$\text{H}_2\text{O}$ structure decays in 1–2 $\sigma$ layers; ion structure decays $\kappa^{-1}$	yes, for ions in Stern layer	two regions: inner (Stern) layer of counterions and outer (diffuse) layer of co-ions normal to the interface; $\text{H}_2\text{O}^+$ ions pack in layers	NR	1269
Ferrofluids	$\sim$ 5 nm NaOe stabilized $\text{Fe}_3\text{O}_4$ nanoparticles in $\text{H}_2\text{O}$	layered particle structures structure decays in 1–30 $\sigma$	yes	layered particle structures; depends on system composition/particule concentration, surface properties, and field strength/direction; pronounced smectic-like ordering possible at high field	NR	878
Polymer Melts	polydimethylsiloxane (MW 3700 g mol $^{-1}$ )	layered chains; structure decays in 1–2 $R_g$ layers	yes	oscillatory segment density profile a few $R_g$ normal to the interface; bond orientation varies between normal and parallel to the surface; structure depends on length of chain, cross-linking, etc.	NR	1264
Molten Salts	sodium chloride (NaCl)	alternating ion layers ('ABABA') layering decays in 1–5 $\sigma_{\text{ip}}$	no; likely exceptions	oscillatory alternating ion density profile a few nm normal to the interface; no preferred ion orientation in layers; layering more pronounced with surface bias	NR	1270
Ionic Liquids	protic [ $\text{C}_n\text{A}][\text{NO}_3]aprotic [\text{C}_n\text{min}][\text{NTf}_2]fluorous [\text{C}_n\text{A}][\text{OF}]$	ion pairs $1 \leq n \leq 2$ lamellar-like ion pairs $8 \leq n \leq 10$ lamellar-like $\text{NR}_j$ lamellar-like?	worm-like $n \geq 2$ worm-like $2 \leq n \leq 4$ micelle-like $\text{NR}_j$ tricontinuous; micelle-like?	oscillatory ion density profile many nm normal to the interface (decay in 2–10 $\sigma_{\text{ip}}$ ); preferred ion orientation in layers; ions A $^+$ B $^-$ can layer as: • ion pairs (AB/AB) $\rightarrow$ distance detected $\sigma_{\text{ip}}$ • lamellar-like (ABBA/ABBA) $\rightarrow$ distance detected “ $2\sigma_{\text{ip}}$ ”	NR	1257
	cationic [ $\text{C}_n(\text{min})_2][\text{BF}_4]_2$ magnetic [ $\text{C}_n\text{min}][\text{FeCl}_4]$ polymeric [s-vb- $\text{C}_n\text{min}][\text{NTf}_2]$ solvate [ $\text{Li}[\text{G}_4]][\text{NTf}_2]$ AOT/n-decane/brine A	NR <sub>j</sub> like aprotics of $\sim$ ?	single ions (A $^+$ or B $^-$ if strong IL–surface interaction); normal structure decays in 2–10 $\sigma_{\text{ip}}$ structure sensitive to surface (charge, roughness, etc.) and temp	NR	911	
Microemulsions	5CB	NR <sub>j</sub> like polyelectrolyte/melt? lamellar-like structure lamellar-like structures	NR <sub>j</sub> globular? yes	surface flattens and aligns bulk self-assembled structure well-defined structure normal to and laterally along interface	0.2	1126
Liquid Crystals					0.2	1271

<sup>a</sup>Abbreviations used are as follows:  $\sigma_{\text{IP}}$  = ion pair diameter;  $\sigma$  = solvent diameter;  $\kappa^{-1}$  = Debye length;  $R_g$  = radius of gyration; s-vb = styrene-vinylbenzyl; C<sub>n</sub>A = primary alkylammonium cation; C<sub>n</sub>mim = 1-alkyl-3-methylimidazolium cation for alkyl chain lengths  $n$ ; AOT = sodium bis(2-ethylhexyl) sulfosuccinate; NaOe = sodium oelite; SCB = 4-*n*-pentyl 4-cyanobiphenyl. NR refers to "not reported". Note a rich diversity of structures exists in most liquid types; here, the typical example is described in comparison to ILs.

aggregate structures in solvents such as primary alcohols (chain-like aggregates),<sup>1204,1210</sup> formic acid (dimers),<sup>1211</sup> or formamide (cyclic hexamers).<sup>1212,1213</sup>

Molten salts display isotropic charge ordering; an oscillatory structure exists around each ion in solution, beginning with the species of unlike charge in the first coordination shell, and then regions of successively alternating sign.<sup>1214</sup> This satisfies local electroneutrality and is qualitatively different from the van der Waals model of hard-sphere packing. Because ion–ion separations become smaller, not bigger, than in the solid state and there is a large 10–25% volume of fusion expansion upon melting, hole theory<sup>1215,1216</sup> has found some use in modeling the bulk phase of molten salts.

Thus, IL self-assembled structure is remarkable because virtually every other class of molecular solvent lacks solvent structure beyond a preferred organization between adjacent molecules (cf., Table 3). As a consequence, ILs have a preferred separation, orientation between ions, and repeat correlation length ( $d$ ) between polar and apolar domains. Moreover, IL self-assembly is analogous to other self-assembled phases; however, the length-scales of the structure in ILs are at least an order of magnitude smaller. In the first instance, this means that many of the same concepts used in modeling traditional surfactant organization<sup>91,92</sup> can be employed for predicting IL structure, although it is likely, but not fully established, that IL thermodynamic properties (enthalpy, entropy, internal energy) are as closely related to ion arrangements. Interestingly, the time scales of IL structure as revealed by measured diffusion coefficients are considerably slower than for other solvents. This suggests that the bulk phase nanostructure of ILs exists over much longer lifetimes than typically observed in other liquids. These structural differences and similarities in the bulk phase are highlighted in Table 3.

## 6.2. At Solid Interfaces

When liquids meet an interface, the molecular arrangement is altered as compared to the bulk. Liquid molecules tend to pack in discrete strata parallel to smooth solid surfaces. This structure, commonly referred to as “solvation layers”,<sup>9,890</sup> is characterized by an oscillatory molecular density profile  $\rho(r)$  versus distance  $r$  normal to the interface; the local density alternates between values higher than and lower than  $\rho_{\text{BULK}}$ , in level planes equal to the solvent’s molecular size ( $\sigma$ ).<sup>1241</sup> The  $\rho(r)$  profile is akin to the well-known radial distribution function  $g(r)$  used to describe bulk structure except for a few key differences. First, the  $\rho(r)$  wave emanates as a 2D plane away from the interface and not from a reference central molecule. Second, the origin of the layered structure is different; whereas bulk  $g(r)$  order captures the balance of intermolecular forces plus some packing considerations (cf., section 6.1), solvation layers are mainly of geometric origin because they represent the most efficient molecular packing up against a hard wall and occur in the absence of attractive/repulsive forces. Finally (apart from the first layer where solvent interactions with the surface may be strong), solvation layers are usually modeled with no preferred orientation in the layers, although this may not be true for all systems, for example, anisometric molecules, that self-assemble or where liquid structure is highly cooperative.

Whether we consider atomic liquids (Al<sup>1242</sup> and Ga<sup>1243</sup>), molecular liquids (water,<sup>1244–1246</sup> benzene,<sup>1247</sup> *n*-alkanes,<sup>1247–1250</sup> *n*-alcohols,<sup>1249,1251–1253</sup> octamethylcyclotetrasiloxane,<sup>1249,1254,1255</sup> and tetrachloromethane<sup>1247,1255</sup>), polymer melts (polydimethylsiloxane<sup>1256</sup>), or molten salts

(NaCl<sup>1257,1258</sup>), an oscillatory density profile is a hallmark of solvent ordering close to solid interfaces. The structure typically decays to the bulk arrangement after 1–10  $\sigma$  and is controlled by the solvent identity; more layers and higher push-through forces to displace these layers are required when the molecular geometry is spherical, rigid, and nonflexible. Conversely, molecules that are linear or with flexible chemical groups display fewer layers and have weaker solvation force. Roughness<sup>1259</sup> in the order of the size of the solvent will disrupt this layering, again because of changed packing considerations. This is summarized in Table 4.

The lateral structure of liquids is generally more complex than the normal structure and has been the subject of far fewer investigations. This is because tools to study this with molecular resolution did not exist until recently. In fact, most revelations of this are for liquids held under conditions of extreme confinement where the solvent has surface-crystallized.<sup>1004,1260–1262</sup> In general, lateral structure is most likely to be found in the layer flanking the interface such that the solvent order in some way reflects structural features (e.g., charge distribution, crystallographic order) of the underlying substrate. For subsequent solvation layers, a lateral structure may exist, but it will be harder to detect as the average molecular separation (or orientation) approaches bulk values. Clear evidence of lateral structure has been observed for liquids that self-assemble (surfactant solutions,<sup>906,921,1263</sup> ferrofluids<sup>1264,1265</sup>); in every case, the structure is a flatter and surface-templated version of the bulk organization. Recently, AFM has even shown that ions in aqueous electrolytes<sup>878,901</sup> possess a lateral structure, which is not explained in traditional EDL models.

Hence, the solid–IL interface is interesting from a fundamental point of view because there is exceptional diversity of possible structures, uniting features of simple, molecular, and self-assembled liquid systems. While not every IL type has yet been studied, the ions are highly organized in both normal and lateral directions. Interestingly, the associated push-through forces are typically larger in ILs than for solvation layers of most other solvent types (cf., Table 4). This indicates that IL interfacial structure is much more pronounced than other solvents, similar to the bulk phase (cf., Table 3) due to strong cohesive interactions. Because the segregation of polar and apolar groups is retained normal to and laterally along the interface, it is preferable to use (1) terms like “layered”, “lamellar-like”, or “bilayer” in place of “solvation layers” to describe normal structure and (2) the language of self-assembly (worm-like, micelle-like, etc.) for lateral structure. Above all, elucidating the transitions between different ion arrangements is of great importance: When is (normal) structure more lamellar-like than ion pairs?<sup>82,911,920</sup> When is lateral structure more worm-like than micelle-like?<sup>899</sup> How long must an alkyl chain be to form poly(IL)-like structures?<sup>1266</sup>

## 7. DISCUSSION

The structure of ILs plays a key role in many applications and processes. In the first instance, there are many opportunities to mix, match, and incorporate different IL atoms, functional groups, or ion types in ILs to optimize performance. However, solvent properties and thus function are strongly influenced by the net organization of ions in the bulk. This requires deeper understanding of the role of IL self-assembly, and how it can be exploited for technological advances.

In the following section, we critically assess how to control IL self-assembly. Afterward, we highlight fields of research (ILs for

making things, ILs for processing things, and ILs for transporting things) where both the chemical and the self-assembled structure can be exploited to unlock the economic potential of ILs. We do not seek to comprehensively survey all IL applications, but instead to provide some perspective on the challenges and opportunities that could be realized with better control over IL structure.

### 7.1. Factors That Dictate Self-Assembly in ILs

**7.1.1. Coulombic Interactions.** Coulombic interactions are the most important factor in ion self-assembly, as the force is at least an order of magnitude stronger than other ion–ion interactions.<sup>9</sup> In the bulk, it enforces an electroneutral distribution of positive and negative charges, thus lowering system energy. However, the high ionic concentration ( $\sim 10\text{ M}$ ) and dielectric constants ( $\sim 20\text{--}30$ )<sup>159</sup> of ILs lead to Debye lengths smaller than ion dimensions. This means that Coulombic interactions are weaker and felt over shorter distances in the bulk as compared to ions in a vacuum or in aqueous electrolyte solutions. This means that the response of bulk ILs to external electric fields is weak.

Coulombic interactions lead to the formation of polar domains. This is observed in many ILs because (1) cation charged groups selectively solvate the anion's charged groups (and vice versa) and (2) uncharged groups are expelled from this region. The localization of Coulombic charge on the ions leads to strong charge–charge correlations, which assists in polar domain formation.

**7.1.2. Solvophobic Interactions.** Like the hydrophobic effect in water,<sup>355</sup> solvophobic interactions are entropy-driven and increase in strength with cation alkyl chain length. Thus, the structural effect of increasing alkyl chain length is to promote larger, more distinct, apolar domains, and consequently more well-defined solvent nanostructure.

The concentration of polar/apolar interfaces in ILs is exceptionally high, and repeats every  $\sim 1\text{ nm}$  (depending on the IL's repeat bulk correlations). This is just above the critical radius for a stable amphiphile self-assembly.<sup>1273,1274</sup> This indicates that IL nanostructure with an ethyl group may be the smallest example of amphiphile self-assembly. The absence of tail–tail correlations in methylammonium nitrate<sup>440</sup> is consistent with this.

**7.1.3. Packing Geometry.** The relative dimensions of the polar and nonpolar moieties of cations and anions define a packing geometry ( $a_{\text{alkyl}}/a_{\text{polar}}$ ), akin to the critical packing parameter,<sup>91,92</sup> which controls the preferred arrangement of polar and nonpolar domains, captured by bulk correlation peak in scattering measurements. This is the principle way in which the anions influence nanostructure for ILs with amphiphilic cations; depending on the cation alkyl chain length, it occupies a relatively large or small volume in the polar domains. It is likely that the polar/apolar interface is subject to an area-minimization constraint as in L<sub>3</sub>-sponges,<sup>441</sup> although the “tension” of this interface must be extremely low. On a related note, more rigorous theoretical treatment of the IL nanostructures, and how their topology and nodal surfaces compare to classical self-assembled phases,<sup>443,444</sup> has not been performed. This may be important for understanding the underlying physics of non-aqueous self-assembly, for example, curvature and bending energy of the nanostructures.

**7.1.4. Hydrogen Bonding.** In general, the importance of H-bonding toward ILs structure has been overstated. In PILs, Evans et al.'s hypothesis of 3D H-bond network in EAN<sup>179</sup> is widely

accepted in the literature and is consistent with established models of structure in molecular protic liquids.<sup>424</sup> However, this has led to the belief in some quarters that all PILs can build up H-bond networks structures.<sup>1205</sup> Moreover, many studies continue to emphasize the similarity of PIL H-bond networks to that found in water<sup>152,437,682,761,847,1275–1292</sup> or other protic solvents.<sup>1293</sup> It is common to find statements such as “PILs can build up hydrogen bonding networks similar to water molecules due to their protic nature and general solvent properties”<sup>1294</sup> in reference to ion arrangements.

While a 3D H-bond network does form in the majority of PILs, it is quite different from that in water, and is confined within the polar domain of the liquid's nanostructure. Even for anions with different capacities to H-bond, there is little discernible effect on bulk structure; the overriding effect of electrostatic interactions and packing consideration is stronger than that due to differences in H-bonds. In some respects, this is analogous to well-established concepts of H-bonding in protein folding,<sup>1295</sup> as H-bonds do not control self-assembly, but form between adjacent donor and acceptor sites in the nanostructure. H-bonds are accommodated between ions as best they can, but are not the principal drivers of structure.

At the other extreme, some studies still ignore H-bonding in ILs<sup>183,184,1296–1299</sup> and/or treat these solvents as unstructured media<sup>100,1300–1307</sup> of uniform polarity. This is reflective, at least in part, of the classical view of liquids as an “unstructured” homogeneous state of matter.<sup>12</sup>

H-bonds are important for understanding IL solvent properties. In PILs, trends in melting point, glass transition temperature, ionic conductivity, and viscosity can be correlated with the nature of H-bonds.<sup>427</sup> This has far reaching implications for solvent selection as the nature of H-bonds present in the nanostructure is reflective of PIL behavior; whether the H-bonds are strong or weak correlates with the strength of the cohesive interactions and thus PIL properties. For some time now, ILs have been touted as “designer solvents” due to the promise that macroscopic properties can be tuned by variation in ion structure. The results suggest this can be achieved by greater understanding of IL H-bonding, and ways to control it via ion self-assembly. This is a widely used approach in crystal engineering,<sup>188</sup> where the strength/geometry of H-bonds is modified to achieve desired physical properties. For example, distorting the H-bond network may be advantageous where PILs are required as solvents, with melting points below room temperature. In other cases, a less constrained H-bond network is desirable as it will facilitate faster proton transfer in the bulk. This will become increasingly important as PILs are explored as electrolytes for hydrogen fuel cells<sup>1136,1308</sup> and pharmaceutical compounds<sup>1309</sup> where labile protons are key to process efficiency.

**7.1.5. IL–Surface Interactions.** In addition to the factors that control structure in the bulk, the self-assembly of ions near solid interfaces is influenced by IL–surface interactions. While the focus here is on solid interfaces, in principle this description also holds for air and liquid interfaces.

The surface properties of all of the substrates described in this Review vary substantially, leading to key differences in the ion arrangements close to the interface. In general, ions organize into lamellar-like layers at the solid–IL interface. This is because the interface aligns the pre-existing morphology present in the bulk phase, similar to aqueous surfactant dispersions.<sup>1176</sup> The ion arrangements here are closely related to, but more ordered than, the bulk phase, as IL–surface interactions have an organizing

effect. The main features that influence self-assembly are surface: (1) charge (positive vs negative vs neutral), (2) polarizability (polarizable vs unpolarisable), (3) topology (smooth vs rough, curved vs flat, surface defects), (4) crystallinity (crystallographic vs amorphous), (5) porosity, (6) reactivity (exchangeable ions or groups vs inert substrate), (7) reconstructions, and (8) the volume of IL interacting with the substrate (monolayer vs bilayer vs liquid film vs bulk liquid).

To a greater or lesser extent, all of these surface properties can change self-assembly. The response of the IL is not so easy to predict as these can alter (1) what part of the IL interacts with the surface (anion vs cation, charged moiety vs uncharged moiety), (2) the strength of the IL–surface interaction, (3) the number of ion layers arranged normal to the interface, (4) the lateral structure<sup>899</sup> of ion layers, and (5) ion packing normal to, and laterally along, the interface. The most prominent changes are noted for the ions flanking the substrate; however, longer range (5–10 nm) effects in the transition zone between the interfacial layer and bulk phase have been observed.

As an aside, no experiments have explicitly demonstrated whether the flow of ILs at solid surfaces reversibly alters interfacial chemistry. Recently, this has been demonstrated for aqueous solutions at salt surfaces,<sup>1310</sup> and such an effect in ILs has implications for many applications where there is a (free-flowing or induced) collective motion of ions parallel to the surface.

## 7.2. How To Control IL Self-Assembly

**7.2.1. In the Bulk Phase.** With so many ways to modify chemical structure, and such diversity of possible responses on short and long length or time scales, it is surprising that for nearly every reported IL type, the net organization is governed by ion amphiphilicity. This is the principal way in which researchers can control IL self-assembly; highly amphiphilic ions provide a strong basis for solvophobic segregation of charged and uncharged groups into polar and apolar domains. “Nonamphiphilic” ions that possess (1) short alkyl chains, (2) multiple, sterically hindered charged groups, or (3) electrostatic charge distributed over a large molecular volume have a reduced tendency to self-assemble.

Because solvophobic alkyl chains are normally found on IL cations, IL amphiphilicity is largely a function of cation molecular structure, with more pronounced structure reported with increasing cation alkyl chain length and localization of positive charge. Experiments have shown the role of common anions is less significant because amphiphilic anions are rarely employed. Anions are, however, an important reporter of structure in scattering experiments,<sup>428,432</sup> and are important for controlling local structure in the polar domains.

If the ions are weakly amphiphilic, the bulk structure is largely determined by Coulombic forces and simple packing. In this case, the bulk organization is reminiscent of molten salts with alternating anion/cation three-dimensional shells that satisfy local and bulk electroneutrality. This is because the driving force for apolar domain formation is reduced and so the structure resembles the radially symmetric “onionskin” model suggested by Hardacre et al.<sup>301</sup> At a critical asymmetry, when the IL ions are sufficiently amphiphilic, short-range solvophobic interactions drive self-assembly of polar and apolar groups. This enables a bicontinuous phase morphology to form in the bulk through the mutual attraction of polar and apolar groups.

For an amphiphilic IL, the dimensions and geometry of the self-assembled structure can be predicted by considering the area ratio of charged/uncharged or solvophilic/solvophobic groups in

the ion pair ( $a_{\text{alkyl}}/a_{\text{polar}}$ ). This exploits the fact that amphiphilic ions resemble ionic surfactants but on smaller length scales. Thus, it is possible to apply relationships akin to the critical packing parameter<sup>91,92</sup> to IL ions to describe the overall arrangement. While it may not be applicable to all anion/cation combinations (see below), its application, alongside evidence of a peak at low- $Q$  in scattering experiments, should distinguish between weakly/strongly or curved/flat IL nanostructures in terms of amphiphilicity, and hence whether bicontinuous ordering forms in the bulk.

Introducing polar or H-bonding moieties (hydroxyl, ether, thiol, amine, fluorous, etc.) onto uncharged groups interferes with amphiphilicity. When the number of polar substitutions is low, amphiphilicity is usually disrupted, which forces a bicontinuous morphology into a more disordered, clustered nanostructure. However, as exemplified by fluorous ILs, with increasing numbers of the polar groups, a tricontinuous nanostructure can form.<sup>467,469,471</sup> This is because some polar moieties can self-associate, and form a separate domain.

The organization of dicationic ILs is consistent with this model of ion self-assembly; the degree of nanostructure scales with cation amphiphilicity. However, the presence of two charged sites on the cation means that the segregation of polar and apolar domains is less pronounced than the corresponding monovalent IL. In this case, the link to bolaform or gemini surfactants is striking;<sup>474–476</sup> “spacer” length and anion volume are the key indicators of nanostructure. It is likely that these principles will also hold for dianionic ILs, which have yet been characterized in the literature.

In magnetic ILs, the evidence from crystal structures suggests that the segregation of charged and uncharged groups will also be present in the bulk liquid. However, this is still to be verified experimentally or via simulation, and it is still unclear how the strong magnetic moments affect long-range solvent ordering.

Conversely, a surfactant-like chemical structure is not present for solvate ILs. Thus, amphiphilicity is not a key to nanostructure formation in these ILs. Instead, the ion sizes as well as the number and position of chelating groups dictate self-assembly.

Another way of controlling self-assembly is via the dissolution of solutes. While the IL resists changes in its self-assembled structure, at sufficient concentration a different but related nanostructure will form. These can be predicted using ideas captured in the  $a_{\text{alkyl}}/a_{\text{polar}}$  ratio, by considering whether the solute prefers to be solvated by the charged or uncharged groups and its relative size or concentration in the bulk. Again, this highlights the importance of ion amphiphilicity for controlling the arrangement not only of the IL itself but also of the structure of species dissolved in the solvent. Additionally (and unlike most solvents), IL ions often act as cosurfactants on account of their amphiphilicity. This provides a new criterion for distinguishing how ILs can be used as self-assembly media as compared to traditional solvents.

External variables can also be used to tune self-assembly in ILs. To date, the evidence suggests that ion conformations can be altered by increased pressure; no explicit data have shown a change in the overall self-assembled nanostructure. The effect of temperature is more complicated and likely IL specific. In general, ILs respond to increasing temperature as per molecular liquids. However, modest increases in temperature can lead to well-defined polar domains, and thus more ordered nanostructure.<sup>559</sup>

**7.2.2. At the Solid Interface.** In most respects, the model previously developed for structure at the solid–IL interface<sup>82,85</sup> is

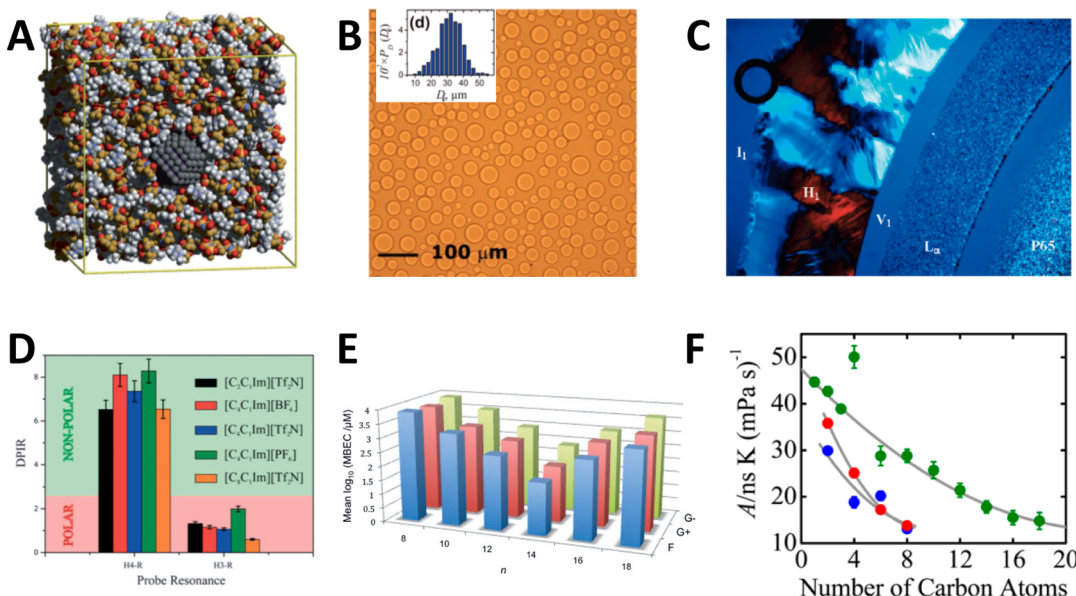


**Figure 26.** Exploiting IL bulk (nano)structure for making things. (A) MD simulation of Ru nanoparticle solvation in  $[C_4\text{mim}][\text{NTf}_2]$ . (B) Optical micrographs of the structure and size distribution of cationic DDAB vesicles dispersed in both a  $L_3$ -surfactant and EAN's  $L_3$ -solvent phase. (C) Polarizing optical micrograph of  $L_\omega$ ,  $V_1$ ,  $H_1$ , and  $I_1$  phases of P65 in EAN. (D) Partition coefficient (DPIR) for resonances of the RAFT agent in the polar ( $H_3\text{-R}$ ) and apolar ( $H_4\text{-R}$ ) domains of several ILs. (E) Mean minimum biofilm eradication concentration (MBEC) of different fungi for three ILs as a function of alkyl chain length  $n$ . (F) How the number of carbons on cation chain influences rotational diffusion of polar solutes. Reproduced with permission from refs 837 (Copyright 2011 John Wiley and Sons), 152 (Copyright 2012 American Chemical Society), 494 (Copyright 2009 American Chemical Society), 1360 (Copyright 2013 Royal Society of Chemistry), 1418 (Copyright 2010 Royal Society of Chemistry), and 1422 (Copyright 2012 American Chemical Society).

retained: ions form a lamellar-like morphology close to the surface surface due to specific, molecular, (bulk) liquid, and surface effects. The most important recent development has been increased recognition of lateral structure within the ion layers.<sup>899</sup> Again, this is a consequence of ion amphiphilicity, but the structure formed reflects both ion–ion and ion–surface interactions.

The strength of IL–surface interaction and number of ion layers can now be changed at will by variation in ion chemical structure,<sup>82,922</sup> surface type,<sup>82,1011</sup> surface charge,<sup>82,572,922,1011</sup> etc., and for many situations (porous surfaces, analytical separations, particle stability), thinking about self-assembly at the solid–IL interface in 2D is sufficient. However, in phenomena like capacitance, surface wetting, and friction, understanding the 3D lateral structure is important, and more research still needs to be performed in this area. Thus, by assessing the degree of ion amphiphilicity, packing arguments<sup>86</sup> and surface properties can predict ion self-assembly at the interface, although there are likely related kinetic or hydrodynamic effects yet to be uncovered.

### 7.3. Exploiting (Nano)structure to Make Things

**7.3.1. Nanoscience and Nanomaterials.** In the last 40 years, nanoscience and nanotechnology have developed rapidly with precise control over matter achieved down to the atomic level.<sup>1311</sup> This has seen an enormous number of nanostructures and nanomaterials characterized in the literature, showing many interesting chemical, physical, electronic, thermal, and optical properties.<sup>4</sup> Despite these successes, the synthesis of modern nanomaterials remains challenging due to the unique operating conditions, for example, tiny length and time scales and high surface-to-volume ratios of components. In general, this has often seen nanoscale processes resulting in lower efficiencies or prone to deviations from expected behavior as compared to

macroscopic chemical processes. Currently, synthetic nanoreactors<sup>1312,1313</sup> are being explored to bridge this efficiency gap, because they provide a reasonably well-defined nanospace or cavity in which reactions can occur. Others have focused on self-assembled phases,<sup>1314</sup> which exploit the polar/apolar domains of surfactant and copolymer amphiphiles formed in an aqueous media. However, scaling up these systems for mass nanofabrication has not been achieved, and so they cannot be easily integrated into existing macroscopic technologies and devices.

To this end, ILs have been suggested as potential self-assembled nanoreactors.<sup>1315</sup> Unlike traditional nanoreactors<sup>1312,1313</sup> and aqueous self-assembled phases,<sup>1314</sup> no complex encapsulation techniques or critical ion concentrations are required to induce self-assembly in ILs; the bicontinuous phase forms spontaneously in the pure liquid, and the structure is quite robust to high water content.<sup>426,597</sup> This indicates that ILs are well-placed to be integrated into nanotechnology revolution via deeper consideration of structure. For example, the strong interaction of imidazolium-based ions with carbon-nanomaterials<sup>631,632,966,985,1011</sup> can be exploited to form stable dispersions of graphene,<sup>1316,1317</sup> hybrid materials,<sup>1318</sup> nanoribbons,<sup>955</sup> nanotubes,<sup>196</sup> carbon nanodots,<sup>1319</sup>  $\pi$ -conjugated polymer devices,<sup>499</sup> or functional surfaces.<sup>1320</sup>

Nano- and microsized particles are routinely prepared in many IL solvents without aggregation. Here, consideration needs to be made for both number of ion layers formed at the solid–IL interface and the overall viscosity of the solvent.<sup>156,940,1144,1321,1322</sup> When grown in ILs, the size distribution of metal nanoparticles is related to the degree of internal structure of the IL (cf., Figure 26A).<sup>1323–1326</sup> This is because nucleation and growth of the metal appears to be localized in the nonpolar regions of the liquid,<sup>1327</sup> and so is limited by the dimensions of these domains. An interesting extension of this work would be the solvation of Janus<sup>1328</sup> or “patchy”<sup>1329</sup>

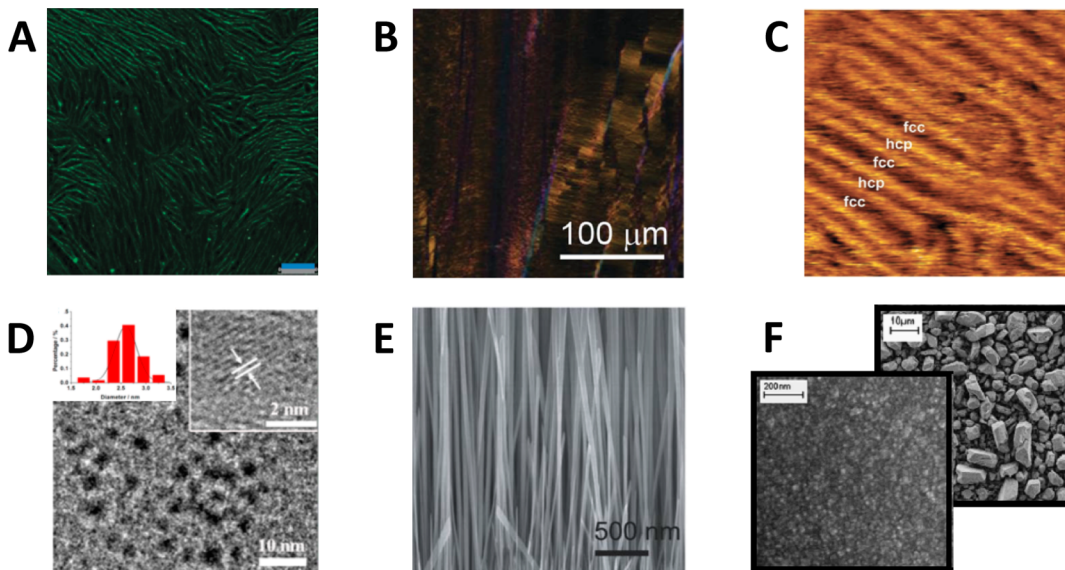


**Figure 27.** Exploiting IL interfacial (nano)structure for making things. (A) Confocal image of cyclic peptide nanotubes on PVDF membrane aligned using  $[C_8\text{mim}]^+\text{Cl}^-$  (scale bar 1  $\mu\text{m}$ ). (B) Polarized microscopy image of compressed thin film of PB16TTT polymer structured by  $[C_2\text{mim}]^+[\text{NTf}_2]^-$ . (C) In situ  $30 \times 30$  nm STM image of herringbone rearrangement of Au(111) surface mediated by  $[\text{Py}_{1,4}]^+\text{FAP}$  adsorption at  $-1.2$  V. (D) Structure and size distribution of IL-carbon nanodots from TEM and HRTEM. (E) SEM image of the quasi-aligned ZnS nanowires grown off Au nanoparticles from  $[C_4\text{mim}]^+[\text{AuCl}_4]^-$ . (F) SEM images of nano- (left) and micro- (right) crystalline Al electrodeposited on Au from  $[\text{Py}_{1,4}]^+$  and  $[C_2\text{mim}]^+$ -based ILs. Reproduced with permission from refs 1347 (Copyright 2013 Royal Society of Chemistry), 1350 (Copyright 2014 John Wiley & Sons), 573 (Copyright 2011 Royal Society of Chemistry), 1319 (Copyright 2014 American Chemical Society), 1351 (Copyright 2012 Royal Society of Chemistry), and 883 (Copyright 2009 American Chemical Society).

(nano)particles in ILs. It is likely that the hydrophobic and hydrophilic domains will be selectively solvated by corresponding groups on the ions. This may open new ways of controlling orientation<sup>1330</sup> of colloid particles in the bulk or the adsorbed particle structure at liquid–liquid interfaces.<sup>1328,1331,1332</sup>

Similar control of zeolite<sup>1333,1334</sup> or metal organic framework<sup>1335,1336</sup> architectures should also be possible if the reaction is slow, enabling the IL to template a desired topology or crystallinity. This is because the nanostructure will grow and selectively recruit reagents dissolved in a favored domain, propagating one local structure/crystallographic plane over time. Currently, different nanostructures have only been demonstrated by varying IL ion size or chirality. For example, small IL ions with localized charge centers can be occluded into the materials' pores, leading to substantial changes in catalytic activity and near-surface conductivity.<sup>1337</sup> Alternatively, chiral nanostructures from achiral reagents have been reported using chiral ILs.<sup>1338</sup> The origin of the chiral effect is still unclear as it is unlikely that the nanostructure of a chiral IL is substantially different from that of the achiral ILs.<sup>1339,1340</sup>

An even greater degree of control has been demonstrated at the solid–IL interface, because the IL nanostructure is more well-defined than in the bulk (cf., Figure 27). Already, scientists are creating novel materials with (nano)structure that have been templated and aligned by the ion arrangement, for example, nanowires,<sup>1341–1346</sup> nanotubes,<sup>1347</sup> Janus nanosheets,<sup>1348</sup> electropolished surfaces,<sup>1349</sup> or polymer semiconductor films.<sup>1350</sup> For example, Goldberg et al. created centimeter-long ZnS nanowire arrays from a silica substrate.<sup>1351</sup> By choosing an  $[\text{AuCl}_4]^-$ -based IL, a uniform pattern of gold nanoparticles could be templated onto the substrate, from which ZnS adsorbs and grows nanowires. As near surface IL structures can be controllably varied, exquisite control of functional interfaces or coatings<sup>1352</sup> through judicious IL selection is within our reach,

and applicable to the creation of other assemblies, for example, supported IL membranes<sup>1353,1354</sup> or self-assembled monolayers.<sup>1355,1356</sup>

For polymers, ILs offer many advantages, either as solvents for polymerization or as functional additives.<sup>147,493,501</sup> Both hydrophobic and hydrophilic monomers and long chain polymers are soluble in ILs due to solvent nanostructure. This can be further exploited to separate growing monomer chains from the catalysts in ATRP and thus reduce the extent of side-reactions.<sup>1357</sup> Moreover, the efficacy of ILs as additives (plasticizers and porogenic agents) is related to ion amphiphilicity, suggesting self-assembly plays a direct role in controlling structure. It is possible to achieve similar outcomes for IL ions entrained in the polymer matrix; properties of polymer electrolytes<sup>1358</sup> and melts<sup>1359</sup> can be solvent tuned with surfactants. Notably, the kinetics in and products of polymerizations<sup>1360–1362</sup> are influenced by IL self-assembly, which offers further opportunities to tune the structure and properties of polymeric materials (cf., Figure 26D); it would be interesting to see whether this could be exploited in IL-based 3D printing<sup>1363,1364</sup> or in lithography to fabricate surface nanostructures.<sup>1365,1366</sup>

Other opportunities in nanoscience abound. Solvent nanostructure itself has been implicated in the speed of sound<sup>1367,1368</sup> or thermal conductivity<sup>161</sup> of ILs, which will be further harnessed in future sonochemistry<sup>1369</sup> or heat transfer<sup>1370</sup> applications, respectively.

**7.3.2. Organic Synthesis.** There is longstanding and widespread interest in the use of ILs for organic synthesis and catalysis,<sup>24,25,1140,1371</sup> with the advent of air- and water-stable ILs, organic chemists quickly recognized their scientific potential as alternative “green” solvents. An impressive array of organic reactions has now been demonstrated in ILs, spanning most, if not all, of the transformations and coupling reactions that have been achieved in molecular solvents.<sup>24,25</sup> However, the outcomes

of a reaction are markedly different when conducted in an IL as compared to a molecular solvent (or between different ILs); yields, favored product/s, byproducts, reaction rates, reagent solubility, material reactivity, transition states, intermediates, or activation energies vary depending on IL used. Likewise, ILs are not benign solvents and can be reactive to dissolved materials.<sup>1372</sup> In many early publications, the origin of these solvent effects is not explored because the solvent was treated as a homogeneous continuum of dissociated ions<sup>1373</sup> with uniform polarity.<sup>100</sup> Since then, greater attention has been paid to IL structure. For instance, it has been recognized that solvent polarity measurements by dielectric spectroscopy or probe dyes fail to capture ion translations<sup>24,1374</sup> or polar/apolar domains<sup>24,28,233</sup> (respectively). More recently, the contribution of IL steric factors,<sup>1375</sup> H-bonding,<sup>1375,1376</sup> solvophobic interactions,<sup>1377</sup> solvent entropy,<sup>1378,1379</sup> ion self-assembly,<sup>1375</sup> and clathrate formation<sup>1380</sup> has been used to control the reaction mechanisms, selectivity, or rates. Others have demonstrated that IL nanostructure influences the rotational diffusion constant of solutes (cf., Figure 26F),<sup>622,623</sup> which likely has implications tuning reaction mechanisms. Similar but less specific structural effects were noted in multicomponent reactions<sup>1381</sup> and microwave synthesis,<sup>1382</sup> the latter because IL ions possess many groups active in the microwave region.

As pointed out by Hallet and Welton,<sup>24</sup> even standard transition-state theory<sup>2</sup> is not so easily applied in ILs as consequences of self-assembly. This is because the reorganization of solvent ions or functional groups in polar/apolar may not be fast as compared to the reacting species. This means that static, activation, and dynamically controlled reactions are possible in ILs, depending on the degree of internal structure in the IL, and the extent to which this slows ion motion in either the polar or the apolar domains. The picture that is emerging is a solvent environment much more complex than in molecular liquids as there are multiple ways in which structure can influence the reaction.

**7.3.3. Electrodeposition.** STM has been used to engineer nanostructure formation at the metal–IL interface (Fe clusters,<sup>1383</sup> nanowires<sup>1341–1346,1384</sup>) and to investigate electrodeposition of materials from ILs (cf., Figure 27C). An array of metals, semiconductors, and alloys can be safely and rapidly electrodeposited from ILs including Al,<sup>1385–1388</sup> Bi,<sup>1389</sup> Co,<sup>1390</sup> Cu,<sup>1391–1393</sup> Ge,<sup>1344,1394–1396</sup> In,<sup>1391,1393</sup> Nb,<sup>1397,1398</sup> Pb,<sup>1399</sup> Sb,<sup>1400,1401</sup> Se,<sup>1393</sup> Si,<sup>1344,1394,1402</sup> Sn,<sup>1390</sup> Ta,<sup>1397,1403,1404</sup> and Zn.<sup>1405</sup> Notably, most of these cannot be isolated in traditional (usually aqueous) electrolytes<sup>36</sup> as the electrochemical window is too small, and thus the solvent itself breaks down before isolating the material of interest. The ion chemical structure and solvent structure may contribute to the large electrochemical windows of ILs, insofar as the lateral organization at the electrode interface will determine which ion functional groups are susceptible to one-electron reduction/oxidation by bond scission.<sup>1406,1407</sup>

The size and morphology of the electrodeposit appears to be related to the strength of the ion–surface interactions (usually the cation) and thus near-surface IL structure; if the interaction strength is strong, nanocrystalline deposits are isolated, whereas larger coarse, micrometer-sized deposits are achieved when the interaction is weak (cf., Figure 27F).<sup>883,1408</sup> There is great scope for further research along these lines varying IL ion and solvent nanostructure, with the goal to electrodeposit cheap, commercial-grade quantities of these materials in ILs.

**7.3.4. Medicines and Medical Research.** One novel area of IL interest is in medical research. ILs were generally slow to

enter this field as IL ions/solvents generally were believed to be toxic and susceptible to bioaccumulation. This situation is now rapidly changing, and IL medicines were a focus of a Gordon Research conference in 2014.<sup>1409</sup> Medical applications abound and include ILs as active pharmaceutical ingredients, prodrugs, disinfectants, preservatives, antiseptics, antibiofilm agents, and plasticizers/antimicrobial agents for medical polymers, often by tuning ion structure to match or resemble a neutral molecular analogue.<sup>1309,1410–1416</sup>

The ionic nature of ILs is crucial to function and in many ways highlights their pedigree for medical science; around one-half of all drugs are currently administered as (solid) salts.<sup>1417</sup> This is important because ions interact strongly with water molecules, aiding *in vivo* solubility. To date, much of the research effort is focused on tailoring structure so that melting occurs below 37 °C. This enables the candidate IL to be administered, and remain as a fluid in the human body. A liquid compound is also advantageous as there are no issues related to solid polymorphism. Here, the anion, cation, or both can be adapted to create novel medicines. An enormous library of neutral compounds from medicinal chemistry provides a comprehensive roadmap for IL researchers; the challenge is often creating the ionic analogue by incorporating a permanent charged site on the compound without loss of, or indeed improving, drug efficacy. Fortunately, many of these target molecules have proton-donating/-accepting functional groups so that a protic analogue is often possible. Likewise, these molecules are typically large and asymmetric, meaning that a liquid salt should be achievable if paired with an appropriate counterion.

Systematic screening of structure–activity relationships in IL drugs has not been performed, at least to the extent that it has for most other prospective pharmaceutical compounds. However, the activity of 1-alkylquinolinium ILs suitable against Gram-positive and Gram-negative bacteria, fungi, and algae is related to cation alkyl chain length (cf., Figure 26E).<sup>1418</sup> A similar effect was noted for ammonium-, phosphonium-, or imidazolium-based ILs on human tumor cell lines.<sup>1419–1421</sup> This suggests features related to the IL self-assembly are important for their efficacy, although the molecular origin of this behavior has not been elucidated, and is likely to be highly specific to the target of interest.

What is still to be performed for ILs in medical research? We suggest that it may be possible to make sunscreens with photoresponsive ions or radiopharmaceuticals from ILs with radioactive atoms. Neither of these examples has been reported in the scientific literature.

#### 7.4. Exploiting (Nano)structure to Process Things

**7.4.1. Cellulose Dissolution.** One of the most promising and eagerly awaited applications of ILs is their use for biomass processing or biofuels, because large biomolecules including cellulose, wood, lignin, etc., can be dissolved and regenerated under benign conditions.<sup>589,1423,1424</sup> While much of the literature rationalizes cellulose solubility in ILs or molecular solvents via H-bonds, a recent review of the fundamental experimental evidence has pointed to the importance of hydrophobic interactions.<sup>1425–1427</sup> Cellulose is itself amphiphilic, and hydrophobic associations in cellulose stabilize the crystal over the solution phase.<sup>1425</sup> In fact, every example of successful dissolution of cellulose in an IL has been achieved with one of the ions (usually the cation) being amphiphilic. As described throughout this Review, the signature of hydrophobic (solvophobic) interactions in ILs is ion self-assembly, leading to well-defined nanostructures

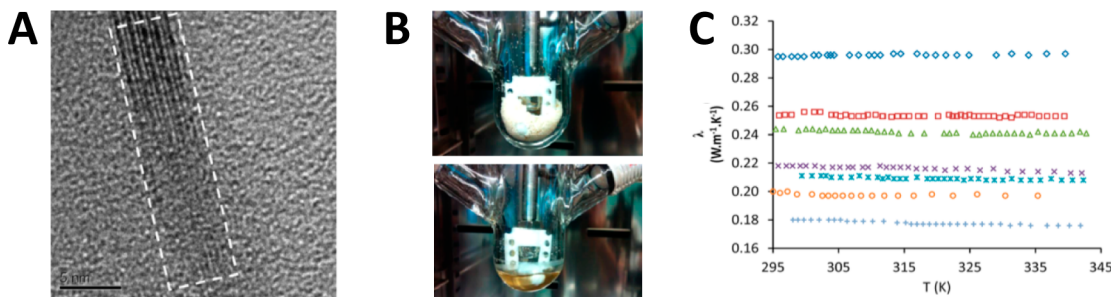


**Figure 28.** Exploiting IL bulk and interfacial (nano)structure for processing things. (A) TEM image of microcrystalline cellulose in 1-allyl-3-methylimidazolium chloride. (B) The pure IL  $[P_{2,2,2,2}][BnIm]$  at 70 °C (top) and at 0.15 bar  $CO_2$  (bottom). In (C) thermal conductivity  $\lambda$  versus temperature for several PILs with different bulk nanostructure; ETAN (blue  $\diamond$ ), EAHS (red  $\square$ ), EAN (green  $\triangle$ ), PAN (purple  $\times$ ), EASCN (blue \*), BAN (orange  $\circ$ ), and BASCN (blue +). Reproduced with permission from refs 1429 (Copyright 2012 Royal Society of Chemistry), 1485 (Copyright 2014 American Chemical Society), and 161 (Copyright 2014 Royal Society of Chemistry).

in the bulk or at interfaces. What is therefore required is greater understanding of how ion self-assembly mediates cellulose/biomass dissolution<sup>1428</sup> and whether we can pattern different types of cellulose structures<sup>1429</sup> from ILs (cf., Figure 28A). The biology of the problem is important too as amphiphilic ILs appear to inhibit microbial growth, decreasing the efficiency of biofuel production. This was recently addressed by Ruegg et al.<sup>1430</sup> who genetically engineering microbes tolerant to imidazolium ILs.

**7.4.2. Mineral Extraction.** A special case of ILs for analytical separations<sup>1138,1431</sup> is in mineral processing. Recovering precious materials from an ore is highly energy-intensive and requires enormous volume of solvent.<sup>1432</sup> Because the cost of ILs is significantly greater than water, it is unlikely that ILs will ever be used as wholesale replacements in current approaches of, for example, froth flotation, even with solvent recycling. Nonetheless, ILs represent an alternate solvent additive to control surface tension due to their surfactant-like behavior at interfaces. Several groups have shown peculiar interaction between ILs and minerals (ores of coal,<sup>1433,1434</sup> Au,<sup>1435,1436</sup> Ag,<sup>1435,1436</sup> Cu,<sup>1436,1437</sup> etc.), which could be exploited in small volume extraction/treatment of precious materials.<sup>1438</sup> To date, successful extractions have matched IL anion types to the corresponding acid ( $H_2SO_4$ ) used in aqueous systems. This suggests that IL ion types are likely to be rate-determining for material extraction. However, understanding self-assembly is likely key to designing future recovery strategies of the material from the IL. This underscores the need for more research into IL solvation, as recovery could proceed via simple precipitation, aggregation, or nucleation.

ILs may find use in the treatment of waste products from minerals extraction, thus preventing contamination in terrestrial environments. For example, biodegradable PILs appear well-placed to be used as buffers of acidic or basic discharges from mine sites. In a similar vein, solvate ILs with alkali metal cations could be employed to precipitate out cyanide anions; it is not difficult to envision other cases where careful selection of IL anions could be used to scavenge heavy metal ions in aqueous runoff treatment.

**7.4.3. Energy Storage.** ILs have been touted for a host of energy-based applications including fuel cells,<sup>1136</sup> batteries,<sup>697</sup> capacitors,<sup>553</sup> solar cells,<sup>1063</sup> and heat transport fluids,<sup>1370</sup> with the field subject to detailed reviews.<sup>1439,1440</sup> Again, controlling both chemical and self-assembled structure is crucial to delivering superior performance, particularly at interfaces. However, much fundamental research is still to be performed here as there are many components (electrodes, air– or liquid–liquid interfaces,

porous membranes, etc.) and solutes ( $Li^+$  ions, organic dyes, polymers, electrons/holes, nanoparticles) interacting with the IL, each of which has a different and sometimes competing chemistry. Interestingly, examples of superior performance have been obtained with solid- or quasi-solid IL electrolytes,<sup>1136,1441–1443</sup> suggesting that future reports of IL crystal or glass structures will not be unrewarded.<sup>1444–1447</sup> Likewise, the charge transport mechanism<sup>1448</sup> and thermal conductivity<sup>161</sup> of ILs in the bulk fluid is correlated to the degree of ion self-assembly (cf., Figure 28C). For all of these reasons, more basic science is required to inform the design of the IL, the structure formed, and overall process efficiency.

At interfaces, EDL structures of protic or polymeric ILs are still underdeveloped for their use as hydrogen fuel cell<sup>1136</sup> or polymeric electrolytes,<sup>1137</sup> respectively. While protic ions can be used in place of  $H_3O^+$  or  $OH^-$  ions as proton carriers, unlike AILs, experiments to elucidate ion arrangements at charge electrode interfaces have not been performed and are limited to Au(111) and graphite. In the case of photovoltaic cells, surprisingly little is known about ion organization at  $TiO_2$ , ITO, perovskite, or conductive polymer substrates under working conditions and how this affects related phenomena, for example, recombination/regeneration kinetics<sup>1449</sup> or adsorbed dye morphology.<sup>1450</sup> Related studies of the IL–rubrene<sup>1066,1007,1451</sup> interface have highlighted the challenges for controlling near-surface structure in organic field effect transistors. For batteries, the immediate challenge is to link the observed potential-dependent interfacial structure to charging kinetics,<sup>1133,1452</sup> pore effects,<sup>1453–1455</sup> ion–solvent complexes,<sup>1456</sup> or (preventing) dendrite growth<sup>1457</sup> that are key overall to performance. Interestingly, droplets of concentrated aqueous electrolytes moving on along graphene can also be used to generate electricity,<sup>1458</sup> which should be applicable to ILs so that energy is harvested by tuning the IL EDL structure itself.

Likewise, we have the tools but not sufficient control of ion self-assembly to create cubic or related nanostructures with columnar polar domains. As envisioned by Angell,<sup>1459</sup> this could be used to prepare PILs with a self-assembled structure that replicates the fast proton conduction of nanochannel proteins for use in a hydrogen fuel cell. Some developments along these lines for liquid crystal ILs have been achieved.<sup>1460–1462</sup>

In other instances, some of the groundwork has already been performed. For example, the strong, potential-dependent IL–electrode structure<sup>572</sup> with slow ion kinetics<sup>1463,1464</sup> will be used to build better IL capacitors or corrosion-resistant surfaces.<sup>1465</sup> These effects may also explain the suppression of the metal–

insulator transition in  $\text{VO}_2^{1466,1467}$  by electric field gating or controlling surface electronic states<sup>1468</sup> on metallic systems.

**7.4.4. Microfluidics.** Microfluidics is the science of plumbing on tiny dimensions.<sup>5,1469</sup> Relatively few scientists work with ILs in microfluidics<sup>1470–1473</sup> as the field largely employs cheaper aqueous solvents. It is now feasible to use ILs in microfluidic devices due to recent advances in understanding confined IL structure. However, high IL viscosities are still an issue, and most of the dimensionless groups<sup>1474</sup> used to assess microfluidic solvents have not been reported for ILs. This is important as they control the ratio of turbulent and lamellar liquid flow of the solvent, and are likely tunable with different chemical structures.

The strong interactions that induce IL self-assembly offer many opportunities to manipulate the solvent in microfluidic devices. For example, the amphiphilic nature of ILs provides openings to tune solid–liquid interactions at hydrophobic, hydrophilic, or metallic interfaces. The lubricity of microfluidic interfaces is also switchable depending on whether an anion, cation, or an uncharged moiety is adsorbed to the channel wall. The number of ion layers arranged near the wall is also important for lubrication at these length scales, and may even be used to control the level of lamellar flow on nanoscopic dimensions. Likewise, external electric fields could be used in flow-focusing<sup>1475</sup> of the IL or in electrochemical gating,<sup>1476–1478</sup> such that the density of either charge carrier is precisely controlled. This offers a novel way to pump the solvent around a device or to separate dissolved species.

More broadly, ILs offer the possibility of combining microfluidics and microprocessing devices of the Information Age. This is because the flow of ILs in the channel is both a movement of mobile solvent and a movement of electrical charge. This could be exploited to prepare integrated circuits with microfluidic platforms and vice versa. To our knowledge, this has not been developed in the literature.

**7.4.5.  $\text{CO}_2$  Capture.** ILs are promising solvents for postcombustion capture of  $\text{CO}_2$  gas.<sup>72,376,1479–1483</sup> Significant research efforts are currently underway in this area due to the link between anthropogenic global warming and  $\text{CO}_2$  emissions. ILs are envisioned as processing technologies to be fitted in the design of coal-fired power stations for separating  $\text{CO}_2$  from flue gas. In principle, much of the basic physical chemistry and proof of concept studies have been performed; the challenge now is to tailor IL ion reactivity, self-assembly, and selectivity for  $\text{CO}_2$  trapping so that the technology can be scaled up and become economically feasible.

Two different separation scenarios are reported: ion structures that react with  $\text{CO}_2$  or those that physically dissolve  $\text{CO}_2$  (usually under pressure). Chemically trapping  $\text{CO}_2$  is promising because ILs ions can be easily functionalized with amine groups, leading to better reaction stoichiometries than obtained for molecular solvents such as monoethanolamine.<sup>1481</sup> One drawback of this approach is that it can lead to large increases in solvent viscosity. This can be overcome via counterions that do not support a H-bond network<sup>1484</sup> or possibly by constraining any H-bonds that may form in a highly curved nanostructure. Another more interesting approach is to use benzimidazolide-ILs that change phase (solid → liquid) upon  $\text{CO}_2$  dissolution (cf., Figure 28B).<sup>1485</sup> This may enable the solvent heat of fusion to be employed in ultimate release of  $\text{CO}_2$  from the absorbent. Unlike chemical trapping, physical separation of  $\text{CO}_2$  is generally harder to achieve, because it must be selectively dissolved over other gaseous components and the solvent must have the capacity to

store high quantities at the partial pressures used in the flue mixture.

**7.4.6. Biomolecule Stabilization.** Surprisingly, ILs, particularly PILs, have been shown to be useful materials for the stabilization of biomolecules<sup>132,586,1486–1489</sup> (or even viruses<sup>1490</sup>) in their native state. This has been demonstrated for pure ILs or IL+ $\text{H}_2\text{O}$  mixtures and often results in better (and reversible) stabilization than can be achieved with existing approaches using phosphate buffers. The structure in these systems is incredibly complex and poses more questions than we currently have answers for. Any complete model for this behavior must consider IL self-assembly, Hofmeister<sup>1491</sup> and hydrophobic<sup>355</sup> effects, proton activity/buffer capacity,<sup>1492</sup> ion–biomolecule interactions, protein folding, and the role of water molecules trapped at the biomolecule surface. The presence of hydrophobic and hydrophilic groups on IL ions is likely important to this stabilization as are revelations that water's 3D H-bond network can remain largely intact at high IL content due to ion self-assembly.<sup>426,597</sup>

**7.4.7. Nuclear Fuel Processing.** ILs may also have a role in treatment, separation, and recycling schemes in nuclear fuel processing.<sup>1493</sup> Both the chemical and the self-assembled structures of ions play a role in performance. For example, ILs with boron or chlorine atoms have wide neutron cross sections<sup>1494</sup> and thus can quench chain reactions as control fluids for nuclear industry. Separation of spent radioactive lanthanides and actinides compounds has been demonstrated in ILs via liquid–liquid extractions (usually from an aqueous solvent)<sup>701,702</sup> as charged f-block compounds are generally well-solvated in the bulk polar domains of the ILs. It should also be noted that ILs display complex (hyper-<sup>1495</sup>)reactivity to radiation.<sup>1496</sup> For example, ionizing radiation creates “presolvent” electrons that persist in the IL bulk for much longer lifetimes as compared to molecular liquids. This is due to the high viscosity of the IL solvent and means that there is potential for side reactions or radical decomposition of the IL, dissolved solutes, or the substrate unless the electron is recaptured. To overcome this, ILs with aromatic groups are preferable because they can effectively scavenge free electrons and have low-lying  $\pi^*$ -LUMO orbitals. While promising, this field is still in its infancy, with much fundamental physical chemistry still to be performed.

## 7.5. Exploiting (Nano)structure to Transport Things

**7.5.1. Lubrication.** ILs offer many important advantages over conventional lubricants and antiwear compounds due to their (1) capacity to self-assemble, either in the bulk or confined at interfaces, and (2) strong interaction with surfaces. This means that ILs resist being “squeezed out” under surface compression, resulting in a robust boundary film that is stable at higher forces than a comparable molecular lubricant.<sup>909</sup> The capacity to self-assemble is retained even when dissolved in a second solvent, paving the way for IL additives in tribology.<sup>1139,1497,1498</sup> If the second solvent supports amphiphile self-assembly, 100-fold dilution of the IL is as effective as the pure IL to lubricate surfaces!<sup>1499</sup> This shows that cost need not be an insurmountable barrier for IL lubricants in large-scale applications;<sup>1500</sup> similar (or enhanced) performance as compared to conventional oils is economically feasible once the surface is half saturated in IL ions.

The key barrier to integration is that the molecular mechanisms of ILs lubrication are only just beginning to emerge.<sup>903,917–919,1010,1501–1504</sup> The majority of existing studies have examined macroscopic lubrication and shown mixed

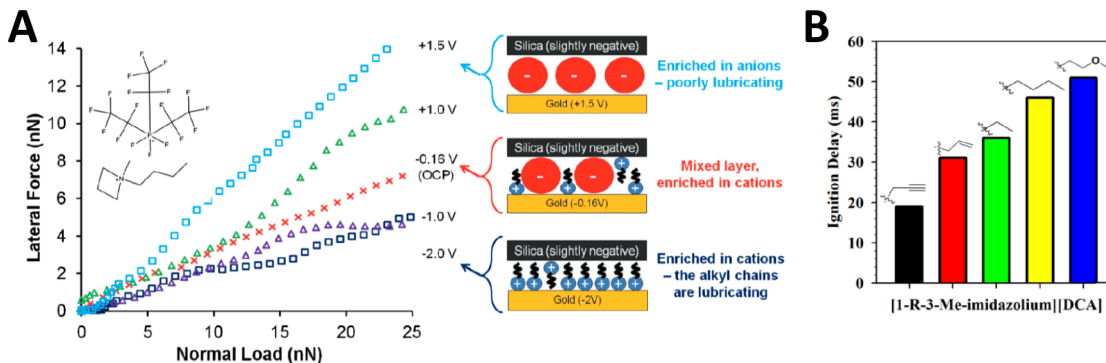


**Figure 29.** Exploiting IL bulk and interfacial (nano)structure for transporting things. (A) Lateral force versus normal load for  $[\text{Py}_{1,4}] \text{FAP}$  of a confined IL layer with varying composition due to different surface potentials between a silica colloid probe and the Au(111) electrode surface. (B) Measured ignition delay for several hypergolic ILs. Reproduced with permission from refs 1121 (Copyright 2012 American Physical Society) and 1516 (Copyright 2014 American Chemical Society).

results; in some cases, the IL performs better than a conventional oil, in other cases worse.<sup>1139</sup> It has recently been shown that the structures in both the near surface ion layer and subsequent layers control nanoscale friction.<sup>903</sup> The AFM data revealed that lubricity varies with the number and lateral structure of confined ion layers. In a related study, Sweeney and co-workers showed that nanoscale friction depends on applied surface potential (cf., Figure 29A),<sup>1121</sup> and is part of broader interest in electrochemical control of friction.<sup>913,1505–1509</sup> This paper exploits the fact that ILs are comprised of both an anion and a cation, which show different patterns of self-assembly under confinement. This study, confirmed by recent molecular dynamics simulations,<sup>1510</sup> offers the tantalizing prospect of tuning friction on small dimensions without changing surfaces with a self-replenishing layer, and could be easily integrated into niche situations, for example, lubrication of electrical contacts<sup>1511</sup> or of surfaces prone to contact electrification,<sup>1512</sup> because ILs are cheaper than existing nonconducting molecular lubricants (polytetrafluoroethylene). On a related note, different surface freezing behavior may be apparent in ILs at different potentials on certain substrates. This effect has long been known for water,<sup>1513</sup> and could be exploited in IL tribology.

**7.5.2. Fuels.** Some IL ions are known to be chemically<sup>1372</sup> or physically<sup>1514</sup> reactive materials. This paves the way for tuning ion structure to store chemical energy as fuelstocks. Perhaps the most promising area of IL fuel research is as hypergolic materials.<sup>1515</sup> In these systems, energy is controllably released via self-ignition when the fuel and oxidizer are mixed.<sup>1516–1521</sup> This has potential to be used as projectile propellants or for igniting engines and moving pistons. Unlike conventional hypergolic fuels, ILs generally display high energy densities and large heats of formation. Ion chemical structure is crucial to function in hypergolic IL fuels, while self-assembled structure appears less important, although we note that IL heat capacities have recently been linked to solvent nanostructure.<sup>161,1522</sup> Typically, ions with multiple reactive N=N, C≡N, or B–H bonds are employed. Recently, a systematic study of structure–property relationships for 38 ILs was performed by McCray et al.,<sup>1516</sup> who showed that fast ignition times (<40 ms) could be obtained by selecting cations with high electron density (cf., Figure 29B).

ILs have also been employed as pretreatment agents for conventional fuels (e.g., for extractive desulfurization<sup>1523–1525</sup>). This is based upon the solubility and/or preferential affinity of these compounds for the IL phase. Here, matching functional

groups and ion types to the target molecules is essential, as it likely proceeds via a solvophobic or  $\pi$ – $\pi$  interaction mechanism.

## 8. CONCLUSIONS

A central theme of this Review is that ILs are more complex than molecular solvents and thus their bulk and interfacial structures are markedly different. ILs show rich structural diversity both in the nature of ions that can be employed as well as in the organization of these ions in the liquid phase. While ILs have been modeled in several different ways including as ionic continua, collapsed crystal lattices, ion pairs, and H-bond networks, the evidence that IL ions self-assemble into amphiphilic nanostructures is now overwhelming. This is the unifying thread across all of the different IL types in the bulk liquid, as well as ion arrangements near interfaces or in the solid crystal phase. The existence of such well-defined solvent structure is the origin of much past, current, and future interest in ILs and is implicated in almost all aspects of their chemistry. Further, it is consistent with established models<sup>91,92</sup> for organization of ionic surfactant dispersions, although we stress that it is not a prerequisite for ILs to be dissolved in a second solvent; self-assembly occurs spontaneously in the pure liquid, or when mixed with (charged or uncharged) solutes and other ILs because at least one of the constituent ions are amphiphilic.

Therefore, ILs should now be thought of as fluids that are nanoheterogeneous, coherent, and essentially regular. This represents a clear departure from Bernal's classical picture of liquids as homogeneous, coherent, and essentially irregular. Heterogeneity in ILs arises because they are composed of two components, anions and cations, or, alternatively, charged and uncharged groups, and leads to repeating, correlated structure in the bulk and at interfaces on nanometer dimensions. The capacity for IL to self-assemble imparts regularity to ion arrangements, and means that the time-averaged structure can often be predicted from first principles. Recent advances in experimental and theoretical methods have led to unprecedented sensitivity in measuring this degree of regularity in ILs, with a goal to develop design rules for tailoring solvent properties.

### 8.1. Outlook

To build a competitive edge in the future, society needs creative, evidence-based solutions from chemistry research, with strong attention to solvents. ILs are a new, innovative class of materials with the potential to impact across many areas of scientific research.

When ILs first caught the attention of organic and electrochemists, little was known about the structure of these solvents except that they were pure ionic fluids. Since then, detailed understanding of IL structure has been obtained from simulation and experiment, and an unexpected diversity of solvent structures has been reported due to the capacity for IL ions to self-assemble. This has catalyzed research in ILs, and now their chemical and self-assembled structures can be used to unlock their considerable, but largely unfulfilled, potential in industry. As the field matures, there needs to be increasing cost/benefit economic analysis of ILs,<sup>63,1499,1526,1527</sup> which will be critical for ILs to compete with established solvent technologies. Also, the dynamics of ILs, and how this is linked to self-assembly, is not sufficiently developed and may in fact be a criteria to distinguish between structure in ILs and the organization of other solvents or dissolved (molecular, charged, amphiphilic) solutes. One can anticipate that progress in experimental and simulation techniques will enable an even larger body of IL structures to be screened,<sup>1528,1529</sup> and more structure–property relationships to be established. Thus, at this point, we ask: Do we need new ILs, new additives, and new IL structures to achieve this or a reappraisal of existing structures? The answer most likely is both, as there are many (unexploited) opportunities for manipulating IL structure to control function. Even among the vast IL literature, the usual suspects from the Periodic Table are ubiquitous in common IL ions (C, H, N, O, P, S); a large number of metals or gaseous elements have to date not been incorporated into an IL. We likely have only scratched the surface of IL structure.

## AUTHOR INFORMATION

### Corresponding Author

\*E-mail: rob.atkin@newcastle.edu.au.

### Present Address

<sup>§</sup>Department of Material Science & Engineering, The University of Illinois, 1304 West Green Street, Urbana, Illinois 61801, United States.

### Notes

The authors declare no competing financial interest.

### Biographies



Robert Hayes obtained his B.Sc. (Hons I) from the University of Newcastle under the supervision of Prof. Rob Atkin in 2009. He completed his Ph.D. within the same research group in 2014, examining the bulk and interfacial structure of ionic liquids using a combination of neutron diffraction, Monte Carlo simulations, and atomic force microscopy. Robert is currently working as a postdoctoral research

associate in the laboratory of Prof. Steve Granick at the University of Illinois at Urbana–Champaign.



Gregory Warr is Professor of Physical Chemistry at the University of Sydney. Greg completed his B.Sc. (Hons I) (1982) and Ph.D. (1986) at the University of Melbourne. He has held postdoctoral or visiting appointments at the University of Minnesota, Princeton University, the Centre d'Etudes Nucléaires, Saclay, the U.S. National Institute of Standards and Technology Centre for Neutron Research, and the CNRS Centre de Recherche Paul Pascale in Bordeaux. He has over 170 peer-reviewed journal publications and 8 book chapters, and has supervised 17 Ph.D. and M.Sc. completions and over 30 Honours projects at Sydney and elsewhere. Greg is a former Head of the School of Chemistry at the University of Sydney (2007–2012). He has served on the Editorial Advisory Boards of *Langmuir*, *The Journal of Colloid and Interface Science*, *Advances in Colloid and Interface Science*, and *The Australian Journal of Chemistry*. His research interests include amphiphile self-assembly, complex fluids, and interfacial structure.



Rob Atkin is Professor and ARC Future Fellow at University of Newcastle (Australia) where he leads the Nanostructure and Ionic Liquids (NaIL) group. Rob obtained his B.Sc. (Hons I) from the University of Newcastle and then completed a Ph.D. at Newcastle in 2003. Rob then joined the group of Prof. Brian Vincent at Bristol University working on microencapsulation. In 2005 he was awarded an Australian Research Council Postdoctoral Fellowship to study surfactant self-assembly in ionic liquids in collaboration with Greg Warr at the University of Sydney. He returned to Newcastle as a University Research Fellow in 2007, and was awarded an ARC Future Fellowship in 2012. He has published over 90 peer-reviewed journal articles and 5 book chapters.

## ACKNOWLEDGMENTS

This research was supported by ARC Discovery Projects, the AMRFP, ISIS beamtime grants, and the University of Newcastle

via a Ph.D. stipend. R.H. thanks the AINSE for a PGRA and Kenneth Schweizer (UIUC) for comments in Table 3. R.A. acknowledges receipt of a Future Fellowship. We would like to thank all of the anonymous Reviewers for their helpful comments and current members of the Newcastle & Sydney ILs groups for corrections during proofs. It is a pleasure to acknowledge long-standing collaborations and discussions with Frank Endres, Silvia Imberti, Mark Rutland, Tamar Greaves, Grant Webber, Roland Bennewitz, Alister Page, and Kislon Voitchovsky.

## GLOSSARY

OAc <sup>-</sup>	acetate anion
[Py <sub>n,n</sub> ] <sup>+</sup>	1-alkyl-1-alkylpyrrolidinium cation ( <i>n</i> = carbon chain length)
[C <sub>n</sub> C <sub>m</sub> mim] <sup>+</sup>	1-alkyl-3-alkylimidazolium cation ( <i>n</i> = carbon chain length)
[C <sub>n</sub> mim] <sup>+</sup>	1-alkyl-3-methylimidazolium cation ( <i>n</i> = carbon chain length)
<i>l</i> <sub>c</sub>	alkyl chain length (nm)
<i>v</i> <sub>c</sub>	alkyl chain volume (nm <sup>3</sup> )
Å	angstrom (=10 <sup>-10</sup> m)
AIL	aprotic ionic liquid
AFM	atomic force microscopy
S <sub>N</sub> 2	bimolecular substitution reaction
NPf <sub>2</sub> <sup>-</sup>	bis(pentafluoroethylsulfonyl)imide anion
NTf <sub>2</sub> <sup>-</sup>	bis(trifluoromethanesulfonyl)imide anion
T <sub>b</sub>	boiling point (°C)
Br <sup>-</sup>	bromide anion
Cl <sup>-</sup>	chloride anion
CARS	coherent anti-Stokes Raman scattering
$\kappa^{-1}$	Debye length (nm)
DFT	Density Functional Theory
N(CN) <sub>2</sub> <sup>-</sup>	dicyanamide anion
$\epsilon$	dielectric permittivity
DRS	dielectric relaxation spectroscopy
<i>D</i>	diffusion coefficient
DLS	dynamic light scattering
DLVO	Derjaguin, Landau, Verwey, Overbeek theory
EAN	ethylammonium nitrate
EDL	electrical double layer
EIS	electrochemical impedance spectroscopy
EPSR	empirical potential structure refinement
ESI-MS	electrospray ionization mass spectrometry
FAB-MS	fast atom bombardment mass spectrometry
fs-IR	femtosecond infrared spectroscopy
F <sup>-</sup>	fluoride anion
FTIR	Fourier transfer infrared spectroscopy
<i>T</i> <sub>g</sub>	glass transition temperature (°C)
G	glycolate anion
C	heat capacity (thermal) (J mol <sup>-1</sup> K <sup>-1</sup> )
HFB	heptafluorobutyrate anion
H-bond	hydrogen bond
HSO <sub>4</sub> <sup>-</sup>	hydrogen sulfate anion
I <sup>-</sup>	iodide anion
$\kappa$	ionic conductivity (S cm <sup>-1</sup> )
IL	ionic liquid
<i>I</i>	ionic strength (mol L <sup>-1</sup> )
L <sup>-</sup>	lactate anion
<i>L</i> <sub><math>\alpha</math></sub>	lamellar phase
LAXS	large-angle X-ray scattering
% <sub>linear</sub>	linear H-bond percentage
<i>m/z</i>	mass to charge ratio
<i>T</i> <sub>m</sub>	melting point (°C)
CH <sub>3</sub> SO <sub>3</sub> <sup>-</sup>	methylsulfate anion
MD	molecular dynamics
MW	molecular weight (g mol <sup>-1</sup> )
MC	Monte Carlo
nm	nanometer (=10 <sup>-9</sup> m)
nN	nanonewton (=10 <sup>-9</sup> N)
NICISS	neutral impact collision ion scattering spectroscopy
ND	neutron diffraction
IM <sub>24</sub> <sup>-</sup>	(nonafluorobutanesulfonyl)(pentafluoroethanesulfonyl)imide anion
IM <sub>14</sub> <sup>-</sup>	(nonafluorobutanesulfonyl)(trifluoromethanesulfonyl)imide anion
C <sub>i</sub> E <sub>j</sub>	nonionic alkyl polyglycolether surfactant ( <i>i</i> = glycol units, <i>j</i> = ether units)
NMR	nuclear magnetic resonance
NOE	nuclear Overhauser effect
NOESY	nuclear Overhauser effect spectroscopy
OA <sup>-</sup>	octanoate anion
TOTO	oligoether-carboxylate
OCP	open circuit potential
OKE	optical Kerr effect
OB <sup>-</sup>	orthoborate anion
OF	pentadecafluoroctanoate anion
ClO <sub>4</sub> <sup>-</sup>	perchlorate anion
FBS <sup>-</sup>	perfluorobutanesulfonate anion
$\pi$ - $\pi$	pi–pi (interaction or force)
PAN	propylammonium nitrate
PES	photoelectron spectroscopy
PIL	protic ionic liquid
QENS	quasi-elastic neutron scattering
<i>d</i>	quasi-periodic repeat distance (nm)
<i>g</i> ( <i>r</i> )	radial distribution function
<i>n</i> <sub>D</sub>	refractive index
RTIL	room-temperature ionic liquid
STM	scanning tunneling microscopy
<i>Q</i>	scattering (wave) vector (Å <sup>-1</sup> )
SANS	small-angle neutron scattering
SAXS	small-angle X-ray scattering
SWAXS	small- and wide-angle X-ray scattering
L <sub>3</sub>	sponge phase
SFG	sum frequency generation spectroscopy
SERAS	surface-enhanced infrared or Raman spectroscopy
SFA	surface forces apparatus
N <sub><i>n,n,n,n</i></sub> <sup>+</sup>	tetraalkylammonium cation ( <i>n</i> = carbon chain length)
P <sub><i>n,n,n,n</i></sub> <sup>+</sup>	tetraalkylphosphonium cation ( <i>n</i> = carbon chain length)
AlCl <sub>4</sub> <sup>-</sup>	tetrachloroaluminate anion
BF <sub>4</sub> <sup>-</sup>	taetrafluoroborate anion
SCN <sup>-</sup>	thiocyanate anion
ToF-SIMS	time of flight secondary ion mass spectrometry
CH <sub>3</sub> PhSO <sub>3</sub> <sup>-</sup>	tosylate anion
TF	triflate anion
TFA <sup>-</sup>	trifluoroacetate anion
OFT <sup>-</sup>	trifluoromethanesulfonate anion
FAP <sup>-</sup>	tris(pentafluoroethyl)trifluorophosphate anion
<i>P</i>	vapor pressure (Pa)
$\eta$	viscosity (Pa s)
<i>V</i> <sub>alkyl</sub>	volume of apolar groups (nm <sup>3</sup> )
<i>V</i> <sub>polar</sub>	volume of polar groups (nm <sup>3</sup> )
$\gamma$	surface tension (N m <sup>-1</sup> )
vdW	van der Waals (force or interaction)

WAXS	wide-angle X-ray scattering
XPS	X-ray photoelectron spectroscopy
XRD	X-ray diffraction
XRR	X-ray reflectivity

## REFERENCES

- (1) Crick, F. H. *What Mad Pursuit: A Personal View of Scientific Discovery*; Basic Books: New York, 1988.
- (2) Reichardt, C.; Welton, T. *Solvents and Solvent Effects in Organic Chemistry*, 4th ed.; Wiley-VCH: Weinheim, 2011.
- (3) Wypych, G.; Wypych, J. *Handbook of Solvents*; ChemTec Publishing: Canada, 2001.
- (4) *Springer Handbook of Nanotechnology*, 3rd ed.; Springer: New York, 2010.
- (5) Prakash, S.; Yeom, J. *Nanofluidics and Microfluidics: Systems and Applications*; Elsevier: New York, 2014.
- (6) Tanaka, K. *Solvent-Free Organic Synthesis*; Wiley-VCH: New York, 2009.
- (7) Hartman, R. L.; McMullen, J. P.; Jensen, K. F. *Angew. Chem., Int. Ed.* **2011**, *50*, 7502–7519.
- (8) Tabor, D. *Gases, Liquids, and Solids: and Other States of Matter*, 3rd ed.; Cambridge University Press: New York, 1991.
- (9) Israelachvili, J. N. *Intermolecular and Surface Forces*, 3rd ed.; Elsevier: London, 2011.
- (10) Bishop, K. J. M.; Wilmer, C. E.; Soh, S.; Grzybowski, B. A. *Small* **2009**, *5*, 1600–1630.
- (11) Donaldson, S. H.; Røyne, A.; Kristiansen, K.; Rapp, M. V.; Das, S.; Gebbie, M. A.; Lee, D. W.; Stock, P.; Valtiner, M.; Israelachvili, J. *Langmuir* **2015**, *31*, 2051–2064.
- (12) Bernal, J. D. *Proc. R. Soc. London, Ser. A* **1964**, *280*, 299–322.
- (13) Head-Gordon, T.; Hura, G. *Chem. Rev.* **2002**, *102*, 2651.
- (14) Soper, A. K. *Pure Appl. Chem.* **2010**, *82*, 1855.
- (15) Paesani, F.; Voth, G. A. *J. Phys. Chem. B* **2009**, *113*, 5702–5719.
- (16) Headen, T. F.; Howard, C. A.; Skipper, N. T.; Wilkinson, M. A.; Bowron, D. T.; Soper, A. K. *J. Am. Chem. Soc.* **2010**, *132*, 5735–5742.
- (17) Böhmera, R.; Gainaru, C.; Richert, R. *Phys. Rep.* **2014**, *545*, 125–195.
- (18) *Faraday Discuss.* **2013**, *167*, 1–2.
- (19) Parsegian, V. A. *Van der Waals Forces: A Handbook for Biologists, ChemistsEngineers, and Physicists*; Cambridge University Press: New York, 2005.
- (20) Ray, A. *Nature* **1971**, *231*, 313–315.
- (21) Mahanty, J.; Ninham, B. W. *Dispersion Forces*; Academic Press: London, 1976.
- (22) Jeffrey, G. A. *An Introduction to Hydrogen Bonding*; Oxford University Press: New York, 1997.
- (23) Metrangolo, P.; Resnati, G. *Halogen Bonding: Fundamentals and Applications*; Springer: Berlin, 2008.
- (24) Hallett, J. P.; Welton, T. *Chem. Rev.* **2011**, *111*, 3508.
- (25) Welton, T. *Chem. Rev.* **1999**, *99*, 2071.
- (26) Endres, F.; Zein El Abedin, S. *Phys. Chem. Chem. Phys.* **2006**, *8*, 2101–2116.
- (27) Rogers, R. D.; Seddon, K. R. *Science* **2003**, *302*, 792–793.
- (28) Greaves, T. L.; Drummond, C. J. *Chem. Rev.* **2008**, *108*, 206–237.
- (29) Angell, C. A. *ECS Trans.* **2010**, *33*, 3–18.
- (30) Angell, C. A.; Ansari, Y.; Zhao, Z. *Faraday Discuss.* **2012**, *154*, 9–27.
- (31) Forsyth, S.; A. P. J. M.; Macfarlane, D. R. *Aust. J. Chem.* **2004**, *57*, 113.
- (32) MacFarlane, D. R.; Seddon, K. R. *Aust. J. Chem.* **2007**, *60*, 3.
- (33) Castner, E. W. J.; Wishart, J. F. *J. Chem. Phys.* **2010**, *132*, 120901.
- (34) El Abedin, S. Z.; Endres, F. *Acc. Chem. Res.* **2007**, *40*, 1106.
- (35) Plechkova, N. V.; Seddon, K. R. *Chem. Soc. Rev.* **2008**, *37*, 123–150.
- (36) Endres, F.; Abbott, A.; MacFarlane, D. R. *Electrodeposition from Ionic Liquids*; Wiley-VCH: New York, 2008.
- (37) Ohno, H. *Electrochemical Aspects Ionic Liquids*; John Wiley & Sons, Inc.: NJ, 2005.
- (38) *Ionic Liquids in Synthesis*, 2nd ed.; Wasserscheid, P., Welton, T., Eds.; Wiley-VCH: New York, 2008.
- (39) Plechkova, N. V.; Seddon, K. R. *Ionic Liquids UnCOILED: Critical Expert Overviews*; John Wiley & Sons: New York, 2012.
- (40) *Molten Salts and Ionic Liquids: Never the Twain?*; John Wiley & Sons: New York, 2010.
- (41) Plechkova, N. V.; Seddon, K. R. *Ionic Liquids futher UnCOILED: Critical Expert Overviews*; John Wiley & Sons: New York, 2014.
- (42) *The Structure of Ionic Liquids*; Caminiti, R., Gontrani, L., Eds.; Springer: New York, 2014.
- (43) Wishart, J. F.; Castner, E. W. *J. Phys. Chem. B* **2007**, *111*, 4639–4640.
- (44) Endres, F. *Phys. Chem. Chem. Phys.* **2010**, *12*, 1648.
- (45) Endres, F. *Phys. Chem. Chem. Phys.* **2012**, *14*, 5008.
- (46) Rogers, R. D., MacFarlane, D. R., Zhang, S., Eds. Web Themed Issue, *Chem. Commun.* **2012**.
- (47) MacFarlane, D. R., Ed. Web Collection from 5th Congress on Ionic Liquids, *Chem. Commun.* **2013**.
- (48) *Faraday Discuss.* **2012**, *154*, 1–2.
- (49) Wasserscheid, P.; Schröer, W. *J. Mol. Liq.* **2014**, *192*, 1–2.
- (50) Bendova, M.; Jacquemin, J. *J. Solution Chem.* **2015**, *44*, 379.
- (51) Ludwig, R.; Maginn, E.; Balasubramanian, S. *ChemPhysChem* **2012**, *13*, 1603–1603.
- (52) Ionic Liquids Database - ILThermo.bounder.nist.gov, 2013.
- (53) Beyersdorff, T.; Schubert, T. J. S.; Welz-Biermann, U.; Pitner, W.; Abbott, A. P.; McKenzie, K. J.; Ryder, K. S. In *Electrodeposition from Ionic Liquids*; Endres, F., MacFarlane, D. R., Abbott, A. P., Eds.; Wiley-VCH: New York, 2008.
- (54) Davis, J. H.; Gordon, C. M.; Hilgers, C.; Wasserscheid, P. In *Ionic Liquids in Synthesis*; Wasserscheid, P., Welton, T., Eds.; Wiley-VCH: New York, 2007.
- (55) Slattery, J. M.; Daguerre, C.; Dyson, P. J.; Schubert, T. J. S.; Krossing, I. *Angew. Chem.* **2007**, *119*, 5480–5484.
- (56) Paduszyński, K.; Domańska, U. *J. Chem. Inf. Model.* **2014**, *54*, 1311–1324.
- (57) Lei, Z.; Chen, B.; Li, C.; Liu, H. *Chem. Rev.* **2008**, *108*, 1419–1455.
- (58) Yoshizawa, M.; Xu, W.; Angell, C. A. *J. Am. Chem. Soc.* **2003**, *125*, 15411–15419.
- (59) Fisher, M. E.; Levin, Y. *Phys. Rev. Lett.* **1993**, *71*, 3826–3829.
- (60) Weingärtner, H.; Schröer, W. *Adv. Chem. Phys.* **2001**, *116*, 1.
- (61) Short, P. L. *Chem. Eng. News* **2006**, *84*, 15–21.
- (62) Freemantle, M. *Chem. Eng. News* **1998**, *76*, 32.
- (63) Chen, L.; Sharifzadeh, M.; Mac Dowell, N.; Welton, T.; Shah, N.; Hallett, J. P. *Green Chem.* **2014**, *16*, 3098–3106.
- (64) Earle, M. J.; Seddon, K. R. *Pure Appl. Chem.* **2000**, *72*, 1391–1398.
- (65) Lui, M. Y.; Crowhurst, L.; Hallett, J. P.; Hunt, P. A.; Niedermeyer, H.; Welton, T. *Chem. Sci.* **2011**, *2*, 1491–1496.
- (66) Niedermeyer, H.; Hallett, J. P.; Villar-Garcia, I. J.; Hunt, P. A.; Welton, T. *Chem. Soc. Rev.* **2012**, *41*, 7780–7802.
- (67) Sharma, R.; Mahajan, R. K. *RSC Adv.* **2014**, *4*, 748–774.
- (68) Chatel, G.; Pereira, J. F. B.; Debeti, V.; Wang, H.; Rogers, R. D. *Green Chem.* **2014**, *16*, 2051.
- (69) Earle, M. J.; Katdare, S. P.; Seddon, K. R. *Org. Lett.* **2004**, *6*, 707–710.
- (70) McCrary, P. D.; Rogers, R. D. *Chem. Commun.* **2013**, *49*, 6011–6014.
- (71) Kohno, Y.; Ohno, H. *Chem. Commun.* **2012**, *48*, 7119–7130.
- (72) Cevasco, G.; Chiappe, C. *Green Chem.* **2014**, *16*, 2375–2385.
- (73) Dupont, J. J. *Braz. Chem. Soc.* **2004**, *15*, 341–350.
- (74) Castner, E. W. J.; Margulis, C. J.; Maroncelli, M.; Wishart, J. F. *Annu. Rev. Phys. Chem.* **2011**, *62*, 85–105.
- (75) Hardacre, C.; Holbrey, J. D.; Nieuwenhuyzen, M.; Youngs, T. G. *A. Acc. Chem. Res.* **2007**, *40*, 1146–1155.
- (76) Weingärtner, H. *Angew. Chem., Int. Ed.* **2008**, *47*, 654–670.
- (77) Chen, S.; S. Z.; Lui, X.; Wang, J.; Wang, J.; Dong, K.; Sun, J.; Xu, B. *Phys. Chem. Chem. Phys.* **2014**, *16*, 5893–5906.
- (78) Russina, O.; Triolo, A.; Gontrani, L.; Caminiti, R. *J. Phys. Chem. Lett.* **2011**, *27*–33.

- (79) Greaves, T. L.; Drummond, C. J. *Chem. Soc. Rev.* **2013**, *42*, 1096–1120.
- (80) Wijaya, E. C.; Greaves, T. L.; Drummond, C. *Faraday Discuss.* **2013**, *167*, 191–215.
- (81) Fayer, M. D. *Chem. Phys. Lett.* **2014**, *616–617*, 259–274.
- (82) Hayes, R.; Warr, G. G.; Atkin, R. *Phys. Chem. Chem. Phys.* **2010**, *12*, 1709–1723.
- (83) Atkin, R.; Borisenko, N.; Drüscher, M.; Endres, F.; Hayes, R.; Huber, B.; Roling, B. *J. Mol. Liq.* **2013**, *192*, 44–54.
- (84) Endres, F.; Borisenko, N.; El Abedin, S. Z.; Hayes, R.; Atkin, R. *Faraday Discuss.* **2012**, *154*, 221–233.
- (85) Hayes, R.; Wakeham, D.; Atkin, R. In *Ionic Liquids UnCOILED: Critical Expert Overviews*; Seddon, K. R., Plechkova, N., Eds.; John Wiley & Sons: New York, 2012.
- (86) Smith, A. M.; Lovelock, K. R. J.; Perkin, S. *Faraday Discuss.* **2013**, *167*, 279–292.
- (87) Perkin, S. *Phys. Chem. Chem. Phys.* **2012**, *14*, 5052–5062.
- (88) Freyland, W. In *Ionic Liquids UnCOILED: Critical Expert Overviews*; Seddon, K. R., Plechkova, N., Eds.; John Wiley & Sons: New York, 2012.
- (89) Su, Y.-Z.; Fu, Y.-C.; Wei, Y.-M.; Yan, J.-W.; Mao, B.-W. *ChemPhysChem* **2010**, *11*, 2764–2778.
- (90) Lovelock, K. R. J. *Phys. Chem. Chem. Phys.* **2012**, *14*, 5071–5089.
- (91) Israelachvili, J. N.; Marčelja, S.; Horn, R. G. *Q. Rev. Biophys.* **1980**, *13*, 121–200.
- (92) Israelachvili, J. N.; Mitchell, D. J.; Ninham, B. W. *J. Chem. Soc., Faraday Trans. 2* **1976**, *72*, 1526–1568.
- (93) Iwashashi, T.; Sakai, Y.; Kanai, K.; Kim, D.; Ouchi, Y. *Phys. Chem. Chem. Phys.* **2010**, *12*, 12943–12946.
- (94) Iwashashi, T.; Sakai, Y.; Kim, D.; Ishiyama, T.; Morita, A.; Ouchi, Y. *Faraday Discuss.* **2012**, *154*, 289–301.
- (95) Sangoro, J. R.; Serghei, A.; Naumov, S.; Galvosas, P.; Kärger, J.; Wespe, C.; Bordusa, F.; Kremer, F. *Phys. Rev. E* **2008**, *77*, 051202.
- (96) Taylor, A. W.; Licence, P.; Abbott, A. P. *Phys. Chem. Chem. Phys.* **2011**, *13*, 10147–10154.
- (97) Ueno, K.; Tokuda, H.; Watanabe, M. *Phys. Chem. Chem. Phys.* **2010**, *12*, 1649–1658.
- (98) MacFarlane, D. R.; Forsyth, M.; Izgorodina, E. I.; Abbott, A. P.; Annat, G.; Fraser, K. *Phys. Chem. Chem. Phys.* **2009**, *11*, 4962–4967.
- (99) Hollóczki, O.; Malberg, F.; Welton, T.; Kirchner, B. *Phys. Chem. Chem. Phys.* **2014**, *16*, 16880–16890.
- (100) Reichardt, C. *Green Chem.* **2005**, *7*, 339.
- (101) Ab Rani, M. A.; Brant, A.; Crowhurst, L.; Dolan, A.; Lui, M.; Hassan, N. H.; Hallett, J. P.; Hunt, P. A.; Niedermeyer, H.; Perez-Arlandis, J. M.; Schrems, M.; Welton, T.; Wilding, R. *Phys. Chem. Chem. Phys.* **2011**, *13*, 16831–16840.
- (102) Wakai, C.; Oleinikova, A.; Ott, M.; Weingärtner, H. *J. Phys. Chem. B* **2005**, *109*, 17028.
- (103) Chaban, V. *Phys. Chem. Chem. Phys.* **2011**, *13*, 16055–16062.
- (104) Yan, T.; Burnham, C. J.; Del Pópolo, M. G.; Voth, G. A. *J. Phys. Chem. B* **2004**, *108*, 11877–11881.
- (105) Walden, P. *Bull. Acad. Imp. Sci. St.-Petersbourg* **1914**, *8*, 405–422.
- (106) Arrhenius, S. Z. *Phys. Chem.* **1887**, *1*, 631.
- (107) Walden, P. Z. *Phys. Chem.* **1906**, *55*, 207.
- (108) Gabriel, S.; Weiner, J. *Ber. Dtsch. Chem. Ges.* **1888**, *21*, 2669.
- (109) Rogers, R. D. *Nature* **2007**, *447*, 917.
- (110) Wilkes, J. S. *Green Chem.* **2002**, *4*, 73.
- (111) Hussey, C. L. In *Chemistry of Nonaqueous Solutions*; Mamantov, G., Popov, A. I., Eds.; VCH Publisher Inc.: New York, 1994.
- (112) Anastas, P. T.; Warner, J. C. *Green Chemistry: Theory and Practice*; Oxford University Press: New York, 2000.
- (113) Reichardt, C. *Org. Process Res. Dev.* **2007**, *11*, 105.
- (114) Rogers, R. D.; Seddon, K. R.; Volkov, S. *Green Industrial Applications of Ionic Liquids*; Kluwer Academic: Dordrecht, Netherlands, 2002.
- (115) Ubbelohde, A. R. *Nature* **1973**, *244*, 487.
- (116) Davis, J. H. 5th Congress on Ionic Liquids (COILS), Algarve, Portugal, 2013.
- (117) Murray, S. M.; O'Brien, R. A.; Mattson, K. M.; Ceccarelli, C.; Sykora, R. E.; West, K. N.; Davis, J. H. *Angew. Chem., Int. Ed.* **2010**, *49*, 2755–2758.
- (118) Sinensky, M. *Proc. Natl. Acad. Sci. U.S.A.* **1974**, *71*, 522–525.
- (119) Lopez-Martin, I.; Burello, E.; Davey, P. N.; Seddon, K. R.; Rothenberg, G. *ChemPhysChem* **2007**, *8*, 690–695.
- (120) Bradley, A. E.; Hardacre, C.; Holbrey, J. D.; Johnston, S. E. J.; McMath, M.; Nieuwenhuyzen, M. *Chem. Mater.* **2002**, *14*, 629–635.
- (121) Dzyuba, S. V.; Bartsch, R. A. *ChemPhysChem* **2002**, *3*, 161–166.
- (122) Gordon, C. M.; Holbrey, J. D.; Kennedy, A. R.; Seddon, K. R. *J. Mater. Chem.* **1998**, *8*, 2627–2636.
- (123) Hamaguchi, H.; Ozawa, R. *Adv. Chem. Phys.* **2005**, *131*, 85.
- (124) Angell, C. A.; Byrne, N.; Belieres, J.-P. *Acc. Chem. Res.* **2007**, *40*, 1228–1236.
- (125) Parker, A. J. *Q. Rev., Chem. Soc.* **1962**, *16*, 163–187.
- (126) Mirjafari, A.; Pham, L. N.; McCabe, J. R.; Mobarrez, N.; Salter, E. A.; Wierzbicki, A.; West, K. N.; Sykora, R. E.; Davis, J. H. *RSC Adv.* **2013**, *3*, 337–340.
- (127) Chen, L.; Mullen, G. E.; Le Roch, M.; Cassity, C. G.; Gouault, N.; Fadamiro, H. Y.; Barletta, R. E.; O'Brien, R. A.; Sykora, R. E.; Stenson, A. C.; West, K. N.; Horne, H. E.; Hendrich, J. M.; Xiang, K. R.; Davis, J. H. *Angew. Chem., Int. Ed.* **2014**, *53*, 11762–11765.
- (128) Xu, W.; Angell, C. A. *Science* **2003**, *302*, 422.
- (129) Noda, A.; Susan, M. A. B. H.; Kudo, K.; Mitsushima, S.; Hayamizu, K.; Watanabe, M. *J. Phys. Chem. B* **2003**, *107*, 4024–4033.
- (130) Miran, M. S.; Yasuda, T.; Susan, M. A. B. H.; Dokko, K.; Watanabe, M. *J. Phys. Chem. C* **2014**, *118*, 27631–27639.
- (131) Belieres, J. P.; Angell, C. A. *J. Phys. Chem. B* **2007**, *111*, 4926–4937.
- (132) Mann, J. P.; McCluskey, A.; Atkin, R. *Green Chem.* **2009**, *11*, 785–792.
- (133) Breisacher, P.; Takimoto, H. H.; Denault, G. C.; Hicks, W. A. *Combust. Flame* **1970**, *14*, 397.
- (134) Estager, J.; Holbrey, J. D.; Swadzba-Kwasny, M. *Chem. Soc. Rev.* **2014**, *43*, 847–886.
- (135) Ding, J.; Armstrong, D. W. *Chirality* **2005**, *17*, 281.
- (136) Santos, E.; Albo, J.; Irabien, A. *RSC Adv.* **2014**, *4*, 40008–40018.
- (137) Mecerreyes, D. *Prog. Polym. Sci.* **2011**, *36*, 1629–1648.
- (138) Shen, Y.; Kennedy, D. F.; Greaves, T. L.; Weerawardena, A.; Mulder, R. J.; Kirby, N.; Drummond, C. J. *Phys. Chem. Chem. Phys.* **2012**, *14*, 7981–7992.
- (139) Zech, O.; Kellermeier, M.; Thomaier, S.; Maurer, E.; Klein, R.; Schreiner, C.; Kunz, W. *Chem.—Eur. J.* **2009**, *15*, 1341–1345.
- (140) Ohno, H.; Fukumoto, K. *Acc. Chem. Res.* **2007**, *40*, 1122–1129.
- (141) Ahrens, S.; Peritz, A.; Strassner, T. *Angew. Chem., Int. Ed.* **2009**, *48*, 7908–7910.
- (142) Kremer, K.; Grest, G. S. *J. Chem. Phys.* **1990**, *92*, 5057–5086.
- (143) Munstedt, H. *Soft Matter* **2011**, *7*, 2273–2283.
- (144) Gladysz, J. A.; Curran, D. P.; Horváth, I., Eds. *Handbook of Fluorous Chemistry*; Wiley-VCH: Weinheim, 2005.
- (145) Holm, C.; Weis, J. J. *Curr. Opin. Colloid Interface Sci.* **2005**, *10*, 133–140.
- (146) Jain, N.; Wang, Y.; Jones, S. K.; Hawkett, B. S.; Warr, G. G. *Langmuir* **2009**, *26*, 4465–4472.
- (147) Greaves, T. L.; Drummond, C. J. *Chem. Soc. Rev.* **2008**, *37*, 1709–1726.
- (148) Greaves, T. L.; Weerawardena, A.; Fong, C.; Drummond, C. J. *Langmuir* **2007**, *23*, 402–404.
- (149) Araos, M. U.; Warr, G. G. *J. Phys. Chem. B* **2005**, *109*, 14275–14277.
- (150) Atkin, R.; Bobillier, S. M. C.; Warr, G. G. *J. Phys. Chem. B* **2010**, *114*, 1350–1360.
- (151) López-Barrón, C. R.; Basavaraj, M. G.; DeRita, L.; Wagner, N. J. *J. Phys. Chem. B* **2011**, *116*, 813–822.
- (152) López-Barrón, C. R.; Li, D.; DeRita, L.; Basavaraj, M. G.; Wagner, N. J. *J. Am. Chem. Soc.* **2012**, *134*, 20728–20732.
- (153) López-Barrón, C. R.; Li, D.; Wagner, N. J.; Caplan, J. L. *Macromolecules* **2014**, *47*, 7484–7495.

- (154) Bockris, J. O. M.; Reddy, A. K. N. *Modern Electrochemistry*; Plenum Press: New York, 1970.
- (155) Lide, D. R. *CRC Handbook of Chemistry and Physics: A Ready-reference Book of Chemical and Physical Data*, 85th ed.; CRC Press: New York, 2004.
- (156) Smith, J. A.; Webber, G. B.; Warr, G. G.; Atkin, R. *J. Phys. Chem. B* **2013**, *117*, 13930–13935.
- (157) Emel'yanenko, V. N.; Boeck, G.; Verevkin, S. P.; Ludwig, R. *Chem.—Eur. J.* **2014**, *20*, 11594.
- (158) Page, A. J. Personal communication, 2015.
- (159) Huang, M.-M.; Jiang, Y.; Sasisanker, P.; Driver, G. W.; Weingärtner, H. *J. Chem. Eng. Data* **2011**, *56*, 1494–1499.
- (160) Allen, M.; Evans, D. F.; Lumry, R. *J. Solution Chem.* **1985**, *14*, 549–560.
- (161) Murphy, T.; Varela, L. M.; Webber, G. B.; Warr, G. G.; Atkin, R. *J. Phys. Chem. B* **2014**, *118*, 12017–12024.
- (162) Carda-Broch, S.; Berthod, A.; Armstrong, D. W. *Anal. Bioanal. Chem.* **2003**, *375*, 191–199.
- (163) Tokuda, H.; Hayamizu, K.; Ishii, K.; Susan, M. A. B. H.; Watanabe, M. *J. Phys. Chem. B* **2004**, *108*, 16593–16600.
- (164) Gomes de Azevedo, R.; Esperança, J. M. S. S.; Najdanovic-Visak, V.; Visak, Z. P.; Guedes, H. J. R.; Nunes da Ponte, M.; Rebello, L. P. N. J. *Chem. Eng. Data* **2005**, *50*, 997–1008.
- (165) Fan, W.; Zhou, Q.; Sun, J.; Zhang, S. *J. Chem. Eng. Data* **2009**, *54*, 2307–2311.
- (166) Paulechka, Y. U.; Kabo, G. J.; Blokhin, A. V.; Vydrov, O. A.; Magee, J. W.; Frenkel, M. *J. Chem. Eng. Data* **2003**, *48*, 457–462.
- (167) Freire, M. G.; Carvalho, P. J.; Fernandes, A. M.; Marrucho, I. M.; Queimada, A. J.; Coutinho, J. A. P. *J. Colloid Interface Sci.* **2007**, *314*, 621.
- (168) Tomida, D.; Kenmochi, S.; Tsukada, T.; Qiao, K.; Yokoyama, C. *Int. J. Thermophys.* **2007**, *28*, 1147.
- (169) Bloom, H.; Peyer, B. M. *Aust. J. Chem.* **1965**, *18*, 777.
- (170) Nachtrieb, N. H.; Petit, J. *J. Chem. Phys.* **1956**, *24*, 746–750.
- (171) Holz, M.; Heil, S. R.; Sacco, A. *Phys. Chem. Chem. Phys.* **2000**, *2*, 4740–4742.
- (172) McCool, M. A.; Collings, A. F.; Woolf, L. A. *J. Chem. Soc., Faraday Trans. 1* **1972**, *68*, 1489.
- (173) Janz, G. *J. Molten Salts Handbook*; Academic Press Inc.: New York, 1967.
- (174) Smallwood, I. M. *Handbook of Organic Solvent Properties*; Halsted: New York, 1996.
- (175) Ramires, M. L. V.; Nieto de Castro, C. A.; Nagasaka, Y.; Nagashima, A.; Assael, M. J.; Wakeham, W. A. *J. Phys. Chem. Ref. Data* **1995**, *24*, 1377–1381.
- (176) Assael, M. J.; Ramires, M. L. V.; Nieto de Castro, C. A.; Wakeham, W. A. *J. Phys. Chem. Ref. Data* **1990**, *19*, 113–117.
- (177) Nagasaka, Y.; Nakazawa, N.; Nagashima, A. *Int. J. Thermophys.* **1992**, *13*, 555–574.
- (178) Izgorodina, E. I.; MacFarlane, D. R. *J. Phys. Chem. B* **2011**, *115*, 14659–14667.
- (179) Evans, D. F.; Chen, S.-H.; Schriver, G. W.; Arnett, E. M. *J. Am. Chem. Soc.* **1981**, *103*, 481–482.
- (180) Ludwig, R. *J. Phys. Chem. B* **2009**, *113*, 15419–15422.
- (181) Canongia Lopes, J. N. A.; Padua, A. A. H. *J. Phys. Chem. B* **2006**, *110*, 3330–3335.
- (182) Burba, C. M.; Janzen, J.; Butson, E. D.; Coltrain, G. L. *J. Phys. Chem. B* **2013**, *117*, 8814–8820.
- (183) Bou Malham, I.; Letellier, P.; Mayaffre, A.; Turmine, M. *J. Chem. Thermodyn.* **2007**, *39*, 1132–1143.
- (184) Bouguerra, S.; Bou Malham, I.; Letellier, P.; Mayaffre, A.; Turmine, M. *J. Chem. Thermodyn.* **2008**, *40*, 146–154.
- (185) Desiraju, G. R. *J. Am. Chem. Soc.* **2013**, *135*, 9952–9967.
- (186) Mudring, A. *Aust. J. Chem.* **2010**, *63*, 544–564.
- (187) Dean, P. M.; Turanjanin, J.; Yoshizawa-Fujita, M.; MacFarlane, D. R.; Scott, J. L. *Cryst. Growth Des.* **2008**, *9*, 1137–1145.
- (188) Rogers, R. D. *Aust. J. Chem.* **2010**, *63*, 533–534.
- (189) Muldoon, M. J.; Nockemann, P.; Lagunas, M. C. *CrystEngComm* **2012**, *14*, 4873–4873.
- (190) Laughlin, R. G. *The Aqueous Phase Behavior of Surfactants*; Academic Press: New York, 1996.
- (191) Suarez, P. A. Z.; Einloft, S.; Dullius, J. E. L.; de Souza, R. F.; Dupont, J. *J. Chim. Phys.* **1998**, *95*, 1626.
- (192) Ciajolo, M. R.; Corradini, P.; Pavone, V. *Acta Crystallogr., Sect. B* **1977**, *33*, 553.
- (193) Paradies, H. H.; Habben, F. *Acta Crystallogr., Sect. C* **1993**, *49*, 744–747.
- (194) Wilkes, J. S.; Zaworotko, M. J. *J. Chem. Soc., Chem. Commun.* **1992**, 965.
- (195) Dieter, K. M.; Dymek, C. J.; Heimer, N. E.; Rovang, J. W.; Wilkes, J. S. *J. Am. Chem. Soc.* **1988**, *110*, 2722–2726.
- (196) Fukushima, T.; Kosaka, A.; Ishimura, Y.; Yamamoto, T.; Takigawa, T.; Ishii, N.; Aida, T. *Science* **2003**, *300*, 2072–2074.
- (197) Carper, W. R.; Pflug, J. L.; Elias, A. M.; Wilkes, J. S. *J. Phys. Chem.* **1992**, *96*, 3828–3833.
- (198) Ananikov, V. P. *Chem. Rev.* **2010**, *111*, 418–454.
- (199) Hamaguchi, H.; Saha, S.; Ozawa, R.; Hayashi, S. In *Ionic Liquids IIIA: Fundamentals, Progress, Challenges, and Opportunities, Properties and Structure*; Rogers, R. D., Seddon, K. R., Eds.; American Chemical Society: Washington, DC, 2005.
- (200) Hayashi, S.; Ozawa, R.; Hamagushi, H. *Chem. Lett.* **2003**, *32*, 498.
- (201) Ozawa, R.; Hayashi, S.; Saha, S.; Kobayashi, A.; Hamaguchi, H. *Chem. Lett.* **2003**, *32*, 948.
- (202) Holbrey, J. D.; Reichert, W. M.; Rogers, R. D. *Dalton Trans.* **2004**, *0*, 2267–2271.
- (203) Sutor, D. J. *Nature* **1962**, *195*, 68–69.
- (204) Deetlefs, M.; Hardacre, C.; Nieuwenhuyzen, M.; Padua, A. A. H.; Sheppard, O.; Soper, A. K. *J. Phys. Chem. B* **2006**, *110*, 12055–12061.
- (205) Lu, X.; Cao, Q.; Wu, X.; Xie, H.; Lei, Q.; Fang, W. *J. Phys. Chem. B* **2014**, *118*, 9085–9095.
- (206) Henderson, W. A.; Fylstra, P.; De Long, H. C.; Trulove, P. C.; Parsons, S. *Phys. Chem. Chem. Phys.* **2012**, *14*, 16041–16046.
- (207) Ratcliffe, C. I.; Sherman, W. I.; Wilkinson, G. R. *J. Raman Spectrosc.* **1982**, *13*, 189.
- (208) Migliorati, V.; Ballirano, P.; Gontrani, L.; Russina, O.; Caminiti, R. *J. Phys. Chem. B* **2011**, *115*, 11805–11815.
- (209) Binnemans, K. *Chem. Rev.* **2005**, *105*, 4148–4204.
- (210) Yang, M.; Mallick, B.; Mudring, A.-V. *Cryst. Growth Des.* **2014**.
- (211) Goossens, K.; Nockemann, P.; Driesen, K.; Goderis, B.; Görller-Walrand, C.; Van Hecke, K.; Van Meervelt, L.; Pouzet, E.; Binnemans, K.; Cardinaels, T. *Chem. Mater.* **2007**, *20*, 157–168.
- (212) Paleos, C. M. *Mol. Cryst. Liq. Cryst. Sci. Technol., Sect. A* **1994**, *243*, 159–183.
- (213) Arkas, M.; Yannakopoulou, K.; Paleos, C. M.; Weber, P.; Skoulios, A. *Liq. Cryst.* **1995**, *18*, 563–569.
- (214) Tschierske, C. *Prog. Polym. Sci.* **1996**, *21*, 775–852.
- (215) Maximo, G. J.; Santos, R. J. B. N.; Lopes-da-Silva, J. A.; Costa, M. C.; Meirelles, A. J. A.; Coutinho, J. A. P. *ACS Sustainable Chem. Eng.* **2013**, *2*, 672–682.
- (216) Beneduci, A.; Cospito, S.; La Deda, M.; Veltri, L.; Chidichimo, G. *Nat. Commun.* **2014**, *5*.
- (217) Arkas, M.; Paleos, C. M.; Skoulios, A. *Liq. Cryst.* **1997**, *22*, 735–742.
- (218) Busico, V.; Corradini, P.; Vacatello, M. *J. Phys. Chem.* **1982**, *86*, 1033–1034.
- (219) Busico, V.; Cernicchiaro, P.; Corradini, P.; Vacatello, M. *J. Phys. Chem.* **1983**, *87*, 1631–1635.
- (220) Matsunaga, Y.; Nishida, K. *Bull. Chem. Soc. Jpn.* **1988**, *61*, 3435–3437.
- (221) Tsiourvas, D.; Paleos, C. M.; Skoulios, A. *Liq. Cryst.* **1999**, *26*, 953–957.
- (222) Matsunaga, Y.; Tsujimura, T. *Mol. Cryst. Liq. Cryst.* **1991**, *200*, 103–108.
- (223) Ito, M.; Matsunaga, Y.; Matsuzaki, H.; Shimojima, S. *Bull. Chem. Soc. Jpn.* **1989**, *62*, 3919–3922.
- (224) Paleos, C.; Arkas, M.; Seghrouchni, R.; Skoulios, A. *Mol. Cryst. Liq. Cryst. Sci. Technol., Sect. A* **1995**, *268*, 179–182.

- (225) Paleos, C. M.; Arkas, M.; Skoulios, A. *Mol. Cryst. Liq. Cryst. Sci. Technol., Sect. A* **1998**, *309*, 237–250.
- (226) Neto, B. A. D.; Meurer, E. C.; Galaverna, R.; Bythell, B. J.; Dupont, J.; Cooks, R. G.; Eberlin, M. N. *J. Phys. Chem. Lett.* **2012**, *3*, 3435–3441.
- (227) Armstrong, J. P.; Hurst, C.; Jones, R. G.; Licence, P.; Lovelock, K. R. J.; Satterley, C. J.; Villar-Garcia, I. *J. Phys. Chem. Chem. Phys.* **2007**, *9*, 982–990.
- (228) Leal, J. P.; Esperança, J. M. S. S.; Minas da Piedade, M. E.; Canongia Lopes, J. N.; Rebelo, L. P. N.; Seddon, K. R. *J. Phys. Chem. A* **2007**, *111*, 6176–6182.
- (229) Schröer, W.; Weingärtner, H. *Pure Appl. Chem.* **2004**, *76*, 19–27.
- (230) Bjerrum, N. *Danske Videnskab. Selsk. Mater.-Fys. Medd.* **1926**, *7*.
- (231) Weingärtner, H. S.; Merkel, T.; Käshammer, S.; Schröer, W.; Wiegand, S. *Ber. Bunsen-Ges. Phys. Chem.* **1993**, *97*, 970.
- (232) Schröer, W.; Wiegand, S.; Weingärtner, H. S. *Ber. Bunsen-Ges. Phys. Chem.* **1993**, *97*, 975.
- (233) Hayes, R.; Imberti, S.; Warr, G. G.; Atkin, R. *Phys. Chem. Chem. Phys.* **2011**, *13*, 3237–3247.
- (234) Weingärtner, H.; Knocke, A.; Schrader, W.; Kaatze, U. *J. Phys. Chem. A* **2001**, *105*, 8646–8650.
- (235) Moynihan, C. T. In *Ionic Interactions. From Dilute Solutions to Fused Salts*; Petrucci, S., Ed.; Academic Press: New York, 1971; Vol. 1.
- (236) Hunt, P. A.; Kirchner, B.; Welton, T. *Chem.—Eur. J.* **2006**, *12*, 6762–6775.
- (237) Izgorodina, E. I. *Phys. Chem. Chem. Phys.* **2011**, *13*, 4189–4207.
- (238) Köddermann, T.; Wertz, C.; Heintz, A.; Ludwig, R. *ChemPhysChem* **2006**, *7*, 1944–1949.
- (239) Hunt, P. A.; Gould, I. R. *Aust. J. Chem.* **2006**, *60*, 9–14.
- (240) Pakiari, A. H.; Siahrostami, S.; Ziegler, T. *J. Mol. Struct. (THEOCHEM)* **2010**, *955*, 47–52.
- (241) Li, W.; Wu, X.; Qi, C.; Rong, H.; Gong, L. *J. Mol. Struct. (THEOCHEM)* **2010**, *942*, 19–25.
- (242) Xuan, X.; Guo, M.; Pei, Y.; Zheng, Y. *Spectrochim. Acta, Part A* **2011**, *78*, 1492–1499.
- (243) Tanzi, L.; Benassi, P.; Nardone, M.; Ramondo, F. *J. Phys. Chem. A* **2014**, *118*, 12229–12240.
- (244) Tsuzuki, S.; Shinoda, W.; Miran, M. S.; Kinoshita, H.; Yasuda, T.; Watanabe, M. *J. Chem. Phys.* **2013**, *139*, 174504.
- (245) Avent, A. G.; Chaloner, P. A.; Day, M. P.; Seddon, K. R.; Welton, T. *J. Chem. Soc., Dalton Trans.* **1994**, *0*, 3405–3413.
- (246) Schulz, P. S.; Müller, N.; Bösmann, A.; Wasserscheid, P. *Angew. Chem.* **2007**, *119*, 1315–1317.
- (247) Katoh, R.; Hara, M.; Tsuzuki, S. *J. Phys. Chem. B* **2008**, *112*, 15462.
- (248) Every, H. A.; Bishop, A. G.; MacFarlane, D. R.; Oradd, G.; Forsyth, M. *Phys. Chem. Chem. Phys.* **2004**, *6*, 1758.
- (249) Gebbie, M. A.; Valtiner, M.; Banquy, X.; Fox, E. T.; Henderson, W. A.; Israelachvili, J. N. *Proc. Natl. Acad. Sci. U.S.A.* **2013**, *110*, 9674–9679.
- (250) Gebbie, M. A.; Valtiner, M.; Banquy, X.; Fox, E. T.; Henderson, W. A.; Israelachvili, J. N. *Proc. Natl. Acad. Sci. U.S.A.* **2013**, *110*, E4122.
- (251) Perkin, S.; Salanne, M.; Madden, P. A.; Lynden-Bell, R. M. *Proc. Natl. Acad. Sci. U.S.A.* **2013**, *110*, E4121.
- (252) Daguenet, C.; Dyson, P. J.; Krossing, I.; Oleinikova, A.; Slattery, J. M.; Wakai, C.; Weingärtner, H. *J. Phys. Chem. B* **2006**, *110*, 12782.
- (253) Weingärtner, H. S.; Sasisanker, P.; Daguenet, C.; Dyson, P. J.; Krossing, I.; Slattery, J. M.; Shubert, T. *J. Phys. Chem. B* **2007**, *111*, 4775.
- (254) Schrödle, S.; Annat, G.; MacFarlane, D. R.; Forsyth, M.; Buchner, R.; Heftner, G. *Chem. Commun.* **2006**, 1748.
- (255) Turton, D. A.; Sonnleitner, T.; Ortnew, A.; Walther, M.; Heftner, G.; Seddon, K. R.; Stana, S.; Plechko, N.; Buchner, R.; Wynne, K. *Faraday Discuss.* **2012**, *154*, 145–153.
- (256) Weingärtner, H. *Curr. Opin. Colloid Interface Sci.* **2013**, *18*, 183–189.
- (257) Zhao, W.; Leroy, F.; Heggen, B.; Zahn, S.; Kirchner, B.; Balasubramanian, S.; Müller-Plathe, F. *J. Am. Chem. Soc.* **2009**, *131*, 15825.
- (258) Kohagen, M.; Brehm, M.; Thar, J.; Zhao, W.; Müller-Plathe, F.; Kirchner, B. *J. Phys. Chem. B* **2010**, *115*, 693–702.
- (259) Lynden-Bell, R. M. *Phys. Chem. Chem. Phys.* **2010**, *12*, 1733.
- (260) Lee, A. A.; Vella, D.; Perkin, S.; Goriely, A. *J. Phys. Chem. Lett.* **2015**, *6*, 159.
- (261) Fraser, K. J.; Izgorodina, E. I.; Forsyth, M.; Scott, J. L.; MacFarlane, D. R. *Chem. Commun.* **2007**, *40*, 3817–3819.
- (262) Doi, H.; Song, X.; Minofar, B.; Kanzaki, R.; Takamuku, T.; Umebayashi, Y. *Chem.—Eur. J.* **2013**, *19*, 11522.
- (263) Bernardes, C. E. S.; Minas da Piedade, M. E.; Canongia Lopes, J. N. *J. Phys. Chem. B* **2011**, *115*, 2067–2074.
- (264) Niazi, A. A.; Rabideau, B. D.; Ismail, A. E. *J. Phys. Chem. B* **2013**, *117*, 1378–1388.
- (265) Fazio, B.; Triolo, A.; Di Marco, G. *J. Raman Spectrosc.* **2008**, *39*, 233–237.
- (266) Schröder, C.; Hunger, J.; Stoppa, A.; Buchner, R.; Steinhauser, O. *J. Chem. Phys.* **2008**, *129*, 184501.
- (267) Spickermann, C.; Thar, J.; Lehmann, S. B. C.; Zahn, S.; Hunger, J.; Buchner, R.; Hunt, P. A.; Welton, T.; Kirchner, B. *J. Chem. Phys.* **2008**, *129*, 104505.
- (268) Pierola, I. F.; Agzenai, Y. *J. Phys. Chem. B* **2012**, *116*, 3973–3981.
- (269) Stange, P.; Fumino, K.; Ludwig, R. *Angew. Chem., Int. Ed.* **2013**, *52*, 2990–2994.
- (270) Ghatee, M. H.; Zolghadr, A. R. *J. Phys. Chem. C* **2013**, *117*, 2066–2077.
- (271) Ekka, D.; Roy, M. N. *RSC Adv.* **2014**, *4*, 19831–19845.
- (272) Gestblom, B.; Songstad, J. *Acta Chem. Scand., Ser. B* **1987**, *41*, 396–409.
- (273) Dupont, J.; Suarez, P. A. Z.; Consorti, C. S.; de Souza, R. F. *Org. Synth.* **2002**, *79*, 236.
- (274) Dupont, J.; Suarez, P. A. Z.; de Souza, R. F.; Burrow, R. A.; Kintzinger, J. P. *Chem.—Eur. J.* **2000**, *6*, 2377.
- (275) Mele, A.; Tran, C. D.; Lacerda, S. H. P. *Angew. Chem., Int. Ed.* **2003**, *42*, 4364.
- (276) Bhat, M. A.; Konar, A.; Ingole, P. P.; Pandith, A. H. *J. Phys. Org. Chem.* **2012**, *25*, 1243–1246.
- (277) Fry, A. J. *J. Electroanal. Chem.* **2003**, *546*, 35–39.
- (278) Del Popolo, M.; Mullan, C. L.; Holbrey John, D.; Hardacre, C.; Ballone, P. *J. Am. Chem. Soc.* **2008**, *130*, 7032.
- (279) Hardacre, C.; Holbrey, J. D.; Mullan, C. L.; Nieuwenhuyzen, M.; Youngs, T. G. A.; Bowron, D. T.; Teat, S. J. *Phys. Chem. Chem. Phys.* **2010**, *12*, 1842–1853.
- (280) Hallett, J. P.; Liotta, C. L.; Ranieri, G.; Welton, T. *J. Org. Chem.* **2009**, *74*, 1864–1868.
- (281) Evans, D. F.; Yamauchi, A.; Roman, R.; Casassa, E. Z. *J. Colloid Interface Sci.* **1982**, *88*, 89–96.
- (282) Evans, D. F.; Yamauchi, A.; Wei, G. J.; Bloomfield, V. A. *J. Phys. Chem.* **1983**, *87*, 3537–3541.
- (283) Fumino, K.; Wulf, A.; Ludwig, R. *Angew. Chem., Int. Ed.* **2009**, *48*, 3184.
- (284) Fumino, K.; Reichert, E.; Wittler, K.; Hempelmann, R.; Ludwig, R. *Angew. Chem., Int. Ed.* **2012**, *51*, 6236–6240.
- (285) Fumino, K.; Reimann, S.; Ludwig, R. *Phys. Chem. Chem. Phys.* **2014**, *16*, 21903–21929.
- (286) Grimme, S.; J. Antony, J.; Ehrlich, S.; Krieg, H. *J. Chem. Phys.* **2010**, *132*, 154104.
- (287) Steiner, T. *Angew. Chem., Int. Ed.* **2002**, *41*, 48–76.
- (288) Desiraju, G. R. *Angew. Chem., Int. Ed.* **2011**, *50*, 52–59.
- (289) Schwalbe, C. H. *Crystallogr. Rev.* **2012**, *18*, 191–206.
- (290) Ribeiro, M. C. C. *J. Phys. Chem. B* **2012**, *116*, 7281–7290.
- (291) Fumino, K.; Wulf, A.; Ludwig, R. *Angew. Chem., Int. Ed.* **2008**, *47*, 8731–8734.
- (292) Fumino, K.; Wulf, A.; Ludwig, R. *Angew. Chem., Int. Ed.* **2008**, *47*, 3830–3834.
- (293) Katsyuba, S. A.; Dyson, P. J.; Vandyukova, E. E.; Chernova, A. V.; Vidiš, A. *Helv. Chim. Acta* **2004**, *87*, 2556–2565.
- (294) Wulf, A.; Fumino, K.; Ludwig, R. *Angew. Chem., Int. Ed.* **2010**, *49*, 449–453.

- (295) Fumino, K.; Wittler, K.; Ludwig, R. *J. Phys. Chem. B* **2012**, *116*, 9507–9511.
- (296) Mele, A.; Tran, C. D.; De Paoli Lacerda, S. H. *Angew. Chem. Int. Ed.* **2003**, *42*, 4500–4502.
- (297) Jodry, J. J.; Mikami, K. *Tetrahedron Lett.* **2004**, *45*, 4429–4431.
- (298) Huang, J.-F.; Chen, P.-Y.; Sun, I. W.; Wang, S. P. *Inorg. Chim. Acta* **2001**, *320*, 7–11.
- (299) Katsyuba, S. A.; Vener, M. V.; Zvereva, E. E.; Fei, Z.; Scopelliti, R.; Laurenczy, G.; Yan, N.; Paunescu, E.; Dyson, P. J. *J. Phys. Chem. B* **2013**, *117*, 9094–9105.
- (300) Roth, C.; Peppel, T.; Fumino, K.; Köckerling, M.; Ludwig, R. *Angew. Chem., Int. Ed.* **2010**, *49*, 10221–10224.
- (301) Hardacre, C.; Holbrey, J. D.; McMath, J. S. E.; Bowron, D. T.; Soper, A. K. *J. Chem. Phys.* **2003**, *118*, 273.
- (302) Hunt, P. A. *J. Phys. Chem. B* **2007**, *111*, 4844–4853.
- (303) Skarmoutsos, I.; Dellis, D.; Matthews, R. P.; Welton, T.; Hunt, P. A. *J. Phys. Chem. B* **2012**, *116*, 4921–4933.
- (304) Dong, K.; Zhang, S.; Wang, D.; Yao, X. *J. Phys. Chem. A* **2006**, *110*, 9775–9782.
- (305) Dong, K.; Song, Y.; Liu, X.; Cheng, W.; Yao, X.; Zhang, S. *J. Phys. Chem. B* **2011**, *116*, 1007–1017.
- (306) Thar, J.; Brehm, M.; Seitsonen, A. P.; Kirchner, B. *J. Phys. Chem. B* **2009**, *113*, 15129–15132.
- (307) Kohagen, M.; Brehm, M.; Lingscheid, Y.; Giernoth, R.; Sangoro, J.; Kremer, F.; Naumov, S.; Iacob, C.; Kärger, J.; Valiullin, R.; Kirchner, B. *J. Phys. Chem. B* **2011**, *115*, 15280–15288.
- (308) Skarmoutsos, I.; Welton, T.; Hunt, P. A. *Phys. Chem. Chem. Phys.* **2014**, *16*, 3675–3685.
- (309) Ossowicz, P.; Janus, E.; Schroeder, G.; Rozwadowski, Z. *Molecules* **2013**, *18*, 4986–5004.
- (310) Dong, K.; Zhang, S. *Chem.—Eur. J.* **2012**, *18*, 2748–2761.
- (311) Fumino, K.; Wulf, A.; Ludwig, R. *Phys. Chem. Chem. Phys.* **2009**, *11*, 8790–8794.
- (312) Fracnk, H. S.; Wen, W.-Y. *Discuss. Faraday Soc.* **1957**, *24*, 133.
- (313) Wernet, P.; Nordlund, D.; Bergmann, U.; Cavalleri, M.; Odellius, M.; Ogasawara, H.; Näslund, L. Å.; Hirsch, T. K.; Ojamäe, L.; Glatzel, P.; Pettersson, L. G. M.; Nilsson, A. *Science* **2004**, *304*, 995–999.
- (314) Huang, C.; Wikfelgdt, K. T.; Tokushima, T.; Nordlund, D.; Harada, Y.; Bergmann, U.; Niebuhr, M.; Weiss, T. M.; Horikawa, Y.; Leetmaa, M.; Ljungberg, M. P.; Takahashi, O.; Lenz, A.; Ojamäe, L.; Lyubartsev, A. P.; Shin, S.; Pettersson, L. G. M.; Nilsson, A. *Proc. Natl. Acad. Sci. U.S.A.* **2009**, *106*, 15214–15218.
- (315) Angell, C. A.; Zhao, Z. *Faraday Discuss.* **2013**, *167*, 625–641.
- (316) Gozzo, F. C.; Santos, L. S.; Augusti, R.; Consorti, C. S.; Dupont, J.; Eberlin, M. N. *Chem.—Eur. J.* **2004**, *10*, 6187–6193.
- (317) Bini, R.; Bortolini, O.; Chiappe, C.; Pieraccini, D.; Siciliano, T. *J. Phys. Chem. B* **2006**, *111*, 598–604.
- (318) Consorti, C. S.; Suarez, P. A. Z.; de Souza, R. F.; Burrow, R. A.; Farrar, D. H.; Lough, A. J.; Loh, W.; da Silva, L. H. M.; Dupont, J. *J. Phys. Chem. B* **2005**, *109*, 4341–4349.
- (319) DaSilveira Neto, B. A.; Santos, L. S.; Nachtigall, F. M.; Eberlin, M. N.; Dupont, J. *Angew. Chem.* **2006**, *118*, 7409–7412.
- (320) Dyson, P. J.; Khalaila, I.; Luettgen, S.; McIndoe, J. S.; Zhao, D. *Chem. Commun.* **2004**, *0*, 2204–2205.
- (321) Dorbritz, S.; Ruth, W.; Kragl, U. *Adv. Synth. Catal.* **2005**, *347*, 1273–1279.
- (322) Kennedy, D. F.; Drummond, C. J. *J. Phys. Chem. B* **2009**, *113*, 5690.
- (323) Xu, W.; Cooper, E. I.; Angell, C. A. *J. Phys. Chem. B* **2003**, *107*, 6170–6178.
- (324) Bodo, E.; Mangialardo, S.; Ramondo, F.; Ceccacci, F.; Postorino, P. *J. Phys. Chem. B* **2012**, *116*, 13878–13888.
- (325) Addicoat, M. A.; Stefanovic, R.; Webber, G. B.; Atkin, R.; Page, A. *J. J. Chem. Theory Comput.* **2014**, *10*, 4633–4643.
- (326) Hunger, J.; Sonnleitner, T.; Liu, L.; Buchner, R.; Bonn, M.; Bakker, H. *J. J. Phys. Chem. Lett.* **2012**, *3*, 3034–3038.
- (327) Ho, S. S. J.; Coddens, M. E.; Poole, C. F. *Org. Mass Spectrom.* **1985**, *20*, 377–379.
- (328) Poole, C. F.; Kersten, B. R.; Ho, S. S. J.; Coddens, M. E.; Furton, K. G. *J. Chromatogr. A* **1986**, *352*, 407.
- (329) AbdulSada, A. K.; Elaiwi, A. E.; Greenway, A. M.; Seddon, K. R. *Eur. Mass Spectrom.* **1997**, *3*, 245.
- (330) Greaves, T. L.; Kennedy, D. F.; Kirby, N.; Drummond, C. J. *J. Phys. Chem. Chem. Phys.* **2011**, *13*, 13501–13509.
- (331) Greaves, T. L.; Kennedy, D. F.; Weerawardena, A.; Tse, N. M. K.; Kirby, N.; Drummond, C. J. *J. Phys. Chem. B* **2011**, *115*, 2055.
- (332) Wakeham, D.; Nelson, A.; Warr, G. G.; Atkin, R. *Phys. Chem. Chem. Phys.* **2011**, *13*, 20828–20835.
- (333) Wakeham, D.; Niga, P.; Ridings, C.; Andersson, G.; Nelson, A.; Warr, G. G.; Baldelli, S.; Rutland, M. W.; Atkin, R. *Phys. Chem. Chem. Phys.* **2012**, *14*, 5106–5114.
- (334) Ridings, C.; Lockett, V.; Andersson, G. *Phys. Chem. Chem. Phys.* **2011**, *13*, 17177–17184.
- (335) Burrell, G. L.; Dunlop, N. F.; Separovic, F. *Soft Matter* **2010**, *6*, 2080–2086.
- (336) Umebayashi, Y.; Mitsugi, T.; Fujii, K.; Seki, S.; Chiba, K.; Yamamoto, H.; Canongia Lopes, J. N.; Pádua, A. A. H.; Takeuchi, M.; Kanzaki, R.; Ishiguro, S.-i. *J. Phys. Chem. B* **2009**, *113*, 4338–4346.
- (337) Umebayashi, Y.; Mori, S.; Fujii, K.; Tsuzuki, S.; Seki, S.; Hayamizu, K.; Ishiguro, S.-i. *J. Phys. Chem. B* **2010**, *114*, 6513–6521.
- (338) Berg, R. W.; Deetlefs, M.; Seddon, K. R.; Shim, I.; Thompson, J. M. *J. Phys. Chem. B* **2005**, *109*, 19018–19025.
- (339) Johnson, C. J.; Fournier, J. A.; Wolke, C. T.; Johnson, M. A. J. *Chem. Phys.* **2013**, *139*, 224305.
- (340) Umebayashi, Y.; Fujimori, T.; Sukizaki, T.; Asada, M.; Fujii, K.; Kanzaki, R.; Ishiguro, S.-i. *J. Phys. Chem. A* **2005**, *109*, 8976–8982.
- (341) Ludwig, R. *Angew. Chem., Int. Ed.* **2001**, *40*, 1808–1827.
- (342) Fannin, A. A.; King, L. A.; Levisky, J. A.; Wilkes, J. S. *J. Phys. Chem.* **1984**, *88*, 2609–2614.
- (343) Wilkes, J. S.; Hussey, C. L.; Sanders, J. R. *Polyhedron* **1986**, *5*, 1567–1571.
- (344) Hussey, C. L.; Sun, I.-W.; Strubinger, S. K. D.; Barnard, P. A. J. *Electrochim. Soc.* **1990**, *137*, 2515.
- (345) Noda, A.; Hayamizu, K.; Watanabe, M. *J. Phys. Chem. B* **2001**, *105*, 4603–4610.
- (346) Tokuda, H.; Hayamizu, K.; Ishii, K.; Susan, M. A. B. H.; Watanabe, M. *J. Phys. Chem. B* **2005**, *109*, 6103–6110.
- (347) Margulis, C. J. *Mol. Phys.* **2004**, *102*, 829.
- (348) Taraskin, S. N.; Elliott, S. R.; Klinger, M. *J. Non-Cryst. Solids* **1995**, *193*, 263.
- (349) Lee, J. H.; Elliott, S. R. *J. Non-Cryst. Solids* **1995**, *193*, 133.
- (350) Parker, D. R.; Wilson, M.; Madden, P. A.; Medvedev, N. N.; Geiger, A. *Phys. Rev. E* **2000**, *62*, 1427–1430.
- (351) Law, G.; Watson, P. R. *Langmuir* **2001**, *17*, 6138.
- (352) Abbott, A. P. *ChemPhysChem* **2004**, *5*, 1242–1246.
- (353) Triolo, A.; Russina, O.; Fazio, B.; Triolo, R.; Di Cola, E. *Chem. Phys. Lett.* **2008**, *457*, 362–365.
- (354) Greaves, T. L.; Kennedy, D. F.; Mudie, S. T.; Drummond, C. J. *J. Phys. Chem. B* **2010**, *114*, 10022–10031.
- (355) Tanford, C. A. *The Hydrophobic Effect: Formation of Micelles and Biological Membranes*, 2nd ed.; Wiley: New York, 1980.
- (356) Schröder, U.; Wadhawan, J. D.; Compton, R. G.; Marken, F.; Suarez, P. A. Z.; Consorti, C. S.; de Souza, R. F.; Dupont, J. *New J. Chem.* **2000**, *24*, 1009.
- (357) Hu, Z.; Margulis, C. J. *Proc. Natl. Acad. Sci. U.S.A.* **2006**, *103*, 831.
- (358) Wang, Y.; Voth, G. A. *J. Am. Chem. Soc.* **2005**, *127*, 12192–12193.
- (359) Wang, Y.; Voth, G. A. *J. Phys. Chem. B* **2006**, *110*, 18601–18608.
- (360) Urahata, S. M.; Ribeiro, M. C. C. *J. Chem. Phys.* **2004**, *120*, 1855.
- (361) Canongia Lopes, J. N.; Costa Gomes, M. F.; Padua, A. A. H. *J. Phys. Chem. B* **2006**, *110*, 16818.
- (362) Santos, L. M. N. B. F.; Canongia Lopes, J. N.; Coutinho, J. A. P.; Esperança, J. M. S. S.; Gomes, L. R.; Marrucho, I. M.; Rebelo, L. P. N. J. *Am. Chem. Soc.* **2006**, *129*, 284–285.
- (363) Triolo, A.; Russina, O.; Bleif, H. J.; DiCola, E. *J. Phys. Chem. B* **2007**, *111*, 4641–4644.

- (364) Triolo, A.; Russina, O.; Fazio, B.; Appeteccchi, G. B.; Carewska, M.; Passerini, S. *J. Chem. Phys.* **2009**, *130*, 164521.
- (365) Bodo, E.; Gontrani, L.; Triolo, A.; Caminiti, R. *J. Phys. Chem. Lett.* **2010**, *1*, 1095–1100.
- (366) Russina, O.; Triolo, A.; Gontrani, L.; Caminiti, R.; Xiao, D.; L. G., Jr.; Bartsch, R. A.; Quitevis, E. L.; Plechkova, N.; Seddon, K. R. *J. Phys.: Condens. Matter* **2009**, *21*, 424121.
- (367) Triolo, A.; Russina, O.; Caminiti, R.; Shirota, H.; Lee, H. Y.; Santos, C. S.; Murthy, N. S.; Castner, J. E. W. *Chem. Commun.* **2012**, *48*, 4959–4961.
- (368) Jiang, W.; Yan, T.; Wang, Y.; Voth, G. A. *J. Phys. Chem. B* **2008**, *112*, 3121.
- (369) Jiang, W.; Wang, Y.; Voth, G. A. *Acc. Chem. Res.* **2008**, *40*, 1193.
- (370) Jiang, W.; Wang, Y.; Voth, G. A. *J. Phys. Chem. B* **2007**, *111*, 4812–4818.
- (371) Wang, Y.; Izvekov, S.; Voth, G. A. *J. Phys. Chem. B* **2006**, *110*, 3564.
- (372) Canongia Lopes, J. N.; Rebelo, L. P. N.; Costa Gomes, M. F.; Padua, A. A. H. Congress on Ionic Liquids III, Carins, 2009.
- (373) Shimizu, K.; Bernardes, C. E. S.; Canongia Lopes, J. N. *Pure Appl. Chem.* **2014**, *86*, 119–133.
- (374) Bhargava, B. L.; Devane, R.; Klein, M. L.; Balasubramanian, S. *Soft Matter* **2007**, *3*, 1395–1400.
- (375) Bhargava, B. L.; Balasubramanian, S. *J. Chem. Phys.* **2007**, *127*, 114510.
- (376) Bhargava, B. L.; Balasubramanian, S. *J. Phys. Chem. B* **2007**, *111*, 4477–4487.
- (377) Bhargava, B. L.; Balasubramanian, S. *J. Phys. Chem. B* **2008**, *112*, 7566–7573.
- (378) Karimi-Varzaneh, H. A.; Müller-Plathe, F.; Balasubramanian, S.; Carbone, P. *Phys. Chem. Chem. Phys.* **2010**, *12*, 4714–4724.
- (379) Raju, S. G.; Balasubramanian, S. *J. Phys. Chem. B* **2010**, *114*, 6455–6463.
- (380) Salanne, M.; Siqueira, L. J.; Seitsonen, A. P.; Madden, P. A.; Kirchner, B. *Faraday Discuss.* **2012**, *154*, 171.
- (381) Paredes, X.; Fernández, J.; Pádua, A. A. H.; Malfreyt, P.; Malberg, F.; Kirchner, B.; Pensado, A. S. *J. Phys. Chem. B* **2014**, *118*, 731–742.
- (382) Weber, H.; Hollóczki, O.; Pensado, A. S.; Kirchner, B. *J. Chem. Phys.* **2013**, *139*, 084502.
- (383) Bhargava, B. L.; Balasubramanian, S.; Klein, M. L. *Chem. Commun.* **2008**, 3339–3351.
- (384) Bhargava, B. L.; Yasaka, Y.; Klein, M. L. *Chem. Commun.* **2011**, *47*, 6228–6241.
- (385) Lynden-Bell, R. M. *Phys. Chem. Chem. Phys.* **2010**, *12*, 1733–1740.
- (386) Lynden-Bell, R. M.; Del Popolo, M. G.; Youngs, T. G. A.; Kohanoff, J.; Hanke, C. G.; Harper, J. B.; Pinilla, C. C. *Acc. Chem. Res.* **2007**, *40*, 1138–1145.
- (387) Hanke, C. G.; Atamas, N. A.; Lynden-Bell, R. M. *Green Chem.* **2002**, *4*, 107–111.
- (388) Hanke, C. G.; Price, S. L.; Lynden-Bell, R. M. *Mol. Phys.* **2001**, *99*, 801–809.
- (389) Maginn, E. J. *J. Phys.: Condens. Matter* **2009**, *21*, 373101.
- (390) Morrow, T. I.; Maginn, E. J. *J. Phys. Chem. B* **2002**, *106*, 12807–12813.
- (391) Maginn, E. J. *Acc. Chem. Res.* **2007**, *40*, 1200–1207.
- (392) Gutowski, K. E.; Maginn, E. J. *J. Am. Chem. Soc.* **2008**, *130*, 14690–14704.
- (393) Shah, J. K.; Brennecke, J. F.; Maginn, E. J. *Green Chem.* **2002**, *4*, 112–118.
- (394) Del Pópolo, M. G.; Kohanoff, J.; Lynden-Bell, R. M. *J. Phys. Chem. B* **2006**, *110*, 8798–8803.
- (395) Izgorodina, E. I.; Forsyth, M.; MacFarlane, D. R. *Aust. J. Chem.* **2007**, *60*, 15–20.
- (396) Addicoat, M. A.; Fukuoka, S.; Page, A. J.; Irle, S. *J. Comput. Chem.* **2013**, *34*, 2591–2600.
- (397) Koßmann, S.; Thar, J.; Kirchner, B.; Hunt, P. A.; Welton, T. *J. Chem. Phys.* **2006**, *124*, 174506.
- (398) Izgorodina, E. I.; Rigby, J.; MacFarlane, D. R. *Chem. Commun.* **2012**, *48*, 1493–1495.
- (399) Liu, Z.; Huang, S.; Wang, W. *J. Phys. Chem. B* **2004**, *108*, 12978.
- (400) Canongia Lopes, J. N.; Deschamps, J.; Pádua, A. A. H. *J. Phys. Chem. B* **2004**, *108*, 2038–2047.
- (401) Margulis, C. J.; Stern, H. A.; Berne, B. J. *J. Phys. Chem. B* **2002**, *106*, 12017.
- (402) Micaelo, N. M.; Baptista, A. M.; Soares, C. M. *J. Phys. Chem. B* **2006**, *110*, 14444–14451.
- (403) Köddermann, T.; Reith, D.; Ludwig, R. *ChemPhysChem* **2013**, *14*, 3368–3374.
- (404) Borodin, O. *J. Phys. Chem. B* **2009**, *113*, 11463–11478.
- (405) Chaban, V. V.; Prezhdo, O. V. *Phys. Chem. Chem. Phys.* **2011**, *13*, 19345–19354.
- (406) Chaban, V. V.; Voroshlyova, I. V.; Kalugin, O. N. *Phys. Chem. Chem. Phys.* **2011**, *13*, 7910–7920.
- (407) Kobrak, M. N.; Li, H. *Phys. Chem. Chem. Phys.* **2010**, *12*, 1922–1932.
- (408) Zhao, H.-Q.; Shi, R.; Wang, Y.-T. *Commun. Theor. Phys.* **2011**, *56*, 499–50.
- (409) Izgorodina, E. I.; Golze, D.; Maganti, R.; Armel, V.; Taige, M.; Schubert, T. J. S.; MacFarlane, D. R. *Phys. Chem. Chem. Phys.* **2014**.
- (410) Matthews, R. P.; Welton, T.; Hunt, P. A. *Phys. Chem. Chem. Phys.* **2014**, *16*, 3238–3253.
- (411) Rocha, M. A. A.; Neves, C. M. S. S.; Freire, M. G.; Russina, O.; Triolo, A.; Coutinho, J. A. P.; Santos, L. M. N. B. F. *J. Phys. Chem. B* **2013**, *117*, 10889–10897.
- (412) Kashyap, H. K.; Santos, C. S.; Murthy, N. S.; Hettige, J. J.; Kerr, K.; Ramati, S.; Gwon, J.; Gohdo, M.; Lall-Ramnarine, S. I.; Wishart, J. F.; Margulis, C. J.; Castner, E. W. *J. Phys. Chem. B* **2013**, *117*, 15328–15337.
- (413) Butler, S. N.; Müller-Plathe, F. *J. Mol. Liq.* **2014**, *192*, 114–117.
- (414) Raju, S. G.; Balasubramanian, S. *J. Phys.: Condens. Matter* **2009**, *21*, 035105.
- (415) Dommert, F.; Wendler, K.; Berger, R.; Site, L. D.; Holm, C. *ChemPhysChem* **2012**, *13*, 1625–1637.
- (416) Bhushan, B. *Wear* **2005**, *259*, 1507–1531.
- (417) Zahn, S.; Brehm, M.; Brüssela, M.; Hollóczki, O.; Kohagen, M.; Lehmann, S.; Malberg, F.; Pensado, A. S.; Schöppke, M.; Weber, H.; Kirchner, B. *J. Mol. Liq.* **2014**, *192*, 71–76.
- (418) Shimizu, K.; Costa Gomes, M. F.; Padua, A. A. H.; Rebelo, L. P. N.; Canongia Lopes, J. N. *J. Mol. Struct. (THEOCHEM)* **2010**, *946*, 70–76.
- (419) Shimizu, K.; Padua, A. A. H.; Canongia Lopes, J. N. *J. Phys. Chem. B* **2010**, *114*, 15635–15641.
- (420) Pott, T.; Méléard, P. *Phys. Chem. Chem. Phys.* **2009**, *11*, 5469–5475.
- (421) Hardacre, C.; McMath, S. E. J.; Nieuwenhuyzen, M.; Bowron, D. T.; Soper, A. K. *J. Phys.: Condens. Matter* **2003**, *1*, S159.
- (422) Hardacre, C.; Holbrey, J. D.; Mullan, C. L.; Youngs, T. G. A.; Bowron, D. T. *J. Chem. Phys.* **2010**, *133*, 074510.
- (423) McLain, S. E.; Soper, A. K.; Luzar, A. *J. Chem. Phys.* **2006**, *124*, 074502.
- (424) Soper, A. K. *Chem. Phys.* **2000**, *258*, 121–137.
- (425) Hayes, R.; Imberti, S.; Warr, G. G.; Atkin, R. *Phys. Chem. Chem. Phys.* **2011**, *13*, 13544.
- (426) Hayes, R.; Imberti, S.; Warr, G. G.; Atkin, R. *Angew. Chem., Int. Ed.* **2012**, *51*, 7468–7471.
- (427) Hayes, R.; Imberti, S.; Warr, G. G.; Atkin, R. *Angew. Chem., Int. Ed.* **2013**, *52*, 4623–4627.
- (428) Hayes, R.; Imberti, S.; Warr, G. G.; Atkin, R. *J. Phys. Chem. C* **2014**, *118*, 13998–14008.
- (429) Binnemans, K. *Chem. Rev.* **2005**, *105*, 4148–4204.
- (430) Annapureddy, H. V. R.; Kashyap, H. K.; De Biase, P. M.; Margulis, C. J. *J. Phys. Chem. B* **2010**, *114*, 16838–16846.
- (431) Kashyap, H. K.; Hettige, J. J.; Annapureddy, H. V. R.; Margulis, C. J. *Chem. Commun.* **2012**, *48*, 5103–5105.
- (432) Hettige, J. J.; Kashyap, H. K.; Annapureddy, H. V. R.; Margulis, C. J. *J. Phys. Chem. Lett.* **2013**, *4*, 105–110.
- (433) Teubner, M.; Strey, R. *J. Chem. Phys.* **1987**, *87*, 3195–3200.

- (434) Atkin, R.; Warr, G. G. *J. Phys. Chem. B* **2008**, *112*, 4164–4166.
- (435) Umebayashi, Y.; Chung, W.; Mitsugi, T.; Fukuda, S.; Takeuchi, M.; Fuji, K.; Takamuku, T.; Kanzaki, R.; Ishiguro, S. *J. Comput. Chem. Jpn.* **2008**, *7*, 125.
- (436) Hayes, R. Structure in Ionic Liquids. Ph.D. Thesis, Discipline of Chemistry, The University of Newcastle, Australia, 2014.
- (437) Iglesias, M.; Torres, A.; Gonzalez-Olmos, R.; Salvatierra, D. *J. Chem. Thermodyn.* **2008**, *40*, 119–133.
- (438) Gontrani, L.; Bodo, E.; Triolo, A.; Leonelli, F.; D'Angelo, P.; Migliorati, V.; Caminiti, R. *J. Phys. Chem. B* **2012**, *116*, 13024–13032.
- (439) Campetella, M.; Gontrani, L.; Bodo, E.; Ceccacci, F.; Marincola, F. C.; Caminiti, R. *J. Chem. Phys.* **2013**, *138*, 184506.
- (440) Zahn, S.; Thar, J.; Kirchner, B. *J. Chem. Phys.* **2010**, *132*, 124506.
- (441) Scriven, L. E. *Nature* **1976**, *263*, 123.
- (442) Hyde, S. T. *J. Phys. Chem.* **1989**, *93*, 1458–1464.
- (443) Hyde, S. T.; Blum, Z.; Landh, T.; Lidin, S.; Ninham, B. W.; Andersson, S.; Larsson, K. *The Language of Shape: The Role of Curvature in Condensed Matter: Physics, Chemistry and Biology*; Elsevier: Amsterdam, 1997.
- (444) Hyde, S. T.; Schröder, G. E. *Curr. Opin. Colloid Interface Sci.* **2003**, *8*, 5–14.
- (445) Santos, C. S.; Annareddy, H. V. R.; Murthy, N. S.; Kashyap, H. K.; Castner, E. W. J.; Margulis, C. J. *J. Chem. Phys.* **2011**, *134*, 064501.
- (446) Kashyap, H. K.; Santos, C. S.; Annareddy, H. V. R.; Murthy, N. S.; Margulis, C. J.; Castner, E. W. J. *Faraday Discuss.* **2011**, *154*, 133–143.
- (447) Freitas, A. A.; Shimizu, K.; Canongia Lopes, J. N. *J. Chem. Eng. Data* **2014**, *59*, 3120–3129.
- (448) Shimizu, K.; Bernardes, C. E. S.; Canongia Lopes, J. N. *J. Phys. Chem. B* **2014**, *118*, 567–576.
- (449) Bernardes, C. E. S.; Shimizu, K.; Lobo Ferreira, A. I. M. C.; Santos, L. M. N. B. F.; Canongia Lopes, J. N. *J. Phys. Chem. B* **2014**, *118*, 6885–6895.
- (450) Russina, O.; Triolo, A. *Faraday Discuss.* **2012**, *154*, 97–109.
- (451) Shimizu, K.; Bernardes, C. E. S.; Triolo, A.; Canongia Lopes, J. N. *Phys. Chem. Chem. Phys.* **2013**, *15*, 16256–16262.
- (452) Wei, K.; Deng, L.; Wang, Y.; Ou-Yang, Z.-C.; Wang, G. *J. Phys. Chem. B* **2014**, *118*, 3642–3649.
- (453) Fakhraee, M.; Zand Karimi, B.; Salari, H.; Gholami, M. R. *J. Phys. Chem. B* **2014**, *118*, 14410–14428.
- (454) Lee, H. Y.; Shirota, H.; Castner, E. W. J. *J. Phys. Chem. Lett.* **2013**, *4*, 1477–1483.
- (455) Rocha, M. A. A.; Neves, C. M. S. S.; Freire, M. G.; Russina, O.; Triolo, A.; Coutinho, J. o. A. P.; Santos, L. M. N. B. F. *J. Phys. Chem. B* **2013**.
- (456) Morgado, P.; Shimizu, K.; Esperança, J. M. S. S.; Reis, P. M.; Rebelo, L. P. N.; Canongia Lopes, J. N.; Filipe, E. J. M. *J. Phys. Chem. Lett.* **2013**, *4*, 2758–2762.
- (457) Castiglione, F.; Simonutti, R.; Mauri, M.; Mele, A. *J. Phys. Chem. Lett.* **2013**, *4*, 1608–1612.
- (458) Men, S.; Lovelock, K. R. J.; Licence, P. *Phys. Chem. Chem. Phys.* **2012**, *13*, 15244–15255.
- (459) Hurisso, S.; Lovelock, K. R. J.; Licence, P. *Phys. Chem. Chem. Phys.* **2011**, *13*, 17737–17748.
- (460) Licence, P. *Angew. Chem., Int. Ed.* **2012**, *51*, 4789–4791.
- (461) Monduzzi, M. *Curr. Opin. Colloid Interface Sci.* **1998**, *3*, 467–477.
- (462) Guittard, F.; Taffin de Givenchy, E.; Geribaldi, S.; Cambon, A. J. *Fluorine Chem.* **1999**, *100*, 85–96.
- (463) Hoffmann, H.; Würtz, J. *J. Mol. Liq.* **1997**, *72*, 191–230.
- (464) Chambers, R. D. *Fluorine in Organic Chemistry*; Wiley: New York, 2004.
- (465) Dolbier, W. R., Jr. *J. Fluorine Chem.* **2005**, *126*, 157–163.
- (466) Greaves, T. L.; Kennedy, D. F.; Shen, Y.; Hawley, A.; Song, G.; Drummond, C. J. *Phys. Chem. Chem. Phys.* **2013**, *15*, 7592–7598.
- (467) Shen, Y.; Kennedy, D. F.; Greaves, T. L.; Weerawardena, A.; Mulder, R. J.; Kirby, N.; Song, G.; Drummond, C. J. *Phys. Chem. Chem. Phys.* **2012**, *14*, 7981–7992.
- (468) Russina, O.; Lo Celso, F.; Di Michiel, M.; Passerini, S.; Appeteccchi, G. B.; Castiglione, F.; Mele, A.; Caminiti, R.; Triolo, A. *Faraday Discuss.* **2013**, *167*, 499–513.
- (469) Pereiro, A. B.; Pastoriza-Gallego, M. J.; Shimizu, K.; Marrucho, I. M.; Canongia Lopes, J. N.; Pineiro, M. M.; Rebelo, L. P. N. *J. Phys. Chem. B* **2013**, *117*, 10826–10833.
- (470) Smith, G. D.; Borodin, O.; Magda, J. J.; Boyd, R. H.; Wang, Y.; Bara, J. E.; Miller, S.; Gin, D. L.; Noble, R. D. *Phys. Chem. Chem. Phys.* **2010**, *12*, 7064–7076.
- (471) Hettige, J. J.; Araque, J. C.; Margulis, C. J. *J. Phys. Chem. B* **2014**, *118*, 12706–12716.
- (472) Zeng, X.; Ungar, G.; Imperor-Clerc, M. *Nat. Mater.* **2005**, *4*, 562–567.
- (473) Davey, T. W.; Warr, G. G.; Almgren, M.; Asakawa, T. *Langmuir* **2001**, *17*, 5283–5287.
- (474) Fuhrhop, J. H.; Wang, T. *Chem. Rev.* **2004**, *104*, 2901–2937.
- (475) Menger, F. M.; Littau, C. A. *J. Am. Chem. Soc.* **1993**, *115*, 10083–10090.
- (476) Zana, R. In *Specialist Surfactants*; Robb, I. D., Ed.; Blackie Academic and Professional: London, 1997.
- (477) Li, S.; Banuelos, J. L.; Zhang, P.; Feng, G.; Dai, S.; Rother, G.; Cummings, P. T. *Soft Matter* **2014**, *10*, 9193–9200.
- (478) Ishida, T.; Shirota, H. *J. Phys. Chem. B* **2012**, *117*, 1136–1150.
- (479) Yeganegi, S.; Soltanabadi, A.; Farmanzadeh, D. *J. Phys. Chem. B* **2012**, *116*, 11517–11526.
- (480) Bodo, E.; Chiricotto, M.; Caminiti, R. *J. Phys. Chem. B* **2011**, *115*, 14341–14347.
- (481) Li, S.; Feng, G.; Leobardo Bañuelos, J.; Rother, G.; Fulvio, P. F.; Dai, S.; Cummings, P. T. *J. Phys. Chem. C* **2013**, *117*, 18251–18257.
- (482) Shirota, H. I. T. *J. Phys. Chem. B* **2011**, *115*, 10860–10870.
- (483) Payagala, T.; Huang, J.; Breitbach, Z. S.; Sharma, P. S.; Armstrong, D. W. *Chem. Mater.* **2007**, *19*, 5848–5850.
- (484) Shirota, H.; Mandai, T.; Fukazawa, H.; Kato, T. *J. Chem. Eng. Data* **2011**, *56*, 2453–2459.
- (485) Brown, P.; Butts, C. P.; Eastoe, J.; Padron Hernandez, E.; Machado, F. L. d. A.; de Oliveira, R. *J. Chem. Commun.* **2013**, *49*, 2765–2767.
- (486) Men, Y.; Schalaad, H.; Voelkel, A.; Yuan, J. *Polym. Chem.* **2014**, *5*, 3719–3724.
- (487) Fei, Z.; Zhu, D.-R.; Yan, N.; Scopelliti, R.; Katsuba, S. A.; Laurenczy, G.; Chisholm, D. M.; McIndoe, J. S.; Seddon, K. R.; Dyson, P. J. *Chem.—Eur. J.* **2014**, n/a–n/a.
- (488) Tadesse, H.; Blake, A. J.; Champness, N. R.; Warren, J. E.; Rizkallah, P. J.; Licence, P. *CrystEngComm* **2012**, *14*, 4886–4893.
- (489) Bhargava, B. L.; Klein, M. L. *J. Chem. Theory Comput.* **2010**, *6*, 873–879.
- (490) Bhargava, B. L.; Klein, M. L. *J. Phys. Chem. B* **2011**, *115*, 10439–10446.
- (491) Santos, C. S.; Murthy, N. S.; Baker, G. A.; Castner, E. W. *J. J. Chem. Phys.* **2011**, *134*, 121101–121103.
- (492) In, M.; Warr, G. G.; Zana, R. *Phys. Rev. Lett.* **1999**, *83*, 2278–2281.
- (493) Carmichael, A. J.; Haddleton, D. M. In *Ionic Liquids in Synthesis*; Wasserscheid, P.; Welton, T., Eds.; Wiley-VCH: New York, 2007.
- (494) Atkin, R.; De Fina, L.-M.; Kiederling, U.; Warr, G. G. *J. Phys. Chem. B* **2009**, *113*, 12201–12213.
- (495) Werzer, O.; Atkin, R. *Phys. Chem. Chem. Phys.* **2011**, *13*, 13479–13485.
- (496) Werzer, O.; Warr, G. G.; Atkin, R. *J. Phys. Chem. B* **2010**, *115*, 648–652.
- (497) Werzer, O.; Warr, G. G.; Atkin, R. *Langmuir* **2011**, *27*, 3541–3549.
- (498) Triolo, A.; Russina, O.; Keiderling, U.; Kohlbrecher, J. *J. Phys. Chem. B* **2006**, *110*, 1513–1515.
- (499) Lu, W.; Fadeev, A. G.; Qi, B.; Smela, E.; Mattes, B. R.; Ding, J.; Spinks, G. M.; Mazurkiewicz, J.; Zhou, D.; Wallace, G. G.; MacFarlane, D. R.; Forsyth, S. A.; Forsyth, M. *Science* **2002**, *297*, 983–987.
- (500) Booker, K.; Bower, M. C.; Lennard, C. J.; Holdsworth, C. I.; McCluskey, A. *Chem. Commun.* **2006**, *1*, 1730.

- (501) Lu, J.; Yan, F.; Texter, J. *Prog. Polym. Sci.* **2009**, *34*, 431–448.
- (502) Dobbelen, M.; Jovanovski, V.; Llarena, I.; Claros Marfil, L. J.; Cabanero, G.; Rodriguez, J.; Mecerreyres, D. *Polym. Chem.* **2011**, *2*, 1275–1278.
- (503) Yuan, J.; Antonietti, M. *Polymer* **2011**, *52*, 1469–1482.
- (504) Yuan, J.; Mecerreyres, D.; Antonietti, M. *Prog. Polym. Sci.* **2013**, *38*, 1009–1036.
- (505) Yuan, J.; Soll, S.; Drechsler, M.; Müller, A. H. E.; Antonietti, M. *J. Am. Chem. Soc.* **2011**, *133*, 17556–17559.
- (506) Weber, R. L.; Ye, Y.; Schmitt, A. L.; Banik, S. M.; Elabd, Y. A.; Mahanthappa, M. K. *Macromolecules* **2011**, *44*, 5727–5735.
- (507) Carrasco, P. M.; Ruiz de Luzuriaga, A.; Constantinou, M.; Georgopanos, P.; Rangou, S.; Avgeropoulos, A.; Zafeiropoulos, N. E.; Grande, H.-J.; Cabaniero, G. n.; Mecerreyres, D.; Garcia, I. *Macromolecules* **2011**, *44*, 4936–4941.
- (508) de Gennes, P. G. *J. Chem. Phys.* **1971**, *55*, 572–579.
- (509) Sing, C. E.; Zwanikken, J. W.; Olvera de la Cruz, M. *Nat. Mater.* **2014**, *13*, 694–698.
- (510) Sing, C. E.; Zwanikken, J. W.; Olvera de la Cruz, M. *ACS Macro Lett.* **2013**, *2*, 1042–1046.
- (511) Sing, C. E.; Olvera de la Cruz, M. *ACS Macro Lett.* **2014**, *3*, 698–702.
- (512) Jain, N.; Zhang, X.; Hawkett, B. S.; Warr, G. G. *ACS Appl. Mater. Interfaces* **2011**, *3*, 662–667.
- (513) Jain, N.; Liu, C. K.; Hawkett, B. S.; Warr, G. G.; Hamilton, W. A. *J. Appl. Crystallogr.* **2014**, *47*, 41–52.
- (514) Butter, K.; Bomans, P. H. H.; Frederik, P. M.; Vroege, G. J.; Philipse, A. P. *Nat. Mater.* **2003**, *2*, 88–91.
- (515) Hayashi, S.; Hamaguchi, H. *Chem. Lett.* **2004**, *33*, 1590–1591.
- (516) Yoshida, Y.; Saito, G. *J. Mater. Chem.* **2006**, *16*, 1254–1262.
- (517) Klee, A.; Prevost, S.; Kunz, W.; Schweins, R.; Kiefer, K.; Gradzielski, M. *Phys. Chem. Chem. Phys.* **2012**, *14*, 15355–15360.
- (518) Panja, S. K.; Saha, S. *RSC Adv.* **2013**, *3*, 14495–14500.
- (519) Bica, K.; Gaertner, P. *Org. Lett.* **2006**, *8*, 733–735.
- (520) Lee, S.; Ha, S.; You, C.-Y.; Koo, Y.-M. *Korean J. Chem. Eng.* **2007**, *24*, 436–437.
- (521) Okuno, M.; Hamaguchi, H.-o.; Hayashi, S. *Appl. Phys. Lett.* **2006**, *89*, 132506–132506–2.
- (522) Mallick, B.; Balke, B.; Felser, C.; Mudring, A.-V. *Angew. Chem., Int. Ed.* **2008**, *47*, 7635–7638.
- (523) Kim, J.-Y.; Kim, J.-T.; Song, E.-A.; Min, Y.-K.; Hamaguchi, H.-o. *Macromolecules* **2008**, *41*, 2886–2889.
- (524) Funasako, Y.; Mochida, T.; Inagaki, T.; Sakurai, T.; Ohta, H.; Furukawa, K.; Nakamura, T. *Chem. Commun.* **2011**, *47*, 4475–4477.
- (525) García-Saiz, A.; de Pedro, I.; Blanco, J. s. A.; González, J. s.; Fernández, J. s. R. *J. Phys. Chem. B* **2013**, *117*, 3198–3206.
- (526) Brown, P.; Bushmelev, A.; Butts, C. P.; Cheng, J.; Eastoe, J.; Grillo, I.; Heenan, R. K.; Schmidt, A. M. *Angew. Chem., Int. Ed.* **2012**, *51*, 2414–2416.
- (527) Sitze, M. S.; Schreiter, E. R.; Patterson, E. V.; Freeman, R. G. *Inorg. Chem.* **2001**, *40*, 2298–2304.
- (528) de Pedro, I.; Rojas, D. P.; Blanco, J. A.; Fernández, J. R. *J. Magn. Magn. Mater.* **2011**, *323*, 1254–1257.
- (529) Li, J.-G.; Hu, Y.-F.; Sun, S.-F.; Ling, S.; Zhang, J.-Z. *J. Phys. Chem. B* **2011**, *116*, 6461–6464.
- (530) Del Sesto, R. E.; McCleskey, T. M.; Burrell, A. K.; Baker, G. A.; Thompson, J. D.; Scott, B. L.; Wilkes, J. S.; Williams, P. *Chem. Commun.* **2008**, *447*–449.
- (531) Krieger, B. M.; Lee, H. Y.; Emge, T. J.; Wishart, J. F.; Castner, J. E. W. *Phys. Chem. Chem. Phys.* **2010**, *12*, 8919–8925.
- (532) Bäcker, T.; Breunig, O.; Valldor, M.; Merz, K.; Vasylyeva, V.; Mudring, A.-V. *Cryst. Growth Des.* **2011**, *11*, 2564–2571.
- (533) Kruszynski, R.; Wyrzykowski, D. *Acta Crystallogr., Sect. E: Struct. Rep. Online* **2006**, *62*, m994–m996.
- (534) Housecroft, C. E.; Sharpe, A. G. *Inorganic Chemistry*, 2nd ed.; Pearson Education Limited: 2005.
- (535) Cotton, F. A.; Wilkinson, G.; Murillo, C. A.; Bochmann, M. *Advanced Inorganic Chemistry*, 5th ed.; Wiley: New York, 1999.
- (536) Lawrence, G. A. *Introduction to Coordination Chemistry*; John Wiley & Sons Ltd.: Chichester, 2010.
- (537) Pratt Lii, H. D.; Rose, A. J.; Staiger, C. L.; Ingersoll, D.; Anderson, T. M. *Dalton Trans.* **2011**, *40*, 11396–11401.
- (538) Mallick, B.; Metlen, A.; Nieuwenhuyzen, M.; Rogers, R. D.; Mudring, A.-V. *Inorg. Chem.* **2011**, *51*, 193–200.
- (539) Inagaki, T.; Mochida, T.; Takahashi, M.; Kanadani, C.; Saito, T.; Kuwahara, D. *Chem.—Eur. J.* **2012**, *18*, 6795–6804.
- (540) Angell, C. A. *J. Electrochem. Soc.* **1965**, *112*, 1224.
- (541) Watanabe, M.; Mandai, T.; Yoshida, K.; Ueno, K.; Dokko, K. *Phys. Chem. Chem. Phys.* **2014**.
- (542) Rees, W. S., Jr.; Moreno, D. A. *J. Chem. Soc., Chem. Commun.* **1991**, 1759–1760.
- (543) Pedersen, C. J.; Frensdorff, H. K. *Angew. Chem.* **1972**, *84*, 16–26.
- (544) Klein, R.; Zech, O.; Maurer, E.; Kellermeier, M.; Kunz, W. *J. Phys. Chem. B* **2011**, *115*, 8961–8969.
- (545) Zech, O.; Kellermeier, M.; Thomaier, S.; Maurer, E.; Klein, R.; Schreiner, C.; Kunz, W. *Chem.—Eur. J.* **2009**, *15*, 1341–1345.
- (546) Zech, O.; Hunger, J.; Sangoro, J. R.; Iacob, C.; Kremer, F.; Kunz, W.; Buchner, R. *Phys. Chem. Chem. Phys.* **2010**, *12*, 14341–14350.
- (547) Justus, E.; Rischka, K.; Wishart, J. F.; Werner, K.; Gabel, D. *Chem.—Eur. J.* **2008**, *14*, 1918–1923.
- (548) Li, X. L.; Zeng, Z.; Garg, S.; Twamley, B.; Shreeve, J. M. *Eur. J. Inorg. Chem.* **2008**, 3353–3358.
- (549) Mehdi, H.; Binnemans, K.; Van Hecke, K.; Van Meervelt, L.; Nockemann, P. *Chem. Commun.* **2010**, *46*, 234–236.
- (550) Tamura, T.; Yoshida, K.; Hachida, T.; Tsuchiya, M.; Nakamura, M.; Kazue, Y.; Tachikawa, N.; Dokko, K.; Watanabe, M. *Chem. Lett.* **2010**, *39*, 753–755.
- (551) Ueno, K.; Yoshida, K.; Tsuchiya, M.; Tachikawa, N.; Dokko, K.; Watanabe, M. *J. Phys. Chem. B* **2012**, *116*, 11323–11331.
- (552) Hayamizu, K.; Akiba, E.; Bando, T.; Aihara, Y. *J. Chem. Phys.* **2002**, *117*, 5929–5939.
- (553) Tamura, T.; Hachida, T.; Yoshida, K.; Tachikawa, N.; Dokko, K.; Watanabe, M. *J. Power Sources* **2010**, *195*, 6095–6100.
- (554) Depuydt, D.; Brooks, N. R.; Schaltin, S.; Van Meervelt, L.; Fransaer, J.; Binnemans, K. *ChemPlusChem* **2013**, *78*, 578–588.
- (555) Eilmes, A.; Kubisak, P. *J. Phys. Chem. B* **2013**, *117*, 12583–12592.
- (556) Tanaka, H. *Faraday Discuss.* **2013**, *167*, 9–76.
- (557) Kashyap, H. K.; Santos, C. S.; Annappureddy, H. V. R.; Murthy, N. S.; Margulis, C. J.; Castner, E. W. *J. Faraday Discuss.* **2011**, *154*, 133–143.
- (558) Tosi, M. P. *Annu. Rev. Phys. Chem.* **1993**, *44*, 173–211.
- (559) Hettige, J. J.; Kashyap, H. K.; Margulis, C. J. *J. Chem. Phys.* **2014**, *140*, 111102.
- (560) Iwata, K.; Okajima, H.; Saha, S.; Hamaguchi, H. *Acc. Chem. Res.* **2007**, *40*, 1174.
- (561) Iwata, K.; Hamaguchi, H. *J. Phys. Chem. A* **1997**, *110*, 632.
- (562) Shigeto, S.; Hamaguchi, H. *Chem. Phys. Lett.* **2006**, *427*, 329.
- (563) Wang, Y. *J. Phys. Chem. B* **2009**, *113*, 11058–11060.
- (564) Shi, R.; Wang, Y. *J. Phys. Chem. B* **2013**, *117*, 5102.
- (565) Aparicio, S.; Atilhan, M.; Pala, N. *J. Chem. Phys.* **2013**, *139*, 224502.
- (566) Zhao, Y.; Dong, K.; Liu, X.; Zhang, S.; Zhu, J.; Wang, J. *Mol. Simul.* **2012**, *38*, 172.
- (567) English, N. J.; Mooney, D. A. *J. Phys. Chem. B* **2009**, *113*, 10128.
- (568) English, N. J.; Mooney, D. A. *Phys. Chem. Chem. Phys.* **2009**, *11*, 9370.
- (569) Sha, M.; Niu, D.; Dou, Q.; Wu, G.; Fang, H.; Hu, J. *Soft Matter* **2011**, *7*, 4228.
- (570) Xie, G.; Luo, J.; Guo, D.; Liu, S. *Appl. Phys. Lett.* **2010**, *96*, 043112.
- (571) Wein, M. *Ann. Phys.* **1928**, *85*, 795.
- (572) Hayes, R.; Borisenko, N.; Tam, M. K.; Howlett, P. C.; Endres, F.; Atkin, R. *J. Phys. Chem. C* **2011**, *115*, 6855–6863.
- (573) Atkin, R.; Borisenko, N.; Drüscher, M.; El Abedin, S. Z.; Endres, F.; Hayes, R.; Huber, B.; Roling, B. *Phys. Chem. Chem. Phys.* **2011**, *13*, 6849.

- (574) Carstens, T.; Hayes, R.; El Abedin, S. Z.; Corr, B.; Webber, G. B.; Borisenko, N.; Atkin, R.; Endres, F. *Electrochim. Acta* **2012**, *82*, 48.
- (575) Trave, A.; Tangney, P.; Scandolo, S.; Pasquarello, A.; Car, R. *Phys. Rev. Lett.* **2002**, *89*, 245504.
- (576) Funamori, N.; Tsuji, K. *Phys. Rev. Lett.* **2002**, *88*, 255508.
- (577) Zhao, Y.; Liu, X.; Lu, X.; Zhang, S.; Wang, J.; Wang, H.; Gurau, G.; Rogers, R. D.; Su, L.; Li, H. *J. Phys. Chem. B* **2012**, *116*, 10876–10884.
- (578) Takekiyo, T.; Hatano, N.; Imai, Y.; Abe, H.; Yoshimura, Y. *High Pressure Research* **2010**, *31*, 35–38.
- (579) Su, L.; Li, M.; Zhu, X.; Wang, Z.; Chen, Z.; Li, F.; Zhou, Q.; Hong, S. *J. Phys. Chem. B* **2010**, *114*, 5061–5065.
- (580) Imai, Y.; Takekiyo, T.; Abe, H.; Yoshimura, Y. *High Pressure Res.* **2010**, *31*, 53–57.
- (581) Yoshimura, Y.; Takekiyo, T.; Imai, Y.; Abe, H. *J. Phys. Chem. C* **2011**, *116*, 2097–2101.
- (582) Faria, L. F. O.; Penna, T. C.; Ribeiro, M. C. C. *J. Phys. Chem. B* **2013**, *117*, 10905–10912.
- (583) Chang, H.-C.; Hung, T.-C.; Wang, H.-S.; Chen, T.-Y. *AIP Adv.* **2013**, *3*, 032147.
- (584) Domanska, U. *Pure Appl. Chem.* **2005**, *77*, 543–557.
- (585) Pereiro, A. B.; Araujo, J. M. M.; Oliveira, F. S.; Esperanca, J. M. S.; Canongia Lopes, J. N.; Marrucho, I. M.; Rebelo, L. P. N. *J. Chem. Thermodyn.* **2012**, *55*, 29–36.
- (586) Summers, C. A.; Flowers, R. A. *Protein Sci.* **2000**, *9*, 2001–2008.
- (587) Liu, H.; Tao, G.-h.; Evans, D. G.; Kou, Y. *Carbon* **2005**, *43*, 1782–1785.
- (588) Lei, Z.; Dai, C.; Chen, B. *Chem. Rev.* **2014**, *114*, 1289–1326.
- (589) Swatoski, R. P.; Spear, S. K.; Holbrey, J. D.; Rogers, R. D. *J. Am. Chem. Soc.* **2002**, *124*, 4974–4975.
- (590) Kyllonen, L.; Parviainen, A.; Deb, S.; Lawoko, M.; Gorlov, M.; Kilpelainen, I.; King, A. W. T. *Green Chem.* **2013**, *15*, 2374–2378.
- (591) Xie, H.; Li, S.; Zhang, S. *Green Chem.* **2005**, *7*, 606–608.
- (592) Francesco, F. D.; Calisi, N.; Creatini, M.; Melai, B.; Salvo, P.; Chiappe, C. *Green Chem.* **2011**, *13*, 1712–1717.
- (593) Sharma, R.; Mahajan, R. K. *RSC Adv.* **2013**.
- (594) Chowdhury, S.; Mohan, R. S.; Scott, J. L. *Tetrahedron* **2007**, *63*, 2363–2389.
- (595) Weber, C. C.; Masters, A. F.; Maschmeyer, T. *Green Chem.* **2013**.
- (596) Acevedo, O. *J. Phys. Chem. A* **2014**, *118*, 11653.
- (597) Bernardes, C. E. S.; Minas da Piedade, M. E.; Canongia Lopes, J. N. *J. Phys. Chem. B* **2011**, *115*, 2067–2074.
- (598) Wu, Y.; Ma, X.; Li, Y.; Guan, W.; Tong, J.; Hu, N. *RSC Adv.* **2014**, *4*, 10531–10541.
- (599) Kattnig, D. R.; Hinderberger, D. *Chem.—Asian J.* **2012**, *7*, 1000–1008.
- (600) Bodo, E.; Mangialardo, S.; Capitani, F.; Gontrani, L.; Leonelli, F.; Postorino, P. *J. Chem. Phys.* **2014**, *140*, 204503.
- (601) Ramya, K. R.; Kumar, P.; Kumar, A.; Venkatnathan, A. *J. Phys. Chem. B* **2014**, *118*, 8839–8847.
- (602) Shirota, H.; Biswas, R. *J. Phys. Chem. B* **2012**, *116*, 13765–13773.
- (603) Cesare Marincola, F.; Piras, C.; Russina, O.; Gontrani, L.; Saba, G.; Lai, A. *ChemPhysChem* **2012**, *13*, 1339–1346.
- (604) Saha, S.; Hamaguchi, H. *J. Phys. Chem. B* **2006**, *110*, 2777–2781.
- (605) Zhang, L.; Xu, Z.; Wang, Y.; Li, H. *J. Phys. Chem. B* **2008**, *112*, 6411–6419.
- (606) Cha, S.; Ao, M.; Sung, W.; Moon, B.; Ahlstrom, B.; Johansson, P.; Ouchi, Y.; Kim, D. *Phys. Chem. Chem. Phys.* **2014**, *16*, 9591–9601.
- (607) Rai, G.; Kumar, A. *J. Phys. Chem. B* **2014**, *118*, 4160–4168.
- (608) Hanke, C. G.; Lynden-Bell, R. M. *J. Phys. Chem. B* **2003**, *107*, 10873–10878.
- (609) Palchowdhury, S.; Bhargava, B. L. *J. Phys. Chem. B* **2014**, *118*, 6241.
- (610) Docampo-Álvarez, B.; Gómez-González, V.; Méndez-Morales, T.; Carrete, J.; Rodriguez, J. R.; Cabeza, O.; Gallego, L. J.; Varela, L. M. *J. Chem. Phys.* **2014**, *140*, 214502.
- (611) Maiti, A.; Kumar, A.; Rogers, R. D. *Phys. Chem. Chem. Phys.* **2012**, *14*, 5139–5146.
- (612) Chaban, V. V.; Prezhdo, O. V. *J. Phys. Chem. Lett.* **2014**, *5*, 1623–1627.
- (613) Bowers, J.; Butts, C. P.; Martin, P. J.; Vergara-Gutierrez, M. C.; Heenan, R. K. *Langmuir* **2004**, *20*, 2191–2198.
- (614) Kamboj, R.; Bharmoria, P.; Chauhan, V.; Singh, S.; Kumar, A.; Mithu, V. S.; Kang, T. S. *Langmuir* **2014**, *30*, 9920–9930.
- (615) Kamboj, R.; Bharmoria, P.; Chauhan, V.; Singh, G.; Kumar, A.; Singh, S.; Kang, T. S. *Phys. Chem. Chem. Phys.* **2014**, *16*, 26040–26050.
- (616) Russina, O.; Sferrazza, A.; Caminiti, R.; Triolo, A. *J. Phys. Chem. Lett.* **2014**, *1738*–1742.
- (617) Roth, C.; Appelhagen, A.; Jobst, N.; Ludwig, R. *ChemPhysChem* **2012**, *13*, 1708–1717.
- (618) Herold, E.; Strauch, M.; Michalik, D.; Appelhagen, A.; Ludwig, R. *ChemPhysChem* **2014**, *15*, 3040–3048.
- (619) Jiang, H. J.; FitzGerald, P. A.; Dolan, A.; Atkin, R.; Warr, G. G. *J. Phys. Chem. B* **2014**, *118*, 9983–9990.
- (620) Chen, M.; Pendrill, R.; Widmalm, G.; Brady, J. W.; Wohlert, J. *J. Chem. Theory Comput.* **2014**, *10*, 4465–4479.
- (621) Murphy, T.; Hayes, R.; Imberti, S.; Warr, G. G.; Atkin, R. *Phys. Chem. Chem. Phys.* **2014**, *16*, 13182–13190.
- (622) Prabhu, S. R.; Dutt, G. B. *J. Phys. Chem. B* **2014**, *118*, 2738–2745.
- (623) Prabhu, S. R.; Dutt, G. B. *J. Phys. Chem. B* **2014**, *118*, 5562–5569.
- (624) Bardak, F.; Xiao, D.; Hines, L. G.; Son, P.; Bartsch, R. A.; Quitevis, E. L.; Yang, P.; Voth, G. A. *ChemPhysChem* **2012**, *13*, 1687–1700.
- (625) Zheng, Y.-Z.; Wang, N.-N.; Luo, J.-J.; Zhou, Y.; Yu, Z.-W. *Phys. Chem. Chem. Phys.* **2013**, *15*, 18055–18064.
- (626) Bešter-Rogač, M.; Stoppa, A.; Buchner, R. *J. Phys. Chem. B* **2014**, *118*, 1426–1435.
- (627) Stoppa, A.; Hunger, J.; Hefter, G.; Buchner, R. *J. Phys. Chem. B* **2012**, *116*, 7509–7521.
- (628) Yang, P.; Voth, G. A.; Xiao, D.; Hines, L. G.; Bartsch, R. A.; Quitevis, E. L. *J. Chem. Phys.* **2011**, *135*, 034502.
- (629) Xiao, D.; Hines, L. G.; Bartsch, R. A.; Quitevis, E. L. *J. Phys. Chem. B* **2009**, *113*, 4544–4548.
- (630) Xue, L.; Tamas, G.; Gurung, E.; Quitevis, E. L. *J. Chem. Phys.* **2014**, *140*, 164512.
- (631) Holbrey, J. D.; Reichert, W. M.; Nieuwenhuyzen, M.; Sheppard, O.; Hardacre, C.; Rogers, R. D. *Chem. Commun.* **2003**, 476–477.
- (632) Deetlefs, M.; Hardacre, C.; Nieuwenhuyzen, M.; Sheppard, O.; Soper, A. K. *J. Phys. Chem. B* **2005**, *109*, 1593–1598.
- (633) Shirota, H. *J. Phys. Chem. B* **2013**, *117*, 7985–7995.
- (634) Lynden-Bell, R. M.; Xue, L.; Tamas, G.; Quitevis, E. L. *J. Chem. Phys.* **2014**, *141*, 044506.
- (635) Wagle, D.; Kamath, G.; Baker, G. A. *J. Phys. Chem. C* **2013**, *117*, 4521–4532.
- (636) Matsugami, M.; Fujii, K.; Ueki, T.; Kitazawa, Y.; Umebayashi, Y.; Watanabe, M.; Shibayama, M. *Anal. Sci.* **2013**, *29*, 311.
- (637) Cao, Z.; Li, S.; Yan, T. *ChemPhysChem* **2012**, *13*, 1743–1747.
- (638) Yang, Y.; Yu, L. *Phys. Chem. Chem. Phys.* **2013**, *15*, 2669–2683.
- (639) Nikitina, V.; Kislenko, S. A.; Nazmutdinov, R.; Bronstein, M. D.; Tsirlina, G. A. *J. Phys. Chem. C* **2014**, *118*, 6151.
- (640) Zheng, Y.-Z.; He, H.-Y.; Zhou, Y.; Yu, Z.-W. *J. Mol. Struct.* **2014**, *1069*, 140–146.
- (641) Russina, O.; Macchiagodena, M.; Kirchner, B.; Mariani, A.; Aoun, B.; Russina, M.; Caminiti, R.; Triolo, A. *J. Non-Cryst. Solids* **2015**, *407*, 333–338.
- (642) Shen, Y.; Greaves, T. L.; Kennedy, D. F.; Weerawardena, A.; Kirby, N.; Song, G.; Drummond, C. *J. Phys. Chem. Chem. Phys.* **2014**, *16*, 21321–21329.
- (643) Maciel, C.; Fileti, E. E. *Chem. Phys. Lett.* **2013**, *568*–*569*, 75–79.
- (644) García, G.; Atilhan, M.; Aparicio, S. *J. Phys. Chem. B* **2014**, *118*, 11330–11340.
- (645) Fukushima, T.; Kosaka, A.; Ishimura, Y.; Yamamoto, T.; Takigawa, T.; Ishii, N.; Aida, T. *Science* **2003**, *300*, 2072.
- (646) Deschamps, J.; Costa Gomes, M. F.; Padua, A. A. H. *ChemPhysChem* **2004**, *5*, 1049.
- (647) Shah, J. K.; Maginn, E. J. *J. Phys. Chem. B* **2005**, *109*, 10395.

- (648) Corvo, M. C.; Sardinha, J.; Menezes, S. C.; Einloft, S.; Seferin, M.; Dupont, J.; Casimiro, T.; Cabrita, E. *J. Angew. Chem.* **2013**, *125*, 13262–13265.
- (649) Kanakybo, M.; Umecky, T.; Hiejima, Y.; Aizawa, T.; Nanjo, H.; Kameda, Y. *J. Phys. Chem. B* **2005**, *109*, 13847.
- (650) Carvalho, P. J.; Alvarez, V. H.; Schröder, B.; Gil, A. M.; Marrucho, I. M.; Aznar, M.; Santos, L. M. N. B. F.; Coutinho, J. A. P. *J. Phys. Chem. B* **2009**, *113*, 6803.
- (651) Cadena, C.; Anthony, J. L.; Shah, J. K.; Morrow, T. I.; Brennecke, J. F.; Maginn, E. *J. Am. Chem. Soc.* **2004**, *126*, 5300.
- (652) Gutowski, K. E.; Maginn, E. *J. Am. Chem. Soc.* **2008**, *130*, 14690.
- (653) Firaha, D. S.; Kirchner, B. *J. Chem. Eng. Data* **2014**, *59*, 3098–3104.
- (654) Zhang, X.; Huo, F.; Liu, Z.; Wang, W.; Shi, W.; Maginn, E. *J. Phys. Chem. B* **2009**, *113*, 7591–7598.
- (655) Huang, X.; Margulis, C. J.; Li, Y.; Berne, B. *J. Am. Chem. Soc.* **2005**, *127*, 17842.
- (656) Seki, T.; Grunwaldt, J.-D.; Baiker, A. *J. Phys. Chem. B* **2009**, *113*, 114–122.
- (657) Costa Gomes, M. F.; Pison, L.; Pensado, A. S.; Padua, A. A. H. *Faraday Discuss.* **2012**, *154*, 41–52.
- (658) Moura, L.; Mishra, M.; Bernales, V.; Fuentealba, P.; Padua, A. A. H.; Santini, C. C.; Costa Gomes, M. F. *J. Phys. Chem. B* **2013**, *117*, 7416–7425.
- (659) Chen, S.; Li, J.; Zhou, C.; Wu, J.; Tempel, D. J.; Henderson, P. B.; Brzozowski, J. R.; Cheng, H. *J. Phys. Chem. B* **2009**, *114*, 904–909.
- (660) Thomas, M.; Brehm, M.; Hollóczki, O.; Kirchner, B. *Chem.—Eur. J.* **2014**, *20*, 1622–1629.
- (661) Paluch, A. S.; Vitter, C. A.; Shah, J. K.; Maginn, E. *J. Chem. Phys.* **2012**, *137*, 184504.
- (662) Greaves, T. L.; Mudie, S. T.; Drummond, C. *Phys. Chem. Chem. Phys.* **2011**, *13*, 20441–20452.
- (663) Topolnicki, I. L.; FitzGerald, P. A.; Atkin, R.; Warr, G. G. *ChemPhysChem* **2014**, *15*, 2485–2489.
- (664) Asai, H.; Fujii, K.; Nishi, K.; Sakai, T.; Ohara, K.; Umebayashi, Y.; Shibayama, M. *Macromolecules* **2013**, *46*, 2369–2375.
- (665) Mondal, J.; Choi, E.; Yethiraj, A. *Macromolecules* **2013**, *47*, 438–446.
- (666) Choi, E.; Yethiraj, A. *J. Phys. Chem. B* **2014**, DOI: 10.1021/jp508876q.
- (667) Chang, H.-C.; Tsai, T.-T.; Kuo, M.-H. *Macromolecules* **2014**, *47*, 3052–3058.
- (668) Youngs, T. G. A.; Hardacre, C.; Holbrey, J. D. *J. Phys. Chem. B* **2007**, *111*, 13765–13774.
- (669) Youngs, T. G. A.; Holbrey, J. D.; Deetlefs, M.; Nieuwenhuyzen, M.; Gomes, M. F. C.; Hardacre, C. *ChemPhysChem* **2006**, *7*, 2279.
- (670) Youngs, T. G. A.; Holbrey, J. D.; Mullan, C. L.; Norman, S. E.; Lagunas, M. C.; D'Agostino, C.; Mantle, M. D.; Gladden, L. F.; Bowron, D. T.; Hardacre, C. *Chem. Sci.* **2011**, *2*, 1594–1605.
- (671) Jarin, Z.; Pfaendtner, J. *J. Chem. Theory Comput.* **2014**, *10*, 507–510.
- (672) Liu, H.; Sale, K. L.; Holmes, B. M.; Simmons, B. A.; Singh, S. J. *Phys. Chem. B* **2010**, *114*, 4293–4301.
- (673) Mostofian, B.; Smith, J.; Cheng, X. *Cellulose* **2014**, *21*, 983–997.
- (674) Zhao, Y.; Liu, X.; Wang, J.; Zhang, S. *ChemPhysChem* **2012**, *13*, 3126–3133.
- (675) Payal, R. S.; Balasubramanian, S. *Phys. Chem. Chem. Phys.* **2014**, *16*, 17458–17465.
- (676) Velioglu, S.; Yao, X.; Devemy, J.; Ahunbay, M. G.; Tantekin-Ersolmaz, S. B.; Dequidt, A.; Costa Gomes, M. F.; Padua, A. A. H. *J. Phys. Chem. B* **2014**, *118*, 14860–14869.
- (677) Gupta, K. M.; Hu, Z.; Jiang, J. *RSC Adv.* **2013**, *3*, 4425–4433.
- (678) Ohtaki, H.; Radnai, T. *Chem. Rev.* **1993**, *93*, 1157.
- (679) Marcus, Y. *Chem. Rev.* **2009**, *109*, 1346–1370.
- (680) Li, T.; Balbuena, P. B. *J. Electrochem. Soc.* **1999**, *146*, 3613–3622.
- (681) Seo, D. M.; Borodin, O.; Han, S.-D.; Ly, Q.; Boylec, P. D.; Henderson, W. A. *J. Electrochem. Soc.* **2012**, *159*, A553–A565.
- (682) Heintz, A.; Lehmann, J. K.; Kozlova, S. A.; Balantseva, E. V.; Bazyleva, A. B.; Ondo, D. *Fluid Phase Equilib.* **2010**, *294*, 187–196.
- (683) Miskolczy, Z.; Sebők-Nagy, K.; Biczók, L.; Göktürk, S. *Chem. Phys. Lett.* **2004**, *400*, 296–300.
- (684) Blesic, M.; Marques, M. H.; Plechko, N. V.; Seddon, K. R.; Rebelo, L. P. N.; Lopes, A. *Green Chem.* **2007**, *9*, 481–490.
- (685) Fan, X.; Zhao, K. *Soft Matter* **2014**, *10*, 3259–3270.
- (686) Chen, Z.; Greaves, T. L.; Caruso, R. A.; Drummond, C. *J. Phys. Chem. B* **2015**, *119*, 179–191.
- (687) Hargreaves, R.; Bowron, D. T.; Edler, K. *J. Am. Chem. Soc.* **2011**, *133*, 16524–16536.
- (688) Hayes, R.; Bernard, S. A.; Imberti, S.; Warr, G. G.; Atkin, R. J. *Phys. Chem. C* **2014**, *118*, 21215–21225.
- (689) Méndez-Morales, T.; Carrete, J.; Bouzón-Capelo, S.; Pérez-Rodríguez, M.; Cabeza, Ó.; Gallego, L. J.; Varela, L. M. *J. Phys. Chem. B* **2013**, *117*, 3207–3220.
- (690) Lawler, C.; Fayer, M. D. *J. Phys. Chem. B* **2013**, *117*, 9768–9774.
- (691) Niu, S.; Cao, Z.; Li, S.; Yan, T. *J. Phys. Chem. B* **2010**, *114*, 877–881.
- (692) Li, Z.; Smith, G. D.; Bedrov, D. *J. Phys. Chem. B* **2012**, *116*, 12801–12809.
- (693) Liu, H.; Maginn, E. *J. Chem. Phys.* **2013**, *139*, 114508.
- (694) Sanchez-Ramirez, N.; Martins, V. L.; Ando, R. A.; Camilo, F. F.; Urahata, S. M.; Ribeiro, M. C. C.; Torresi, R. M. *J. Phys. Chem. B* **2014**, *118*, 8772–8781.
- (695) Nicolau, B. G.; Sturlaugson, A.; Fruchey, K.; Ribeiro, M. C. C.; Fayer, M. D. *J. Phys. Chem. B* **2010**, *114*, 8350–8356.
- (696) Castiglione, F.; Famulari, A.; Raos, G.; Meille, S. V.; Mele, A.; Appeteccchi, G. B.; Passerini, S. *J. Phys. Chem. B* **2014**.
- (697) Lewandowski, A.; Świderska-Mocek, A. *J. Power Sources* **2009**, *194*, 601–609.
- (698) Monti, D.; Jónsson, E.; Palacín, M. R.; Johansson, P. *J. Power Sources* **2014**, *245*, 630–636.
- (699) Jeremias, S.; Giffin, G. A.; Moretti, A.; Jeong, S.; Passerini, S. *J. Phys. Chem. C* **2014**, *118*, 28361–28368.
- (700) Giffin, G. A.; Moretti, A.; Jeong, S.; Passerini, S. *J. Phys. Chem. C* **2014**, *118*, 9966–9973.
- (701) Binnemans, K. *Chem. Rev.* **2007**, *107*, 2592–2614.
- (702) Cocalia, V. A.; Gutowski, K. E.; Rogers, R. D. *Coord. Chem. Rev.* **2006**, *250*, 755–764.
- (703) Tietze, A. A.; Bordusa, F.; Giernoth, R.; Imhof, D.; Lenzer, T.; Maaß, A.; Mrestani-Klaus, C.; Neundorf, I.; Oum, K.; Reith, D.; Stark, A. *ChemPhysChem* **2013**, *14*, 4044–4064.
- (704) Mrestani-Klaus, C.; Richardt, A.; Wespe, C.; Stark, A.; Humpfer, E.; Bordusa, F. *ChemPhysChem* **2012**, *13*, 1836.
- (705) Podgoršek, A.; Macchiagodena, M.; Ramondo, F.; Costa Gomes, M. F.; Pádua, A. A. H. *ChemPhysChem* **2012**, *13*, 1753–1763.
- (706) Seitkalieva, M. M.; Grachev, A. A.; Egorova, K. S.; Ananikov, V. P. *Tetrahedron* **2014**, *70*, 6075–6081.
- (707) Chowdhury, R.; Mojumdar, S. S.; Chattoraj, S.; Bhattacharyya, K. *J. Chem. Phys.* **2012**, *137*, 055104.
- (708) Shao, Q. *J. Chem. Phys.* **2013**, *139*, 115102.
- (709) Haberler, M.; Schröder, C.; Steinhauser, O. *J. Chem. Theory Comput.* **2012**, *8*, 3911–3928.
- (710) Haberler, M.; Steinhauser, O. *Phys. Chem. Chem. Phys.* **2011**, *13*, 17994–18004.
- (711) Haberler, M.; Schroder, C.; Steinhauser, O. *Phys. Chem. Chem. Phys.* **2011**, *13*, 6955–6969.
- (712) Klähn, M.; Lim, G. S.; Wu, P. *Phys. Chem. Chem. Phys.* **2011**, *13*, 18647–18660.
- (713) Jaganathan, M.; Ramakrishnan, C.; Velmurugan, D.; Dhathathreyan, A. *J. Mol. Struct.* **2015**, *1081*, 334–341.
- (714) Khatun, S.; Castner, E. W. *J. Phys. Chem. B* **2014**, DOI: 10.1021/jp509861g.
- (715) D'Angelo, P.; Zitolo, A.; Ceccacci, F.; Caminiti, R.; Aquilanti, G. *J. Chem. Phys.* **2011**, *135*, 154509.
- (716) Méndez-Morales, T.; Carrete, J.; Cabeza, Ó.; Russina, O.; Triolo, A.; Gallego, L. J.; Varela, L. M. *J. Phys. Chem. B* **2014**, *118*, 761–770.

- (717) Russina, O.; Caminiti, R.; Méndez-Morales, T.; Carrete, J.; Cabeza, O.; Gallego, L. J.; Varela, L. M.; Triolo, A. *J. Mol. Liq.* **2015**, *205*, 16–21.
- (718) Mizuhata, M.; Minowa, T.; Maekawa, M.; Deki, S. *ECS Trans.* **2009**, *16*, 69–77.
- (719) Caporali, S.; Chiappe, C.; Ghilardi, T.; Pomelli, C. S.; Pinzino, C. *ChemPhysChem* **2012**, *13*, 1885–1892.
- (720) Watanabe, M.; Takemura, S.; Kawakami, S.; Syounou, E.; Kurosu, H.; Harada, M.; Iida, M. *J. Mol. Liq.* **2013**, *183*, 50–58.
- (721) Chiappe, C.; Malvaldi, M. *Phys. Chem. Chem. Phys.* **2010**, *12*, 11191–11196.
- (722) Schaltin, S.; Brooks, N. R.; Sniekers, J.; Depuydt, D.; Van Meervelt, L.; Binnemans, K.; Fransaer, J. *Phys. Chem. Chem. Phys.* **2013**, *15*, 18934–18943.
- (723) Brooks, N. R.; Schaltin, S.; Van Hecke, K.; Van Meervelt, L.; Fransaer, J.; Binnemans, K. *Dalton Trans.* **2012**, *41*, 6902–6905.
- (724) Wang, Z.; Zhang, L.; Chen, X.; Cukier, R. I.; Bu, Y. *J. Phys. Chem. B* **2009**, *113*, 8222–8226.
- (725) Wang, Z.; Zhang, L.; Cukier, R. I.; Bu, Y. *Phys. Chem. Chem. Phys.* **2010**, *12*, 1854–1861.
- (726) Margulis, C. J.; Annapureddy, H. V. R.; De Biase, P. M.; Coker, D.; Kohanoff, J.; Del Pópolo, M. G. *J. Am. Chem. Soc.* **2011**, *133*, 20186–20193.
- (727) Xu, C.; Durumeric, A.; Kashyap, H. K.; Kohanoff, J.; Margulis, C. *J. Am. Chem. Soc.* **2013**, *135*, 17528–17536.
- (728) Xu, C.; Margulis, C. *J. Phys. Chem. B* **2015**, *119*, 532–542.
- (729) Yu, L.; Clifford, J.; Pham, T. T.; Almaraz, E.; Perry, F.; Caputo, G. A.; Vaden, T. D. *J. Phys. Chem. B* **2013**, *117*, 7057–7064.
- (730) McCune, J. A.; He, P.; Petkovic, M.; Coleman, F.; Estager, J.; Holbrey, J. D.; Seddon, K. R.; Swadzba-Kwasny, M. *Phys. Chem. Chem. Phys.* **2014**, *16*, 23233–23243.
- (731) Gräsvik, J.; Hallett, J. P.; To, T. Q.; Welton, T. *Chem. Commun.* **2014**, *50*, 7258–7261.
- (732) Fruchey, K.; Fayer, M. D. *J. Phys. Chem. B* **2010**, *114*, 2840–2845.
- (733) Fruchey, K.; Lawler, C. M.; Fayer, M. D. *J. Phys. Chem. B* **2012**, *116*, 3054–3064.
- (734) Patra, S.; Samanta, A. *J. Phys. Chem. B* **2012**, *116*, 12275–12283.
- (735) Khara, D. C.; Kumar, J. P.; Mondal, N.; Samanta, A. *J. Phys. Chem. B* **2013**, *117*, 5156–5164.
- (736) Das, S.; Sahu, P.; Sarkar, M. *J. Fluoresc.* **2013**, *23*, 1217–1227.
- (737) Khara, D. C.; Samanta, A. *J. Phys. Chem. B* **2012**, *116*, 13430–13438.
- (738) Jang, H.-S.; Zhao, J.; Lei, Y.; Nieh, M.-P. *ACS Appl. Mater. Interfaces* **2014**, *6*, 14801–14811.
- (739) Chatterjee, A.; Maity, B.; Seth, D. *ChemPhysChem* **2013**, *14*, 3400–3409.
- (740) Wakasa, M.; Yago, T.; Hamasaki, A. *J. Phys. Chem. B* **2009**, *113*, 10559–10561.
- (741) Yago, T.; Wakasa, M. *J. Phys. Chem. C* **2011**, *115*, 2673–2678.
- (742) Taylor, A. W.; Puttick, S.; Licence, P. *J. Am. Chem. Soc.* **2012**, *134*, 15636–15639.
- (743) Marcus, Y. *Solvent Mixtures*; Marcel Decker: New York, 2002.
- (744) Wagle, D. V.; Zhao, H.; Baker, G. A. *Acc. Chem. Res.* **2014**, *47*, 2299–2308.
- (745) Smith, E. L.; Abbott, A. P.; Ryder, K. S. *Chem. Rev.* **2014**, *114*, 11060–11082.
- (746) Peck, R. L.; Brink, N. G.; Kuehl, F. A.; Flynn, E. H.; Walti, A.; Folkers, K. *J. Am. Chem. Soc.* **1945**, *67*, 1866–1867.
- (747) Dixit, S.; Crain, J.; Poon, W. C. K.; Finney, J. L.; Soper, A. K. *Nature* **2002**, *416*, 829–832.
- (748) Towey, J. J.; Soper, A. K.; Dougan, L. *J. Phys. Chem. B* **2011**, *115*, 7799–7807.
- (749) MacCallum, J. L.; Tieleman, D. P. *J. Am. Chem. Soc.* **2003**, *124*, 15085.
- (750) Mancinelli, R.; Bruni, F.; Ricci, M. A.; Imberti, S. *J. Chem. Phys.* **2013**, *138*, 204503.
- (751) Soper, A. K.; Luzar, A. *J. Chem. Phys.* **1992**, *97*, 1320–1331.
- (752) Xiao, D.; Rajian, J. R.; Li, S.; Bartsch, R. A.; Quitevis, E. *L. J. Phys. Chem. B* **2006**, *110*, 16174–16178.
- (753) Xiao, D.; Rajian, J. R.; Hines, L. G.; Li, S.; Bartsch, R. A.; Quitevis, E. *L. J. Phys. Chem. B* **2008**, *112*, 13316–13325.
- (754) Stoppa, A.; Buchner, R.; Hefter, G. *J. Mol. Liq.* **2010**, *153*, 46–51.
- (755) Canongia Lopes, J. N.; Cordeiro, T. C.; Esperança, J. M. S. S.; Guedes, H. J. R.; Huq, S.; Rebelo, L. P. N.; Seddon, K. R. *J. Phys. Chem. B* **2005**, *109*, 3519–3525.
- (756) Navia, P.; Troncoso, J.; Romaní, L. *J. Chem. Eng. Data* **2007**, *52*, 1369–1374.
- (757) Annat, G.; MacFarlane, D. R.; Forsyth, M. *J. Phys. Chem. B* **2007**, *111*, 9018–9024.
- (758) Annat, G.; Forsyth, M.; MacFarlane, D. R. *J. Phys. Chem. B* **2012**, *116*, 8251–8258.
- (759) Omar, S.; Lemus, J.; Ruiz, E.; Ferro, V. R.; Ortega, J.; Palomar, J. *J. Phys. Chem. B* **2014**, *118*, 2442–2450.
- (760) Navia, P.; Troncoso, J.; Romaní, L. *J. Solution Chem.* **2008**, *37*, 677–688.
- (761) Thomaier, S.; Kunz, W. *J. Mol. Liq.* **2007**, *130*, 104–107.
- (762) Li, N.; Zhang, S.; Zheng, L.; Dong, B.; Li, X.; Yu, L. *Phys. Chem. Chem. Phys.* **2008**, *10*, 4375–4377.
- (763) Zech, O.; Thomaier, S.; Bauduin, P.; Rück, T.; Touraud, D.; Kunz, W. *J. Phys. Chem. B* **2008**, *113*, 465–473.
- (764) Brussel, M.; Brehm, M.; Voigt, T.; Kirchner, B. *Phys. Chem. Chem. Phys.* **2011**, *13*, 13617–13620.
- (765) Brussel, M.; Brehm, M.; Pensado, A. S.; Malberg, F.; Ramzan, M.; Stark, A.; Kirchner, B. *Phys. Chem. Chem. Phys.* **2012**, *14*, 13204–13215.
- (766) Payal, R. S.; Balasubramanian, S. *Phys. Chem. Chem. Phys.* **2013**, *15*, 21077–21083.
- (767) Shimizu, K.; Tariq, M.; Rebelo, L. P. N.; Canongia Lopes, J. N. *J. Mol. Liq.* **2010**, *153*, 52–56.
- (768) Aparicio, S.; Atilhan, M. *J. Phys. Chem. B* **2012**, *116*, 2526–2537.
- (769) Castejón, H. J.; Lashock, R. J. *J. Mol. Liq.* **2012**, *167*, 1–4.
- (770) Andanson, J.-M.; Beier, M. J.; Baiker, A. *J. Phys. Chem. Lett.* **2011**, *2*, 2959–2964.
- (771) Fumino, K.; Bonsa, A.-M.; Golub, B.; Paschek, D.; Ludwig, R. *ChemPhysChem* **2015**, *16*, 299–304.
- (772) D'Anna, F.; Marullo, S.; Vitale, P.; Noto, R. *ChemPhysChem* **2012**, *13*, 1877–1884.
- (773) Castiglione, F.; Raos, G.; Battista Appetecchi, G.; Montanino, M.; Passerini, S.; Moreno, M.; Famulari, A.; Mele, A. *Phys. Chem. Chem. Phys.* **2010**, *12*, 1784–1792.
- (774) Villar-Garcia, I. J.; Lovelock, K. R. J.; Men, S.; Licence, P. *Chem. Sci.* **2014**, *5*, 2573–2579.
- (775) Chen, S.-H.; Huang, J.; Tartaglia, P.; Kahlweit, M. *Structure and Dynamics of Strongly Interacting Colloids and Supramolecular Aggregates in Solution*; Springer: Netherlands, 1992; Vol. 369.
- (776) Schubert, K.-V.; Streiter, R.; Kline, S. R.; Kaler, E. W. *J. Chem. Phys.* **1994**, *101*, 5343.
- (777) Turton, D. A.; Hunger, J.; Stoppa, A.; Hefter, G.; Thoman, A.; Walther, M.; Buchner, R.; Wynne, K. *J. Am. Chem. Soc.* **2009**, *131*, 11140.
- (778) Hunger, J.; Stoppa, A.; Schrodle, S.; Hefter, G.; Buchner, R. *ChemPhysChem* **2009**, *10*, 723.
- (779) Fruchey, K.; Fayer, M. D. *J. Phys. Chem. B* **2010**, *114*, 2840.
- (780) Mamontov, E.; Luo, H.; Dai, S. *J. Phys. Chem. B* **2008**, *113*, 159–169.
- (781) Triolo, A.; Russina, O.; Arrighi, V.; Juranyi, F.; Janssen, S.; Gordon, C. M. *J. Chem. Phys.* **2003**, *119*, 8549.
- (782) Triolo, A.; Russina, O.; Hardacre, C.; Nieuwenhuyzen, M.; Gonzalez, M. A.; Grimm, H. *J. Phys. Chem. B* **2005**, *109*, 22061.
- (783) Zheng, Z.-P.; Fan, W.-H.; Roy, S.; Mazur, K.; Nazet, A.; Buchner, R.; Bonn, M.; Hunger, J. *Angew. Chem., Int. Ed.* **2014**, *S4*, 687.
- (784) Puertas, A. M.; Fuchs, M.; Cates, M. *J. Chem. Phys.* **2004**, *121*, 2813.
- (785) Cates, M.; Fuchs, M.; Kroy, K.; Poon, W. C. K.; Puertas, A. M. *J. Phys.: Condens. Matter* **2004**, *16*, S4861.

- (786) Pham, K. N.; Puertas, A. M.; Bergenholz, J.; Egelhaaf, S. U.; Moussaid, A.; Pusey, P. N.; Schofeild, A. B.; Cates, M.; Fuchs, M.; Poon, W. C. K. *Science* **2002**, *296*, 104.
- (787) Hu, Z.; Margulis, C. *J. Acc. Chem. Res.* **2007**, *40*, 1097.
- (788) Sciortino, F.; Geiger, A.; Stanley, H. E. *J. Chem. Phys.* **1992**, *96*, 3857.
- (789) Giovanbattista, N.; Mazza, M. G.; Buldyrev, S. V.; Starr, F. W.; Stanley, H. E. *J. Phys. Chem. B* **2004**, *108*, 6655.
- (790) Ohmine, I.; Tanaka, H. *Chem. Rev.* **1993**, *93*, 1157–1204.
- (791) Wang, B.; Kuo, J.; Bae, S. C.; Granick, S. *Nat. Mater.* **2012**, *11*, 481–485.
- (792) Giraud, G.; Gordon, C. M.; Dunkin, I. R.; Wynne, K. *J. Chem. Phys.* **2003**, *393*, 372.
- (793) Chiappe, C. *Monatsh. Chem.* **2007**, *138*, 1035.
- (794) Xiao, D.; Rajian, D. R.; Li, S.; Bartsch, R. A.; Quitevis, E. L. *J. Phys. Chem. B* **2006**, *110*, 16174.
- (795) Xiao, D.; Rajian, J. R.; Cady, A.; Li, S.; Bartsch, R. A.; Quitevis, E. L. *J. Phys. Chem. B* **2007**, *111*, 4669–4677.
- (796) Hoarfrost, M. L.; Tyagi, M.; Segalman, R. A.; Reimer, J. A. *J. Phys. Chem. B* **2012**, *116*, 8201–8209.
- (797) Triolo, A.; Mandanici, A.; Russina, O.; Rodriguez-Mora, V.; Cutroni, M.; Hardacre, C.; Nieuwenhuyzen, M.; Bleif, H.-J.; Keller, L.; Ramos, M. A. *J. Phys. Chem. B* **2006**, *110*, 21357–21364.
- (798) Nelson, A.; Hayes, R.; Tyagi, M.; Mamontov, E.; Diallo, S.; Atkin, R.; Warr, G. G.; Peterson, V. K., in prep.
- (799) Burankova, T.; Hempelmann, R.; Wildes, A.; Embs, J. P. *J. Phys. Chem. B* **2014**, *118*, 14452–14460.
- (800) Burrell, G. L.; Burgar, I. M.; Gong, Q.; Dunlop, N. F.; Separovic, F. *J. Phys. Chem. B* **2010**, *114*, 11436–11443.
- (801) Daschakraborty, S.; Biswas, R. *Chem. Phys. Lett.* **2012**, *545*, 54–59.
- (802) Krüger, M.; Huang, M.-M.; Bründermann, E.; Weingärtner, H.; Havenith, M. *IEEE Trans. Tetra. Sci. Technol.* **2011**, *1*, 313.
- (803) Bhargava, B. L.; Balasubramanian, S. *J. Chem. Phys.* **2005**, *123*, 144505.
- (804) Downard, A.; Earle, M. J.; Hardacre, C.; McMath, S. E. J.; Nieuwenhuyzen, M.; Teat, S. J. *Chem. Mater.* **2003**, *16*, 43–48.
- (805) Kirchner, B.; Seitsonen, A. P. *Inorg. Chem.* **2007**, *46*, 2751–2754.
- (806) Macchiagodena, M.; Ramondo, F.; Triolo, A.; Gontrani, L.; Caminiti, R. *J. Phys. Chem. B* **2012**, *116*, 13448–13458.
- (807) Russina, O.; Gontrani, L.; Fazio, B.; Lombardo, D.; Triolo, A.; Caminiti, R. *Chem. Phys. Lett.* **2010**, *493*, 259–262.
- (808) Takahashi, S.; Suzuya, K.; Kohara, S.; Koura, N.; Curtiss, L. A.; Saboungi, M. L. *Z. Phys. Chem.* **1999**, 209.
- (809) Bhargava, B. L.; Balasubramanian, S. *J. Chem. Phys.* **2007**, *127*, 114510.
- (810) Szefczyk, B.; Sokalski, W. A. *J. Phys. Chem. B* **2014**, *118*, 2147–2156.
- (811) Macchiagodena, M.; Gontrani, L.; Ramondo, F.; Triolo, A.; Caminiti, R. *J. Chem. Phys.* **2011**, *134*, 114521.
- (812) Kowsari, M. H.; Alavi, S.; Ashrafizaadeh, M.; Najafi, B. *J. Chem. Phys.* **2008**, *129*, 224508.
- (813) Kowsari, M. H.; Alavi, S.; Ashrafizaadeh, M.; Najafi, B. *J. Chem. Phys.* **2009**, *130*, 014703.
- (814) Russina, O.; Fazio, B.; Schmidt, C.; Triolo, A. *Phys. Chem. Chem. Phys.* **2011**, *13*, 12067–12074.
- (815) Kofu, M.; Nagao, M.; Ueki, T.; Kitazawa, Y.; Nakamura, Y.; Sawamura, S.; Watanabe, M.; Yamamoto, O. *J. Phys. Chem. B* **2013**, *117*, 2773–2781.
- (816) Kanzaki, R.; Mitsugi, T.; Fukuda, S.; Fujii, K.; Takeuchi, M.; Soejima, Y.; Takamuku, T.; Yamaguchi, T.; Umebayashi, Y.; Ishiguro, S.-i. *J. Mol. Liq.* **2009**, *147*, 77–82.
- (817) Resende Prado, C. E.; Gomide Freitas, L. C. *J. Mol. Struct. (THEOCHEM)* **2007**, *847*, 93–100.
- (818) Moreno, M.; Castiglione, F.; Mele, A.; Pasqui, C.; Raos, G. *J. Phys. Chem. B* **2008**, *112*, 7826–7836.
- (819) Yan, T.; Burnham, C. J.; Del Pópolo, M. G.; Voth, G. A. *J. Phys. Chem. B* **2004**, *108*, 11877–11881.
- (820) Del Pópolo, M. G.; Voth, G. A. *J. Phys. Chem. B* **2004**, *108*, 1744–1752.
- (821) Ji, Y.; Shi, R.; Wang, Y.; Saielli, G. *J. Phys. Chem. B* **2013**, *117*, 1104–1109.
- (822) Bowron, D. T.; D'Agostino, C.; Gladden, L. F.; Hardacre, C.; Holbrey, J. D.; Lagunas, M. C.; McGregor, J.; Mantle, M. D.; Mullan, C. L.; Youngs, T. G. *A. J. Phys. Chem. B* **2010**, *114*, 7760–7768.
- (823) Ding, Z.-D.; Chi, Z.; Gu, W.-X.; Gu, S.-M.; Wang, H.-J. *J. Mol. Struct.* **2012**, *1015*, 147–155.
- (824) Tsuzuki, S.; Katoh, R.; Mikami, M. *Mol. Phys.* **2008**, *106*, 1621–1629.
- (825) Hunt, P. A.; Gould, I. R. *J. Phys. Chem. A* **2006**, *110*, 2269–2282.
- (826) Kuang, Q.; Zhang, J.; Wang, Z. *J. Phys. Chem. B* **2007**, *111*, 9858.
- (827) Shukla, M.; Srivastava, N.; Saha, S. *J. Mol. Struct.* **2010**, *975*, 349–356.
- (828) Aoun, B.; Goldbach, A.; Gonzalez, M. A.; Kohara, S.; Price, D. L.; Saboungi, M.-L. *J. Chem. Phys.* **2011**, *134*, 104509.
- (829) Aoun, B.; Goldbach, A.; Kohara, S.; Wax, J.-F. o.; González, M. A.; Saboungi, M.-L. *J. Phys. Chem. B* **2010**, *114*, 12623–12628.
- (830) D'Angelo, P.; Zitolo, A.; Migliorati, V.; Bodo, E.; Aquilanti, G.; Hazemann, J. L.; Testemale, D.; Mancini, G.; Caminiti, R. *J. Chem. Phys.* **2011**, *135*, 074505.
- (831) Zitolo, A.; Migliorati, V.; Aquilanti, G.; D'Angelo, P. *Chem. Phys. Lett.* **2014**, *591*, 32–36.
- (832) Katayanagi, H.; Hayashi, S.; Hamaguchi, H.-o.; Nishikawa, K. *Chem. Phys. Lett.* **2004**, *392*, 460–464.
- (833) Fujii, K.; Seki, S.; Fukuda, S.; Kanzaki, R.; Takamuku, T.; Umebayashi, Y.; Ishiguro, S.-i. *J. Phys. Chem. B* **2007**, *111*, 12829–12833.
- (834) Fujii, K.; Soejima, Y.; Kyoshioin, Y.; Fukuda, S.; Kanzaki, R.; Umebayashi, Y.; Yamaguchi, T.; Ishiguro, S.-i.; Takamuku, T. *J. Phys. Chem. B* **2008**, *112*, 4329–4336.
- (835) Fujii, K.; Seki, S.; Ohara, K.; Kameda, Y.; Doi, H.; Saito, S.; Umebayashi, Y. *J. Solution Chem.* **2014**, *43*, 1655–1668.
- (836) Russina, O.; Beiner, M.; Pappas, C.; Russina, M.; Arrighi, V.; Unruh, T.; Mullan, C. L.; Hardacre, C.; Triolo, A. *J. Phys. Chem. B* **2009**, *113*, 8469–8474.
- (837) Pensado, A. S.; Pádua, A. A. H. *Angew. Chem., Int. Ed.* **2011**, *50*, 8683–8687.
- (838) Schwenzer, B.; Kerisit, S. N.; Vijayakumar, M. *RSC Adv.* **2014**, *4*, 5457–5464.
- (839) Kiefer, J.; Pye, C. C. *J. Phys. Chem. A* **2010**, *114*, 6713–6720.
- (840) Lü, R.; Qu, Z.; Yu, H.; Wang, F.; Wang, S. *Comput. Theor. Chem.* **2012**, *988*, 86–91.
- (841) Fujii, K.; Mitsugi, T.; Takamuku, T.; Yamaguchi, T.; Umebayashi, Y.; Ishiguro, S. *Chem. Lett.* **2009**, *38*, 340–341.
- (842) Bodo, E.; Postorino, P.; Mangialardo, S.; Piacente, G.; Ramondo, F.; Bosi, F.; Ballirano, P.; Caminiti, R. *J. Phys. Chem. B* **2011**, *115*, 13149–13161.
- (843) Mylrajan, M.; Srinivasan, T. K. K.; Sreenivasamurthy, G. *J. Crystallogr. Spectrosc. Res.* **1985**, *15*, 493–500.
- (844) Zahn, S.; Wendler, K.; Delle Site, L.; Kirchner, B. *Phys. Chem. Chem. Phys.* **2011**, *13*, 15083–15093.
- (845) Song, X.; Hamano, H.; Minofar, B.; Kanzaki, R.; Fujii, K.; Kameda, Y.; Kohara, S.; Watanabe, M.; Ishiguro, S.; Umebayashi, Y. *J. Phys. Chem. B* **2012**, *116*, 2801–2813.
- (846) Bodo, E.; Sferrazza, A.; Caminiti, R.; Mangialardo, S.; Postorino, P. *J. Chem. Phys.* **2013**, *139*, 144309.
- (847) Krüger, M.; Bründermann, E.; Funkner, S.; Weingärtner, H.; Havenith, M. *J. Chem. Phys.* **2010**, *132*, 101101.
- (848) Ishida, H.; Weiss, A. *Ber. Bunsen-Ges. Phys. Chem.* **1988**, *92*, 511–514.
- (849) Migliorati, V.; Ballirano, P.; Gontrani, L.; Triolo, A.; Caminiti, R. *J. Phys. Chem. A* **2011**, *115*, 4887–4899.
- (850) Campetella, M.; Gontrani, L.; Leonelli, F.; Bencivenni, L.; Caminiti, R. *ChemPhysChem* **2014**, *16*, 197.
- (851) Aparicio, S.; Atilhan, M.; Khraisheh, M.; Alcalde, R. *J. Phys. Chem. B* **2011**, *115*, 12473–12486.

- (852) Siqueira, L. J. A.; Ribeiro, M. C. C. *J. Chem. Phys.* **2011**, *135*, 204506.
- (853) Siqueira, L. J. A.; Ribeiro, M. C. C. *J. Phys. Chem. B* **2007**, *111*, 11776–11785.
- (854) Siqueira, L. J. A.; Ribeiro, M. C. C. *J. Phys. Chem. B* **2009**, *113*, 1074–1079.
- (855) Borodin, O.; Smith, G. D. *J. Phys. Chem. B* **2006**, *110*, 11481–11490.
- (856) Li, S.; Bañuelos, J. L.; Guo, J.; Anovitz, L.; Rother, G.; Shaw, R. W.; Hillesheim, P. C.; Dai, S.; Baker, G. A.; Cummings, P. T. *J. Phys. Chem. Lett.* **2011**, *3*, 125–130.
- (857) Lethesh, K. C.; Van Hecke, K.; Van Meervelt, L.; Nockemann, P.; Kirchner, B.; Zahn, S.; Parac-Vogt, T. N.; Dehaen, W.; Binnemans, K. *J. Phys. Chem. B* **2011**, *115*, 8424–8438.
- (858) Wang, Y.-L.; Shah, F. U.; Glavatskikh, S.; Antzutkin, O. N.; Laaksonen, A. *J. Phys. Chem. B* **2014**, *118*, 8711–8723.
- (859) Gontrani, L.; Russina, O.; Celso, F. L.; Caminiti, R.; Annat, G.; Triolo, A. *J. Phys. Chem. B* **2009**, *113*, 9235–9240.
- (860) Sun, H.; Qiao, B.; Zhang, D.; Liu, C. *J. Phys. Chem. A* **2010**, *114*, 3990–3996.
- (861) Cadena, C.; Maginn, E. J. *J. Phys. Chem. B* **2006**, *110*, 18026–18039.
- (862) Li, S.; Han, K. S.; Feng, G.; Hagaman, E. W.; Vlcek, L.; Cummings, P. T. *Langmuir* **2013**, *29*, 9744–9749.
- (863) Fujii, K.; Seki, S.; Fukuda, S.; Takamuku, T.; Kohara, S.; Kameda, Y.; Umebayashi, Y.; Ishiguro, S.-i. *J. Mol. Liq.* **2008**, *143*, 64–69.
- (864) Hayamizu, K.; Tsuzuki, S.; Seki, S.; Fujii, K.; Suenaga, M.; Umebayashi, Y. *J. Chem. Phys.* **2010**, *133*, 194505.
- (865) Canongia Lopes, J. N.; Shimizu, K.; Pádua, A. A. H.; Umebayashi, Y.; Fukuda, S.; Fujii, K.; Ishiguro, S.-i. *J. Phys. Chem. B* **2008**, *112*, 1465–1472.
- (866) Fujimori, T.; Fujii, K.; Kanzaki, R.; Chiba, K.; Yamamoto, H.; Umebayashi, Y.; Ishiguro, S.-i. *J. Mol. Liq.* **2007**, *131*–*132*, 216–224.
- (867) Triolo, A.; Russina, O.; Fazio, B.; Appetecchi, G. B.; Carewska, M.; Passerini, S. *J. Chem. Phys.* **2009**, *130*, 164521.
- (868) Hardacre, C.; Holbrey, J. D.; Mullan, C. L.; Nieuwenhuyzen, M.; Youngs, T. G. A.; Bowron, D. T. *J. Phys. Chem. B* **2008**, *112*, 8049–8056.
- (869) Carlson, P. J.; Bose, S.; Armstrong, D. W.; Hawkins, T.; Gordon, M. S.; Petrich, J. W. *J. Phys. Chem. B* **2011**, *116*, 503–512.
- (870) Liu, Y.; Zhang, L.; Wang, G.; Wang, L.; Gong, X. *J. Phys. Chem. C* **2012**, *116*, 16144–16153.
- (871) Daschakraborty, S.; Biswas, R. *Chem. Phys. Lett.* **2012**, *545*, 54–59.
- (872) Granick, S. *Science* **1991**, *253*, 1374–1379.
- (873) Zaera, F. *Chem. Rev.* **2012**, *112*, 2920–2986.
- (874) Bain, C. D. *J. Chem. Soc., Faraday Trans.* **1995**, *91*, 1281.
- (875) Voitchovsky, K. *Phys. Rev. E* **2013**, *88*, 022407.
- (876) Voitchovsky, K.; Kuna, J. J.; Contera, S. A.; Tosatti, E.; Stellacci, F. *Nat. Nanotechnol.* **2010**, *5*, 401–405.
- (877) Kuna, J. J.; Voitchovsky, K.; Singh, C.; Jiang, H.; Mwenifumbo, S.; Ghorai, P. K.; Stevens, M. M.; Glotzer, S. C.; Stellacci, F. *Nat. Mater.* **2009**, *8*, 837–842.
- (878) Ricci, M.; Spijker, P.; Voitchovsky, K. *Nat. Commun.* **2014**, *5*, 4400.
- (879) Contera, S. A.; Voitchovsky, K.; Ryan, J. F. *Nanoscale* **2010**, *2*, 222–229.
- (880) Heberle, J. A. *Biophys. J.* **2004**, *87*, 2105–2106.
- (881) Zhang, C.; Knyazev, D. G.; Vereshaga, Y. A.; Ippoliti, E.; Nguyen, T. H.; Carloni, P.; Pohl, P. *Proc. Natl. Acad. Sci. U.S.A.* **2012**, *109*, 9744–9749.
- (882) Davy, H. *Researches, Chemical and Philosophical*; Biggs and Cottle: Bristol, 1800.
- (883) Atkin, R.; El Abedin, S. Z.; Hayes, R.; Gasparotto, L. H. S.; Borisenko, N.; Endres, F. *J. Phys. Chem. C* **2009**, *113*, 13266.
- (884) Hayes, R.; El Abedin, S. Z.; Atkin, R. *J. Phys. Chem. B* **2009**, *113*, 7049.
- (885) Wakeham, D.; Hayes, R.; Warr, G. G.; Atkin, R. *J. Phys. Chem. B* **2009**, *113*, 5961.
- (886) Horn, R. G.; Evans, D. F.; Ninham, B. W. *J. Phys. Chem.* **1988**, *92*, 3531.
- (887) Mezger, M.; Schramm, S.; Schroder, H.; Reichart, H.; Deutsch, M.; De Souza, E. J.; Okasinski, J. S.; Ocko, B. M.; Honkimaki, V.; Dosch, H. *J. Chem. Phys.* **2009**, *131*, 094701.
- (888) Mezger, M.; Schroder, H.; Reichert, H.; Schramm, S.; Okasinski, J. S.; Schoder, S.; Honkimaki, V.; Deutsch, M.; Ocko, B. M.; Ralston, J.; Rohwerder, M.; Stratmann, M.; Dosch, H. *Science* **2008**, *322*, 424–428.
- (889) Lim, R.; O’Shea, S. *J. Phys. Rev. Lett.* **2002**, *88*, 246101–1.
- (890) Israelachvili, J. *Acc. Chem. Res.* **1987**, *20*, 415–421.
- (891) Sotnikov, A. I.; Esin, O. A. *Proc. of Third All-Soviet Conferences Khimia*; Leningrad, 1966; p 209.
- (892) Graves, A. D. *Electroanal. Chem.* **1970**, *25*, 349.
- (893) Graves, A. D. *Electroanal. Chem.* **1970**, *25*, 357.
- (894) Heyes, D. M.; Clarke, J. H. *J. Chem. Soc., Faraday Trans. 2* **1981**, *77*, 1089.
- (895) Atkin, R.; Craig, V. S. J.; Wanless, E. J.; Biggs, S. *Adv. Colloid Interface Sci.* **2003**, *103*, 219–304.
- (896) Warr, G. G. *Curr. Opin. Colloid Interface Sci.* **2000**, *5*, 88–94.
- (897) Gaines, G. L.; Tabor, D. *Nature* **1969**, *178*, 1304–1305.
- (898) Iler, R. K. *The Chemistry of Silica*; Wiley-Interscience Publishers: New York, 1979.
- (899) Elbourne, A.; Voitchovsky, K.; Warr, G.; Atkin, R. *Chem. Sci.* **2015**, *6*, 527–536.
- (900) Qi, G.; Yang, Y.; Yan, H.; Guan, L.; Li, Y.; Qiu, X.; Wang, C. *J. Phys. Chem. C* **2008**, *113*, 204–207.
- (901) Ricci, M.; Spijker, P.; Stellacci, F.; Molinari, J.-F.; Voitchovsky, K. *Langmuir* **2013**, *29*, 2207–2216.
- (902) Segura, J. J.; Elbourne, A.; Wanless, E. J.; Warr, G. G.; Voitchovsky, K.; Atkin, R. *Phys. Chem. Chem. Phys.* **2013**, *15*, 3320.
- (903) Elbourne, A.; Sweeney, J.; Webber, G. B.; Wanless, E. J.; Warr, G. G.; Rutland, M. W.; Atkin, R. *Chem. Commun.* **2013**, *49*, 6797.
- (904) Seddon, J. R. T. *J. Phys. Chem. C* **2014**, *118*, 22197–22201.
- (905) Manne, S.; Gaub, H. E. *Science* **1995**, *270*, 1480–1482.
- (906) Wanless, E. J.; Ducker, W. A. *J. Phys. Chem.* **1996**, *100*, 3207–3214.
- (907) Wanless, E. J.; Ducker, W. A. *Langmuir* **1997**, *13*, 1463.
- (908) Werzer, O.; Cranston, E. D.; Warr, G. G.; Atkin, R.; Rutland, M. W. *Phys. Chem. Chem. Phys.* **2012**, *14*, 5147–5152.
- (909) Perkin, S.; Albrecht, T.; Klein, J. *Phys. Chem. Chem. Phys.* **2010**, *12*, 1243–1247.
- (910) Perkin, S.; Crowhurst, L.; Niedermeyer, H.; Welton, T.; Smith, A. M.; Gosvami, N. *Chem. Commun.* **2011**, *47*, 6572–6574.
- (911) Smith, A. M.; Lovelock, K. R. J.; Gosvami, N.; Licence, P.; Dolan, A.; Welton, T.; Perkin, S. *J. Phys. Chem. Lett.* **2013**, *4*, 378.
- (912) Min, Y.; Akbulut, M.; Sangoro, J. R.; Kremer, F.; Prud’homme, R. K.; Israelachvili, J. *J. Phys. Chem. C* **2009**, *113*, 16445.
- (913) Israelachvili, J. N.; Kristiansen, K.; Gebbie, M.; Lee, D. W.; Donaldson, S. H.; Das, S.; Rapp, M.; Banquy, X.; Valtiner, M.; Yu, J. *J. Phys. Chem. B* **2013**, *117*, 16369–16387.
- (914) Espinosa-Marzal, R. M.; Arcifa, A.; Rossi, A.; Spencer, N. D. *J. Phys. Chem. Lett.* **2013**, *5*, 179–184.
- (915) Bou-Malham, I.; Bureau, L. *Soft Matter* **2010**, *6*, 4062.
- (916) Ueno, K.; Kasuya, M.; Watanabe, M.; Mizukami, M.; Kurihara, K. *Phys. Chem. Chem. Phys.* **2010**, *12*, 4066.
- (917) Smith, A. M.; Parkes, M. A.; Perkin, S. *J. Phys. Chem. Lett.* **2014**, *5*, 4032–4037.
- (918) Espinosa-Marzal, R. M.; Arcifa, A.; Rossi, A.; Spencer, N. D. *J. Phys. Chem. C* **2014**, *118*, 6419.
- (919) Smith, A. M.; Lovelock, K. R. J.; Gosvami, N. N.; Welton, T.; Perkin, S. *Phys. Chem. Chem. Phys.* **2013**, *15*, 15317–15320.
- (920) Atkin, R.; Warr, G. G. *J. Phys. Chem. C* **2007**, *111*, 5162–5168.
- (921) Wydro, M. J.; Warr, G. G.; Atkin, R. *Langmuir* **2015**, *31*, 5513.
- (922) Li, H.; Endres, F.; Atkin, R. *Phys. Chem. Chem. Phys.* **2013**.
- (923) Antelmi, D. A.; Kekicheff, P.; Richetti, P. *Langmuir* **1999**, *15*, 7774.
- (924) Peñalber, C. Y.; Baker, G. A.; Baldelli, S. *J. Phys. Chem. B* **2013**, *117*, 5939–5949.
- (925) Baldelli, S. *Acc. Chem. Res.* **2008**, *41*, 421.

- (926) Baldelli, S. *J. Phys. Chem. Lett.* **2012**, *4*, 244–252.
- (927) Ichii, T.; Negami, M.; Sugimura, H. *J. Phys. Chem. C* **2014**, *118*, 26803–26807.
- (928) Payal, R. S.; Balasubramanian, S. *ChemPhysChem* **2012**, *13*, 1764–1771.
- (929) Payal, R. S.; Balasubramanian, S. *ChemPhysChem* **2012**, *13*, 3085–3086.
- (930) Zhou, H.; Rouha, M.; Feng, G.; Lee, S. S.; Docherty, H.; Fentner, P.; Cummings, P. T.; Fulvio, P. F.; Dai, S.; McDonald, J.; Presser, V.; Gogotsi, Y. *ACS Nano* **2012**, *6*, 9818.
- (931) Dragoni, D.; Manini, N.; Ballone, P. *ChemPhysChem* **2012**, *13*, 1772–1780.
- (932) Sieffert, N.; Wipff, G. *J. Phys. Chem. C* **2008**, *112*, 19590–19603.
- (933) Wang, Y.-L.; Laaksonen, A. *Phys. Chem. Chem. Phys.* **2014**, *16*, 23329–23339.
- (934) Romero, C.; Baldelli, S. *J. Phys. Chem. B* **2006**, *110*, 6213–6223.
- (935) Romero, C.; MooreH, J.; Lee, T. R.; Baldelli, S. *J. Phys. Chem. C* **2007**, *111*, 240–247.
- (936) Payal, R. S.; Balasubramanian, S. *J. Phys.: Condens. Matter* **2014**, *26*, 284101.
- (937) Heinz, H.; Vaia, R. A.; Krishnamoorti, R.; Farmer, B. L. *Chem. Mater.* **2006**, *19*, 59–68.
- (938) Duarte, D.; Salanne, M.; Rotenberg, B.; Bizeto, M. A.; Siqueira, L. J. A. *J. Phys.: Condens. Matter* **2014**, *26*, 284107.
- (939) Martins, M. J. F.; Ferreira, A. R.; Konstantinova, E.; de Abreu, H. A.; Souza, W. F.; Chiaro, S. S. X.; Dias, L. G.; Leitão, A. A. *Int. J. Quantum Chem.* **2012**, *112*, 3234–3239.
- (940) Smith, J.; Webber, G. B.; Warr, G. G.; Atkin, R. *Langmuir* **2014**, *30*, 1506–1513.
- (941) Asencio, R. Á.; Cranston, E. D.; Atkin, R.; Rutland, M. W. *Langmuir* **2012**, *28*, 9967–9976.
- (942) Fitchett, B. D.; Conboy, J. C. *J. Phys. Chem. B* **2004**, *108*, 20255–20262.
- (943) Rollins, J. B.; Fitchett, B. D.; Conboy, J. C. *J. Phys. Chem. B* **2007**, *111*, 4990–4999.
- (944) Wang, P.; Zakeeruddin, S. M.; Comte, P.; Exnar, I.; Grätzel, M. J. *Am. Chem. Soc.* **2003**, *125*, 1166–1167.
- (945) Stefanopoulos, K. L.; Romanos, G. E.; Vangeli, O. C.; Mergia, K.; Kanellopoulos, N. K.; Koutsoubas, A.; Lairez, D. *Langmuir* **2011**, *27*, 7980–7985.
- (946) Göbel, R.; Hesemann, P.; Weber, J.; Möller, E.; Friedrich, A.; Beuermann, S.; Taubert, A. *Phys. Chem. Chem. Phys.* **2009**, *11*, 3653–3662.
- (947) Wu, C.-M.; Lin, S.-Y.; Kao, K.-Y.; Chen, H.-L. *J. Phys. Chem. C* **2014**, *118*, 17764–17772.
- (948) Gupta, A. K.; Verma, Y. L.; Singh, R. K.; Chandra, S. *J. Phys. Chem. C* **2013**, *118*, 1530–1539.
- (949) Verma, Y. L.; Singh, R. K.; Oh, I.-K.; Chandra, S. *RSC Adv.* **2014**, *4*, 39978–39983.
- (950) Gupta, A. K.; Singh, R. K.; Chandra, S. *RSC Adv.* **2014**, *4*, 22277–22287.
- (951) Singh, M. P.; Singh, R. K.; Chandra, S. *J. Phys. Chem. B* **2011**, *115*, 7505–7514.
- (952) Ichii, T.; Negami, M.; Fujimura, M.; Murase, K.; Sugimura, H. *Electrochemistry* **2014**, *82*, 380–384.
- (953) Shimizu, K.; Pensado, A.; Malfreyt, P.; Padua, A. A. H.; Canongia Lopes, J. N. *Faraday Discuss.* **2012**, *154*, 155–169.
- (954) Tuteja, A.; Choi, W.; Mabry, J. M.; McKinley, G. H.; Cohen, R. E. *Proc. Natl. Acad. Sci. U.S.A.* **2008**, *105*, 18200–18205.
- (955) Lu, J.; Yang, J.-x.; Wang, J.; Lim, A.; Wang, S.; Loh, K. P. *ACS Nano* **2009**, *3*, 2367–2375.
- (956) Chaban, V. V.; Maciel, C.; Fileti, E. E. *J. Solution Chem.* **2014**, *43*, 1019.
- (957) Balducci, A.; Dugas, R.; Taberna, P. L.; Simon, P.; Plee, D.; Mastragostino, M.; Passerini, S. *J. Power Sources* **2007**, *165*, 922.
- (958) Chmiola, J.; Yushin, G.; Gogotsi, Y.; Portet, C.; Simon, P.; Taberna, P. L. *Science* **2006**, *313*, 1760–1763.
- (959) Atkin, R.; Warr, G. G. *J. Am. Chem. Soc.* **2005**, *127*, 11940–11941.
- (960) Luque, N. B.; Schmickler, W. *Electrochim. Acta* **2012**, *71*, 82–85.
- (961) Aparicio, S.; Atilhan, M. *J. Phys. Chem. C* **2012**, *116*, 12055–12065.
- (962) Maolin, S.; Fuchun, Z.; Guozhong, W.; Haiping, F.; Chunlei, W.; Shimou, C.; Yi, Z.; Jun, H. *J. Chem. Phys.* **2008**, *128*, 134504.
- (963) Merlet, C.; Rotenberg, B.; Madden, P. A.; Taberna, P.-L.; Simon, P.; Gogotsi, Y.; Salanne, M. *Nat. Mater.* **2012**, *11*, 306–310.
- (964) Sha, M.; Wu, G.; Fang, H.; Zhu, G.; Liu, Y. *J. Phys. Chem. C* **2008**, *112*, 18584–18587.
- (965) Sha, M.; Wu, G.; Liu, Y.; Tang, Z.; Fang, H. *J. Phys. Chem. C* **2009**, *113*, 4618–4622.
- (966) Carstens, T.; Gustus, R.; Höft, O.; Borisenko, N.; Endres, F.; Li, H.; Wood, R. J.; Page, A. J.; Atkin, R. *J. Phys. Chem. C* **2014**, *118*, 10833.
- (967) Merlet, C.; Salanne, M.; Rotenberg, B.; Madden, P. A. *J. Phys. Chem. C* **2011**, *115*, 16613.
- (968) Page, A. J.; Elbourne, A.; Stefanovic, R.; Addicoat, M. A.; Warr, G. G.; Voitchovsky, K.; Atkin, R. *Nanoscale* **2014**, *6*, 8100.
- (969) Vatamanu, J.; Borodin, O.; Smith, G. D. *J. Am. Chem. Soc.* **2010**, *132*, 14825–14833.
- (970) Merlet, C.; Pean, C.; Rotenberg, B.; Madden, P. A.; Simon, P.; Salanne, M. *J. Phys. Chem. Lett.* **2013**, *4*, 264–268.
- (971) Merlet, C.; Salanne, M.; Rotenberg, B.; Madden, P. A. *Electrochim. Acta* **2013**, *101*, 262–271.
- (972) Merlet, C.; Limmer, D. T.; Salanne, M.; Van Roij, R.; Madden, P. A.; Chandler, D.; Rotenberg, B. *J. Phys. Chem. C* **2014**, *118*, 18291.
- (973) Dou, Q.; Sha, M.; Fu, H.; Wu, G. *ChemPhysChem* **2010**, *11*, 2438–2443.
- (974) Dou, Q.; Sha, M. L.; Fu, H. Y.; Wu, G. *Z. J. Phys.: Condens. Matter* **2011**, *23*, 175001.
- (975) Hu, Z.; Vatamanu, J.; Borodin, O.; Bedrov, D. *Phys. Chem. Chem. Phys.* **2013**, *15*, 14234–14247.
- (976) Kornyshev, A. A.; Luque, N. B.; Schmickler, W. *J. Solid State Electrochem.* **2013**, *1*, 1–5.
- (977) Van Aken, K. L.; McDonough, J. K.; Li, S.; Feng, G.; Chathoth, S. M.; Mamontov, E.; Fulvio, P. F.; Cummings, P. T.; Dai, S.; Gogotsi, Y. J. *Phys.: Condens. Matter* **2014**, *26*, 284104.
- (978) Vatamanu, J.; Borodin, O.; Smith, G. D. *J. Phys. Chem. B* **2011**, *115*, 3073–3084.
- (979) Vatamanu, J.; Cao, L.; Borodin, O.; Bedrov, D.; Smith, G. D. *J. Phys. Chem. Lett.* **2011**, *2*, 2267–2272.
- (980) Liu, X.; Han, Y.; Yan, T. *ChemPhysChem* **2014**, *15*, 2503–2509.
- (981) Pensado, A. S.; Malberg, F.; Gomes, M. F. C.; Padua, A. A. H.; Fernandez, J.; Kirchner, B. *RSC Adv.* **2014**, *4*, 18017–18024.
- (982) Fedorov, M. V.; Lynden-Bell, R. M. *Phys. Chem. Chem. Phys.* **2012**, *14*, 2552.
- (983) Aparicio, S.; Atilhan, M. *J. Phys. Chem. C* **2013**, *117*, 22046–22059.
- (984) Ivaniščev, V.; Fedorov, M. V.; Lynden-Bell, R. M. *J. Phys. Chem. C* **2014**, *118*, 5841.
- (985) Ivaniščev, V.; Fedorov, M. V.; Lynden-Bell, R. M. *J. Phys. Chem. C* **2014**, *118*, 5841–5847.
- (986) Li, S.; Feng, G.; Cummings, P. T. *J. Phys.: Condens. Matter* **2014**, *26*, 284106.
- (987) Uysal, A.; Zhou, H.; Feng, G.; Lee, S. S.; Li, S.; Fenter, P.; Cummings, P. T.; Fulvio, P. F.; Dai, S.; McDonough, J. K.; Gogotsi, Y. J. *Phys. Chem. C* **2013**, *118*, 569–574.
- (988) Ghatee, M. H.; Moosavi, F. *J. Phys. Chem. C* **2011**, *115*, 5626–5636.
- (989) Pensado, A.; Malberg, F.; Costa Gomes, M. F.; Padua, A. A. H.; Fernandes, J.; Kirchner, B. *RSC Adv.* **2014**, *14*, 18017.
- (990) Wang, Y.-L.; Laaksonen, A.; Lu, Z.-Y. *Phys. Chem. Chem. Phys.* **2013**, *15*, 13559–13569.
- (991) Mendez-Morales, T.; Carrete, J.; Perez-Rodriguez, M.; Cabeza, O.; Gallego, L. J.; Lynden-Bell, R. M.; Varela, L. M. *Phys. Chem. Chem. Phys.* **2014**, *16*, 13271–13278.
- (992) Wang, Y.-L.; Lu, Z.-Y.; Laaksonen, A. *Phys. Chem. Chem. Phys.* **2014**, *16*, 20731–20740.
- (993) Mendonça, A. C. F.; Fomin, Y. D.; Malfreyt, P.; Padua, A. A. H. *Soft Matter* **2013**, *9*, 10606–10616.

- (994) Shim, Y.; Kim, H. J. *ACS Nano* **2009**, *3*, 1693.
- (995) Dong, K.; Zhou, G.; Liu, X.; Yao, X.; Zhang, S.; Lyubartsev, A. J. *Phys. Chem. C* **2009**, *113*, 10013–10020.
- (996) Singh, R.; Monk, J.; Hung, F. R. *J. Phys. Chem. C* **2010**, *114*, 15478–15485.
- (997) Monk, J.; Singh, R.; Hung, F. R. *J. Phys. Chem. C* **2011**, *115*, 3034–3042.
- (998) Rajput, N. N.; Monk, J.; Singh, R.; Hung, F. R. *J. Phys. Chem. C* **2012**, *116*, 5169–5181.
- (999) Singh, R.; Monk, J.; Hung, F. R. *J. Phys. Chem. C* **2011**, *115*, 16544–16554.
- (1000) Dou, Q.; Sha, M.; Fu, H.; Wu, G. *J. Phys. Chem. C* **2011**, *115*, 18946–18951.
- (1001) Rajput, N. N.; Monk, J.; Hung, F. R. *J. Phys. Chem. C* **2014**, *118*, 1540–1553.
- (1002) Bañuelos, J. L.; Feng, G.; Fulvio, P. F.; Li, S.; Rother, G.; Dai, S.; Cummings, P. T.; Wesolowski, D. J. *Chem. Mater.* **2013**, *26*, 1144–1153.
- (1003) Zhao, C.; Ren, B.; Song, Y.; Zhang, J.; Wei, L.; Chen, S.; Zhang, S. *RSC Adv.* **2014**, *4*, 16267–16273.
- (1004) Christenson, H. K. *J. Phys.: Condens. Matter* **2001**, *13*, R95.
- (1005) Weingarth, D.; Drummond, R.; Foelske-Schmitz, A.; Kotz, R.; Presser, V. *Phys. Chem. Chem. Phys.* **2014**, *16*, 21219–21224.
- (1006) Yokota, Y.; Hara, H.; Harada, T.; Imanishi, A.; Uemura, T.; Takeya, J.; Fukui, K. *Chem. Commun.* **2013**, *49*, 10596.
- (1007) Yokota, Y.; Hara, H.; Morino, Y.; Bando, K.; Imanishi, A.; Uemura, T.; Takeya, J.; Fukui, K. *Appl. Phys. Lett.* **2014**, *104*, 263102.
- (1008) Shakourian-Fard, M.; Kamath, G.; Jamshidi, Z. *J. Phys. Chem. C* **2014**, *118*, 26003–26016.
- (1009) Black, J. M.; Walters, D.; Labuda, A.; Feng, G.; Hillesheim, P. C.; Dai, S.; Cummings, P. T.; Kalinin, S. V.; Proksch, R.; Balke, N. *Nano Lett.* **2013**, *13*, 5954–5960.
- (1010) Li, H.; Wood, R. J.; Rutland, M. W.; Atkin, R. *Chem. Commun.* **2014**, *50*, 4368–4370.
- (1011) Li, H.; Wood, R. J.; Endres, F.; Atkin, R. *J. Phys.: Condens. Matter* **2014**, *26*, 284115.
- (1012) Lee, S. H.; Rossky, P. J. *J. Chem. Phys.* **1994**, *100*, 3334.
- (1013) Hogshead, C. G.; Manias, E.; Williams, P.; Lupinsky, A.; Painter, P. *Energy Fuels* **2010**, *25*, 293–299.
- (1014) Borisenko, N.; El Abedin, S. Z.; Endres, F. *J. Phys. Chem. B* **2006**, *110*, 6250–6256.
- (1015) Carstens, T.; El Abedin, S. Z.; Endres, F. *ChemPhysChem* **2008**, *9*, 439.
- (1016) Gasparotto, L. H. S.; Borisenko, N.; Bocchi, N.; Zein El Abedin, S.; Endres, F. *Phys. Chem. Chem. Phys.* **2009**, *11*, 11140–11145.
- (1017) Waldmann, T.; Huang, H.-H.; Hoster, H. E.; Höft, O.; Endres, F.; Behm, R. J. *ChemPhysChem* **2011**, *12*, 2565–2567.
- (1018) Su, Y.-Z.; Yan, J.-W.; Li, M.-G.; Xie, Z.-X.; Mao, B.-W.; Tian, Z.-Q. *Z. Phys. Chem.* **2012**, *226*, 979–994.
- (1019) Pan, G.-B.; Freyland, W. *Chem. Phys. Lett.* **2006**, *427*, 96–100.
- (1020) Gnahn, M.; Pajkossy, T.; Kolb, D. M. *Electrochim. Acta* **2010**, *55*, 6212–6217.
- (1021) Lin, L. G.; Wang, J. W.; Yuan, Y. Z.; Xiang, J.; Mao, B.-W. *Electrochim. Commun.* **2009**, *5*, 995.
- (1022) Gnahn, M.; Berger, C.; Arkhipova, M.; Kunkel, H.; Pajkossy, T.; Maas, G.; Kolb, D. M. *Phys. Chem. Chem. Phys.* **2012**, *14*, 10647–10652.
- (1023) Uhl, B.; Buchner, F.; Alwast, D.; Wagner, N.; Behm, R. J. r. *Beilstein J. Nanotechnol.* **2013**, *4*, 903–918.
- (1024) Uhl, B.; Buchner, F.; Alwast, D.; Wagner, N.; Behm, R. J. r. *Beilstein J. Nanotechnol.* **2013**, *4*, 903–918.
- (1025) Su, Y.; Yan, J.; Li, M.; Zhang, M.; Mao, B. J. *Phys. Chem. C* **2012**, *117*, 205–212.
- (1026) Su, Y.-Z.; Fu, Y.-C.; Yan, J.-W.; Chen, Z.-B.; Mao, B.-W. *Angew. Chem.* **2009**, *121*, 5250–5253.
- (1027) Buchner, F.; Forster-Tonigold, K.; Uhl, B.; Alwast, D.; Wagner, N.; Farkhondeh, H.; Groß, A.; Behm, R. J. *ACS Nano* **2013**.
- (1028) Uhl, B.; Buchner, F.; Gabler, S.; Bozorgchenani, M.; Jurgen Behm, R. *Chem. Commun.* **2014**, *50*, 8601–8604.
- (1029) Tamura, K.; Miyaguchi, S.-i.; Sakaue, K.; Nishihata, Y.; Mizuki, J. i. *Electrochim. Commun.* **2011**, *13*, 411–413.
- (1030) Chen, C. J. *Introduction to Scanning Tunneling Microscopy*; Oxford University Press: New York, 1993.
- (1031) Zobel, M.; Neder, R. B.; Kimber, S. A. J. *Science* **2015**, *347*, 292–294.
- (1032) Binetti, E.; Panniello, A.; Tommasi, R.; Agostiano, A.; Fantini, S.; Curri, M. L.; Striccoli, M. *J. Phys. Chem. C* **2013**, *117*, 12923–12929.
- (1033) Andanson, J.-M.; Baiker, A. *J. Phys. Chem. C* **2013**, *117*, 12210–12217.
- (1034) Podgoršek, A.; Pensado, A. S.; Santini, C. C.; Costa Gomes, M. F.; Pádua, A. A. H. *J. Phys. Chem. C* **2013**, *117*, 3537–3547.
- (1035) Tariq, M.; Serro, A. P.; Colaço, R.; Saramago, B.; Lopes, J. N. C.; Rebelo, L. P. N. *Colloids Surf., A* **2011**, *377*, 361–366.
- (1036) Labuda, A.; Grütter, P. *Langmuir* **2012**, *28*, 5319–5322.
- (1037) Manini, N.; Cesaratto, M.; Del Pópolo, M. G.; Ballone, P. J. *Phys. Chem. B* **2009**, *113*, 15602–15609.
- (1038) Aliaga, C.; Baldelli, S. *J. Phys. Chem. C* **2008**, *112*, 3064–3072.
- (1039) Olszewski, M.; Gustus, R.; Marszewski, M.; Hofft, O.; Endres, F. *Phys. Chem. Chem. Phys.* **2014**.
- (1040) Neouze, M.-A.; Litschauer, M. *J. Phys. Chem. B* **2008**, *112*, 16721–16725.
- (1041) Tamam, L.; Ocko, B. M.; Reichert, H.; Deutsch, M. *Phys. Rev. Lett.* **2011**, *106*, 197801.
- (1042) Alam, M. T.; Islam, M. M.; Okajima, T.; Ohsaka, T. *J. Phys. Chem. C* **2008**, *112*, 2601–2606.
- (1043) Alam, M. T.; Islam, M. M.; Okajima, T.; Ohsaka, T. *J. Phys. Chem. C* **2007**, *111*, 18326–18333.
- (1044) Costa, R.; Pereira, C. M.; Silva, F. *RSC Adv.* **2013**, *3*, 11697–11706.
- (1045) Muller, E. A.; Strader, M. L.; Johns, J. E.; Yang, A.; Caplins, B. W.; Shearer, A. J.; Suich, D. E.; Harris, C. B. *J. Am. Chem. Soc.* **2013**, *135*, 10646–10653.
- (1046) Spohr, E. *J. Electroanal. Chem.* **1998**, *450*, 327–334.
- (1047) Liu, L.; Li, S.; Cao, Z.; Peng, Y.; Li, G.; Yan, T.; Gao, X. P. J. *Phys. Chem. C* **2007**, *111*, 12161–12164.
- (1048) Yan, T.; Wang, S.; Zhou, Y.; Cao, Z.; Li, G. *J. Phys. Chem. C* **2009**, *113*, 19389–19392.
- (1049) Aliaga, C.; Baldelli, S. *J. Phys. Chem. C* **2008**, *112*, 3064–3072.
- (1050) Valencia, H.; Kohyama, M.; Tanaka, S.; Matsumoto, H. *J. Chem. Phys.* **2009**, *131*, 244705.
- (1051) Valencia, H.; Kohyama, M.; Tanaka, S.; Matsumoto, H. *Phys. Rev. B* **2008**, *78*, 205402.
- (1052) Klaver, T. P. C.; Luppi, M.; Sluiter, M. H. F.; Kroon, M. C.; Thijssse, B. J. *J. Phys. Chem. C* **2011**, *115*, 14718–14730.
- (1053) Mendonça, A. C. F.; Malfreyt, P.; Pádua, A. A. H. *J. Chem. Theory Comput.* **2012**, *8*, 3348–3355.
- (1054) Mendonça, A. C. F.; Pádua, A. A. H.; Malfreyt, P. *J. Chem. Theory Comput.* **2013**, *9*, 1600–1610.
- (1055) Jha, K. C.; Liu, H.; Bockstaller, M. R.; Heinz, H. *J. Phys. Chem. C* **2013**, *117*, 25969–25981.
- (1056) Zhang, M.; Yu, L.-J.; Huang, Y.-F.; Yan, J.-W.; Liu, G.-K.; Wu, D.-Y.; Tian, Z.-Q.; Mao, B.-W. *Chem. Commun.* **2014**, *50*, 14740–14743.
- (1057) Jalili, N.; Ansari, N.; Vines, F.; Illas, F.; Nazari, F. *J. Phys. Chem. C* **2014**, *118*, 1568–1575.
- (1058) Fedorov, M. V.; Kornyshev, A. A. *Chem. Rev.* **2014**, *114*, 2978–3036.
- (1059) Borisenko, N. *Bunsenmagazin* **2013**, 21–25.
- (1060) Borisenko, N.; Atkin, R.; Endres, F. *Interface* **2014**, *23*, 59.
- (1061) Ivaniščev, V.; O'Connor, S.; Fedorov, M. V. *Electrochim. Commun.* **2014**, *48*, 61–64.
- (1062) Endres, F. *ChemPhysChem* **2002**, *3*, 144–154.
- (1063) Gorlov, M.; Kloot, L. *Dalton Trans.* **2008**, 2655–2666.
- (1064) Pinilla, C.; Del Popolo, M. G.; Lynden-Bell, R. M.; Kohanoff, J. *J. Phys. Chem. B* **2005**, *109*, 17922–17927.
- (1065) Li, H.; Paneru, M.; Sedev, R.; Ralston, J. *J. Am. Chem. Soc.* **2013**, *128*, 3098–3101.
- (1066) Millefiorini, S.; Tkaczyk, A. H.; Sedev, R.; Efthimiadis, J.; Ralston, J. *J. Am. Chem. Soc.* **2006**, *128*, 3098–3101.

- (1067) Zhang, X.; Cai, Y. *Angew. Chem.* **2013**, *125*, 2345–2348.
- (1068) Ivaniščev, V.; Fedorov, M. V. *Interface* **2014**, *23*, 65.
- (1069) Kornyshev, A. A. *J. Phys. Chem. B* **2007**, *111*, 5545–5557.
- (1070) Wu, J.; Jiang, T.; Jiang, D.-e.; Jin, Z.; Henderson, D. *Soft Matter* **2011**, *7*, 11222–11231.
- (1071) Henderson, D.; Wu, J. *J. Phys. Chem. B* **2012**, *116*, 2520–2525.
- (1072) Henderson, D.; Lamperski, S. a.; Bari Bhuiyan, L.; Wu, J. *J. Chem. Phys.* **2013**, *138*, 144704.
- (1073) Henderson, D.; Jiang, D.-e.; Jin, Z.; Wu, J. *J. Phys. Chem. B* **2012**, *116*, 11356–11361.
- (1074) Lamperski, S. a.; Kaja, M.; Bhuiyan, L. B.; Wu, J.; Henderson, D. *J. Chem. Phys.* **2013**, *139*, 054703.
- (1075) Fedorov, M. V.; Kornyshev, A. A. *J. Phys. Chem. B* **2008**, *112*, 11868–11872.
- (1076) Bhuiyan, L. B.; Lamperski, S. a.; Wu, J.; Henderson, D. *J. Phys. Chem. B* **2012**, *116*, 10364–10370.
- (1077) Fedorov, M. V.; Georgi, N.; Kornyshev, A. A. *Electrochim. Commun.* **2010**, *12*, 296–299.
- (1078) Lynden-Bell, R. M.; Frolov, A. I.; Fedorov, M. V. *Phys. Chem. Chem. Phys.* **2012**, *14*, 2693–2701.
- (1079) Sha, M.; Wu, G.; Dou, Q.; Tang, Z.; Fang, H. *Langmuir* **2010**, *26*, 12667–12672.
- (1080) Vatamanu, J.; Xing, L.; Li, W.; Bedrov, D. *Phys. Chem. Chem. Phys.* **2014**, *16*, 5174–5182.
- (1081) Sha, M.; Dou, Q.; Luo, F.; Zhu, G.; Wu, G. *ACS Appl. Mater. Interfaces* **2014**.
- (1082) Sha, M.; Dou, Q.; Luo, F.; Zhu, G.; Wu, G. *ACS Appl. Mater. Interfaces* **2014**, *6*, 12556–12565.
- (1083) Hu, Z.; Vatamanu, J.; Borodin, O.; Bedrov, D. *Electrochim. Acta* **2014**, *145*, 40.
- (1084) Li, S.; Van Aken, K. L.; McDonough, J. K.; Feng, G.; Gogotsi, Y.; Cummings, P. T. *J. Phys. Chem. C* **2014**, *118*, 3901–3909.
- (1085) Turesson, M.; Szparaga, R.; Ma, K.; Woodward, C. E.; Forsman, J. *Soft Matter* **2014**.
- (1086) Breitsprecher, K.; Košovan, P.; Holm, C. *J. Phys.: Condens. Matter* **2014**, *26*, 284108.
- (1087) Breitsprecher, K.; Košovan, P.; Holm, C. *J. Phys.: Condens. Matter* **2014**, *26*, 284114.
- (1088) Kirchner, K.; Kirchner, T.; Ivaniščev, V.; Fedorov, M. V. *Electrochim. Acta* **2013**, *110*, 762–771.
- (1089) Bazant, M. Z.; Storey, B. D.; Kornyshev, A. A. *Phys. Rev. Lett.* **2011**, *106*, 046102.
- (1090) Jiang, X.; Huang, J.; Zhao, H.; Sumpter, B. G.; Qiao, R. *J. Phys.: Condens. Matter* **2014**, *26*, 284109.
- (1091) Yochelis, A. *Phys. Chem. Chem. Phys.* **2014**, *16*, 2836–2841.
- (1092) Yochelis, A. *J. Phys. Chem. C* **2014**, *118*, 5716–5724.
- (1093) Singh, M. B.; Kant, R. *J. Phys. Chem. C* **2014**, *118*, 8766.
- (1094) Oldham, K. B. *J. Electroanal. Chem.* **2008**, *613*, 131.
- (1095) Feng, G.; Jiang, X.; Qiao, R.; Kornyshev, A. A. *ACS Nano* **2014**, *8*, 11685.
- (1096) Baldelli, S. *J. Phys. Chem. B* **2005**, *109*, 13049.
- (1097) Rivera-Rubero, S.; Baldelli, S. *J. Phys. Chem. B* **2004**, *108*, 15133–15140.
- (1098) Lockett, V.; Horne, M.; Sedev, R.; Rodopoulos, T.; Ralston, J. *Phys. Chem. Chem. Phys.* **2010**, *12*, 12499–12512.
- (1099) Lockett, V.; Sedev, R.; Harmer, S.; Ralston, J.; Horne, M.; Rodopoulos, T. *Phys. Chem. Chem. Phys.* **2010**, *12*, 13816–13827.
- (1100) Feng, G.; Zhang, J. S.; Qiao, R. *J. Phys. Chem. C* **2009**, *113*, 4549–4559.
- (1101) Lauw, Y.; Horne, M. D.; Rodopoulos, T.; Leermakers, F. A. M. *Phys. Rev. Lett.* **2009**, *103*, 117801.
- (1102) Lauw, Y.; Horne, M. D.; Rodopoulos, T.; Nelson, A.; Leermakers, F. A. M. *J. Phys. Chem. B* **2010**, *114*, 11149–11154.
- (1103) Lockett, V.; Sedev, R.; Ralston, J.; Horne, M.; Rodopoulos, T. *J. Phys. Chem. C* **2008**, *112*, 7486–7495.
- (1104) Nanjundiah, C.; McDevitt, S. F.; Koch, V. R. *J. Electrochem. Soc.* **1997**, *144*, 3392–3397.
- (1105) Costa, R.; Pereira, C. M.; Silva, A. F. *Electrochim. Acta* **2014**, *116*, 306–313.
- (1106) Cannes, C. I.; Cachet, H.; Debiemme-Chouvy, C.; Deslouis, C.; de Sanoit, J.; Le Naour, C.; Zinov'yeva, V. A. *J. Phys. Chem. C* **2013**, *117*, 22915–22925.
- (1107) Zhou, W.; Xu, Y.; Ouchi, Y. *ECS Trans.* **2013**, *50*, 339–348.
- (1108) Drüscher, M.; Huber, B.; Passerini, S.; Roling, B. *J. Phys. Chem. C* **2010**, *114*, 3614–3617.
- (1109) Motobayashi, K.; Minami, K.; Nishi, N.; Sakka, T.; Osawa, M. *J. Phys. Chem. Lett.* **2013**, *4*, 3110–3114.
- (1110) Uysal, A.; Zhou, H.; Feng, G.; Lee, S. S.; Li, S.; Fenter, P.; Cummings, P. T.; Fulvio, P. F.; Dai, S.; McDonough, J. K.; Gogotsi, Y. *J. Phys. Chem. C* **2014**, *118*, 569–574.
- (1111) Endres, F.; El Abedin, S. Z.; Borisenco, N. *Z. Phys. Chem.* **2006**, *220*, 1377–1394.
- (1112) Hayes, R.; Borisenco, N.; Corr, B.; Webber, G. B.; Endres, F.; Atkin, R. *Chem. Commun.* **2012**, *48*, 10246–10248.
- (1113) Gouy, G. *Compt. Rend.* **1910**, *149*, 654.
- (1114) Chapman, D. L. *Philos. Mag.* **1913**, *25*, 475.
- (1115) Stern, O. Z. *Elektrochim.* **1924**, *30*, 508.
- (1116) Parsons, R. *Chem. Rev.* **1990**, *90*, 813–826.
- (1117) Hillier, A. C.; Kim, S.; Bard, A. J. *J. Phys. Chem.* **1996**, *100*, 18808–18817.
- (1118) Raiteri, R.; Grattarola, M.; Butt, H.-J. *J. Phys. Chem.* **1996**, *100*, 16700–16705.
- (1119) Barten, D.; Kleijn, J. M.; Duval, J.; Lyklema, J.; Cohen Stuart, M. A. *Langmuir* **2003**, *19*, 1133–1139.
- (1120) Wang, J.; Bard, A. J. *J. Phys. Chem. B* **2001**, *105*, 5217–5222.
- (1121) Sweeney, J.; Hausen, F.; Hayes, R.; Webber, G. B.; Endres, F.; Rutland, M. W.; Bennewitz, R.; Atkin, R. *Phys. Rev. Lett.* **2012**, *109*, 155502.
- (1122) Zhang, X.; Zhong, Y.-X.; Yan, J.-W.; Su, Y.-Z.; Zhang, M.; Mao, B.-W. *Chem. Commun.* **2012**, *48*, 582–584.
- (1123) Negami, M.; Ichii, T.; Murase, K.; Sugimura, H. *ECS Trans.* **2013**, *50*, 349–355.
- (1124) Hoth, J.; Hausen, F.; Müser, M. H.; Bennewitz, R. *J. Phys.: Condens. Matter* **2014**, *26*, 284110.
- (1125) Zhong, Y.-X.; Yan, J.-W.; Li, M.-G.; Zhang, X.; He, D.-W.; Mao, B.-W. *J. Am. Chem. Soc.* **2014**, *136*, 14682.
- (1126) McLean, B.; Li, H.; Stefanovic, R.; Wood, R. J.; Webber, G. B.; Ueno, K.; Watanabe, M.; Warr, G.; Page, A.; Atkin, R. *Phys. Chem. Chem. Phys.* **2014**, *17*, 325.
- (1127) Yamamoto, R.; Morisaki, H.; Sakata, O.; Shimotani, H.; Yuan, H.; Iwasa, Y.; Kimura, T.; Wakabayashi, Y. *Appl. Phys. Lett.* **2012**, *101*, -.
- (1128) Lauw, Y.; Horne, M. D.; Rodopoulos, T.; Lockett, V.; Akgun, B.; Hamilton, W. A.; Nelson, A. R. *J. Langmuir* **2012**, *28*, 7374–7381.
- (1129) Wakeham, D.; Niga, P.; Warr, G. G.; Rutland, M. W.; Atkin, R. *Langmuir* **2010**, *26*, 8313–8318.
- (1130) Yang, Y.-Y.; Zhang, L.-N.; Osawa, M.; Cai, W.-B. *J. Phys. Chem. Lett.* **2013**, *4*, 1582–1586.
- (1131) Liu, Y.; Yuan, Y.-X.; Wang, X.-R.; Zhang, N.; Xu, M.-M.; Yao, J.-L.; Gu, R.-A. *J. Electroanal. Chem.* **2014**, *728*, 10–17.
- (1132) Liu, Y.; Lu, C.; Twigg, S.; Ghaffari, M.; Lin, J.; Winograd, N.; Zhang, Q. *M. Sci. Rep.* **2013**, *3*.
- (1133) Jiang, J.; Cao, D.; Jiang, D.-e.; Wu, J. *J. Phys. Chem. Lett.* **2014**, *5*, 2195–2200.
- (1134) Shotwell, J. B.; Flowers, R. A., II. *Electroanalysis* **2000**, *12*, 223–226.
- (1135) Lee, S.-Y.; Ogawa, A.; Kanno, M.; Nakamoto, H.; Yasuda, T.; Watanabe, M. *J. Am. Chem. Soc.* **2010**, *132*, 9764–9773.
- (1136) Yasudaa, T.; Watanabe, M. *MRS Bull.* **2013**, *38*, 560–566.
- (1137) Hallinan, D. T.; Balsara, N. P. *Annu. Rev. Mater. Res.* **2013**, *43*, 503–525.
- (1138) Sun, P.; Armstrong, D. W. *Anal. Chim. Acta* **2010**, *661*, 1–16.
- (1139) Somers, A.; Howlett, P.; MacFarlane, D.; Forsyth, M. *Lubricants* **2013**, *1*, 3–21.
- (1140) Parvulescu, V. I.; Hardacre, C. *Chem. Rev.* **2007**, *107*, 2615–2665.
- (1141) Huang, P.; Latham, J.-A.; MacFarlane, D. R.; Howlett, P. C.; Forsyth, M. *Electrochim. Acta* **2013**, *110*, 501–510.

- (1142) McIntosh, E. M.; Ellis, J.; Jardine, A. P.; ALicence, P.; Jones, R. G.; Allison, W. *Chem. Sci.* **2014**, *5*, 667–676.
- (1143) Restolho, J.; Mata, J. L.; ColaÃ±o, R. r.; Saramago, B. *J. Phys. Chem. C* **2013**, *117*, 10454–10463.
- (1144) Smith, J. A.; Werzer, O.; Webber, G. B.; Warr, G. G.; Atkin, R. *J. Phys. Chem. Lett.* **2010**, *1*, 64–68.
- (1145) Wang, Z.; Priest, C. *Langmuir* **2013**, *29*, 11344–11353.
- (1146) Beattie, D. A.; Espinosa-Marzal, R. M.; Ho, T. T. M.; Popescu, M. N.; Ralston, J.; Richard, C. J. E.; Sellapperumage, P. M. F.; Krasowska, M. *J. Phys. Chem. C* **2013**, *117*, 23676–23684.
- (1147) Deyko, A.; Cremer, T.; Rietzler, F.; Perkin, S.; Crowhurst, L.; Welton, T.; SteinrÃ¼ck, H. P.; Maier, F. *J. Phys. Chem. C* **2013**, *117*, 5101–5111.
- (1148) Gong, X.; Frankert, S.; Wang, Y.; Li, L. *Chem. Commun.* **2013**, *49*, 7803–7805.
- (1149) Anaredy, R. S.; Lucio, A. J.; Shaw, S. K. *ECS Trans.* **2014**, *64*, 135–144.
- (1150) HÃ¶fft, O.; Bahr, S.; Kempfer, V. *Langmuir* **2008**, *24*, 11562–11566.
- (1151) Cremer, T.; Stark, M.; Deyko, A.; C. J. Margulis, J. P. C.; Maier, F. *Langmuir* **2011**, *27*, 3662–3671.
- (1152) Rietzler, F.; Piermaier, M.; Deyko, A.; SteinrÃ¼ck, H.-P.; Maier, F. *Langmuir* **2014**, *30*, 1063–1071.
- (1153) Cremer, T.; Wibmer, L.; Calderon, S. K.; Deyko, A.; Maier, F.; SteinrÃ¼ck, H. P. *Phys. Chem. Chem. Phys.* **2012**, *14*, 5153–5163.
- (1154) Schernich, S.; Wagner, V.; Taccardi, N.; Wasserscheid, P.; Laurin, M.; Libuda, J. *Langmuir* **2014**, *30*, 6846–6851.
- (1155) Schernich, S.; Kostyshyn, D.; Wagner, V.; Taccardi, N.; Laurin, M.; Wasserscheid, P.; Libuda, J. *J. Phys. Chem. C* **2014**, *118*, 3188–3193.
- (1156) SteinrÃ¼ck, H.-P. *Surf. Sci.* **2010**, *604*, 481–484.
- (1157) Li, H.; Sede, R.; Ralston, J. *Phys. Chem. Chem. Phys.* **2011**, *13*, 3952–3959.
- (1158) An, R.; Zhu, Y.; Wu, N.; Xie, W.; Lu, J.; Feng, X.; Lu, X. *ACS Appl. Mater. Interfaces* **2013**, *5*, 2692–2698.
- (1159) Huang, J. Y.; Lo, Y.-C.; Niu, J. J.; Kushima, A.; Qian, X.; Zhong, L.; Mao, S. X.; Li, J. *Nat. Nano* **2013**, *8*, 277–281.
- (1160) Cremer, T.; Stark, M.; Deyko, A.; SteinrÃ¼ck, H. P.; Maier, F. *Langmuir* **2011**, *27*, 3662–3671.
- (1161) Cremer, T.; Wibmer, L.; Calderon, S. K.; Deyko, A.; Maier, F.; SteinrÃ¼ck, H. P. *Phys. Chem. Chem. Phys.* **2012**, *14*, 5153–5163.
- (1162) Schernich, S.; Laurin, M.; Lykhach, Y.; SteinrÃ¼ck, H.-P.; Tsud, N.; Skla, T.; Prince, K. C.; Taccardi, N.; Matolan, V.; Wasserscheid, P.; Libuda, J. *J. Phys. Chem. Lett.* **2013**, *4*, 30.
- (1163) Li, C.; Wang, Y.; Guo, X.; Jiang, Z.; Jiang, F.; Zhang, W.; Zhang, W.; Fu, H.; Xu, H.; Wu, G. *J. Phys. Chem. C* **2014**, *118*, 3140–3144.
- (1164) Chen, S.; Kobayashi, K.; Kitaura, R.; Miyata, Y.; Shinohara, H. *ACS Nano* **2011**, *5*, 4902–4908.
- (1165) Mansfeld, U.; Hoepfner, S.; Schubert, U. S. *Adv. Mater.* **2013**, *25*, 761–765.
- (1166) He, Y.; Li, Z.; Simone, P.; Lodge, T. P. *J. Am. Chem. Soc.* **2006**, *128*, 2745–2750.
- (1167) Li, H.; Su, L.; Zhu, X.; Cheng, X.; Yang, K.; Yang, G. *J. Phys. Chem. B* **2014**, *118*, 8684–8690.
- (1168) Liu, Y.; Zhang, Y.; Wu, G.; Hu, J. *J. Am. Chem. Soc.* **2006**, *128*, 7456–7457.
- (1169) Bovio, S.; Podesta, A.; Lenardi, C.; Milani, P. *J. Phys. Chem. B* **2009**, *113*, 6600.
- (1170) Bovio, S.; Podesta, A.; Milani, P.; Ballone, P.; Popolo, M. G. D. *J. Phys.: Condens. Matter* **2009**, *21*, 424118.
- (1171) Yokota, Y.; Harada, T.; Fukui, K. *Chem. Commun.* **2010**, *46*, 8627.
- (1172) KÃ¶hler, R.; Restolho, J.; Krastev, R.; Shimizu, K.; Canongia Lopes, J. N.; Saramago, B. *J. Phys. Chem. Lett.* **2011**, *2*, 1551–1555.
- (1173) Coasne, B.; Viau, L.; Vioux, A. *J. Phys. Chem. Lett.* **2011**, *2*, 1150–1154.
- (1174) Kanakubo, M.; Hiejima, Y.; Minami, K.; Aizawa, T.; Nanjo, H. *Chem. Commun.* **2006**, 1828–1839.
- (1175) Castillo, M. R.; Fraile, J. M.; Mayoral, J. A. *Langmuir* **2012**, *28*, 11364–11375.
- (1176) Hamilton, W. A.; Porcar, L.; Butler, P. D.; Warr, G. G. *J. Chem. Phys.* **2002**, *116*, 8533–8546.
- (1177) Niga, P.; Wakeham, D.; Nelson, A.; Warr, G. G.; Rutland, M. W.; Atkin, R. *Langmuir* **2010**, *26*, 8282–8288.
- (1178) Chandler, D. *Annu. Rev. Phys. Chem.* **1978**, *29*, 441–471.
- (1179) Kruh, R. F. *Chem. Rev.* **1962**, *62*, 319–346.
- (1180) Rossky, P. J. *Annu. Rev. Phys. Chem.* **1985**, *36*, 321–346.
- (1181) Hansen, J.-P.; McDonald, I. R. *Theory of Simple Liquids*, 3rd ed.; Academic Press: New York, 2006.
- (1182) Bosio, L.; Cortes, R.; Segaud, C. *J. Chem. Phys.* **1979**, *71*, 3595–3600.
- (1183) de Graaf, L. A.; Mozer, B. *J. Chem. Phys.* **1971**, *55*, 4967–4973.
- (1184) Mikolaj, P. G.; Pings, C. *J. Chem. Phys.* **1967**, *46*, 1401–1411.
- (1185) Campbell, J. A.; Hildebrand, J. H. *J. Chem. Phys.* **1943**, *11*, 334–337.
- (1186) van der Waals, J. D. Ph.D. Dissertation, Universiteit of Leiden, 1873.
- (1187) Chandler, D.; Weeks, J. D.; Andersen, H. C. *Science* **1983**, *220*, 787–794.
- (1188) Weeks, J. D.; Chandler, D.; Andersen, H. C. *J. Chem. Phys.* **1971**, *54*, 5237.
- (1189) Berthier, L.; Tarjus, G. *Phys. Rev. Lett.* **2009**, *103*, 170601.
- (1190) Berthier, L.; Tarjus, G. *J. Chem. Phys.* **2011**, *134*, 214503.
- (1191) Celli, M.; Bafile, U.; Formisano, F.; Guarini, E.; Magli, R.; Neumann, M.; Zoppi, M. *Phys. Rev. B* **2005**, *71*, 014205.
- (1192) Zoppi, M.; Bafile, U.; Magli, R.; Soper, A. K. *Phys. Rev. E* **1993**, *48*, 1000.
- (1193) Andreani, C.; Dore, J. C.; Ricci, F. P. *Rep. Prog. Phys.* **1991**, *54*, 731.
- (1194) Bisanti, P.; Sacchetti, F. *Mol. Phys.* **1985**, *54*, 255–264.
- (1195) McLain, S. E.; Benmore, C. J.; Siewenie, J. E.; Urquidi, J.; Turner, J. F. C. *Angew. Chem., Int. Ed.* **2004**, *43*, 1952–1955.
- (1196) Neufeld, J.; Fischer, H. E.; Simonson, J. M.; Idrissi, A.; Schops, A.; Honkimaki, V. *J. Chem. Phys.* **2009**, *130*, 174503.
- (1197) Bowron, D. T.; Finney, J. L.; Soper, A. K. *J. Am. Chem. Soc.* **2006**, *128*, 5119–5126.
- (1198) Arunan, E.; Desiraju, G. R.; Klein, R. A.; Sadlej, J.; Scheiner, S.; Alkorta, I.; Clary, D. C.; Crabtree, R. H.; Dannenberg, J. J.; Hobza, P.; Kjaergaard, H. G.; Legon, A. C.; Mennucci, B.; Nesbitt, D. J. *Pure Appl. Chem.* **2011**, *83*, 1637–1641.
- (1199) Latimer, W. M.; Rodebush, W. H. *J. Am. Chem. Soc.* **1920**, *42*, 1419.
- (1200) Ball, P. *Chem. Rev.* **2008**, *108*, 74–108.
- (1201) Head-Gordon, T.; Johnson, M. E. *Proc. Natl. Acad. Sci. U.S.A.* **2006**, *103*, 7973–7977.
- (1202) Franks, F. *Water. A Comprehensive Treatise*; Plenum: New York, 1973–1982.
- (1203) Henchman, R. H.; Cockram, S. J. *Faraday Discuss.* **2013**, *167*, 529–550.
- (1204) Kosztolanyi, T.; Bako, I.; Palinkas, G. *J. Chem. Phys.* **2003**, *118*, 4546–4555.
- (1205) Ricci, M. A.; Nardone, M.; Ricci, F. P.; Andreani, C.; Soper, A. K. *J. Chem. Phys.* **1995**, *102*, 7650.
- (1206) Towey, J. J.; Soper, A. K.; Dougan, L. *Phys. Chem. Chem. Phys.* **2011**, *13*, 9397–9406.
- (1207) Dougan, L.; Bates, S. P.; Hargreaves, R.; Fox, J. P.; Crain, J.; Reat, V.; Soper, A. K. *J. Chem. Phys.* **2004**, *121*, 6456.
- (1208) Towey, J. J.; Dougan, L. *J. Phys. Chem. B* **2012**, *116*, 1633–1641.
- (1209) Elola, M. D.; Ladanyi, B. M. *J. Chem. Phys.* **2006**, *125*, 184506.
- (1210) Chen, B.; Siepmann, J. I. *J. Phys. Chem. B* **2005**, *110*, 3555–3563.
- (1211) Imberti, S.; Bowron, D. T. *J. Phys.: Condens. Matter* **2010**, *22*, 404212.
- (1212) Chang, Y. J.; Castner, E. W. *J. Chem. Phys.* **1993**, *99*, 113.
- (1213) Ludwig, R.; Weinhold, F.; Farrar, T. C. *J. Chem. Phys.* **1995**, *102*, 5118.
- (1214) Edwards, F. G.; Enderby, J. E.; Page, D. T. *J. Phys. (Paris)* **1975**, *C8*, 3483.

- (1215) Fürth, R. *Proc. Cambridge Philos. Soc.* **1941**, *37*, 276–280.
- (1216) Fürth, R. *Proc. Cambridge Philos. Soc.* **1941**, *37*, 252–275.
- (1217) Henshaw, D. G. *Phys. Rev.* **1957**, *105*, 976–981.
- (1218) Mancinelli, R.; Botti, A.; Bruni, F.; Ricci, M. A.; Soper, A. K. *Phys. Chem. Chem. Phys.* **2007**, *9*, 2959–2967.
- (1219) Ishii, R.; Okazaki, S.; Okada, I.; Furusaka, M.; Watanabe, N.; Misawa, M.; Fukunaga, T. *Chem. Phys. Lett.* **1995**, *240*, 84–88.
- (1220) Bernabei, M.; Botti, A.; Bruni, F.; Ricci, M. A.; Soper, A. K. *Phys. Rev. E* **2008**, *78*, 021505.
- (1221) Ballone, P.; Pastore, G.; Tosi, M. P. *J. Chem. Phys.* **1984**, *81*, 3174.
- (1222) Chen, S. H.; Lin, T. L.; Kotlarchyk, M. Analysis of Critical Scattering Data from AOT/D<sub>2</sub>O/n-Decane Microemulsions. In *Surfactants in Solution*; Lal Mittal, K., Bothorel, P., Eds.; Springer: New York, 1986.
- (1223) Duvail, M.; Dufreche, J.-F.; Arleth, L.; Zemb, T. *Phys. Chem. Chem. Phys.* **2013**, *15*, 7133–7141.
- (1224) Palermo, M. F.; Pizzirusso, A.; Muccioli, L.; Zannoni, C. *J. Chem. Phys.* **2013**, *138*, 204901.
- (1225) Mills, R. *Ber. Bunsen-Ges. Phys. Chem.* **1971**, *75*, 195.
- (1226) Nachtrieb, N. H.; Petit, J. *J. Chem. Phys.* **1956**, *24*, 746.
- (1227) O'Reilly, D. E.; Peterson, E. M. *J. Chem. Phys.* **1977**, *66*, 934–937.
- (1228) Kreitmeir, M.; Bertagnolli, H.; Mortensen, J.; Parrinello, M. *J. Chem. Phys.* **2003**, *118*, 3639–3645.
- (1229) Kratochwill, A.; Hertz, H. G. *J. Chim. Phys.* **1977**, *74*, 814.
- (1230) Tanaka, K. *J. Chem. Soc., Faraday Trans.* **1975**, *71*, 1127–1131.
- (1231) Passiniemi, P.; Liukkonen, S.; Noszticzius, Z. *J. Chem. Soc., Faraday Trans.* **1977**, *73*, 1834–1839.
- (1232) Passiniemi, P. *J. Solution Chem.* **1983**, *12*, 801–813.
- (1233) Etesse, P.; Zega, J. A.; Kobayashi, R. *J. Chem. Phys.* **1992**, *97*, 2022.
- (1234) Lamb, W. J.; Hoffman, G. A.; Jonas, J. *J. Chem. Phys.* **1981**, *74*, 6875.
- (1235) Bartels, C. R.; Graessley, W. W.; Crist, B. *J. Polym. Sci., Polym. Lett. Ed.* **1983**, *21*, 495–499.
- (1236) Janz, G. J.; Bansal, N. P. *J. Phys. Chem. Ref. Data* **1982**, *11*, 505.
- (1237) Tokuda, H.; Tsuzuki, S.; Susan, M. A. B. H.; Hayamizu, K.; Watanabe, M. *J. Phys. Chem. B* **2006**, *110*, 19593–19600.
- (1238) Towey, J. J.; Soper, A. K.; Dougan, L. *Faraday Discuss.* **2013**, *167*, 159–176.
- (1239) Sala, J.; Guàrdia, E.; Martí, J. *J. Chem. Phys.* **2010**, *132*, 214505.
- (1240) Saharay, M.; Balasubramanian, S. *J. Chem. Phys.* **2004**, *120*, 9694.
- (1241) Snook, I. K.; Henderson, D. *J. Chem. Phys.* **1978**, *68*, 2134.
- (1242) Oh, S. H.; Kauffmann, Y.; Scheu, C.; Kaplan, W. D.; Rähle, M. *Science* **2005**, *310*, 661–663.
- (1243) Huisman, W. J.; Peters, J. F.; Zwanenburg, M. J.; de Vries, S. A.; Derry, T. E.; Abernathy, D.; van der Veen, J. F. *Nature* **1997**, *390*, 379–381.
- (1244) Pashley, R. M.; Israelachvili, J. N. *J. Colloid Interface Sci.* **1984**, *101*, 511.
- (1245) Cheng, L.; Fenter, P.; Nagy, K. L.; Schlegel, M. L.; Sturchio, N. C. *Phys. Rev. Lett.* **2001**, *87*, 156103.
- (1246) Toney, M. F.; Howard, J. N.; Richer, J.; Borges, G. L.; Gordon, J. G.; Melroy, O. R.; Wiesler, D. G.; Yee, D.; Sorenson, L. B. *Nature* **1994**, *368*, 444–446.
- (1247) Christenson, H. K. *J. Chem. Phys.* **1983**, *78*, 6906.
- (1248) Porcheron, F.; Rousseau, B.; Schoen, M.; Fuchs, A. H. *Phys. Chem. Chem. Phys.* **2001**, *3*, 1155–1159.
- (1249) Lim, L. T.; Wee, A. T.; O'Shea, S. *J. J. Chem. Phys.* **2009**, *130*, 134703.
- (1250) Christenson, H. K.; Gruen, D. W. R.; Horn, R. G.; Israelachvili, J. N. *J. Chem. Phys.* **1987**, *87*, 1834–1841.
- (1251) Mugele, F.; Baldelli, S.; Somorjai, G. A.; Salmeron, M. *J. Phys. Chem. B* **2000**, *104*, 3140–3144.
- (1252) Hofbauer, W.; Ho, R. J.; R, H.; Gosvami, N. N.; O'Shea, S. *J. Phys. Rev. B* **2009**, *80*, 134104.
- (1253) Franz, V.; Butt, H.-J. *J. Phys. Chem. B* **2002**, *106*, 1703–1708.
- (1254) Horn, R. G.; Israelachvili, J. N. *J. Chem. Phys.* **1981**, *75*, 1400.
- (1255) Yu, C. J.; Richter, A. G.; Kmetko, J.; Dugan, S. W.; Datta, A.; Dutta, P. *Phys. Rev. E* **2001**, *63*, 021205.
- (1256) Horn, R. G.; Israelachvili, J. N. *Macromolecules* **1988**, *21*, 2836–2841.
- (1257) Heyes, D. M.; Clarke, J. H. R. *J. Chem. Soc., Faraday Trans.* **1981**, *77*, 1089–1100.
- (1258) Lanning, O. J.; Madden, P. A. *J. Phys. Chem. B* **2004**, *108*, 11069–11072.
- (1259) Parsons, D. F.; Walsh, R. B.; Craig, V. S. J. *J. Chem. Phys.* **2014**, *140*, 164701.
- (1260) Gee, M. L.; McGuigan, P. M.; Israelachvili, J. N.; Homola, A. *M. J. Chem. Phys.* **1990**, *93*, 1895–1906.
- (1261) Ohnesorge, R.; Löwen, H.; Wagner, H. *Phys. Rev. E* **1994**, *50*, 4801–4809.
- (1262) Algara-Siller, G.; Lehtinen, O.; Wang, F. C.; Nair, R. R.; Kaiser, U.; Wu, H. A.; Geim, A. K.; Grigorieva, I. V. *Nature* **2015**, *519*, 443–445.
- (1263) Manne, S.; Cleveland, J. P.; Gaub, B. E.; Stucky, G. D.; Hansma, P. K. *Langmuir* **1994**, *10*, 4409–4413.
- (1264) Vorobiev, A.; Major, J.; Dosch, H.; Gordeev, G.; Orlova, D. *Phys. Rev. Lett.* **2004**, *93*, 267203.
- (1265) Trasca, R. A.; Klapp, S. H. L. *J. Chem. Phys.* **2008**, *129*, 084702.
- (1266) Israelachvili, J. N.; Kott, S. J. *J. Chem. Phys.* **1988**, *88*, 7162–7166.
- (1267) Sullivan, D. E.; Barker, R.; Gray, C. G.; Streett, W. B.; Gubbins, K. E. *Mol. Phys.* **1981**, *44*, 597–621.
- (1268) Thompson, S. M.; Gubbins, K. E.; Sullivan, D. E.; Gray, C. G. *Mol. Phys.* **1984**, *51*, 21–44.
- (1269) Israelachvili, J. N.; Pashley, R. M. *Nature* **1983**, *306*, 249.
- (1270) Patel, S. S.; Tirrell, M. *Annu. Rev. Phys. Chem.* **1989**, *40*, 597–635.
- (1271) Petrov, P.; Olsson, U.; Wennerström, H. *Langmuir* **1997**, *13*, 3331–3337.
- (1272) Horn, R. G.; Israelachvili, J. N.; Perez, E. *J. Phys. (Paris)* **1981**, *42*, 39–52.
- (1273) Chandler, D. *Nature* **2005**, *437*, 640–646.
- (1274) Raschke, T. M.; Tsai, J.; Levitt, M. *Proc. Natl. Acad. Sci. U.S.A.* **2001**, *98*, 5965.
- (1275) Mirejovsky, D.; Arnett, E. M. *J. Am. Chem. Soc.* **1983**, *105*, 1112.
- (1276) Kang, W.; Dong, B.; Gao, Y.; Zheng, L. *Colloid Polym. Sci.* **2010**, *288*, 1225–1232.
- (1277) Zhang, G.; Chen, X.; Zhao, Y.; Ma, F.; Jing, B.; Qiu, H. *J. Phys. Chem. B* **2008**, *112*, 6578–6584.
- (1278) Zhao, M.; Gao, Y.; Zheng, L. *J. Phys. Chem. B* **2010**, *114*, 11382–11389.
- (1279) Shi, L.; Zheng, L. *J. Phys. Chem. B* **2012**, *116*, 2162–2172.
- (1280) Ammam, M.; Di Caprio, D.; Gaillon, L. *Electrochim. Acta* **2012**, *61*, 207–215.
- (1281) Shi, L.; Zhao, M.; Zheng, L. *Colloids Surf., A* **2011**, *392*, 305–312.
- (1282) Ghosh, S. *J. Colloid Interface Sci.* **2011**, *360*, 672–680.
- (1283) Tamura-Lis, W.; Lis, L. J.; Quinn, P. J. *J. Colloid Interface Sci.* **1992**, *150*, 200–207.
- (1284) Zech, O.; Thomaier, S.; Kolodziejski, A.; Touraud, D.; Grillo, I.; Kunz, W. *J. Colloid Interface Sci.* **2010**, *347*, 227–232.
- (1285) Kanzaki, R.; Uchida, K.; Song, X.; Umebayashi, Y.; Ishiguro, S.-i. *Anal. Sci.* **2008**, *24*, 1347–1349.
- (1286) Xie, L. L. *J. Dispersion Sci. Technol.* **2009**, *30*, 100–103.
- (1287) Jiang, W.; Hao, J.; Wu, Z. *Langmuir* **2008**, *24*, 3150–3156.
- (1288) Galin, M.; Marchal, E.; Mathis, A.; Galin, J.-C. *Polym. Adv. Technol.* **1997**, *8*, 75–86.
- (1289) Zhang, S.; Liu, J.; Li, N.; Yang, X.; Zheng, L. *Colloid Polym. Sci.* **2012**, *290*, 1927–1935.
- (1290) Kumar, A.; Venkatesu, P. *RSC Adv.* **2013**, *3*, 362–367.
- (1291) Wang, X.; Chen, X.; Zhao, Y.; Yue, X.; Li, Q.; Li, Z. *Langmuir* **2011**, *28*, 2476–2484.
- (1292) Debeljuh, N. J.; Sutti, A.; Barrow, C. J.; Byrne, N. *J. Phys. Chem. B* **2013**, *117*, 8430–8435.

- (1293) Grossman, S.; Danielson, N. D. *J. Chromatogr, A* **2009**, *1216*, 3578–3586.
- (1294) Lu, F.; Shi, L.; Gu, Y.; Yang, X.; Zheng, L. *Colloid Polym. Sci.* **2013**, *291*, 2375–2384.
- (1295) Baker, E. N.; Hubbard, R. E. *Prog. Biophys. Mol. Biol.* **1984**, *44*, 97–179.
- (1296) Rao, V. G.; Ghatak, C.; Pramanik, R.; Sarkar, S.; Sarkar, N. *Chem. Phys. Lett.* **2010**, *499*, 89–93.
- (1297) Mulla, S. A. R.; Salama, T. A.; Pathan, M. Y.; Inamdar, S. M.; Chavan, S. S. *Tetrahedron Lett.* **2013**, *54*, 672–675.
- (1298) Bicak, N. *J. Mol. Liq.* **2005**, *116*, 15–18.
- (1299) Dear, R. D.; Worrall, E. K.; Gault, W. D.; Ritchie, G. A. D. *J. Phys. Chem. B* **2013**, *117*, 10567–10571.
- (1300) Yuan, X.; Zhang, S.; Liu, J.; Lu, X. *Fluid Phase Equilib.* **2007**, *257*, 195–200.
- (1301) Tamura-Lis, W.; Lis, L. J.; Quinn, P. J. *Biophys. J.* **1988**, *53*, 489–492.
- (1302) Kanzaki, R.; Uchida, K.; Hara, S.; Umebayashi, Y.; Ishiguro, S.; Nomura, S. *Chem. Lett.* **2007**, *36*.
- (1303) Jiang, W.; Yu, B.; Liu, W.; Hao, J. *Langmuir* **2007**, *23*, 8549–8553.
- (1304) Sarda, S.; Kale, J.; Wasmatkar, S.; Kadam, V.; Ingole, P.; Jadhav, W.; Pawar, R. *Mol. Diversity* **2009**, *13*, 545–549.
- (1305) Kaper, H.; Sallard, S. b.; Djerdj, I.; Antonietti, M.; Smarsly, B. *M. Chem. Mater.* **2010**, *22*, 3502–3510.
- (1306) Zhao, Y.; Cheng, N.; Liu, M.; Yu, L. *Colloid Polym. Sci.* **2013**, *1*–9.
- (1307) Frost, D. S.; Machas, M.; Perea, B.; Dai, L. L. *Langmuir* **2013**, *29*, 10159–10165.
- (1308) Zhao, C.; Burrell, G.; Torriero, A. A. J.; Separovic, F.; Dunlop, N. F.; MacFarlane, D. R.; Bond, A. M. *J. Phys. Chem. B* **2008**, *112*, 6923–6936.
- (1309) Stoimenovski, J.; Dean, P. M.; Izgorodina, E. I.; MacFarlane, D. R. *Faraday Discuss.* **2012**, *154*, 335–352.
- (1310) Lis, D.; Backus, E. H.; Hunger, J.; Parekh, S. H.; Bonn, M. *Science* **2014**, *344*, 1138.
- (1311) Feynman, R. P. *Eng. Sci.* **1960**, *23*.
- (1312) Koblenz, T. S.; Wassenaar, J.; Reek, J. N. H. *Chem. Soc. Rev.* **2008**, *37*, 247–262.
- (1313) Vriezema, D. M.; Comellas Aragonès, M.; Elemans, J. A. A. W.; Cornelissen, J. J. L. M.; Rowan, A. E.; Nolte, R. J. M. *Chem. Rev.* **2005**, *105*, 1445–1490.
- (1314) Busseron, E.; Ruff, Y.; Moulin, E.; Giuseppone, N. *Nanoscale* **2013**, *5*, 7098–7140.
- (1315) Weber, C. C.; Masters, A. F.; Maschmeyer, T. *Angew. Chem., Int. Ed.* **2012**, *51*, 11483–11486.
- (1316) Liu, N.; Luo, F.; Wu, H.; Liu, Y.; Zhang, C.; Chen, J. *Adv. Funct. Mater.* **2008**, *18*, 1518–1525.
- (1317) Zhang, B.; Ning, W.; Zhang, J.; Qiao, X.; Zhang, J.; He, J.; Liu, C.-Y. *J. Mater. Chem.* **2010**, *20*, 5401–5403.
- (1318) Sham, A. Y. W.; Notley, S. M. *Soft Matter* **2013**, *9*, 6645–6653.
- (1319) Li, H.; Chen, L.; Wu, H.; He, H.; Jin, Y. *Langmuir* **2014**, *30*, 15016.
- (1320) Ding, Y.; Sun, X.; Zhang, L.; Mao, S.; Xie, Z.; Liu, Z.-W.; Su, D. *Angew. Chem., Int. Ed.* **2014**, *54*, 231.
- (1321) Szilagyi, I.; Szabo, T.; Desert, A.; Trefalt, G.; Oncsik, T.; Borkovec, M. *Phys. Chem. Chem. Phys.* **2014**, *16*, 9515–9524.
- (1322) Smith, J. A.; Webber, G. B.; Warr, G. G.; Atkin, R. *J. Phys. Chem. B* **2014**, *117*, 13930–13935.
- (1323) Gutel, T.; Garcia-Antón, J.; Pelzer, K.; Philippot, K.; Santini, C. C.; Chauvin, Y.; Chaudret, B.; Basset, J. M. *J. Mater. Chem.* **2007**, *17*, 3290.
- (1324) Yang, M.; Campbell, P. S.; Santini, C. C.; Mudring, A.-V. *Nanoscale* **2014**, *6*, 3367–3375.
- (1325) Redel, E.; Thomann, R.; Janiak, C. *Inorg. Chem.* **2007**, *47*, 14–16.
- (1326) Gindri, I. M.; Frizzo, C. P.; Bender, C. R.; Tier, A. Z.; Martins, M. A. P.; Villetti, M. A.; Machado, G.; Rodriguez, L. C.; Rodrigues, D. C. *ACS Appl. Mater. Interfaces* **2014**, *6*, 11536–11543.
- (1327) Gutel, T.; Santini, C. C.; Philippot, K.; Padua, A.; Pelzer, K.; Chaudret, B.; Chauvin, Y.; Basset, J.-M. *J. Mater. Chem.* **2009**, *19*, 3624–3631.
- (1328) Jiang, S.; Chen, Q.; Tripathy, M.; Luijten, E.; Schweizer, K. S.; Granick, S. *Adv. Mater.* **2010**, *22*, 1060–1071.
- (1329) Granick, S. *Annu. Rev. Phys. Chem.* **2015**, *66*.
- (1330) Chen, Q.; Bae, S. C.; Granick, S. *Nature* **2011**, *469*, 381–384.
- (1331) Park, B. J.; Lee, D. *ACS Nano* **2011**, *6*, 782–790.
- (1332) Kim, J.-W.; Lee, D.; Shum, H. C.; Weitz, D. A. *Adv. Mater.* **2008**, *20*, 3239–3243.
- (1333) Morris, R. E. *Angew. Chem., Int. Ed.* **2008**, *47*, 442–444.
- (1334) Cooper, E. R.; Andrews, C. D.; Wheatley, P. S.; Webb, P. B.; Wormald, P.; Morris, R. E. *Nature* **2004**, *430*, 1012–1016.
- (1335) Dybtsev, D. N.; Chun, H.; Kim, K. *Chem. Commun.* **2004**, 1594–1595.
- (1336) Sindoro, M.; Yanai, N.; Jee, A.-Y.; Granick, S. *Acc. Chem. Res.* **2013**, *47*, 459–469.
- (1337) Morris, R. E. *Chem. Commun.* **2009**, 2990–2998.
- (1338) Lin, Z.; Slawin, A. M. Z.; Morris, R. E. *J. Am. Chem. Soc.* **2007**, *129*, 4880–4881.
- (1339) Lísal, M. *J. Chem. Phys.* **2013**, *139*, 214701.
- (1340) Lísal, M.; Chval, Z.; Storch, J.; Izáka, P. *J. Mol. Liq.* **2014**, *189*, 85–94.
- (1341) Endres, F. *MRS Bull.* **2013**, *38*, 567–571.
- (1342) Al Zoubi, M.; Endres, F. *Electrochim. Acta* **2011**, *56*, 5872–5876.
- (1343) Al-Salman, R.; Endres, F. *J. Mater. Chem.* **2009**, *19*, 7228–7231.
- (1344) Al-Salman, R.; Mallet, J.; Molinari, M.; Fricoteaux, P.; Martineau, F.; Troyon, M.; El Abedin, S. Z.; Endres, F. *Phys. Chem. Chem. Phys.* **2008**, *10*, 6233–6237.
- (1345) Carstens, T.; Prowald, A.; Zein El Abedin, S.; Endres, F. *Solid State Electrochem.* **2012**, *16*, 3479–3485.
- (1346) Zhu, Y.-J.; Wang, W.-W.; Qi, R.-J.; Hu, X.-L. *Angew. Chem.* **2004**, *116*, 1434–1438.
- (1347) Byrne, N.; Menzies, D.; Goujon, N.; Forsyth, M. *Chem. Commun.* **2013**, *49*, 7729–7731.
- (1348) Ji, X.; Zhang, Q.; Liang, F.; Chen, Q.; Qu, X.; Zhang, C.; Wang, Q.; Li, J.; Song, X.; Yang, Z. *Chem. Commun.* **2014**, *50*, 5706–5709.
- (1349) Lebedeva, O.; Kudryavtsev, I.; Kultin, D.; Dzhungurova, G.; Kalmykov, K.; Kustov, L. *J. Phys. Chem. C* **2014**, *118*, 21293–21298.
- (1350) Soeda, J.; Matsui, H.; Okamoto, T.; Osaka, I.; Takimiya, K.; Takeya, J. *Adv. Mater.* **2014**, *26*, 6430–6435.
- (1351) Chen, S.; Li, L.; Wang, X.; Tian, W.; Wang, X.; Tang, D.-M.; Bando, Y.; Golberg, D. *Nanoscale* **2012**, *4*, 2658–2662.
- (1352) Borra, E. F.; Seddiqi, O.; Angel, R.; Eisenstein, D.; Hickson, P.; Seddon, K. R.; Worden, S. P. *Nature* **2007**, *447*, 979–981.
- (1353) Miao, W.; Chan, T. H. *Acc. Chem. Res.* **2006**, *39*, 897–908.
- (1354) Xin, B.; Hao, J. *Chem. Soc. Rev.* **2014**, *43*, 7171.
- (1355) Bain, C. D.; Troughton, E. B.; Tao, Y. T.; Evall, J.; Whitesides, G. M.; Nuzzo, R. G. *J. Am. Chem. Soc.* **1989**, *111*, 321–335.
- (1356) Dai, J.; Cheng, J.; Jin, J.; Li, Z.; Kong, J.; Bi, S. *Electrochim. Commun.* **2008**, *10*, 587–591.
- (1357) Kubisa, P. *Prog. Polym. Sci.* **2004**, *29*, 3–12.
- (1358) Piculell, L.; Lindman, B. *Adv. Colloid Interface Sci.* **1992**, *41*, 149–178.
- (1359) Groot, R. D. *Langmuir* **2000**, *16*, 7493–7502.
- (1360) Puttick, S.; Davis, A. L.; Butler, K.; Irvine, D. J.; Licence, P.; Thurecht, K. J. *Polym. Chem.* **2013**, *4*, 1337–1344.
- (1361) Puttick, S.; Davis, A. L.; Butler, K.; Lambert, L.; El harfi, J.; Irvine, D. J.; Whittaker, A. K.; Thurecht, K. J.; Licence, P. *Chem. Sci.* **2011**, *2*, 1810–1816.
- (1362) Whitley, J. W.; Jeffrey Horne, W.; Danielsen, S. P. O.; Shannon, M. S.; Marshall, J. E.; Hayward, S. H.; Gaddis, C. J.; Bara, J. E. *Eur. Polym. J.* **2014**, *60*, 92–97.
- (1363) Schultz, A. R.; Lambert, P. M.; Chartrain, N. A.; Ruohoniemi, D. M.; Zhang, Z.; Jangu, C.; Zhang, M.; Williams, C. B.; Long, T. E. *ACS Macro Lett.* **2014**, *3*, 1205–1209.
- (1364) Markstedt, K.; Sundberg, J.; Gatenholm, P. *3D Printing Additive Manufacturing* **2014**, *1*, 115–121.

- (1365) Perera-Nuñez, J.; Meíndez-Vilas, A.; Labajos-Broncano, L.; González-Martín, M. L. *Langmuir* **2010**, *26*, 17712–17719.
- (1366) Kaisei, K.; Kobayashi, K.; Matsushige, K.; Yamada, H. *Ultramicroscopy* **2010**, *110*, 733–736.
- (1367) Ribeiro, M. C. C. *J. Chem. Phys.* **2013**, *139*, 114505.
- (1368) Kozlov, D. N.; Kiefer, J.; Seeger, T.; Fröba, A. P.; Leipertz, A. *J. Phys. Chem. B* **2014**, *118*, 14493.
- (1369) Chatel, G.; MacFarlane, D. R. *Chem. Soc. Rev.* **2014**, *43*, 8132–8149.
- (1370) Valkenburg, M. E. V.; Vaughn, R. L.; Williams, M.; Wilkes, J. S. *Thermochim. Acta* **2005**, *425*, 181–188.
- (1371) Olivier-Bourbigou, H.; Magna, L.; Morvan, D. *Appl. Catal., A* **2010**, *373*, 1–56.
- (1372) Chowdhury, S.; Mohan, R. S.; Scott, J. L. *Tetrahedron* **2007**, *63*, 2363–2389.
- (1373) Yau, H. M.; Chan, S. J.; George, S. R. D.; Hook, J. M.; Croft, A. K.; Harper, J. B. *Molecules* **2009**, *14*, 2521–2534.
- (1374) Chiappe, C.; Malvaldi, M.; Pomelli, C. S. *Pure Appl. Chem.* **2009**, *81*, 767.
- (1375) Weber, C. C.; Masters, A. F.; Maschmeyer, T. *Org. Biomol. Chem.* **2013**, *11*, 2534–2542.
- (1376) Aggarwal, A.; Lancaster, N. L.; Sethi, A. R.; Welton, T. *Green Chem.* **2002**, *4*, 517–520.
- (1377) Jaeger, D. A.; Tucker, C. E. *Tetrahedron Lett.* **1989**, *30*, 1785–1788.
- (1378) Yau, H. M.; Croft, A. K.; Harper, J. B. *Faraday Discuss.* **2012**, *154*, 365–371.
- (1379) Yau, H. M.; Howe, A. G.; Hook, J. M.; Croft, A. K.; Harper, J. B. *Org. Biomol. Chem.* **2009**, *7*, 3572–3575.
- (1380) Allen, C.; McCann, B. W.; Acevedo, O. *J. Phys. Chem. B* **2015**, *119*, 743.
- (1381) Al Otaibi, A.; McCluskey, A. *Multicomponent Reactions in Ionic Liquids*, 2013.
- (1382) Hoffmann, J.; Nuchter, M.; Ondruschka, B.; Wasserscheid, P. *Green Chem.* **2003**, *5*, 296–299.
- (1383) Wei, Y.-M.; Zhou, X.-S.; Wang, J.-G.; Tang, J.; Mao, B. W.; Kolb, D. M. *Small* **2008**, *4*, 1355–1358.
- (1384) Endres, F. *MRS Bull.* **2013**, *38*, 567–571.
- (1385) El Abedin, S. Z.; Moustafa, E.; Hempelmann, R.; Natter, H.; Endres, F. *ChemPhysChem* **2006**, *7*, 1535.
- (1386) El Abedin, S. Z.; Moustafa, E.; Hempelmann, R.; Natter, H.; Endres, F. *Electrochim. Commun.* **2005**, *7*, 1111–1116.
- (1387) Giridhar, P.; El Abedin, S. Z.; Endres, F. *Electrochim. Acta* **2012**, *70*, 2010.
- (1388) Abbott, A. P.; Qiu, F.; Abood, H. M. A.; Ali, M. R.; Ryder, K. S. *Phys. Chem. Chem. Phys.* **2010**, *12*, 1862–1872.
- (1389) Fu, Y.-C.; Su, Y.-Z.; Zhang, H.-M.; Yan, J.-W.; Xie, Z.-X.; Mao, B.-W. *ChemPhysChem* **2010**, *11*, 2764–2778.
- (1390) Ispas, A.; Buschbeck, M.; Pitula, S.; Mudring, A.; Uhlemann, M.; Bund, A.; Endres, F. *ECS Trans.* **2009**, *16*, 119–127.
- (1391) El Abedin, S. Z.; Saad, A. Y.; Farag, H. K.; Borisenko, N.; Liua, Q. X.; Endres, F. *Electrochim. Acta* **2007**, *52*, 2746–2754.
- (1392) Giridhar, P.; El Abedin, S. Z.; F. Endres, F. *J. Solid State Electrochem.* **2012**, *16*, 3487–3497.
- (1393) Zein El Abedin, S.; Saad, A. Y.; Farag, H. K.; Borisenko, N.; Liu, Q. X.; Endres, F. *Electrochim. Acta* **2007**, *52*, 2746–2754.
- (1394) Al-Salman, R.; El Abedin, S. Z.; Endres, F. *Phys. Chem. Chem. Phys.* **2008**, *10*, 4650–4657.
- (1395) Meng, X.; Al-Salman, R.; Zhao, J.; Borissenko, N.; Li, Y.; Endres, F. *Angew. Chem., Int. Ed.* **2009**, *48*, 2703–2707.
- (1396) Endres, F. *Phys. Chem. Chem. Phys.* **2001**, *3*, 3165–3174.
- (1397) Krischok, S.; Ispas, A.; Züehlsdorff, A.; Ulbrich, A.; Bund, A.; Endres, F. *ECS Trans.* **2013**, *50*, 229–237.
- (1398) Giridhar, P.; Zein El Abedin, S.; Bund, A.; Ispas, A.; Endres, F. *Electrochim. Acta* **2014**, *129*, 312–317.
- (1399) Wang, F.-X.; Pan, G.-B.; Liu, Y.-D.; Xiao, Y. *Chem. Phys. Lett.* **2010**, *488*, 112–115.
- (1400) Fu, Y.-C.; Yan, J.-W.; Wang, Y.; Tian, J.-H.; Zhang, H.-M.; Xie, Z.-X.; Mao, B.-W. *J. Phys. Chem. C* **2007**, *111*, 10467–10477.
- (1401) Yan, J. W.; Wu, Q.; Shang, W. H.; Mao, B. W. *Electrochim. Commun.* **2004**, *6*, 843–848.
- (1402) Zein El Abedin, S.; Borissenko, N.; Endres, F. *Electrochim. Commun.* **2004**, *6*, 510–514.
- (1403) Ispas, A.; Adolphi, B.; Bund, A.; Endres, F. *Phys. Chem. Chem. Phys.* **2010**, *12*, 1793.
- (1404) Borisenko, N.; Ispas, A.; Zschippang, E.; Liu, Q.; Zein El Abedin, S.; Bund, A.; Endres, F. *Electrochim. Acta* **2009**, *54*, 1519–1528.
- (1405) Liu, Z.; Borisenko, N.; El Abedin, S. Z.; Endres, F. *J. Solid State Electrochem.* **2014**, *18*, 2683.
- (1406) Tian, Y.-H.; Goff, G. S.; Runde, W. H.; Batista, E. R. *J. Phys. Chem. B* **2012**, *116*, 11943–11952.
- (1407) Hayyan, M.; Mjalli, F. S.; Hashim, M. A.; AlNashef, I. M.; Mei, T. X. *J. Ind. Eng. Chem.* **2013**, *19*, 106–112.
- (1408) Endres, F.; Höfft, O.; Borisenko, N.; Gasparotto, L. H. S.; Prowald, A.; Al-Salman, R.; Carstens, T.; Atkin, R.; Bund, A.; El Abedin, S. Z. *Phys. Chem. Chem. Phys.* **2010**, *12*, 1724.
- (1409) Gordon Research Conference “Ionic Liquids: Solvents, Materials, or Medicines?”, Newry, Maine, August, 2014.
- (1410) Ferraz, R.; Branco, L. C.; Prudêncio, C.; Noronha, J. P.; Petrovski, Ž. *ChemMedChem* **2011**, *6*, 975–985.
- (1411) *Ionic Liquid Applications: Pharmaceuticals, Therapeutics, and Biotechnology*; American Chemical Society: Washington, DC, 2010.
- (1412) Bica, K.; Rijksen, C.; Nieuwenhuyzen, M.; Rogers, R. D. *Phys. Chem. Chem. Phys.* **2010**, *12*, 2011–2017.
- (1413) Choi, S. Y.; Rodriguez, H.; Mirjafari, A.; Gilpin, D. F.; McGrath, S.; Malcolm, K. R.; Tunney, M. M.; Rogers, R. D.; McNally, T. *Green Chem.* **2011**, *13*, 1527–1535.
- (1414) Cojocaru, O. A.; Bica, K.; Gurau, G.; Narita, A.; McCrary, P. D.; Shamshina, J. L.; Barber, P. S.; Rogers, R. D. *MedChemComm* **2013**, *4*, 559–563.
- (1415) Stoimenovski, J.; MacFarlane, D.; Bica, K.; Rogers, R. *Pharm. Res.* **2010**, *27*, 521–526.
- (1416) Stoimenovski, J.; MacFarlane, D. R. *Chem. Commun.* **2011**, *47*, 11429–11431.
- (1417) Kumar, V.; Malhotra, S. V. *Ionic Liquid Applications: Pharmaceuticals, Therapeutics, and Biotechnology*; American Chemical Society: Washington, DC, 2010; Vol. 1038.
- (1418) Busetto, A.; Crawford, D. E.; Earle, M. J.; Gilea, M. A.; Gilmore, B. F.; Gorman, S. P.; Laverty, G.; Lowry, A. F.; McLaughlin, M.; Seddon, K. R. *Green Chem.* **2010**, *12*, 420–425.
- (1419) Kumar, V.; Malhotra, S. V. *Bioorg. Med. Chem. Lett.* **2009**, *19*, 4643–4646.
- (1420) Malhotra, S. V.; Kumar, V. *Bioorg. Med. Chem. Lett.* **2010**, *20*, 581–585.
- (1421) Kumar, V.; Malhotra, S. V. *Ionic Liquid Applications: Pharmaceuticals, Therapeutics, and Biotechnology*; American Chemical Society: Washington, DC, 2010; Vol. 1038.
- (1422) Gangamallaiah, V.; Dutt, G. B. *J. Phys. Chem. B* **2012**, *116*, 12819–12825.
- (1423) Kilpeläinen, I.; Xie, H.; King, A.; Granstrom, M.; Heikkilä, S.; Argyropoulos, D. S. *J. Agric. Food Chem.* **2007**, *55*, 9142–9148.
- (1424) Pinkert, A.; Marsh, K. N.; Pang, S.; Staiger, M. P. *Chem. Rev.* **2009**, *109*, 6712–6728.
- (1425) Medronho, B.; Romano, A.; Miguel, M.; Stigsson, L.; Lindman, B. *Cellulose* **2012**, *19*, 581–587.
- (1426) Glasser, W.; Atalla, R.; Blackwell, J.; Malcolm Brown, R., Jr.; Burchard, W.; French, A.; Klemm, D.; Nishiyama, Y. *Cellulose* **2012**, *19*, 589–598.
- (1427) Lindman, B.; Karlström, G.; Stigsson, L. *J. Mol. Liq.* **2010**, *156*, 76–81.
- (1428) Wang, H.; Gurau, G.; Pingali, S. V.; O'Neill, H. M.; Evans, B. R.; Urban, V. S.; Heller, W. T.; Rogers, R. D. *ACS Sustainable Chem. Eng.* **2014**, *2*, 1264–1269.
- (1429) Luo, N.; Lv, Y.; Wang, D.; Zhang, J.; Wu, J.; He, J.; Zhang, J. *Chem. Commun.* **2012**, *48*, 6283–6285.
- (1430) Ruegg, T. L.; Kim, E.-M.; Simmons, B. A.; Keasling, J. D.; Singer, S. W.; Soon Lee, T.; Thelen, M. P. *Nat. Commun.* **2014**, *5*.
- (1431) Lei, Z.; Dai, C.; Zhu, J. *AIChE J.* **2014**, *60*, 3312–3329.

- (1432) Rao, S. R. *Surface Chemistry of Froth Flotation*, 2nd ed.; Kluwer Academic/Plenum Publishers: New York, 2003.
- (1433) Shah, K.; Atkin, R.; Stanger, R.; Wall, T.; Moghtaderi, B. *Fuel* **2014**, *119*, 214–218.
- (1434) Cummings, J.; Shah, K.; Atkin, R.; Moghtaderi, B. *Fuel* **2015**, *143*, 244–252.
- (1435) Whitehead, J. A.; Lawrence, G. A.; McCluskey, A. *Green Chem.* **2004**, *6*, 313–315.
- (1436) Whitehead, J. A.; Zhang, J.; Pereira, N.; McCluskey, A.; Lawrence, G. A. *Hydrometallurgy* **2007**, *88*, 109–120.
- (1437) Dong, T.; Hua, Y.; Zhang, Q.; Zhou, D. *Hydrometallurgy* **2009**, *99*, 33–38.
- (1438) Abbott, A. P.; Frisch, G.; Hartley, J.; Ryder, K. S. *Green Chem.* **2011**, *13*, 471–481.
- (1439) MacFarlane, D. R.; Tachikawa, N.; Forsyth, M.; Pringle, J. M.; Howlett, P. C.; Elliott, G. D.; Davis, J. H.; Watanabe, M.; Simon, P.; Angell, C. A. *Energy Environ. Sci.* **2014**, *7*, 232–250.
- (1440) Wishart, J. F. *Energy Environ. Sci.* **2009**, *2*, 956–961.
- (1441) Chen, X.; Zhao, J.; Zhang, J.; Qiu, L.; Xu, D.; Zhang, H.; Han, X.; Sun, B.; Fu, G.; Zhang, Y.; Yan, F. *J. Mater. Chem.* **2012**, *22*, 18018–18024.
- (1442) Li, Q.; Zhao, J.; Sun, B.; Lin, B.; Qiu, L.; Zhang, Y.; Chen, X.; Lu, J.; Yan, F. *Adv. Mater.* **2012**, *24*, 945–950.
- (1443) Zhang, W.; Yuan, C.; Guo, J.; Qiu, L.; Yan, F. *ACS Appl. Mater. Interfaces* **2014**, *6*, 8723–8728.
- (1444) Cooper, E. I.; O'Sullivan, E. J. *Proc. 8th Int. Symp. Molten Salts, Electrochemical Soc.*; Pennington, NJ, 1992; Vol. 92-16, p 386.
- (1445) Angell, C. A. *ECS Trans.* **2014**, *64*, 9–20.
- (1446) Warner, I. M.; El-Zahab, B.; Siraj, N. *Anal. Chem.* **2014**, *86*, 7184–7191.
- (1447) Reichert, W. M.; Holbrey, J. D.; Vigour, K. B.; Morgan, T. D.; Broker, G. A.; Rogers, R. D. *Chem. Commun.* **2006**, 4767–4779.
- (1448) Griffin, P. J.; Holt, A. P.; Wang, Y.; Novikov, V. N.; Sangoro, J. R.; Kremer, F.; Sokolov, A. P. *J. Phys. Chem. B* **2014**, *118*, 783.
- (1449) Li, F.; Jennings, J. R.; Wang, X.; Fan, L.; Koh, Z. Y.; Yu, H.; Yan, L.; Wang, Q. *J. Phys. Chem. C* **2014**, *118*, 17153–17159.
- (1450) Marquet, P.; Andersson, G.; Snedden, A.; Kloo, L.; Atkin, R. *Langmuir* **2010**, *26*, 9612–9616.
- (1451) Xia, Y.; Xie, W.; Ruden, P. P.; Fisbie, C. D. *Phys. Rev. Lett.* **2010**, *105*, 036802.
- (1452) Kong, X.; Lu, D.; Liu, Z.; Wu, J. *Nano Res.* **2014**, 1–10.
- (1453) Feng, G.; Cummings, P. T. *J. Phys. Chem. Lett.* **2011**, *2*, 2859.
- (1454) Si, X.; Li, S.; Wang, Y.; Ye, S.; Yan, T. *ChemPhysChem* **2012**, *13*, 1671.
- (1455) Wu, P.; Huang, J.; Meunier, V.; Sumpter, B. G.; Qiao, R. *J. Phys. Chem. Lett.* **2012**, *3*, 1732.
- (1456) Kamath, G.; Narayanan, B.; Sankaranarayanan, S. K. R. S. *Phys. Chem. Chem. Phys.* **2014**, *16*, 20387–20391.
- (1457) Schweikert, N.; Hofmann, A.; Schulz, M.; Scheuermann, M.; Boles, S. T.; Hanemann, T.; Hahn, H.; Indris, S. *J. Power Sources* **2013**, *228*, 237–243.
- (1458) Yin, J.; Li, X.; Yu, J.; Zhang, Z.; Zhou, J.; Guo, W. *Nat. Nano* **2014**, *9*, 378–383.
- (1459) Angell, C. A. In *Chapter 1 'Tonic Liquids in the Temperature Range 150–1500 K: Patterns and Problems' Molten Salts and Ionic Liquids*; Gaune-Escard, M., Seddon, K. R., Eds.; John Wiley & Sons, Inc.: New York, 2010.
- (1460) Ichikawa, T.; Yoshio, M.; Hamasaki, A.; Mukai, T.; Ohno, H.; Kato, T. *J. Am. Chem. Soc.* **2007**, *129*, 10662–10663.
- (1461) Soberats, B.; Uchida, E.; Yoshio, M.; Kagimoto, J.; Ohno, H.; Kato, T. *J. Am. Chem. Soc.* **2014**, *136*, 9552–9555.
- (1462) Yoshio, M.; Mukai, T.; Kanie, K.; Yoshizawa, M.; Ohno, H.; Kato, T. *Adv. Mater.* **2002**, *14*, 351–354.
- (1463) Druschler, M.; Borisenko, N.; Wallauer, J.; Winter, C.; Huber, B.; Endres, F.; Roling, B. *Phys. Chem. Chem. Phys.* **2012**, *14*, 5090–5099.
- (1464) Roling, B.; Druschler, M.; Huber, B. *Faraday Discuss.* **2012**, *154*, 303–311.
- (1465) Efthimiadis, J.; Neil, W. C.; Bunter, A.; Howlett, P. C.; Hinton, B. R. W.; MacFarlane, D. R.; Forsyth, M. *ACS Appl. Mater. Interfaces* **2010**, *2*, 1317–1323.
- (1466) Jeong, J.; Aetukuri, N.; Graf, T.; Schladt, T. D.; Samant, M. G.; Parkin, S. S. P. *Science* **2013**, *339*, 1402–1405.
- (1467) Schladt, T. D.; Graf, T.; Aetukuri, N. B.; Li, M.; Fantini, A.; Jiang, X.; Samant, M. G.; Parkin, S. S. P. *ACS Nano* **2013**, *7*, 8074–8081.
- (1468) Nakayama, H.; Ye, J.; Ohtani, T.; Fujikawa, Y.; Ando, K.; Iwasa, Y.; Saitoh, E. *Appl. Phys. Lett.* **2012**, *5*, 023002.
- (1469) Whitesides, G. M. *Nature* **2006**, *442*, 368–373.
- (1470) Dubois, P.; Marchand, G.; Fouillet, Y.; Berthier, J.; Douki, T.; Hassine, F.; Gmouh, S.; Vaultier, M. *Anal. Chem.* **2006**, *78*, 4909–4917.
- (1471) de Mello, A. J.; Habgood, M.; Lancaster, N. L.; Welton, T.; Woottton, R. C. *R. Lab Chip* **2004**, *4*, 417–419.
- (1472) Hoang, P. H.; Park, H.; Kim, D.-P. *J. Am. Chem. Soc.* **2011**, *133*, 14765–14770.
- (1473) Chatterjee, D.; Hetayothin, B.; Wheeler, A. R.; King, D. J.; Garrell, R. L. *Lab Chip* **2006**, *6*, 199–206.
- (1474) Squires, T. M.; Quake, S. R. *Rev. Mod. Phys.* **2005**, *77*, 977–1026.
- (1475) Tan, S. H.; Semin, B.; Baret, J.-C. *Lab Chip* **2014**, *14*, 1099–1106.
- (1476) Chen, F.; Qing, Q.; Xia, J.; Li, J.; Tao, N. *J. Am. Chem. Soc.* **2009**, *131*, 9908–9909.
- (1477) Thiemann, S.; Sachnov, S.; Porscha, S.; Wasserscheid, P.; Zaumseil, J. *J. Phys. Chem. C* **2012**, *116*, 13536–13544.
- (1478) Fujimoto, T.; Awaga, K. *Phys. Chem. Chem. Phys.* **2013**, *15*, 8983–9006.
- (1479) Bara, J. E.; Camper, D. E.; Gin, D. L.; Noble, R. D. *Acc. Chem. Res.* **2009**, *43*, 152–159.
- (1480) Bates, E. D.; Mayton, R. D.; Ntai, I.; Davis, J. H. *J. Am. Chem. Soc.* **2002**, *124*, 926–927.
- (1481) Brennecke, J. F.; Gurkan, B. E. *J. Phys. Chem. Lett.* **2010**, *1*, 3459–3464.
- (1482) Davison, J. *Energy* **2007**, *32*, 1163–1176.
- (1483) Zhang, X.; Zhang, X.; Dong, H.; Zhao, Z.; Zhang, S.; Huang, Y. *Energy Environ. Sci.* **2012**, *5*, 6668–6681.
- (1484) Gurkan, B. E.; Gohndrone, T. R.; McCready, M. J.; Brennecke, J. F. *Phys. Chem. Chem. Phys.* **2013**, *15*, 7796–7811.
- (1485) Seo, S.; Simoni, L. D.; Ma, M.; DeSilva, M. A.; Huang, Y.; Stadtherr, M. A.; Brennecke, J. F. *Energy Fuels* **2014**, *28*, 5968–5977.
- (1486) Byrne, N.; Angell, C. A. *J. Mol. Biol.* **2008**, *378*, 707.
- (1487) Byrne, N.; Angell, C. A. *Chem. Commun.* **2009**, 1046–1048.
- (1488) Byrne, N.; Angell, C. A. *Molecules* **2010**, *15*, 793–803.
- (1489) Vijayaraghavan, R.; Izgorodin, A.; Ganesh, V.; Surianarayanan, M.; MacFarlane, D. R. *Angew. Chem., Int. Ed.* **2010**, *49*, 1631–1633.
- (1490) Byrne, N.; Rodoni, B.; Constable, F.; Varghese, S.; Davis, J. H. *Phys. Chem. Chem. Phys.* **2012**, *14*, 10119–10121.
- (1491) Lo Nostro, P.; Ninham, B. W. *Chem. Rev.* **2012**, *112*, 2286–2322.
- (1492) MacFarlane, D. R.; Vijayaraghavan, R.; Ha, H. N.; Izgorodin, A.; Weaver, K. D.; Elliott, G. D. *Chem. Commun.* **2010**, *46*, 7703–7705.
- (1493) Sun, X.; Luo, H.; Dai, S. *Chem. Rev.* **2011**, *112*, 2100–2128.
- (1494) Harmon, C. D.; Smith, W. H.; Costa, D. A. *Radiat. Phys. Chem.* **2001**, *60*, 157–159.
- (1495) Shkrob, I. A.; Marin, T. W.; Wishart, J. F.; Grills, D. C. *J. Phys. Chem. B* **2014**, *118*, 10477–10492.
- (1496) Wishart, J. F. *J. Phys. Chem. Lett.* **2010**, *1*, 3225–3231.
- (1497) Khemchandani, B.; Somers, A.; Howlett, P.; Jaiswal, A. K.; Sayanna, E.; Forsyth, M. *Tribiol. Int.* **2014**, *77*, 171–177.
- (1498) Yang, X.; Meng, Y.; Tian, Y. *Tribol. Lett.* **2014**, *S6*, 161–169.
- (1499) Li, H.; Cooper, P. K.; Somers, A. E.; Rutland, M. W.; Howlett, P. C.; Forsyth, M.; Atkin, R. *J. Phys. Chem. Lett.* **2014**, *5*, 4095.
- (1500) Wakeham, W. A. *Congress on Ionic Liquids V*, Algarve, Portugal, 2013.
- (1501) Li, H.; Rutland, M. W.; Atkin, R. *Phys. Chem. Chem. Phys.* **2013**, *15*, 14616–14623.
- (1502) Sweeney, J.; Webber, G. B.; Rutland, M. W.; Atkin, R. *Phys. Chem. Chem. Phys.* **2014**, *16*, 16651–16658.

- (1503) Watanabe, S.; Nakano, M.; Miyake, K.; Tsuboi, R.; Sasaki, S. *Langmuir* **2014**, *30*, 8078–8084.
- (1504) Pogodina, N. V.; Amann, T.; Dold, C.; Metwalli, E.; Müller-Buschbaum, P.; Kailer, A.; Fredrich, C. *J. Mol. Liq.* **2014**, *192*, 118.
- (1505) de Wijn, A. S.; Fasolino, A.; Filippov, A. E.; Urbakh, M. *Phys. Rev. Lett.* **2014**, *112*, 055502.
- (1506) Hausen, F.; Gosvami, N. N.; Bennewitz, R. *Electrochim. Acta* **2011**, *56*, 10694–10700.
- (1507) Hausen, F.; Nielinger, M.; Ernst, S.; Baltruschat, H. *Electrochim. Acta* **2008**, *53*, 6058–6063.
- (1508) Xie, G.; Guo, D.; Luo, J. *Tribiol. Int.* **2015**, *84*, 22–35.
- (1509) Manzato, C.; Foster, A. S.; Alava, M. J.; Laurson, L. *Phys. Rev. E* **2015**, *91*, 012504.
- (1510) Fajardo, O. Y.; Bresme, F.; Kornyshev, A. A.; Urbakh, M. *Sci. Rep.* **2015**, *5*, 7698.
- (1511) Chudnovsky, B. H. Proceedings of the 51st IEEE Holm Conference on Electrical Contacts, 2005; pp 107–114.
- (1512) Horn, R. G.; Smith, G. D. *Science* **1992**, *256*, 362–364.
- (1513) Ehre, D.; Lavert, E.; Lahav, M.; Lubomirsky, I. *Science* **2010**, *327*, 672–675.
- (1514) Wellens, S.; Thijs, B.; Binnemans, K. *Green Chem.* **2013**, *15*, 3484–3485.
- (1515) Sebastiao, E.; Cook, C.; Hu, A.; Murugesu, M. *J. Mater. Chem. A* **2014**, *2*, 8153–8173.
- (1516) McCrary, P. D.; Chatel, G.; Alaniz, S. A.; Cojocaru, O. A.; Beasley, P. A.; Flores, L. A.; Kelley, S. P.; Barber, P. S.; Rogers, R. D. *Energy Fuels* **2014**, *28*, 3460–3473.
- (1517) Schneider, S.; Hawkins, T.; Ahmed, Y.; Rosander, M.; Hudgens, L.; Mills, J. *Angew. Chem., Int. Ed.* **2011**, *50*, 5886–5888.
- (1518) Schneider, S.; Hawkins, T.; Rosander, M.; Vaghjiani, G.; Chambreau, S.; Drake, G. *Energy Fuels* **2008**, *22*, 2871–2872.
- (1519) Zhang, Y.; Gao, H.; Guo, Y.; Joo, Y.-H.; Shreeve, J. n. M. *Chem.—Eur. J.* **2010**, *16*, 3114–3120.
- (1520) Zhang, Y.; Gao, H.; Joo, Y.-H.; Shreeve, J. n. M. *Angew. Chem., Int. Ed.* **2011**, *50*, 9554–9562.
- (1521) Zhang, Y.; Shreeve, J. n. M. *Angew. Chem., Int. Ed.* **2011**, *50*, 935–937.
- (1522) Rocha, M. A. A.; Coutinho, J. A. P.; Santos, L. M. N. B. F. *J. Chem. Phys.* **2013**, *139*, 104502.
- (1523) Bosmann, A.; Datsevich, L.; Jess, A.; Lauter, A.; Schmitz, C.; Wasserscheid, P. *Chem. Commun.* **2001**, 2494–2495.
- (1524) Huang, C.; Chen, B.; Zhang, J.; Liu, Z.; Li, Y. *Energy Fuels* **2004**, *18*, 1862–1864.
- (1525) Kulkarni, P. S.; Afonso, C. A. M. *Green Chem.* **2010**, *12*, 1139–1149.
- (1526) Kralisch, D.; Stark, A.; Korsten, S.; Kreisel, G.; Ondruschka, B. *Green Chem.* **2005**, *7*, 301–309.
- (1527) Klein-Marcuschamer, D.; Oleskowicz-Popiel, P.; Simmons, B. A.; Blanch, H. W. *Biotechnol. Bioeng.* **2012**, *109*, 1083–1087.
- (1528) Yan, F.; Lartey, M.; Jariwala, K.; Bowser, S.; Damodaran, K.; Albenze, E.; Luebke, D. R.; Nulwala, H. B.; Smit, B.; Haranczyk, M. *J. Phys. Chem. B* **2014**, *118*, 13609.
- (1529) Greaves, T. L.; Ha, K.; Muir, B.; Howard, S. C.; Weerawardena, A.; Kirby, N.; Drummond, C. *J. Phys. Chem. Chem. Phys.* **2015**, *17*, 2357–2365.